The role of CFTR in lumen formation and maintenance in mammary epithelial cells

Aida Aide Luna Perez

A thesis submitted in partial fulfilment of the requirements for the degree of Doctor of Philosophy

School of Medicine and Population Health

University of Sheffield

February 2024

ABSTRACT

The lumen space is essential to establish the tubular morphology of the mammary gland and its maintenance is crucial for the homeostasis of this organ. Breast cancer development is characterised by altered tissue organisation and loss of lumen space. Understanding lumen formation and maintenance may provide insights into normal mammary gland development and possible molecules dysregulated in breast cancer.

One mechanism proposed to form a single lumen is fluid secretion. The cystic fibrosis transmembrane conductance regulator (CFTR) ion channel is essential for fluid secretion in epithelial cells and organogenesis in different cellular systems; however, its role in lumenogenesis and maintenance in mammary epithelial cells (MECs) is unknown. Lumen formation is a complex process that also relies on cell-extracellular matrix (ECM) interactions. Some cellular interactions with the ECM occur through cell surface receptors, such as the integrins. β-1 integrin regulates lumen formation by orienting the apicobasal polarity axis of MECs surrounding the luminal space. Nevertheless, whether β-1 integrin participates downstream orientation in fluid secretion and single-lumen formation is unknown.

This thesis hypothesises that CFTR regulates the lumen structure in MECs and that β1 integrin regulates lumen expansion downstream of polarity orientation through fluid secretion in MECs. The main aim to explore is the role of CFTR in lumen formation and maintenance in normal mouse MECs, which are capable of forming 3D lumen structures *in vitro* and evaluate the CFTR expression in breast cancer cells, which cannot form a lumen *in vitro.* Likewise, determine whether β1-integrin regulates the paracellular fluids in MECs that could contribute to the lumen formation mechanism.

In normal mouse MECs, CFTR activity and its expression were modified using CFTRinh-172, forskolin and siRNAs. Results showed that CFTR activity and expression are essential for the formation and maintenance of the lumen in normal MECs cultured in 3D conditions with BMM. Consequently, *CFTR* expression in human breast cancer cells (MCF7, CAL51, T47D and MDA-MB-231) and non-tumorigenic cell lines were compared by doing *in silico* analysis of sequencing data and afterwards experimentally by qPCR. Similar *CFTR* expression was detected in the non-tumorigenic and breast cancer cell lines. Conversely, at the protein expression level, only the non-tumorigenic MCF10A cells expressed the mature molecular weight in the membrane protein fraction. An evaluation of lumen formation in breast cancer cells cultured in 3D conditions with BMM was conducted, showing that they were not able to form lumen structures. However, lumen formation was observed after the stimulation of CFTR activity with forskolin in the CAL-51 cells.

The β-1 integrin expression was modified *in vitro* and confirmed its decreased or decreased expression in MECs by immunofluorescence. Paracellular permeability

assays were conducted in mouse MECs to analyse the β-1 integrin role on paracellular permeability. Experiment conditions in both cell models were standardised, and future studies are required to determine the β-1 integrin role in paracellular fluid transport and its participation in forming a single lumen.

The findings in this thesis highlight a novel requirement for CFTR in normal mouse MECs for lumen morphogenesis and maintenance, suggesting that CFTR could be related to the lack of lumen formation in breast cancer cells in which the CFTR protein expression is different.

CONTENTS

FIGURES

TABLES

ACKNOWLEDGEMENTS

I want to thank my supervisors, Dr Mark Fenwick and Dr Helen Bryant, for their support and guidance during this project. I am extremely grateful to my supervisor, Dr Fenwick, for allowing me to be part of his laboratory group, guiding me during this stage of my PhD, sharing his experience and knowledge, and for his mentorship, which played a crucial role in this project. Thanks for being patient and for always having kind and motivating words. Thanks, Dr Akhtar, for your supervision during the first years of my PhD. I would also like to thank Dr Sarah Waite and Matt Fisher for their technical support during my PhD. Thank you a lot, Sarah, for always being supportive and sharing your knowledge. I also want to recognise the contribution of work that the students I supervise did for this project; thanks, Lisa and Joely. I would also like to thank the rest of the research team and lab mates for accompanying me at this stage and for your friendship and support. I would also like to acknowledge the Department of Oncology and Metabolism for its administrative and technical support. Likewise, I would like to thank my sponsor, Educafin, who made my stay during the PhD possible.

Finally, I thank my husband, Miguel, for all his infinite love and support; this would not have been possible without you. Thanks to all my family, especially my mom, for her everlasting love and encouraging me to do everything I dream of. Thanks to my nieces and nephews for being treasures in my life and motivating me to achieve this goal. Thanks to my friends who, from a distance in between, supported and motivated me during my PhD.

Presentations and grants

- Flash talk and poster presentation at the International Association for Breast Cancer Research Conference (IABCR 2023)
- Poster presentation at Annual Medical School Research Meeting.
- Poster presentation at the British Society for Developmental Biology (BSDB) Spring Meeting in 2023.
- Oral and poster presentation at the 14th European Network for Breast Development and Cancer (ENBDC). Annual workshop of methods in mammary gland biology and breast cancer in 2023.
- Early career research grant for the International Association for Breast Cancer Research Conference (IABCR) in 2023.
- Grant for the British Society for Developmental Biology (BSDB) Spring Meeting in 2023.
- Wellcome Trust Biomedical Vacation Scholarship to get funds for a summer project and supervise an undergraduate student.

ABBREVIATIONS

µg	Microgram
µl	Microliter
µm	Micrometre
µM	Micromolar
4-OHT	4-hydroxy tamoxifen
ATP	Adenosine triphosphate
BM	Basement membrane
BMM	Basement membrane matrix
cAMP	Cyclic adenosine monophosphate
cDNA	Complementary DNA
CF	Cystic fibrosis
CFTR	Cystic fibrosis transmembrane conductance regulator
CO_2	Carbon dioxide
dd H_2O	Double-distilled water
DMEM	Dulbecco's Modified Eagle's Medium
DMSO	Dimethyl sulfoxide
DNA	Deoxyribonucleic acid
ECM	Extracellular matrix
FBS	Fetal bovine serum
GAPDH	Glyceraldehyde 3-phosphate dehydrogenase
GEO	Gene Expression Omnibus
GFP	Green fluorescent protein
H2O	Water
HRP	Horse radish peroxidase
IF	Immunofluorescence
IgG	Immunoglobulin G
KD	Knockdown
KO	Knockout
LB	Luria broth
MCDK	Madin-Darby Canine Kidney
MEC	Mammary epithelial cell
mg	Milligram
ml	Millilitre
mRNA	Messenger RNA
NaCl	Sodium chloride
ng	Nanogram
nM	Nanomolar
nTPM	Normalised transcript per million TPM
PBS	Phosphate buffered saline
PCR	Polymerase chain reactions
PTM	Post-translational modifications
RIPA	Radioimmunoprecipitation assay
RNA	Ribonucleic acid
RT-qPCR	Reverse transcription-quantitative polymerase chain reaction
SDS	Sodium dodecyl sulfate
SDS-PAGE	SDS-polyacrylamide gel electrophoresis
SEM	Standard error of the mean

siRNA	Small interfering RNA
SMA	Smooth muscle actin
TBS	Tris-buffered saline
TBS-T	TBS-Tween
TEER	Transepithelial electrical resistance
TEMED	Tetramethylethylenediamine
TJs	Tight junctions
WB	Western blot
ZO-1	Zonula occludens-1

Chapter 1

1. INTRODUCTION AND OVERVIEW

1.1 INTRODUCTION

Breast cancer is the most common type of cancer in women, registering 2.3 million women diagnosed in 2020, which in turn causes the highest number of cancer-related deaths in women in the world (WHO 2020). Breast cancer is a heterogeneous disease with different subtypes that exhibit distinct biological and molecular features. Thus, disrupted tissue architecture is a common feature in all breast cancer subtypes.

Structurally, the mammary gland consists of an interconnected system of hollow tubes lined by polarised epithelia. The epithelial cells consist of a morphologically recognisable basal layer oriented towards the outer extracellular matrix (ECM) and a luminal cell side oriented towards the luminal space of the tubes. This glandular structure is essential for the homeostasis of the mammary tissue as well as the production and transport of milk during lactation (Pechoux, Gudjonsson et al. 1999, Macias and Hinck 2012). Lumen formation is a complex process that relies on different mechanisms and phases, such as the establishment of cell polarity (Bryant, Datta et al. 2010, Datta, Bryant et al. 2011), the orientation of the polar axis (Akhtar and Streuli 2013, Bryant, Roignot et al. 2014), the opening and expansion of micro lumens to a single lumen (Bagnat, Navis et al. 2010, Navis and Bagnat 2015) and the axis of cell division (Jaffe, Kaji et al. 2008, Gao, Yang et al. 2017). The lumen space in the mammary gland is formed during embryonic development, and although the mammary gland undergoes extensive remodelling throughout life, the lumen space is consistently maintained. Therefore, it is expected that some of the mechanisms

involved in lumen formation are those that also regulate its maintenance. However, lumen maintenance in the mammary gland is poorly understood.

The opening and expansion of a lumen are important processes necessary for the development of a luminal structure within the mammary gland. The expansion of a single lumen has recently been explained through the fluid secretion mechanism in other cellular systems (Bagnat, Cheung et al. 2007, Alvers, Ryan et al. 2014). This mechanism explains how microlumens can expand to form a single lumen by a hydrostatic pressure generated from fluid secretion and accumulation in the apical zone (Navis and Bagnat 2015). The polarised secretion of fluids to the apical zone occurs as a consequence of an electrochemical gradient created by the Na+/K+ pump and also by ion channel activities such as the Cystic Fibrosis Transmembrane Conductance Regulator (CFTR) (Bagnat, Cheung et al. 2007). The Na+/K+ pump, a transmembrane ATPase, regulates the cell membrane potential, co-transporting potassium ions into the cell and sodium ions out of the cell. The CFTR ion channel secretes chloride and bicarbonate from the apical membrane to the lumen area and promotes an osmotic gradient in the luminal zone that triggers fluid secretion in epithelial cells. The Na+/K+ pump and CFTR promote water transport by osmotic gradients to the lumen area through specialised systems such as aquaporins and tight junctions (TJs) (Saint-Criq and Gray 2017). The hydrostatic pressure generated by the water transported into the luminal space exerts a force to drive lumen expansion and likely plays an important role in lumen maintenance.

Most of the mechanisms involved in lumen formation depend on the cellular interactions with the ECM. For example, cell polarity and polarity orientation depend on the cell-ECM interactions, and both are indispensable for determining the tissue structure and the lumen space position (Blasky, Mangan et al. 2015, Overeem, Bryant et al. 2015). Cell surface receptors, such as the integrins, are the main communicators between the cells and the ECM. In mammary epithelial cells (MECs), β1 integrin is indispensable for polarity orientation; its absence causes the inversion of the polarity, altering the location of apical components and subsequently affecting lumen formation (Akhtar and Streuli 2013). Alterations in cell-ECM communication cause abnormal lesions in the lumen, leading to the formation of multiple lumens that fill the luminal space by epithelial cells. These types of lesions are characteristic of the initial stages of breast cancer, and the continued filling of the lumen with cells is associated with further progression of a dysregulated phenotype, including stromal invasion and potential metastasis to other organs (Gudjonsson, Adriance et al. 2005, Kaushik, Pickup et al. 2016, Halaoui, Rejon et al. 2017). Therefore, studying the mechanisms and the molecules that participate in lumen formation and maintenance could provide relevant information to further understand mammary gland organisation and its alteration in breast cancer.

1.2 MAMMARY GLAND DEVELOPMENT AND BREAST TISSUE

Breast tissue is made up of the mammary gland, connective tissue, adipose, and skin (Khan, Fakoya et al. 2024). Externally, the breasts consist of skin, a nipple bordered by a round shape pigmented areola that contains sebaceous glands. Embedded in the

fat and connective tissue between the second and sixth rib is the mammary gland, whose primary function is to produce and transport milk for the nutrition of newborns. The mammary gland consists of an interconnected system of 15-25 secretory lobes. Each lobe is composed of smaller lobules, which contain functional glandular units called alveoli, where milk is produced during lactation in response to the hormone prolactin. These alveolar subunits are interconnected and lead to a lactiferous duct that carries milk directly to the nipple (Figure 1.1A). Together, these represent a composite tubular acinar gland with a lumen space covered by adipose tissue and stroma (Zucca-Matthes, Urban et al. 2016, Biswas, Banerjee et al. 2022).

Microscopically, the mammary gland consists of a lumen space enclosed by an epithelial bilayer supported by stroma cells and connective tissue (Khan, Fakoya et al. 2024). The bilayer consists of luminal, cuboidal-shaped epithelial cells and peripheral spindle-shaped myoepithelial cells. The luminal epithelial cells express keratins 8 and 18 and line the lactiferous ducts that terminate at the nipple. The myoepithelial cells express smooth muscle actin (SMA) and keratins 5 and 14. These cells are in direct contact with a laminin-rich basement membrane (BM), which forms part of the ECM (Pechoux, Gudjonsson et al. 1999). Although most of the myoepithelial cells are in direct contact with BM, some luminal cells are also in contact with the BM.

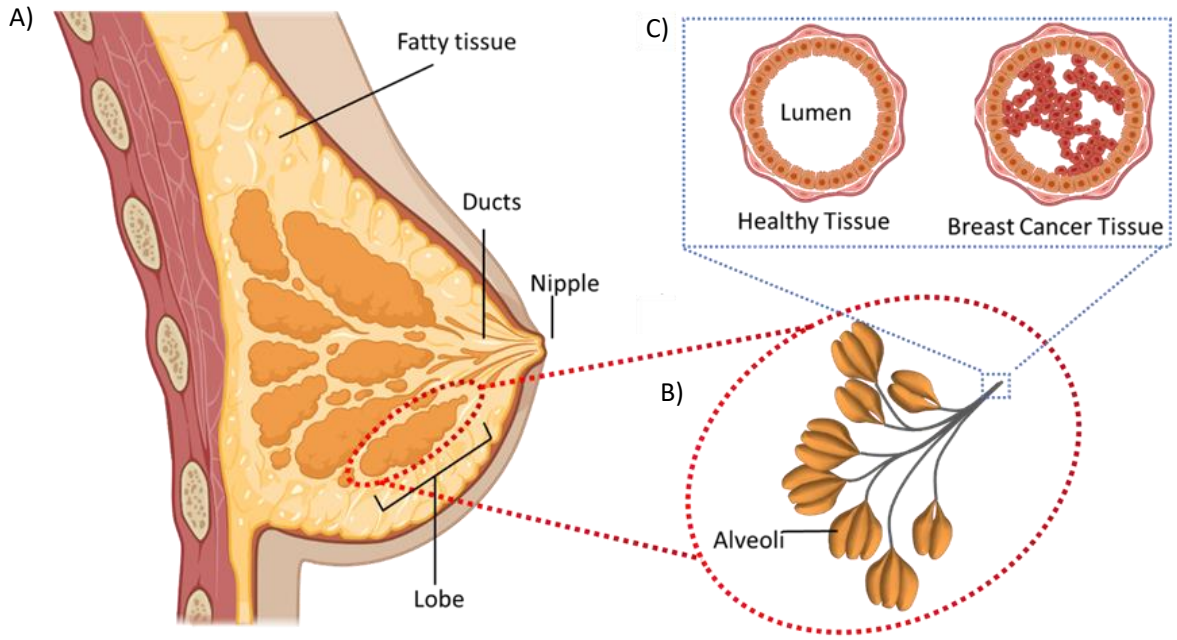

Figure 1.1. Breast tissue. A) Anatomy of the mammary gland. The figure shows a system of lobes and ducts connected to the nipple. B) Alveoli form the lobes. Each lobe has a lactiferous duct that connects to the nipple (Pechoux, Gudjonsson et al. 1999, Zucca-Matthes, Urban et al. 2016, Biswas, Banerjee et al. 2022). C) Lumen space in healthy and breast cancer tissue. The lumen space in healthy tissue is free of cells, while in breast cancer, the lumen area is often reduced by filling it with breast cancer cells (Gudjonsson, Adriance et al. 2005, Kaushik, Pickup et al. 2016). The Illustration was self-drawn (using Biorender) based on the citations mentioned in this figure legend.

The mammary gland undergoes significant changes in different life stages, such as embryogenesis, adolescence and pregnancy (Figure 1.2). In the different stages of development, morphogenetic programs that favour tissue organisation and its interconnected system of hollow ducts that give rise to the luminal space are carried out. During embryogenesis, the primary mammary buds grow downwards to expand into secondary buds in the stroma, reaching the fat pad in the epidermis (Robinson, Karpf et al. 1999). The secondary buds coalesce to give origin to the lumen and the mammary ducts. In mice, lumen formation starts at E16, and in human fetuses, it starts between 15 and 20 weeks (Hogg, Harrison et al. 1983, Biswas, Banerjee et al. 2022). Posteriorly, the nipple is fully developed with smooth muscle fibres. At the end of the

third trimester of embryogenesis, 15-20 lobes with lactiferous ducts are formed (Javed and Lteif 2013).

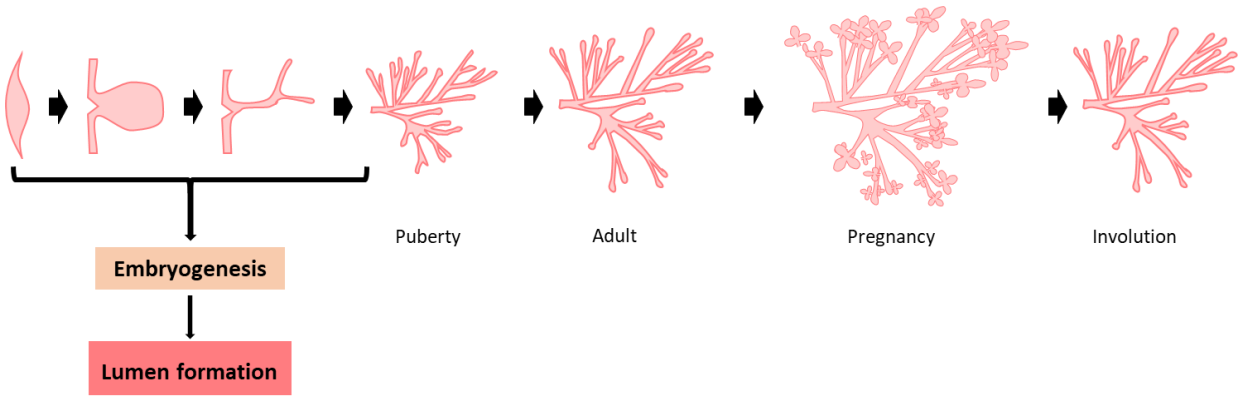

Figure 1.2. Development of the mammary gland and lumen formation. The lumen formation occurs during embryogenesis (between 15 and 20 weeks in human fetuses), and the luminal space is conserved throughout life in the subsequent developmental stages, such as puberty, pregnancy, lactation and involution (Hogg, Harrison et al. 1983, Chen, Wei et al. 2021). The illustration was self-drawn based on the citations mentioned in this figure legend.

After birth and before adolescence, the mammary gland remains relatively quiescent (Lyons 1958). In adolescence, the ducts are elongated and branched from the terminal end buds (TEB), terminal structures rich in stem cells at the end of the ducts. The TEB extension to the mammary fat pad responds to the effect of estrogen, progesterone, and growth factors such as insulin-like growth factor-1 (Ruan and Kleinberg 1999, Bocchinfuso, Lindzey et al. 2000, Sternlicht, Kouros-Mehr et al. 2006). The new duct elongation is subdivided into alveoli that, together with the stroma and the ducts, make up the terminal duct lobular units (Ingthorsson, Briem et al. 2016). Organ maturation is reached around 18-20 years in adult nulliparous women (Javed and Lteif 2013). The following important changes in the mammary gland occur mainly due to the effect of prolactin and progesterone during pregnancy (Brisken, Park et al. 1998, Horseman

1999). Further branching and cell maturation occur in the duct lobular units to produce milk in the acini in the future lactation stage (Sternlicht, Kouros-Mehr et al. 2006). After lactation, a new remodelling process called involution occurs in the mammary gland. Marked apoptosis characterises this process to return the mammary gland architecture to the pre-pregnancy state (Walker, Bennett et al. 1989, Watson 2006). In general, the mammary gland undergoes different changes throughout life and can respond to stimuli such as growth factors and hormones that reshape its structure and physiology. In all these stages, a lumen structure is conserved.

Alterations in the gland structure characterise breast cancer, one of the main features being the loss of the apicobasal polarity and the reduction of lumen size. Generally, the luminal area in breast cancer is reduced due to its filling with cancer cells (Gudjonsson, Adriance et al. 2005, Kaushik, Pickup et al. 2016). Ductal or lobular breast tumour progression starts with ductal hyperplasia and atypical hyperplasia, characterised by the proliferation of monomorphic epithelial cells and some depolarised cells, leading to multilayering (Chatterjee and McCaffrey 2014). Further progression of breast cancer is characterised by lobular carcinoma in situ or ductal carcinoma in situ, which is categorised into low, intermediate, and high grade. Some of these lesions can lead to invasive ductal carcinoma and, subsequently, metastasis (Lukasiewicz, Czeczelewski et al. 2021).

In all the breast cancer stages, the lumen area or its structure becomes altered. Understanding more about the mechanisms and molecules involved in lumen formation and maintenance would provide information to understand better the

mammary gland organisation and thus understand the causes that underlie breast cancer development.

1.3 ECM AND INTEGRINS

The ECM is a three-dimensional macromolecular network composed of collagens, laminins, elastin, proteoglycans, nidogen, fibronectin, and other glycoproteins that provide a scaffold for cells and tissues (Byron, Humphries et al. 2013). In the mammary gland, the ECM participates in the transmission of signals and communication from the microenvironment to the cells that make up the gland. The ECM modulates cellular processes such as adhesion, movement, differentiation and communication with the microenvironment and surrounding cells through cell-ECM interactions (Grobstein 1967). The ECM complex is dynamic, playing an essential role in tissue remodelling and homeostasis, particularly during the involution stage and throughout the menstrual cycle (Schedin, Mitrenga et al. 2004, Atashgaran, Wrin et al. 2016).

Lumen formation is essential to build the functional network of tubes in the mammary gland, and this complex process is dependent on cell-ECM interactions. The integrins consist of a family of transmembrane glycoproteins that preferentially bind to the ECM components and facilitate communication between the extra- and intra-cellular environments, allowing homeostasis in the tissues (Wrighton 2013). These molecules comprise unique and specific heterodimer subunits (alpha and beta) with an intracellular domain, a globular extracellular domain, and an intramembrane domain. Integrins undergo conformational changes from the inactive to the active state,

increasing their affinity for ligands and, once coupled, produce a signal transmission. Activation mainly depends on the molecules that bind to its extracellular domains, representing the outside-in path. However, inside-out activation can also occur in response to the interaction with cytoplasmatic proteins or adaptors in the intracellular domain of the integrins (Luo, Carman et al. 2007, Sun, Costell et al. 2019) (Figure 1.3). The intracellular domain can associate with talin, vinculin, alpha-actinin, tensin and kinases, including focal adhesion kinase within focal adhesion complexes that bind to actin filaments. The extracellular domain binds to collagen, fibronectins and laminins, and the intramembrane domain has hydrophobic amino acids that allow its localisation in the lipid membrane(Hynes 1999, Luo, Carman et al. 2007).

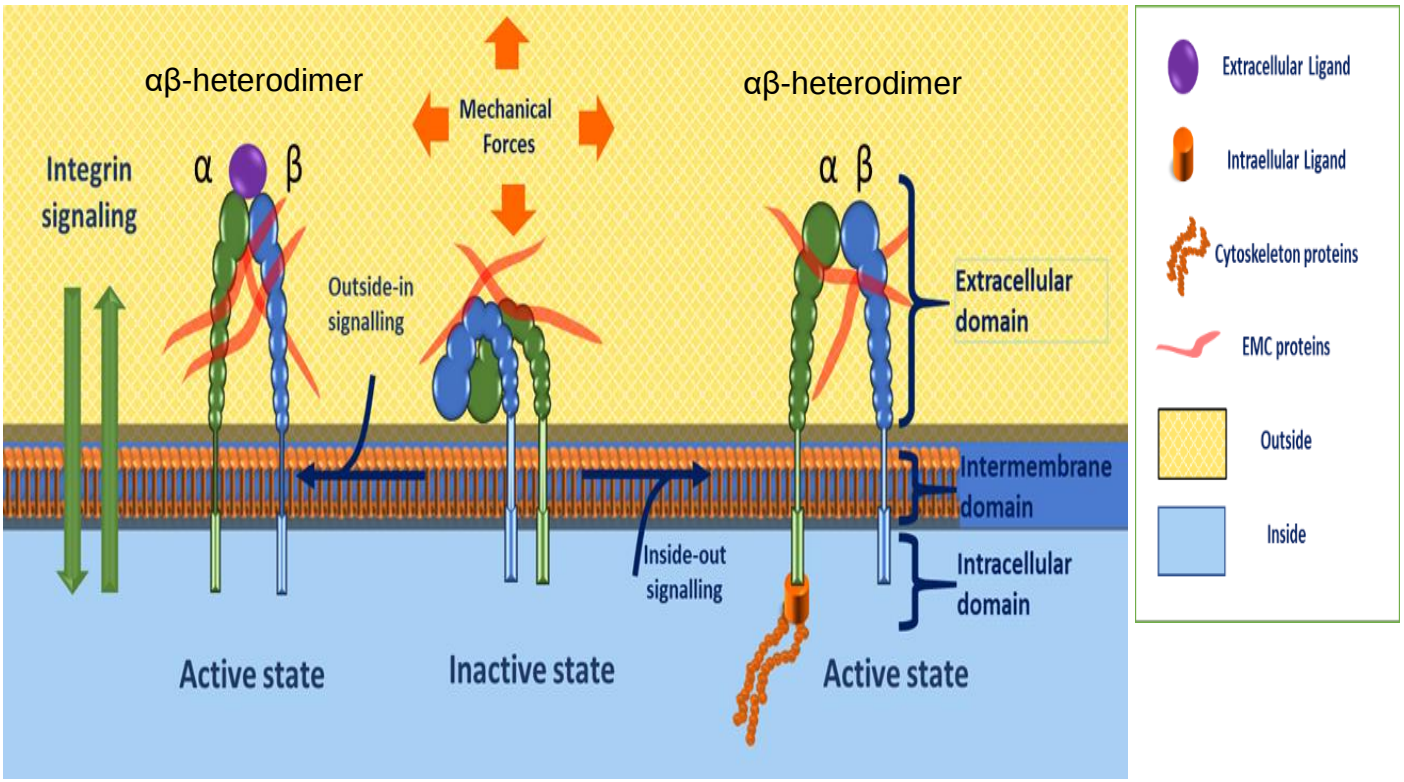

Figure 1.3. States of integrin activity. Integrins change their conformation from bent-closed/extended-closed to extended-open conformation to be activated. The activation signal can come from the outside-in or inside-out of the cells. Integrins interact with proteins in the

ECM such as collagen, fibronectins and laminins; in the cytoskeleton with talin, vinculin, alpha-actinin, and tensin that mediate the binding to the actin cytoskeleton that play an important role in the mechanotransduction (Sun, Costell et al. 2019). The illustration was self-drawn based on the citation mentioned in this figure legend.

There are 24 distinct integrin αβ-heterodimer combinations in mammals (Figure 1.4). The combination and prevalence of the integrins depend on the tissue type (Hynes 2002). In the mammary gland, the subunits α2, α3, α6, β1 are expressed on the luminal and myoepithelial cells, while the α1, α5, and av subunits are expressed only on the myoepithelial cells (Taddei, Faraldo et al. 2003).

β1 integrins are commonly expressed in the epithelial cells of different tissue types, playing an essential role in cell polarity and, consequently, in tissue organisation (Brakebusch, Grose et al. 2000, Aszodi, Hunziker et al. 2003, Schwander, Leu et al. 2003, Belvindrah, Graus-Porta et al. 2007, Nistico, Di Modugno et al. 2014). Deleting the β1 integrin gene in mice has severe consequences on cell adhesion to the BM and spatial arrangement of the cells in the early development after embryo implantation, proving its fundamental role in embryogenesis and morphogenesis (Fassler and Meyer 1995, Stephens, Sutherland et al. 1995, Kim, Sorokin et al. 2022). Also, β1 integrin expression in the mammary gland has been described as essential for maintaining the alveolar structure with a lumen in vivo (Li, Zhang et al. 2005, Naylor, Li et al. 2005).

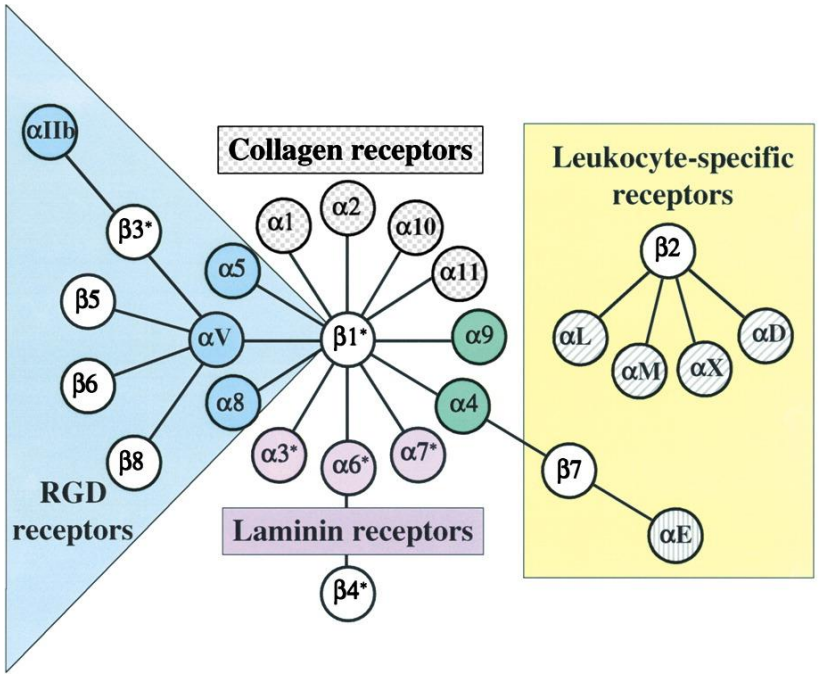

Figure 1.4. Heterodimer association of the integrins in mammals. 8 β subunits can be associated with 18 α subunits to form 24 different integrins. Figure adapted with permission from Cell, Hynes 2002 (see Appendix XV).

Changes in the expression level of the integrins have been associated with a malignant breast cancer phenotype. A high expression of the α2-β1 integrin was identified in normal breast tissue compared with adenocarcinoma tissue at protein and RNA levels (Zutter, Mazoujian et al. 1990, Zutter, Krigman et al. 1993). The Mm5MT cell line is a tumorigenic breast cancer cell line with low expression of α2-β1 integrins. The expression of α2-β1 integrins in the Mm5MT cell by means of expression vectors reduced its malignant and invasive phenotype, suggesting that α2 -β1 could function as a tumour suppressor (Zutter, Santoro et al. 1995). In addition, other studies have shown low β1 integrin expression in human breast cancer tissue (Pignatelli, Hanby et al. 1991, Jones, Critchley et al. 1992). However, the relationship between the expression of β1 integrin and breast cancer is not clear since some studies show that

the expression of β1 integrin is associated with breast cancer (Yao, Zhang et al. 2007, Klahan, Huang et al. 2016, Bui, Rennhack et al. 2019) and its inhibition in cell lines with β1 integrin function-blocking antibodies decrease the proliferation and increases apoptosis in breast cancer cells (Park, Zhang et al. 2006).

1.4 LUMEN FORMATION

The mammary gland is an interconnected system of tubes lined by polarised epithelia with a lumen space. The main function of a lumen in organs is to isolate a compartment for specific functions, such as digestion, or for the transport of fluids, nutrients, gases, and cells, or in the case of the mammary gland during lactation, for the transport of breast milk (Datta, Bryant et al. 2011).

The study of how a new hollow space or lumen is created is called *de novo* lumen formation (Sigurbjornsdottir, Mathew et al. 2014). Different mechanisms of *de novo* lumen formation have been described, including cell hollowing, cord hollowing, cavitation, budding, wrapping and, recently, the mechanism of fluid secretion to expand the microlumens to a single lumen (Iruela-Arispe and Beitel 2013, Sigurbjornsdottir, Mathew et al. 2014, Navis and Bagnat 2015). The budding mechanism is one of the described processes that occurred during the morphogenesis of the mammary gland. In vivo, mammary gland development originates as an epidermal placode that invades the mesenchyme and begins to branch and form microlumens (Figure 1.5). Polarised cells next to the microlumens express junctional complexes, and some non-polarised cells undergo apoptosis. Subsequently, the

microlumens expand to form a single lumen (Hogan and Kolodziej 2002). Another mechanism related to lumen formation in the mammary gland is the cavitation. Some studies *in vivo* and *in vitro* support the idea of necessary apoptosis in the central cells to form a lumen space (Hogan and Kolodziej 2002, Sternlicht 2006). Nevertheless, some studies in the mammary gland and *in vitro* maintain that cavitation is not the central mechanism for lumen formation (Martin-Belmonte, Yu et al. 2008, Pearson, Hughes et al. 2009, Akhtar and Streuli 2013).

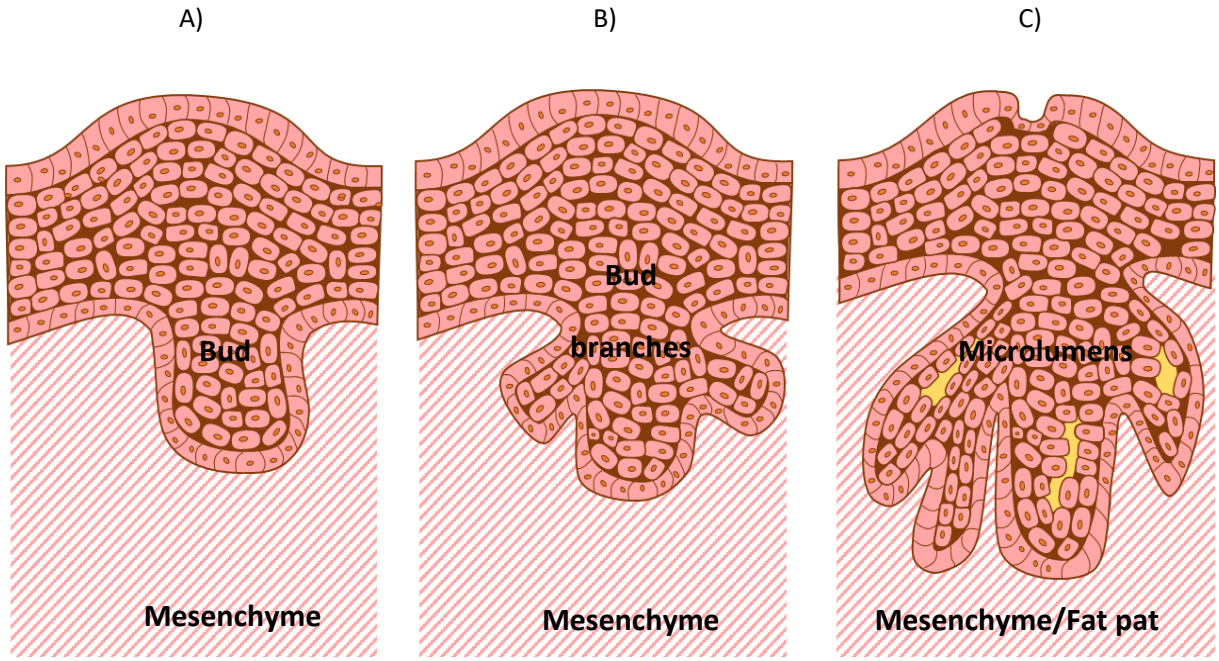

Figure 1.5. Lumen formation of the mammary gland during embryogenesis. A bud from the placode is formed and invades the mesenchyme. B) The primary mammary bud enlarges and branches to form secondary buds. C) The branching and elongation continue, and microlumens are formed to subsequently expand to a single lumen. Figures adapted from: Hogg, Harrison et al. 1983; Hogan and Kolodziej 2002; Javed and Lteif 2013. The illustration was self-drawn based on the citations mentioned in this figure legend.

The entire process and mechanisms necessary for lumen formation in the mammary glands are unclear. Despite some differences in the various mechanisms, it is clear that lumen formation requires a complex coordinate process that involves the

establishment of cell polarity (Bryant, Datta et al. 2010, Datta, Bryant et al. 2011), the orientation of the polar axis (Akhtar and Streuli 2013, Bryant, Roignot et al. 2014), the opening and expansion of micro lumens to a single lumen (Bagnat, Navis et al. 2010, Navis and Bagnat 2015) and the axis of cell division (Jaffe, Kaji et al. 2008, Gao, Yang et al. 2017) (Figure 1.6).

The expansion of the microlumens to a single lumen allows the tubular morphology of the mammary gland to develop. The fluid secretion mechanism proposes how a single lumen is formed and maintained through the secretion of water to the apical zone. The secretion of fluids to the luminal area can come from transcellular or paracellular fluid transport caused by the osmotic gradient produced by ion transporters (Figure 1.6 C). The fluid accumulation on the apical zone generates a hydrostatic pressure favouring expansion of the micro lumens to a single and continuous lumen. This mechanism has been observed in various models such as zebrafish to 3D culture of mammalian cells, including primary prostatic cells and Madin-Darby canine kidney (MDCK) cells (Bagnat, Cheung et al. 2007, Pearson, Hughes et al. 2009, Narayanan, Schappell et al. 2020).

Cell-ECM interactions are also important for establishing the lumen. An example of this is β1 integrin, which participates in the establishment of cell polarity and polarity orientation axis (Martin-Belmonte, Yu et al. 2008, Pearson, Hughes et al. 2009, Zovein, Luque et al. 2010, Akhtar and Streuli 2013).

Currently, it is unknown whether the fluid secretion mechanism for lumen formation occurs in the mammary gland and also which molecules are involved in regulating the

osmotic gradient or the cell-ECM interactions. Understanding the forces and molecules involved in the lumen formation and maintenance could provide valuable information about the organisation of the mammary gland and, with it, a better understanding of the processes that accompany the lumen changes in breast cancer development.

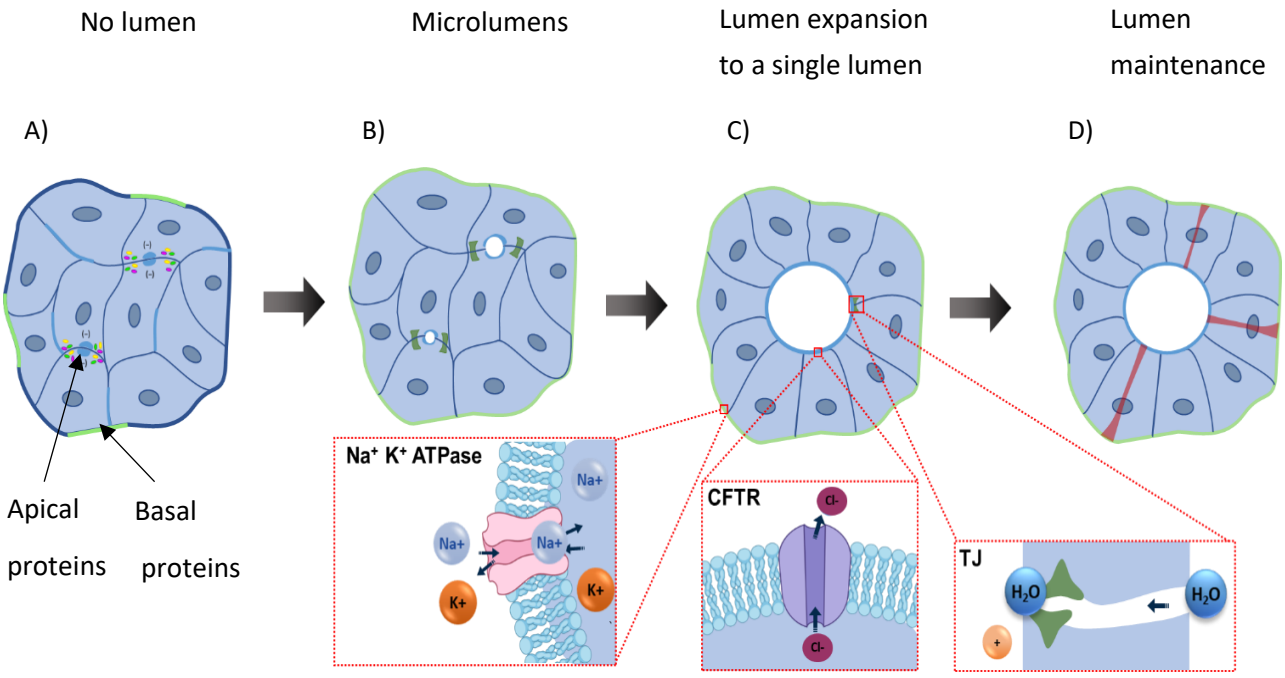

Figure 1.6. Model of lumen formation *in vitro*. A) Establishment of the apical polarity. Apical proteins are transported to the apical membrane (Bryant, Datta et al. 2010, Datta, Bryant et al. 2011). B) The orientation of the polarity axis. Positioning of the apical and basolateral membranes relative to the ECM occurs, and micro lumens appear (Akhtar and Streuli 2013, Bryant, Roignot et al. 2014). C) Fluid secretion mechanism. Fluid transport to the new lumen area occurs in response to an osmotic gradient in the apical zone triggered by the activity of ion transporters such as CFTR (Bagnat, Navis et al. 2010, Navis and Bagnat 2015). Lumen expansion by fluid accumulation occurs, and a single lumen is formed. D) Cell division axis orientation. The positioning of the new daughter cells also defines the lumen structure. The microtubules guide the protein transport to the cell membranes. The polarity after cell division maintains the lumen structure (Jaffe, Kaji et al. 2008, Gao, Yang et al. 2017). The illustration was self-drawn based on the citations mentioned in this figure legend.

1.4.1 Establishment of the apicobasal polarity axis

In the mammary gland, luminal cells have an asymmetric distribution of proteins that determines the apical and basolateral domains. The apical membrane of luminal cells faces the lumen space. The luminal epithelial cells are bound laterally by adherent junctions (AJs) and TJs, which are essential to separate the apical domain that is orientated to the lumen of the duct and the basolateral domain that contacts the myoepithelial cell layer or the BM (Biswas, Banerjee et al. 2022). The first step in establishing a tissue architecture with a lumen space involves cell polarisation and the orientation of an apical membrane next to the lumen (Bryant and Mostov 2008).

An essential set of proteins is required to establish and maintain the cell polarity in epithelia. The three major complexes of proteins that define the cell polarity are made up of: (i) the Crumbs complex (Crb, Pals1 and PATJ) located at the apical membrane, (ii) the Par complex (Par3, Par6 and atypical protein kinase C or aPKC) situated at the TJ, and (iii) in the basolateral side the Scribble complex (Scribble, Dlg and Lgl or Hugl1 and Hugl2 in humans) (Figure 1.7A) (Halaoui and McCaffrey 2015, Rejon, Al-Masri et al. 2016). Depletion of the components of the Scribble complex in the human mammary epithelial cells MCF10A and primary lung epithelial cells affects polarity, increases cell proliferation (in the MCF10A cells), and precedes defects in the lumen structure and its morphogenesis (both cells) (Russ, Louderbough et al. 2012, Yates, Schnatwinkel et al. 2013). Moreover, KD of Par3 in mouse primary MECs induces multilayering in the mammary ducts and alters the proliferation and apoptosis processes (McCaffrey and Macara 2009). In human colorectal adenocarcinoma cells, Caco-2, the KD of Par6 misorients the mitotic spindle, affecting three-dimensional

lumenogenesis (Durgan, Kaji et al. 2011). The Par6 proteins interact directly with aPKC, and this interaction protects Par6 from proteasomal degradation. Both proteins are indispensable for apical membrane development (Horikoshi, Suzuki et al. 2009, Durgan, Kaji et al. 2011). Par6, also interacts with Par3 and Cdc42 proteins during the cell polarisation process. Cdc42, a monomeric GTPase, regulates the interaction of Par3/6 with the TJs, promoting the formation of the apical membrane. In addition, Cdc42 is associated with cell polarisation by controlling microtubule orientation and mitotic spindle, actin polymerisation, and apical endosome transport processes (Blasky, Mangan et al. 2015).

The TJs are not only a reference of cell polarity but also constitute a barrier and transport system in cells. The TJ complex comprises occludins, claudins, binding adhesion molecules (JAM) and linker proteins from the Zonula Occludens (ZO) family. They are a selective barrier which mediates the transport of molecules through the paracellular space, constituting the paracellular transport of ions and solutes (Farquhar and Palade 1963, Anderson and Van Itallie 2009). The AJs are located under the TJs and consist of cadherins, catenins, nectin and afadin. They provide cohesion between epithelial lamina cells and communication of intracellular signals (Gumbiner, Stevenson et al. 1988, Hartsock and Nelson 2008).

Collectively, the three major polarity complexes (Crumbs, Pax and Scrib complex) are key regulators that establish the position and segregation of proteins into the basolateral and apical membrane, thus the location of proteins that face the lumen space. This protein positioning on the cells is carried out by the Rab vesicle transport using two routes: (i) the Biosynthetic Pathway and Recycling and (ii) the Recycling

Pathway Endosome (Grant and Donaldson 2009). Prior to lumen formation, the transport of proteins to the apical membrane occurs via Rab8-Rab11, which is coordinated by the network of activated Cdc42, Par6, aPKC and Par3 proteins. The exocytosis of proteins to the apical membrane promotes the apical membrane initiation site formation (Martin-Belmonte, Gassama et al. 2007, Bryant, Datta et al. 2010). One of the essential cargos for the apical membrane through vesicles mediated by Rab11 (Rab11+ AREs) is the CFTR ion channel, which is expressed on the apical membrane of polarised epithelia and is known to support lumen formation (Bidaud-Meynard, Bossard et al. 2019, Rathbun, Colicino et al. 2020). Furthermore, microtubules also cooperate to define cell polarity by controlling the vesicular trafficking of proteins to the apical and basolateral membranes. The microtubules act as routes to the trafficking of the proteins (Jewett and Prekeris 2018).

The polarity components can also be regulated with direct or indirect interactions by some components of the cell-ECM complex through integrins. A relationship between the expression of β1 integrin and Par3 in endothelial cells has been shown. When the expression of β1 is deleted, the expression of Par3 is decreased, and with this, the polarisation capacity of the endothelial cells, along with lumen formation, is lost (Figure 1.7B) (Zovein, Luque et al. 2010).

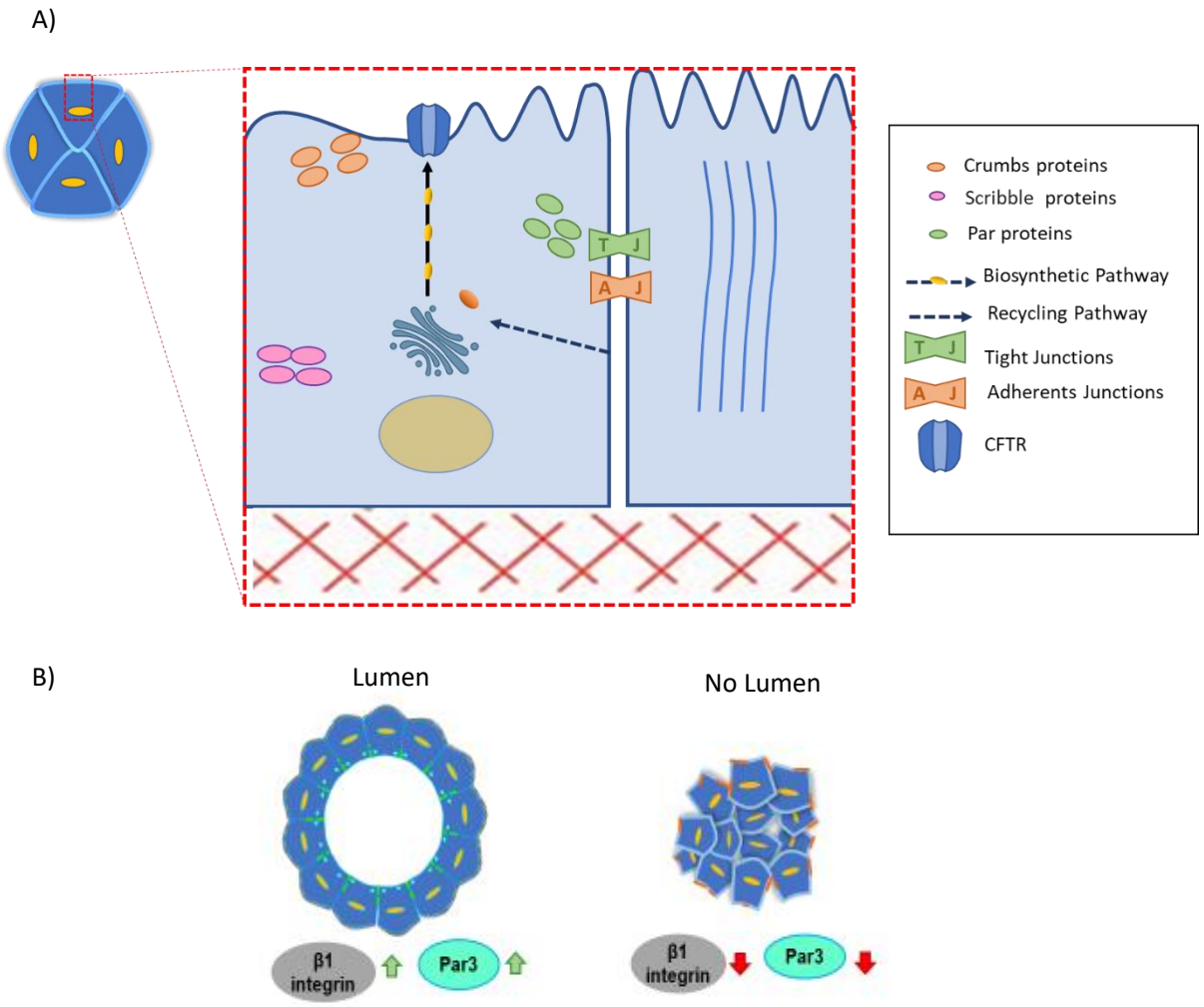

Figure 1.7. Cell polarisation. a) The Scribble proteins are localised in the basolateral membrane, the Crumbs proteins in the apical membrane and the Par proteins near the TJs in epithelial cells. The protein transport for the establishment of polarity is carried out through biosynthetic and recycling pathways (Grant and Donaldson 2009). Scaffolding proteins of the TJs and AJs complexes are transported and spatially positioned to form the scaffolding for their establishment on the membranes (Halaoui and McCaffrey 2015, Rejon, Al-Masri et al. 2016). CFTR is produced and transported to the apical membrane. b) Ablation of β1 integrin expression results in the decreased expression of Par3 in endothelial cells (Zovein, Luque et al. 2010). The illustration was self-drawn based on the citations mentioned in this figure legend.

1.4.2 The orientation of the polarity axis

The cell polarisation of the mammary epithelium is necessary but not sufficient for the formation of the lumen. Each polarised cell must be oriented correctly along with the other cells of the mammary gland to establish a specific geometry and favour the formation and maintenance of the lumen. In the mammary gland, the luminal cells are orientated in a way that the secretory apical surface is placed towards the luminal space and the basolateral surface towards the BM. Some signals necessary to generate correct cell orientation and promote lumen formation come from the ECM; indeed, the interaction of cells with the ECM has been described as a prerequisite in some 3D cell model systems (Weir, Oppizzi et al. 2006, Datta, Bryant et al. 2011). Matrices used to support 3D cell cultures have ECM-rich components in which epithelial cells organise into glandular architecture, allowing examination of the molecular mechanisms related to the orientation of epithelial cysts during their formation.

An epithelial cyst or acini is an organised form of polarised cells where a spherical monolayer of epithelia surrounds a luminal space. The basal surface of the cells is oriented to a BM, and the lateral surface is in contact with neighbouring cells (Zeng, Ferrari et al. 2006). The communication with the cell-ECM is essential for cyst structure. Defects related to the lack of transmission of signals from the ECM to the cells can cause polarity inversion. The apical cell membrane contacts the outside of the cyst, and the basement membrane is oriented towards the central lumen without losing the apicobasal polarity of each cell (Monteleon, Sedgwick et al. 2012). The

correct epithelial orientation enables cells to secrete their products into the lumen space, for example, milk secretion in the mammary gland.

In mammary luminal epithelial cells, β1 integrins are primarily necessary to orient the cell polarity axis such that the apical membrane is positioned next to the lumen space. The genetic deletion of β1integrin in luminal mammary epithelial cells results in apical polarity inversion and the absence of a luminal space (Naylor, Li et al. 2005). The interaction of MECs with BM through β1 integrin is essential for intercellular signalling through ILK that allows the correct position of the lumen. The β1 integrin deletion also affects the Golgi position in MECs, thus affecting the polarised traffic of proteins to the membrane that determines the epithelial orientation and the lumen side. Golgi positioning can be controlled by microtubules that can interact with β1 integrin through EB1 protein, which forms a complex with β1 integrin on the basal surface of the acini (Akhtar and Streuli 2013). However, it is not known what exact role β1 integrin has in lumen opening and expansion.

Once the lumen is formed, the next process is expansion (Mailleux, Overholtzer et al. 2007, Yokoyama, Chen et al. 2007, Datta, Bryant et al. 2011). The mechanism by which micro lumens are formed in the cyst and how they expand to form a single lumen with the appropriate form is not yet completely understood. One of the proposed mechanisms is the transport of ions and fluids in the luminal space, which creates hydrostatic pressure that favours the expansion of the lumen (Navis, Marjoram et al. 2013, Alvers, Ryan et al. 2014, Navis and Bagnat 2015). Another critical factor in the expansion of the lumen is cell proliferation. This must be determined by a cell division axis that will determine the positions of the new cells; in turn, this will determine the

organisation of tissue and its homeostasis. Efficient coordination of cell proliferation and cell polarisation for lumen formation is therefore essential (Andrew and Ewald 2010, Rathbun, Colicino et al. 2020).

1.4.3 Fluid secretion mechanism

The fluid secretion mechanism involves the formation of micro lumens that expand to a single lumen by the secretion of fluid to the apical zone. The fluid displacement into the luminal space responds to an osmotic gradient generated due to the transport of ions to the apical zone by activated protein transporters. (Wilson, Olver et al. 2007, Frizzell and Hanrahan 2012). One example is ATP hydrolysis by Na^+/K^+-ATPase that generates an electrochemical gradient maintaining higher concentrations of potassium intracellularly and sodium extracellularly, triggering the indirect activation of other ion transporters that creates an osmotic gradient resulting in fluid secretion and fluid transport by the epithelial cells (Frizzell and Hanrahan 2012).

The mammary gland is an exocrine gland whose physiological function is to secrete milk into an interconnected system of tubes. The salivary gland is also an exocrine gland with a tubular shape that exhibits a fluid secretion model. Fluid secretion in the salivary gland involves osmotic gradients that arise from the hydrolysis of ATP by Na^+/K^+-ATPase, producing a sodium gradient that releases 3 Na^+ to the extracellular medium and takes $2K^+$ to the intracellular compartment, resulting in an electrochemical gradient of 10–15-fold into the cell (Foskett 1990, Tanimura and Tojyo 2006). This driven force triggers the transport of Cl^- through cotransporters and exchangers such

as Na^+-K^+-$2Cl^-$ and Cl^- / $HCO3^-$(Evans, Park et al. 2000). Subsequently, some Cl^- and K^+ ion channels are activated to secrete ions in their corresponding compartments. One of these activated channels is CFTR, which secretes Cl^- from the apical membrane to the apical zone (Nauntofte and Dissing 1988, Frizzell and Hanrahan 2012, Navis, Marjoram et al. 2013). The chlorine transport into the lumen generates an electrical potential difference that favours the passive transport of cations across the TJs. The result is the accumulation of ions in the space outside the apical region of the cells, which causes water to be transported to that area to balance the ion concentration gradient (Almassy, Siguenza et al. 2018). The water movement to the lumen area can come from paracellular transport through the TJs or by transcellular transport through aquaporins (AQ) present in the apical membrane (Ma, Song et al. 1999) (Figure 1.8).

The accumulation of fluids and its nature of low compressibility in the limited area of micro lumens allow the creation of a hydrostatic pressure that can exert a force on the surrounding cells and favours the opening and expansion of the micro luminal spaces to a single one (Navis, Marjoram et al. 2013, Navis and Bagnat 2015) (Figure 1.9). The fluid pressure creates a difference between the external and internal mechanical forces in the cells that can generate spatial patterns and influence local growth behaviours. The importance of the fluid secretion mechanism has been related to tubulogenesis in different organisms. In the intestines of zebrafish, fluid accumulation has been reported to promote lumen coalescence to a single lumen in the intestinal bulb (Alvers, Ryan et al. 2014). The fluid transport into the intestinal lumen is regulated by claudin 15, a component of TJs and the activity of the Na^+/K^+-ATPase (Bagnat, Cheung et al. 2007).

A)

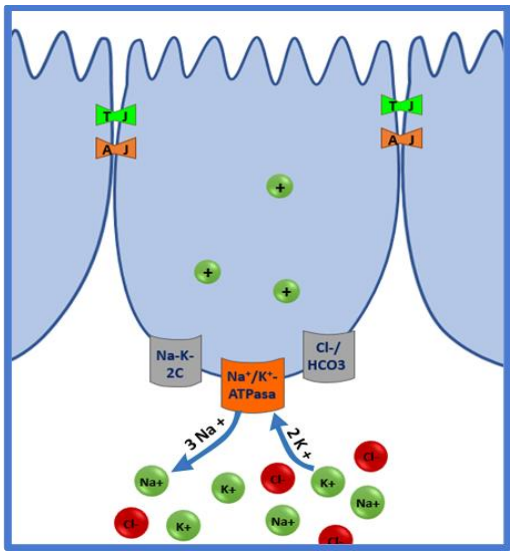
T J
A J
Na-K-2C
Na+/K+-ATPasa
Cl-/HCO3
3 Na+
2 K+
Na+
K+
Cl-

B)

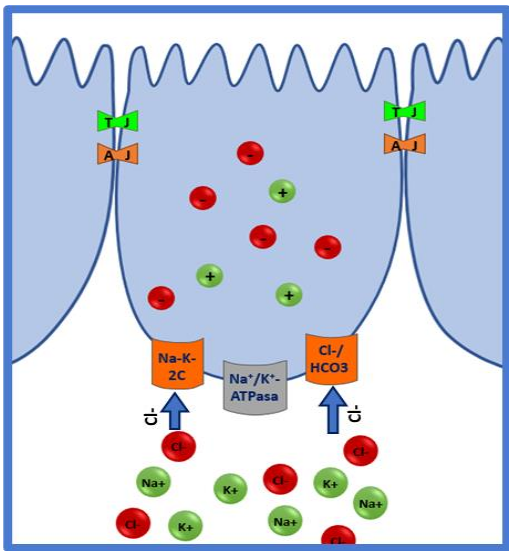
T J
A J
Na-K-2C
Na+/K+-ATPasa
Cl-/HCO3
Cl-
Na+
K+

C)

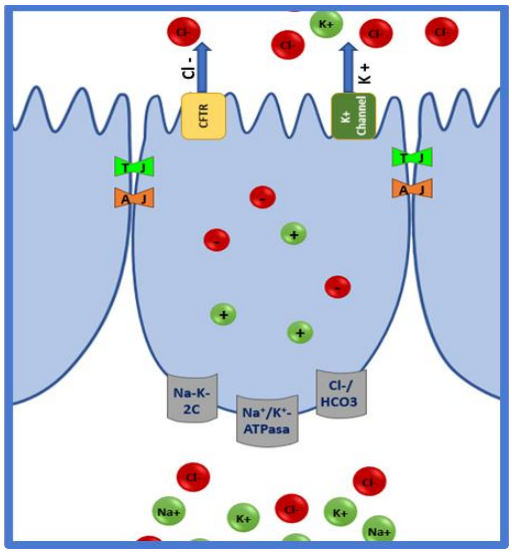
Cl -
K +
CFTR
K+ Channel
T J
A J
Na-K-2C
Na+/K+-ATPasa
Cl-/HCO3
Cl-
Na+
K+

D)

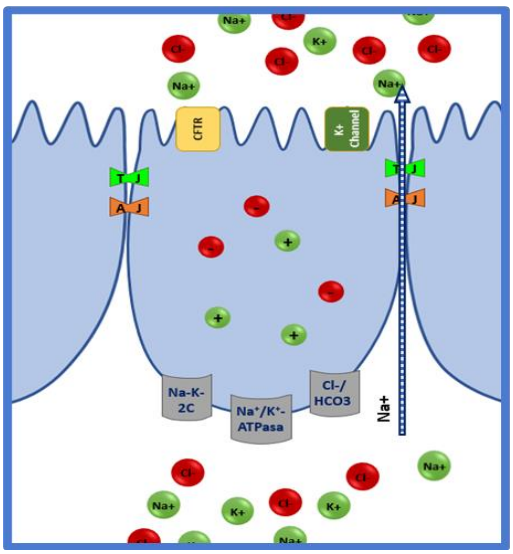
CFTR
K+ Channel
T J
A J
Na-K-2C
Na+/K+-ATPasa
Cl-/HCO3
Na+
Cl-
K+

E)

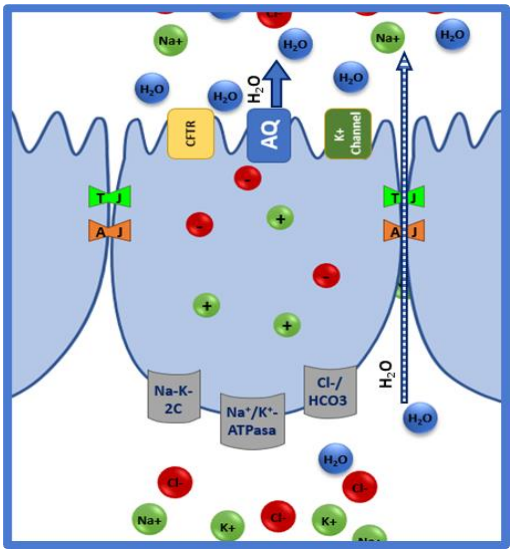
H2O
AQ
CFTR
K+ Channel
T J
A J
Na-K-2C
Na+/K+-ATPasa
Cl-/HCO3
Na+
Cl-
K+

Figure 1.8. Fluid secretion mechanism in the epithelial cells of the salivary gland. A) An electrochemical gradient is generated by the activity of the Na^+/K^+ pump, which introduces to the cell 2 K^+ and excludes 3 Na^+ (Palk, Sneyd et al. 2010, Almassy, Siguenza et al. 2018). B) Chlorine transporters such as Na^+-K^+-2Cl^- and $Cl^-/HCO3^-$ are activated and introduce Cl^- into the cell (Evans, Park et al. 2000, Palk, Sneyd et al. 2010). C) The flow of ions into the cell and its concentrations triggers the activation of other ion transporters, such as the CFTR ion channel that secretes Cl^- from the apical membrane to the apical zone/lumen space (Palk, Sneyd et al. 2010, Frizzell and Hanrahan 2012). D) The secretion of Cl^- and anions to the apical membrane triggers the transport of cations to the apical membrane. The Na+ is transported by the TJs to the apical zone (Palk, Sneyd et al. 2010, Frizzell and Hanrahan 2012). E) The accumulation of ions in the apical zone creates an osmotic gradient that drives paracellular and transcellular fluid transport. The paracellular transport of fluids occurs by the TJs and the transcellular by the aquaporins (Ma, Song et al. 1999, Palk, Sneyd et al. 2010). The illustration was self-drawn based on the citations mentioned in this figure legend.

Although the mechanism of fluid secretion has been described in tubulogenesis in vivo in some organisms and in some in vitro models with mammalian cells, it is unknown whether fluid secretion to the luminal area is a mechanism that occurs during the formation of a single lumen and its maintenance in MECs. Understanding the mechanism and molecules that remodel the lumen in the mammary gland will provide a better understanding of the complex signalling underlying shifts in lumen in breast cancer.

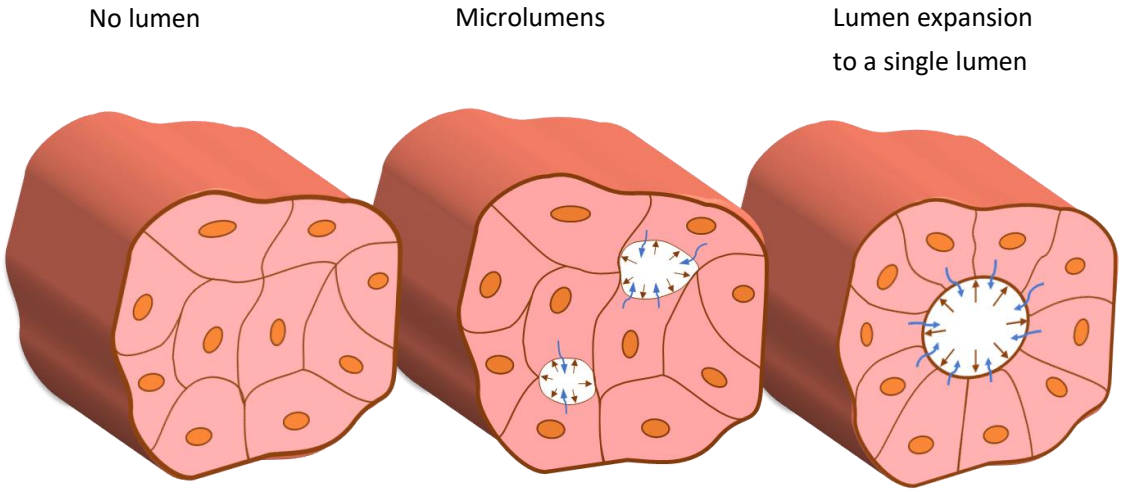

Figure 1.9. Single lumen formation by the influence of fluid secretion in tubular organs. The membranes of two cells separated create a free space of cells, and the fluid secretion and its accumulation in a delimited area create a hydrostatic pressure. The hydrostatic pressure favours the expansion of the micro lumens to a single lumen (Navis, Marjoram et al.

2013, Navis and Bagnat 2015). The illustration was self-drawn based on the citations mentioned in this figure legend.

1.4.4 Cell division axis

The maintenance of the tissue structure also depends on the polarity of the cells that compose the tissue and the polarity of the daughter cells that will compose it. Therefore, the cell division axis is critical to maintaining the architecture of the tissue and lumen structures.

During cell division, the mitotic spindle is formed, and this complex, made of microtubules, kinetochores and centrosomes, guides chromosome segregation (Prosser and Pelletier 2017). The microtubules of the spindle complex connect to the cell cortex, and their alignment is not only important for chromosome segregation but also for the control of protein distribution to cell membranes. The microtubules drive the intracellular traffic of endosomes to the apical or basolateral membrane (Overeem, Bryant et al. 2015, Bergstralh, Dawney et al. 2017). The physical translocation of proteins to the correct domain before and after cell division is crucial for the establishment of cell polarity and cell polarity orientation. Between the G2 and M phases of the cell cycle, the degree of cellular remodelling and redistribution of proteins to the plasma membrane and cytoplasm occurs to ensure the cell division and the cell polarity of the daughter cells are faithfully maintained (Thery and Bornens 2006). This cell organisation during the cell division determines the position of specific apical proteins such as CFTR near the nascent or established lumen (Kravtsov and Ameen 2013, Bidaud-Meynard, Bossard et al. 2019).

3D epithelial cell culture studies have shown that cell division is oriented perpendicularly to the apicobasal axis, where mitotic spindle accommodation favours the generation of daughter cells that properly align their apicobasal axis toward the lumen (Gao, Yang et al. 2017). The orientation of the mitotic spindle is initially controlled by polarity proteins of the Par complex and Cdc42 proteins that control the spindle position for the nascent apical surface. One example is the interaction of Par3 and Par6/aPKC and Cdc42, where the disturbance of these proteins causes the formation of multiple apical lumens in epithelial cells (Horikoshi, Suzuki et al. 2009, Durgan, Kaji et al. 2011). Other protein interactions that define the mitotic spindle orientation are Par3-LGN proteins and LGN (Leu-Gly-Asn repeat-enriched)-NuM (nuclear mitotic apparatus)-Gαi (heterotrimeric G-protein) proteins. The LGN-NuMA-Gαi interaction captures astral microtubules in the cell cortex, reinforcing the correct spindle orientation, representing a link between polarity and the microtubule orientation (Zhu, Wen et al. 2011). In addition, LGN, NuMA and aPKC proteins are related to the ECM interactions. It has been observed these components are delocalised in cells where the expression of β1 integrin is lost. Loss of β1 integrin causes an aberration in the mitotic spindle orientation, leading to loss of orientation in the daughter cells. Mitotic spindles are usually oriented parallel to or perpendicular to the BM; however, cells lacking expression of β1 integrin show a random orientation (Baena-Lopez, Baonza et al. 2005, Fernandez-Minan, Martin-Bermudo et al. 2007).

1.5 CFTR

1.5.1 CFTR structure and fluid secretion function

The CFTR gene is located on the long arm of chromosome 7 in humans and in chromosome 6 in mice. The gene encodes a protein of 1,480 (human) and 1,476 (mice) amino acids, which is exported to the apical membrane of epithelial cells to form an anion channel (Harris and Argent 1993). The CFTR protein comprises two transmembrane domains (TMD1 and TMD2), two cytosolic nucleotide-binding domains (NBD1 and NBD2), one regulatory domain (RD) and one PDZ domain connected to the cytoplasm (Harris and Argent 1993, Zhang, Liu et al. 2018).

Activation of CFTR occurs through the phosphorylation of the R domain by the cAMP-dependent protein kinase (PKA). The gating pore activity depends on the ATP binding to the NBDs domains (Figure 1.10). The channel gate opening occurs by the binding of cytoplasmic ATP to the NBDs domains, causing dimerization of the two NBDs and a conformational change. The closing of the channel gate occurs after ATP hydrolysis (Berger, Travis et al. 1993, Vergani, Nairn et al. 2003, Moran 2017).

The CFTR ion channel belongs to the ATP-binding cassette (ABC) superfamily of transporters. CFTR transports chloride and bicarbonate across the apical membrane, modifying the ion gradient and modulating the activity of other ion channels, such as the epithelial sodium channel (ENaC) (Reddy, Light et al. 1999). Given the role of CFTR in regulating the ion concentration, an ion gradient is created near the apical surface of epithelial cells. This condition triggers fluid secretion and water transport towards the apical section where the lumen is or will be formed. The proper control of fluid transport by CFTR has been described as necessary for epithelial homeostasis and the correct function of organs that physiologically require fluid secretion (Hug, Tamada et al. 2003).

In the salivary gland, the fluid secretion force comes from the transepithelial movement of ions such as Cl^-(Melvin 1999). CFTR is one of the ion channels that contributes to the Cl^- concentration in the luminal area and generates the electrical driving force for the transport of Na^+ through the TJs. The increasing ion concentration in the lumen area drives the fluid transport by the paracellular pathway through the TJs and fluid secretion by transcellular pathways through aquaporins (Foskett 1990, Melvin 1999, Palk, Sneyd et al. 2010, Frizzell and Hanrahan 2012, Almassy, Siguenza et al. 2018). Likewise, the mammary gland is also an exocrine gland, and both share similarities, including the embryological origin and a system made up of acini and ducts. In addition, the main function of the mammary gland during lactation is related to the production and secretion of fluid, the milk. Thus, the mammary epithelium must be in balance between secretion and absorption of fluids to maintain the lumen. Therefore, the mechanism of fluid secretion in the salivary gland could represent a reference for the secretion in the mammary gland.

As was previously mentioned, CFTR is a key regulator of fluid secretion in epithelial cells, and it has been reported that this ion channel regulates fluid secretion in the 31EG4 mouse cells, a non-transformed mammary epithelial cell line. Changes in the transepithelial fluid movement were observed after the CFTR activation using a cAMP-elevating cocktail in 31EG4 cells cultured on chambers. The change was from absorption (3.5 $\mu l \cdot cm^{-2}\ h^{-1}$) to secretion ($-3.0\ \mu l\ cm^{-2}\ h^{-1}$) (Blaug, Hybiske et al. 2001). However, although the expression of CFTR is known to be expressed in human breast tissue and some mammary cell lines (Blaug, Hybiske et al. 2001, Zhang, Jiang et al. 2013, Liu, Dong et al. 2020), its function is very poorly studied in this context.

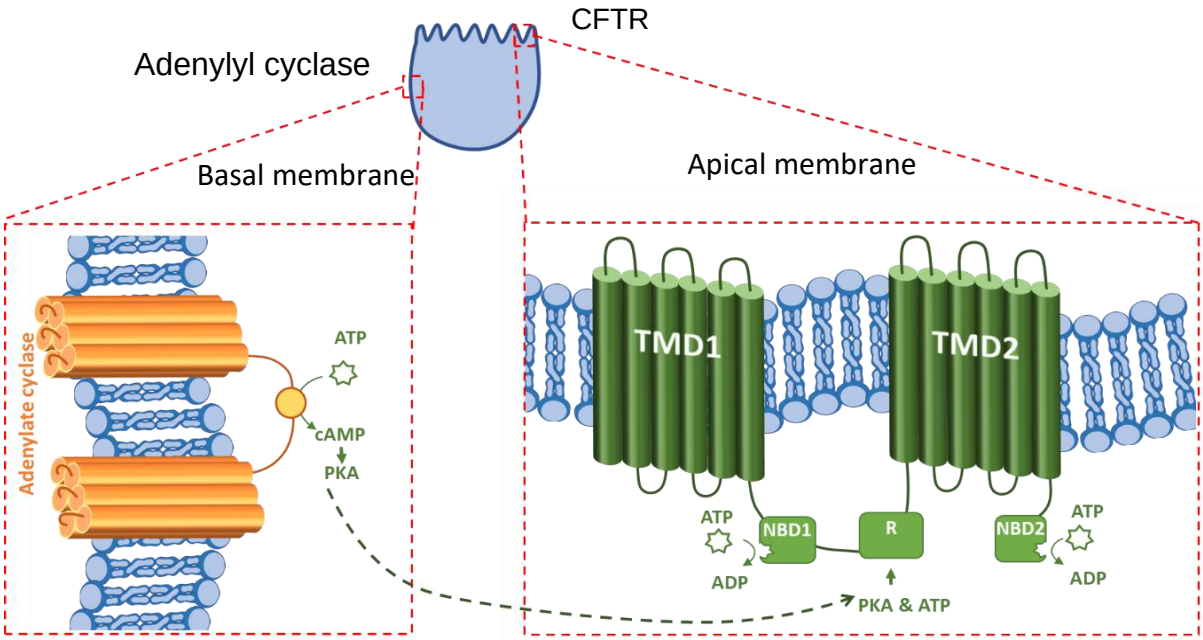

Figure 1.10. The CFTR transmembrane ion channel is located at the apical membrane of epithelial cells. CFTR is composed of two TMD membrane-spanning domains, two NBD nucleotide-binding domains, and one R domain (Harris and Argent 1993, Zhang, Liu et al. 2018). Activation of CFTR is dependent on the activity of the enzyme adenylyl cyclase, which is localised on the basolateral membrane and will activate PKA with cAMP to phosphorylate the R domain. ATP molecules interact with the NBD1 and NBD2 domains to form a strong heterodimer that changes the CFTR conformation, allowing the ion channel to open and Cl^- transport (Berger, Travis et al. 1993, Vergani, Nairn et al. 2003, Moran 2017). The illustration was self-drawn based on the citations mentioned in this figure legend.

1.5.2 CFTR in morphogenesis

Besides the fluid secretion role of CFTR for homeostasis in some organs, its fluid secretion function also plays an important role during tissue morphogenesis (Figure 1.11). Studies *in vivo* in the zebrafish model linked the activity of this ion channel with the lumen expansion in the gut and Kupffer vesicle during embryogenesis; more specifically, loss of CFTR expression or reduction of its activity affects fluid secretion and, as a consequence, the lumen size. By comparison, the activation of CFTR causes fluid accumulation in the lumen area, resulting in an evident lumen expansion (Bagnat, Cheung et al. 2007, Bagnat, Navis et al. 2010).

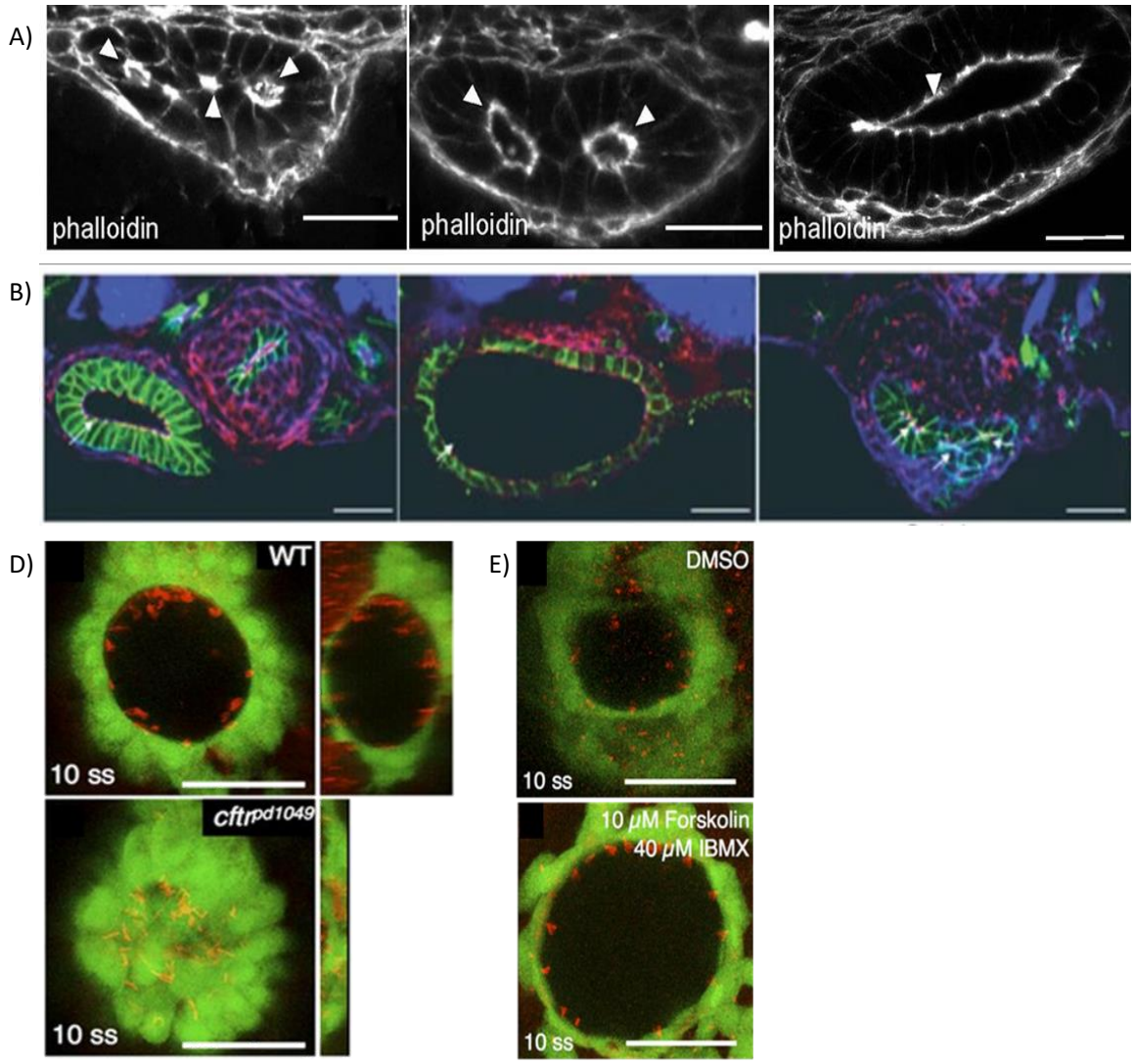

Figure 1.11. Importance of CFTR normal expression and its activity for tubulogenesis in vivo. A) Time course confocal images of single lumen morphogenesis in zebrafish intestine. The cross sections of the zebrafish's intestines were stained with phalloidin, showing a single lumen formed from microlumens. Scale bar of 20μm. Figure adapted with permission from The Company of Biologists, Alvers, Ryan et al. 2014 (see Appendix XVI). B) Confocal images of the gut lumen in zebrafish embryos after the treatment with DMSO (control), Forskolin or Ouabain. The lumen area is bigger after the Forskolin treatment, which activates CFTR and the Na^+/K^+ pump; Ouabain inhibits the Na^+/K^+ pump activity. In red are the ZO-1 proteins; in green are the Cadherin proteins; and in blue are the F actin proteins. Scale bar of 20μm. Figure adapted with permission from Nature Cell Biology, Bagnat, Cheung et al. 2007 (see Appendix XVII). C) Kupffer vesicle images by DIC microscopy of wild-type and CFTR mutant (no functional CFTR) zebrafish. D) Kupffer vesicle after the treatment with Forskolin or DMSO (control). The green signal is for the Tg (sox17:GFP) expression, and Arl13b-mCherry is for positive cilia. Figure adapted with permission of The Company of Biologists, Navis, Marjoram et al. 2013 (see Appendix XVIII).

The importance of CFTR expression is crucial for the normal development of some tubular organs in different organisms. It has been shown that CFTR is critical for the normal tubulogenesis of the trachea (Ornoy, Arnon et al. 1987, Bonvin, Le Rouzic et al. 2008, Meyerholz, Stoltz et al. 2018), lungs (Ornoy, Arnon et al. 1987, Cohen and Larson 2006, Meyerholz, Stoltz et al. 2018), pancreas (Ornoy, Arnon et al. 1987) and gut (Ornoy, Arnon et al. 1987) and its expression is greater during the embryonic development than the adult stage (Broackes-Carter, Mouchel et al. 2002, Cohen and Larson 2006). However, the role of CFTR in lumenogenesis in the mammary gland has not been described.

1.5.3 Cystic Fibrosis

Cystic fibrosis (CF) is an autosomal recessive disease in which CFTR is mutated, affecting its normal production or function. Since the discovery of the CFTR in 1989 and its association with CF (Riordan, Rommens et al. 1989), more than 2500 mutations have been described in CF patients and CFTR-related disorders (Johns Hopkins cystic fibrosis centre, https://hopkinscf.org/). Although CF is a monogenic disease, the type of mutations in the CFTR gene characterises the phenotype and functionality of this protein. The mutations associated with CF have been classified into 6 groups (Class I-IV) according to the molecular defect of CFTR and the functional consequence (Figure 1.12). Class I is related to the lack of expression of CFTR given by mutations that lead to no protein synthesis. Class II is associated with mutations that affect the processing, misfolding and trafficking of CFTR protein. Class III is linked to mutations that affect the ATP binding at the NBD sites of CFTR, causing abnormal pore gating. Class IV is related to mutations that alter channel structure, reducing the

ion conductance. Class V is associated with mutations that alter protein synthesis and abundance. Class VI mutations are related to the instability of the CFTR ion channel in the ER compartments or the plasma membrane after its synthesis (Veit, Avramescu et al. 2016, Deletang and Taulan-Cadars 2022).

The study of the CFTR variants and their cellular manifestations helped to correlate the CFTR dysfunction and the clinical features in CF patients (Figure 1.12). The deletion of the phenylalanine 508 (ΔF508), which is classified as a class II type mutation, is the most common mutation reported in CF patients (more than 88% of prevalence) (Deletang and Taulan-Cadars 2022). The loss of the phenylalanine 508 causes inappropriate CFTR protein folding, leading to its degradation after the quality control post-endoplasmic reticulum. Mutant ΔF508 proteins that reach the plasma membrane have reduced half-life compared to normal CFTR (Lukacs, Chang et al. 1993, Borthwick, Botha et al. 2011).

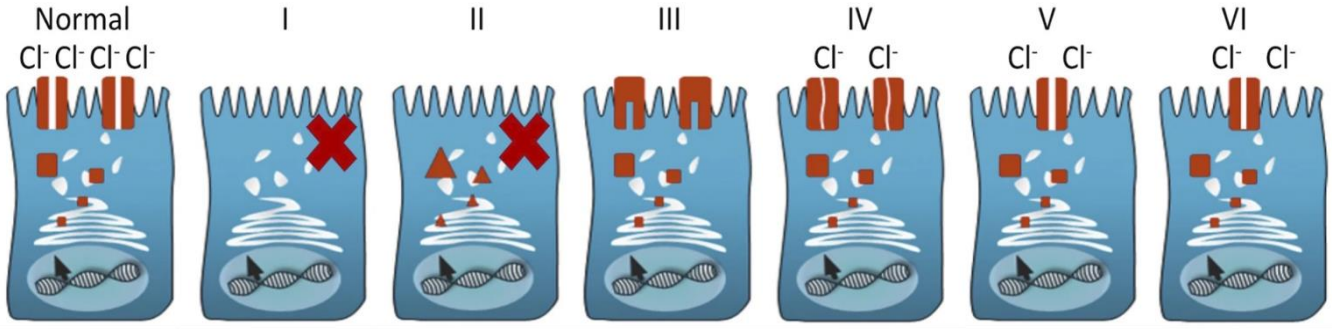

Molecular defect	No CFTR synthesis (mRNA or protein)	CFTR trafficking defect	Defective channel regulation	Decreased channel conductance	Reduced CFTR synthesis	Decreased CFTR stability
Prevalence	10%	88%	4%	< 2%	Rare	
Type of mutations	Nonsense Frameshift Canonical splice	Missense Aminoacid deletion	Missense Aminoacid change		Splicing defect Missense	Missense Aminoacid change
Mutation examples	G542X W1282X R553X R1162X	F508del I507del N1303K M1101K	*G551D* G551S S1255P G178R	R117H R347P R334W R1070W	A455E 3272-26A>G 3849+10kb C>T	4326delTC Gln1412X 4279insA
Therapeutic approach	*Read through** compounds, ELX-02; **kalydeco®** (Ivacaftor)	*Correctors** (+potentiators***)* **Orkambi®** (Lumacaftor +Ivacaftor); **Trikafta®**; GLP222 **; ABBV-3067*	*Potentiators (+correctors)* **kalydeco®**; **Trikafta®** (Elexacaftor + tezacaftor + Ivacaftor); **Symdeko®** (tezacaftor-Ivacaftor)		*Splicing modulators* Antisense oligonucleo-tides; **kalydeco®**; **Trikafta®**	*Stabilizers*

Drugs already in use by patients are noted in bold.
*: read through compounds promote the read through of premature termination codons in *CFTR* mRNA.
**: correctors improve the processing with delivery of functional CFTR protein to the cell surface.
***: potentiators increase the function of CFTR channels on the cell surface.

Figure 1.12 Classification of CFTR mutations. The mutations are categorized into 6 classes based on the molecular defect and functionality of the CFTR protein. The red mark represents the CFTR protein, and the red X represents no CFTR protein in the plasma membrane. The figure was adapted with permission from Spring Nature, Deletang et al., 2022 (see Appendix XIX).

It is estimated that CF affects around 162,428 individuals in 94 countries, mainly Caucasians people. Only 65% of the estimated CF people affected are diagnosed (Guo, Garratt et al. 2022). This disease is characterised by ion and fluid transport

defects into the airway lumen, creating thick mucus secretions that block the ducts of some organs, such as the lungs (Kreda, Davis et al. 2012, Huang, Quach et al. 2021). Some of the CF manifestations are obstructive lung disease, high sweat chloride concentrations, meconium ileus, sinusitis, pancreatic insufficiency, diabetes, liver disease, congenital bilateral absence of vas deference, and others (Ratjen, Bell et al. 2015). All the clinical manifestations mentioned previously are related to organs containing tubular shapes, and their homeostasis depends on fluid secretion.

Histologically, the mammary gland in CF patients has been described with some changes, such as lobular atrophy (Garcia, Galindo et al. 1998). However, there is not much information about the anatomical and histological differences between the non-CF and the CF patients that show affection in breast development. Likewise, the study of the physiology of the mammary gland or risk incidence of pathologies such as breast cancer in this group of patients has not been deepened either. One of the reasons for that is the mean age of the individuals included in the studies, which was lower than the current age of the individuals included in the new studies. Recent reports associate the CF condition with a higher risk of incidence of breast cancer (Stastna, Brat et al. 2023). Archangelidi et al., 2022 reported that breast cancer was the second (after the gastrointestinal) type of cancer with more incidence (13%) of the 98 cases of cancer analysed in CF patients (Archangelidi, Cullinan et al. 2022). These results contradict past studies where no differences in breast cancer incidence between the non-CF and CF patients were observed (Neglia, FitzSimmons et al. 1995, Maisonneuve, Marshall et al. 2013). However, the media age of the CF patients included in the Maisonneuve et al., 2013 study was 19 years, and the breast cancer incidence is related to age. The current media age of cancer diagnosis is 62 years (according to the American Cancer

Society), and in the UK, the incidence rate increases from 35 years (according to Cancer Research UK).

Life expectancy improves notoriously with the approval of pharmacological treatments. The gene that causes CF was identified in 1989 (Riordan, Rommens et al. 1989), and the first treatment (Ivacaftor) for treating CF was approved in 2012 (Whiting, Al et al. 2014). Since then, new treatments have been proposed to treat the different molecular defects of CFTR, increasing the life expectancy and health of CF patients. The median predicted survival of CF patients improved from 27 years in 1985 to 47.7 years in 2016 (Rubin, O'Callaghan et al. 2019). Currently, the median age of survival for CF patients born between 2019 and 2023 is predicted to be 61 years (Cystic Fibrosis Foundation, https://www.cff.org/). The increase in life expectancy in CF patients entails carrying out new epidemiological studies to analyse the incidence of diseases at older ages.

1.5.4 CFTR expression in breast cancer

Clinical breast cancer samples show a significant difference in CFTR expression and localisation in normal tissue samples compared to cancer tissue. In healthy tissue samples, CFTR expression was found to be localised to the apical membrane of luminal cells, whereas breast cancer samples showed lower expression than the adjacent normal tissue and CFTR localisation in the cytoplasm (Figure 1.12A) (Zhang, Jiang et al. 2013, Liu, Dong et al. 2020). This low expression pattern of CFTR has also been seen on human breast cancer samples from databases, and CFTR has been proposed as a prognostic marker for breast cancer since patients with poor Nottingham Prognostic Index have low CFTR expression (transcripts) and patients

with good prognosis have higher CFTR expression (Zhang, Jiang et al. 2013) (Figure 1.12B). Another study carried out with samples from breast cancer patients has found the same pattern of CFTR expression between healthy tissue versus breast cancer tissue. They described that the low expression of CFTR is due to the hypermethylation of its promoter. More specifically, they have found using TCGA data that the promoter methylation level of CFTR is higher in breast cancer samples compared to healthy samples (Liu, Dong et al. 2020). Both research groups also performed functional analyses on cell lines to assess the role of CFTR in invasion and proliferation, and they showed that CFTR suppresses cell invasion and migration. The deficiency of this gene favours the epithelial to mesenchymal transition (EMT) phenotype and, therefore, the invasive and migratory capacity.

The growing information on the involvement of CFTR in breast cancer and other types of cancer in lumen-containing organs such as the intestine, pancreas, prostate, and lung (Zhang, Wang et al. 2018) and its prominent role in fluid secretion for morphogenesis of tubular organs suggests that CFTR could be playing a determining role in the formation of the lumen in the mammary gland and its maintenance.

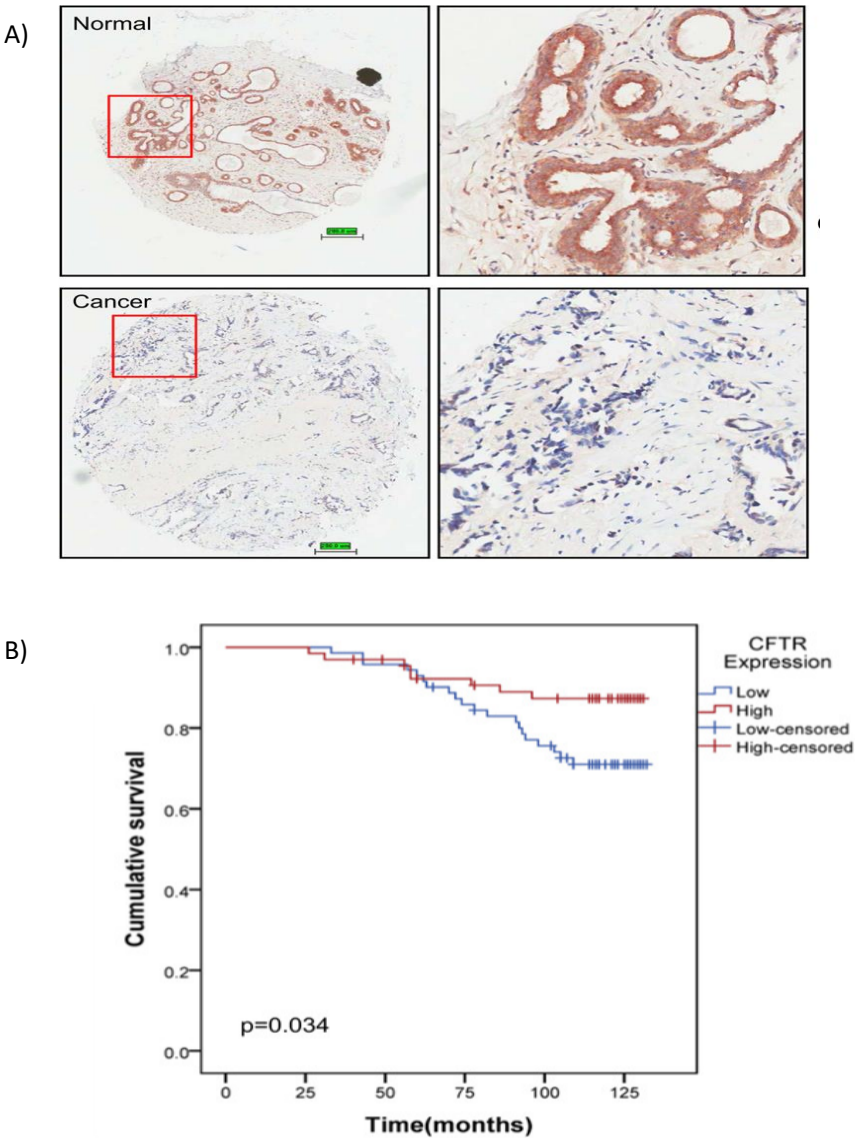

Figure 1.13. Low CFTR expression in breast cancer. A) CFTR protein expression detected by immunohistochemistry in normal adjacent and human breast cancer tissue. CFTR expression in normal tissue is mostly present in the apical membrane of the luminal cells. The breast cancer tissue shows lower CFTR protein expression than the normal tissue. The immunohistochemistry were made with samples from breast tissue microarrays containing 77 no breast cancer and 140 breast cancer samples. The samples were grouped by a score given by the product of staining intensity score and staining positive rate score. It was considered low expression scores lower than 8 and high expression to scores equal to or higher than 8. B) Cumulative survival rate of breast cancer patients. Low CFTR protein expression is associated with poor prognosis (correlation, *P=0.034*). Figure adapted with permission from Cell Biology International, Lui K. et al. 2020 (see Appendix XIX).

1.6 SECRETORY FUNCTION OF B1 INTEGRIN

The mammary gland is an exocrine gland whose primary function is the secretion of breast milk by the luminal cells in the alveoli during lactation. The expression of β1 integrin increases during pregnancy and lactation, showing higher expression during lactation. Cooperation between the signalling pathways of β1 integrin and prolactin, a hormone secreted by the pituitary during lactation, has been described. Prolactin binds to its PRL-R receptor, which causes JAK2 activation and its translocation to the nucleus. Later, JAK2 phosphorylates and translocates to STAT5, favouring the transcription of genes related to lactogenesis. When β1 integrin is not expressed, there is no correct signal transmission, which impedes the prolactin signalling pathway and the transcription of genes related to lactation. Moreover, the lack of β1 integrin expression interferes with alveologenesis (Naylor, Li et al. 2005).

Another study describes β1 integrin as a regulator of cell permeability in proximal tubule cells by modifying the expression of components of TJs. Deletion of integrin β1 integrin increases claudin 7 expression and decreases claudin 2 expression (Elias, Mathew et al. 2014). The claudins are essential membrane proteins that compose the TJs and control paracellular permeability by solute selectivity (Tsukita and Furuse 2000). Altered expression of claudins 2 and 7 decreases paracellular permeability in this cell type and reduces the expression of AQ1, a water channel generally expressed in the apical membrane (Elias, Mathew et al. 2014).

It is unknown whether the multifaceted molecule β1 integrin participates in fluid secretion on MECs, modulating the paracellular permeability of solutes to the luminal space through TJs and thus contributing to the formation and expansion of the lumen. Likewise, it is unknown whether this integrin can directly or indirectly modulate ionic channel activity that influences the secretion of fluids into the lumen and favours its formation and expansion.

1.7 3D CELL CULTURE FOR LUMEN MORPHOGENESIS

The mammary gland is a tubular organ of polarised cells surrounded by an ECM, acquiring a tissue organisation in a 3D structure. The cell culture in 2D or monolayer is a useful tool to study diverse mechanisms in the cell and interactions between the cell-cell and cell-molecules. Nevertheless, its main limitations lie in cell-cell-ECM interactions and the lack of spatial arrangement. This gap given in the 2D cell culture can be covered by the 3D cell culture with a basement membrane matrix (BMM), which allows the cells to acquire the structural conformation mimicking similar conditions of the ECM, promoting spatial organisation (Vidi, Bissell et al. 2013). The advantages of 3D cell culture have been shown over the 2D cell culture, some of which is the study of cell morphology, mechanical forces, physical interactions with other cells in 3 dimensions, and interaction with the ECM. In addition, the cell culture in 3D more clearly reflects the *in vivo* conditions not only for the potential space distribution but also for the different cell behaviour and gene expression that the cells acquire under these conditions (Wicha, Lowrie et al. 1982, Streuli, Bailey et al. 1991, Nelson and Bissell 2005). It has been demonstrated that the gene expression profiling of cells is different in 2D than in 3D conditions. The presence of a BM enables replication of the

in vivo conditions, and the interaction between cell-BM is essential to guarantee the bidirectional cross-talk between proteins, expression, and activation of cell pathways. For example, the inhibition of epidermal growth factor receptor (EGFR) in the human breast cell line T4–2 cells down-regulates the expression of β1 integrin, and conversely, the blocking of β1 integrin function leads to the downregulation of EGFR via the mitogen-activated protein kinase (MAPK) pathway in 3D conditions. Moreover, the effect of these inhibitions was reflected in the growth arrest of the breast cancer cells and the restoration of breast tissue morphogenesis. Interestingly, this bidirectional modulation effect of inhibition was not observed in 2D cell culture (Wang, Weaver et al. 1998).

The morphology and phenotype the cells acquire in 3D conditions allow us to characterise and differentiate normal cells from breast cancer cells. It has been shown that normal breast cells from mammoplasties and non-tumorigenic cell lines compared with the tumorigenic cells from breast carcinoma biopsies and breast cancer cell lines showed notorious differences in growth and morphology in 3D conditions, but these differences are not observed in 2D cell culture. The normal cells in 3D cell culture with BMM were able to form spherical polarised structures with a central lumen recapitulating the structure of the mammary gland in vivo, while the breast cancer cells grown in colonies failed to form the round shape with a lumen structure (Petersen, Ronnov-Jessen et al. 1992). This distinctive capacity of polarised cells to form spheroids or organoids surrounding a lumen space in 3D cell culture represents a valuable model for studying the cell arrangement in the mammary ducts. In addition, the spheroids are also a useful model for breast cancer studies due to their similar structure to the tumours. The outside layer of cells in breast cancer spheroids and

tumours are in contact with the microenvironment and have direct access to nutrients as well as relatively higher levels of oxygen than the inner cells. Also, the cell behaviour is similar in the spheroids and most of the tumours. The proliferation rate is higher in the outside layer than in the inner cells, and necrosis or apoptosis mainly occurs in the core of the cell mass (Mehta, Hsiao et al. 2012).

In more than 90% of the most common carcinomas detected in women, the cells are thought to originate from the ductal epithelium (Silberstein 2001). Histopathology characteristics show a loss of epithelial integrity and lumen from the epithelial atypical to the invasive ductal carcinoma stages (Burstein, Polyak et al. 2004). Therefore, the lumen architecture is compromised from the previous breast cancer stage. Thus, studying lumen structure using models that resemble the *in vivo* conditions is a useful tool for understanding the molecules and mechanisms involved in breast cancer.

The availability of commercial BMM provides a model that largely recapitulates *in vivo* BM components in the 3D cell culture. Their main components are collagen IV, laminin, entactin, heparin sulphate proteoglycans and growth factors (Vukicevic, Kleinman et al. 1992, Zhao, Chen et al. 2022). Although the BMMs available are a good option and offer similar in vivo components, they still have some limitations compared to the BMM *in vivo*. One of these shortcomings is that most commercial products have standard components and concentrations. Some cells (according to their origin) need different components, concentrations and stiffness of the BM. It should also be kept in mind that, like other culture models, important factors such as immune system components, stroma, and vascularisation elements are lacking.

Nevertheless, the 3D cell culture with BMM is a useful tool to allow the molecular bases for tissue structure and spatial distribution.

1.8 HYPOTHESIS AND AIMS

The mammary gland is an organ made up of an interconnected structure of epithelial ducts composed of luminal and myoepithelial cells. The anatomy of this organ involves a lumen space inside the ducts. The lumen is formed during embryogenesis and is maintained for the rest of life despite the dynamic changes to the gland that occur during puberty, pregnancy, and involution. The maintenance of the lumen structure is essential for the homeostasis and functioning of the mammary gland. A decrease in its area or loss of this space has been associated with breast cancer lesions.

This work tries to understand the biology of the development of the lumen in the mammary gland to subsequently understand what mechanism might be dysregulated in breast cancer. The study of the mechanisms of single lumen formation, such as fluid secretion and its regulatory molecules, such as CFTR, may be associated with the formation and maintenance of the lumen and, thus, with the possible altered mechanisms in breast cancer.

Another important factor in establishing a lumen is the interaction between the cell and the ECM. In MECs, β1 integrin is primarily required to generate correct cell polarity orientation and promote lumen formation. Therefore, the hypothesis of this project are:

- **CFTR is a key regulator of fluid secretion and, therefore, for lumen formation and maintenance in mammary epithelial cells.**
- **β1 integrin modulates the fluid transport in mammary epithelial cells.**

A series of studies will address the overall aims of:

- Determining the role of CFTR in lumen formation and maintenance in normal mouse primary MECs and relating the findings to the inability of breast cancer cells to form lumens *in vitro*.
- Determining whether β1-integrin in mouse MECs regulates the paracellular fluids that could contribute to the lumen formation.

Towards these aims, the thesis will address the following specific aims and objectives in the results chapters:

Chapter 3

Aim:

Determine whether CFTR and Na^+/K^+-ATPase activity regulates lumen morphogenesis and maintenance in mouse mammary epithelial cells.

Objectives:

Evaluate the effect of CFTR and Na^+/K^+-ATPase stimulation in lumen formation and lumen area maintenance using forskolin in primary mammary epithelial cells and EpH4 cells cultured in 3D conditions with BMM.

Determine whether the inhibition of CFTR and Na^+/K^+-ATPase activity with CFTR-inh172 or ouabain in primary mammary epithelial cells and EpH4 cells cultured in 3D conditions with BMM alters lumen formation and area.

Chapter 4

Aim:

Determine the requirement for CFTR expression in primary mammary epithelial cells in lumen formation and maintenance processes.

Objectives:

Validate the CFTR KD in mammary epithelial cells after using siRNAs.

Determine whether the CFTR KD impacts lumen formation in mouse primary organoids derived from mammary epithelial cells.

Determine whether CFTR KD alters lumen area in mouse primary organoids derived from MECs.

Chapter 5

Aim:

Determine the CFTR expression in human breast cancer cell lines and evaluate the CFTR role in lumen formation in breast cancer cell lines.

Objectives:

Analyse the expression of CFTR in a range of breast cancer cell lines *in silico* and experimentally by qPCR and WB.

Evaluate the cellular localisation of CFTR in breast cancer cells by IF and WB.

Stimulate CFTR activity using forskolin and evaluate lumen formation in breast cancer cells.

Develop a CFTR over-expression vector to transfect breast cancer cells and evaluate the ability of these cells to form lumens.

Chapter 6

Aim:

Determine whether β1-integrin expression in primary mammary epithelial cells and EpH4 cells regulates the paracellular fluids that could contribute to the formation of a lumen.

Objectives:

Validate the β1 deletion in primary mouse mammary epithelial cells of the β1-integrin fx/fx-K18CreER transgenic mice.

Decrease the β1 expression in the EpH4 cells using the miR-IGTB lentivirus.

Evaluate the paracellular permeability in primary mammary epithelial cells with β1 integrin expression modified using semi-permeable membranes.

Evaluate the paracellular permeability in EpH4 cells with β1 integrin expression modified using semi-permeable membranes.

Chapter 2

2. METHODS

2.1 EQUIPMENT USED

Equipment	Supplier
Fluorescence microscope (Dm1400B)	Leica
Fluorescence inverted microscope (Olympus IX73)	Olympus
Confocal microscope (LSM980)	Zeiss
Light inverted microscope (DMi1)	Leica
Thermocycler (Rotor-Gene)	Qiagen
Gradient Thermocycler	SENSOQUEST
Spectrophotometer (NanoDrop)	Thermo Scientific
pH meter	Fisher Scientific
Centrifuge (Allegra X-22R)	Beckmen Coulter
Centrifuge (3-16K)	SIGMA
High-speed centrifuge (Aventi J26)	Beckmen Coulter
Cell lines incubator (MCO-18ACUV-PE)	SANYO
Bacteria incubator (Orbital incubator, SI500)	stuart
Incubator with shaker (ZHWY-103D)	SciQuip
Culture hood	MICROFLOW
Mini-PROTEAN Tetra cell	BIO-RAD
Trans-Blot SD semi-dry transfer	BIO-RAD
Qubit fluorimeter	Invitrogen
Transilluminator (G:Box)	SYNGENE
Epithelial Voltohmmeter (EVOM2)	World Precision Instruments
EnSight Multimode Plate Reader	Perkin Elmer
Refrigerated microcentrifuge (5417R)	Eppendorf
PowerPac Basic	BIO-RAD

2.2 MOUSE MODELS USED FOR HARVESTING MAMMARY EPITHELIAL

Several transgenic mouse models were available in the lab group, and tissues were harvested for *in vitro* experiments. No interventions were carried out on live animals in this thesis. The maintenance and handling of mice were carried out in accordance with the Animals (Scientific Procedures) Act 1986 (and associated practices) of the UK legislation under Project Licence PP1836785. The mice were kept at 22°C with 40-60% and 12h photoperiod in the Biological Services Unit of the Medical School of the

University of Sheffield. Mice were killed using the Schedule 1 procedure by a trained and registered practitioner. The number of animals used for each experiment is stated in the corresponding results Chapters.

2.2.1 Mouse model used for the drug treatments with forskolin, ouabain and CFTRinh-172

For the stimulation or blocking of the CFTR ion channel and the Na^+/K^+-ATPase in primary mouse MECs, mammary tissue from 8-10 week-old virgin female mice of the β1-integrin fx/fx: YPF: K14-CreERTM transgenic murine model were dissected to obtain the mammary gland tissue. The genetic construction of this mouse model with genetic background from the CD-1 mouse strain allows the deletion of β1-integrin in the myoepithelial cells (K14) in cell culture by adding 4-hydroxy tamoxifen (4-OHT) (Kim, Kim et al. 2018). This tamoxifen-inducible model based on the Cre/lox system uses CreER recombinase to delete the β1-integrin sequence in the cells that express CreER under the K14 promotor. The addition of 4-OHT to the media causes the translocation of CreERT from the cytoplasm to the nuclei for the recombination of the β1 integrin sequence (flanked by the loxP sites) and causes the deletion of the β1 integrin sequence and, subsequently, the KO of β1 integrin in the K14 (myoepithelial) cells. However, the general use of murine mammary tissue (without adding 4-OHT) allows objectively to perform experiments in primary culture to activate and block CFTR and Na^+/K^+-ATPase activity.

2.2.2 Mouse model for permeability experiments

The permeability experiments with primary mouse MECs were done with mammary tissue from 8-12 week-old pregnant β1-integrin fx/fx-K18CreERT mice. This mouse model based on the Cre/lox system allows β1-integrin deletion in luminal cells (K18) under the control of the K18-CreER promoter after adding 4-OHT. The addition of 4-OHT to the media causes the translocation of CreERT from the cytoplasm to the nuclei for the recombination of the β1 integrin sequence (flanked by the loxP sites) and causes the deletion of the β1 integrin sequence and, subsequently, the KO of β1 integrin in the K18 (luminal cells). (Kim, Kim et al. 2018).

2.2.3 Mouse model for CFTR KD experiments

Mammary tissue from 10-14 week-old virgin female mice from the C57BL/6 mouse strain was used to obtain the MECs for the experiments used to knock down CFTR in vitro.

2.3 ISOLATION OF PRIMARY MOUSE MAMMARY EPITHELIAL CELLS FROM BREAST TISSUE

The mammary tissue of the mice was dissected to obtain the MECs and carry out the cell culture experiments. Mice were culled by cervical dislocation, and the mammary glands were dissected. Subsequently, the tissue was chopped into small pieces with sterile blades to be treated enzymatically with a buffer mix of collagenase and trypsin.

This buffer mix contains 9.8 mg/ml collagenase A (Roche Life Sciences, USA), 1.5 mg/ml trypsin (Gibco), 9.8 mg/ml F-10 medium (Sigma-Aldrich), 1.2 mg/ml of NaHCO3 (Sigma-Aldrich, USA), 2.6 mg/ml HEPES-Na (Sigma-Aldrich), 5% (v/v) FBS (Biosera or BioWhittaker) in 47.5 ml of dd H_2O. The tissue was incubated with the buffer for 30 minutes at 37°C using constant agitation. Centrifugation (Allegra X-22R, Beckman Coulter) at 400rpm (31xg) for 2 minutes was carried out to obtain a cell pellet (tube 1) and a supernatant (tube 2). The pellet from tube 1 was digested with the buffer mix for a further 10 minutes and then centrifuged at 900rpm (156xg) for 4 minutes. The obtained pellet was dissolved in 20ml of Ham's F12 media (Lonza or Sigma Aldrich) and stored on ice while the remaining supernatant from tube 1 was centrifuged at 1500rpm (433xg) for 10 minutes to obtain a final pellet. Tube 2 was mixed with Ham's F12 media (filling it up to 40ml) (Lonza or Sigma Aldrich) and centrifuged at 900rpm (156xg) for 4 minutes. The pellet obtained from this centrifugation was kept on ice and resuspended in 40ml of Ham's F12 media (Lonza or Sigma Aldrich) while the supernatant was centrifuged at 1500rpm (433xg) for 10 minutes to obtain another cell pellet from tube 2. The final pellet from tube 2 was combined with the final pellet from tube 1 and washed with Ham's F12 media (Lonza or Sigma Aldrich). Finally, the cells were concentrated by centrifugation at 900rpm (156xg). The cell pellet obtained was resuspended in 20ml of Ham's F12 media (Lonza or Sigma Aldrich) and combined with the first pellet obtained from tube 1. The cells were centrifugated to obtain the final cell pellet used for the designed experiments.

2.4 2D CELL CULTURE MAINTENANCE

2.4.1 HEK 293T cell line

HEK 293T is an immortalised human embryonic kidney cell line expressing the SV40 large T antigen, allowing the expression of proteins that contain the SV40 promotor and is commonly used for lentiviral production. HEK 293T cells were provided by Dr Akhtar's laboratory. Frozen stocks of HEK 293T cells were thawed and transferred to a 15ml tube with complete DMEM F-12 media (Lonza) supplemented with 10% (v/v) FBS (Biosera), 1% (v/v) Ultra-glutamine (Lonza) and 1% (v/v) penicillin/streptomycin (Lonza). The cells were centrifuged at 900rpm (156xg), and the cell pellet was dissolved in complete DMEM F-12 media. The cells were seeded 1:10 in T-75 flasks and maintained at 37°C, 5% carbon dioxide, and 95% humidity.

2.4.2 EpH4 cell line

The EpH4 is a non-tumorigenic cell line from a spontaneously immortalised clone of mouse mammary epithelial cells derived from the female BALB/c mouse. EpH4 cells were provided by Dr Akhtar's laboratory. Frozen stocks of EpH4 cells were thawed and transferred to a 15ml tube with complete DMEM F-12 media (Lonza) supplemented with 5% (v/v) FBS (Biosera) and 1% (v/v) penicillin/streptomycin (Lonza). The cells were centrifuged at 900rpm (156xg), and the cell pellet was dissolved in complete DMEM F-12 media (Lonza). The cells were seeded 1:10 in T-75 flasks and maintained at 37°C, 5% carbon dioxide, and 95% humidity.

2.4.3. CAL-51, MDA-MB-231, MCF7 and T47D cell lines

CAL-51, MCF7, T47D, and MDA-MB-231 cell lines are established breast cancer cells categorised according to the different breast cancer subtypes (Table 2.1). The breast cancer cell lines are useful cell models used to study molecular features in breast cancer. The CAL-51, T47D, and MDA-MB-231 cell lines were provided by Dr Helen Bryant, and the MCF7 cells were provided by Dr Mark Fenwick. Frozen stocks of established breast cancer cell lines (Table 2.1) were thawed and transferred to a 15ml tube with complete DMEM F-12 media (Sigma Aldrich) supplemented with 10% (v/v) FBS (BioWittaker) and 1% (v/v) penicillin/streptomycin (Sigma Aldrich). The cells were centrifuged at 900rpm (156xg), and the cell pellet was dissolved in complete DMEM F-12 media. The cells were seeded 1:10 in T-75 flasks or T-25 flasks according to the desired cell density and maintained at 37°C, 5% carbon dioxide, and 95% humidity.

2.4.4 MCF10A cell line

MCF10A were provided by Dr Chris Toseland. Frozen stocks of the non-tumorigenic human epithelial breast cell line MCF10A were thawed and transferred to a 15ml tube with complete DMEM F-12 media (Sigma) supplemented with 5% (v/v) horse serum (Sigma Aldrich), 20ng/ml EGF (Sigma Aldrich), 0.5mg/ml hydrocortisone (Sigma Aldrich), 100ng/ml Cholera toxin (Sigma Aldrich), 10µg/ml insulin (Sigma Aldrich) and 1% (v/v) penicillin/streptomycin (Sigma Aldrich). The cells were centrifuged at 900rpm (156xg), and the cell pellet was dissolved in complete DMEM F-12 media. The cells were seeded 1:5 in T-75 flasks or in T-25 flasks according to the necessity of cell density and maintained at 37°C, 5% CO_2, and 95% humidity.

Table 2.1 Breast cancer subtype of the breast cancer cell lines used.

Cell line name	**Breast cancer subtype**	**Supplier**
CAL-51	Triple negative	ATCC
MCF7	Luminal A	ATCC
MDA-MB-231	Triple negative	ATCC
T-47D	Luminal A	ATCC

2.5 TIME COURSE LUMEN FORMATION

2.5.1 Lumen formation with cell lines

Confluent T-75 flasks of cells from the different cell lines were detached using 3ml of trypsin/EDTA (Lonza) for 3 minutes. The cells were collected as a pellet and counted to seed them in the desired cell density. $6x10^4$ EpH4 cells were seeded on 100µl of previously solidified (for 15 minutes at 37°C in 24-well plates) Matrigel (standard formulation, Corning B.V. Life Sciences, NL). Breast cancer cells (CAL-51, MCF7, MDA-MB-231 and T-47D) were seeded at a density of $4x10^4$ on 70µl of Cultrex Basement Membrane Extract (Type 2, Pathclear). Subsequently, DMEM F-12 media (Lonza or Sigma Aldrich) supplemented with 1µg/ml Hydrocortisone (Sigma Aldrich), 5ng/ml EGF (Sigma Aldrich), 5µg/ml Insulin (Sigma Aldrich) and 1% of penicillin/streptomycin (Lonza or Sigma Aldrich) were added to each well and incubated at 37°C. The culture media was changed every 2 days. Images of random

sections of the primary and EpH4 samples were taken daily until day 5, and for the breast cancer samples, photos were taken every 2 days until day 11. The photos were taken on the light microscope (Leica DMi1) to track the lumen formation. The number of 3D cell structures with and without lumen was counted and presented as a percentage.

2.5.2 Lumen formation time in mouse primary mammary epithelial cells

For the tracking of lumen formation in mouse primary MECs, cells extracted from mouse mammary glands were seeded with 120µl Matrigel (standard formulation, Corning) in 24-well plates (mammary tissue relation 0.012 mice/well). The embedded cells in Matrigel were incubated for 30 minutes at 37°C to solidify the Matrigel, and DMEM F-12 media (Lonza) containing 5µg/ml insulin (Sigma Aldrich), 1µg/ml hydrocortisone (Sigma Aldrich), 5ng/ml EGF (Sigma Aldrich) and 1% (v/v) of penicillin/streptomycin (Lonza) were added once the solidification had occurred. The media was changed every 2 days. Photographs of the organoids were taken daily for 4 days with the light microscope (Leica DMi1) to follow the lumen formation. The number of organoids with lumen was counted and expressed as a percentage relative to the total number of organoids.

2.6 ORGANOID FORMATION ASSAYS

2.6.1 Mouse primary organoid formation for the drug treatments

For the inhibition or stimulation of the CFTR ion channel or Na^+/K^+-ATPase in primary mouse MECs, cells from mouse mammary glands were mixed and seeded with 120µl Matrigel (standard formulation, Corning) in 24-well plates (mammary tissue relation 0.012 mice7/well). The mixture of cells and Matrigel were seeded on coverslips (treated as described in section 2.9.1) placed in a 24-well plate and incubated at 37°C for 30 minutes. Subsequently, 1ml/well of DMEM F-12 media (Lonza) containing 5µg/ml insulin (Sigma Aldrich), 1µg/ml hydrocortisone (Sigma Aldrich), 5ng/ml EGF (Sigma Aldrich) and 1% (v/v) of penicillin/streptomycin (Lonza) was added to the cells and incubated at 37°C, 5% CO_2, and 95% humidity. The media was changed every 2 days until the experiment day with the addition of forskolin, ouabain or CFTRinh-172.

2.6.2 Mouse primary organoids for the CFTR KD experiments

For the CFTR Knockdown (KD) experiments, the mouse MECs were seeded "with" or "on" 100µl of Cultrex Basement Membrane Extract (Type 2, Pathclear). For the evaluation of CFTR expression in the lumen formation experiments, the embedded cells were seeded in 24-well plates and incubated at 37°C for 30 minutes, while for the lumen maintenance experiments, the cells were seeded on top of the BMM (Cultrex Basement Membrane Extract, Type 2, Pathclear) after solidification (15 minutes at 37°C). Culture media made of DMEM F-12 media (Sigma Aldrich) containing 5µg/ml insulin (Sigma Aldrich), 1µg/ml hydrocortisone (Sigma Aldrich), 5ng/ml EGF (Sigma Aldrich) and 1% (v/v) of penicillin/streptomycin (Sigma Aldrich)

was added to the cells and incubated at 37°C, 5% CO_2, and 95% humidity. The media was changed every 48 hours.

2.7 3D CELL CULTURE OF THE CELL LINES

2.7.1 EpH4 cell line

To form EpH4 acini, $6X10^4$ EpH4 cells were seeded on the surface of 100µl solidified (by incubation at 37°C for 15 minutes) Matrigel (standard formulation, Corning B.V. Life Sciences, NL). 1ml of DMEM F-12 media supplemented with 1µg/ml hydrocortisone (Sigma Aldrich), 5 ng/ml EGF (Sigma Aldrich), 5µg/ml insulin (Sigma Aldrich) and 1% (v/v) of penicillin/streptomycin (Lonza) were added to each 24 well-plate and incubated at 37°C, 5% CO_2, and 95% humidity. The media was changed every 2 days.

2.7.2 Human breast cell lines

$1x10^4$ CAL-51 or MCF10A cells (Table 2.1) were seeded on the top of 30µl of solidified (by incubation at 37°C for 15 minutes) Cultrex Reduced Growth Factor Basement Membrane Extract (Type 2, Pathclear, Biotechne) in a 96-well plate. This cell seeding procedure was followed to allow 3D cell structure formation. The CAL-51 cells were fed with the same media that was used for the 3D cell culture of the EpH4 cells (section 2.6.1). The MCF10A were cultured with DMEN-F12 (Sigma Aldrich) supplemented with 0.5 µg/ml hydrocortisone (Sigma Aldrich), 10ng/ml EGF (Sigma Aldrich), 10µg/ml

insulin (Sigma Aldrich), 1% (v/v) of penicillin/streptomycin (Sigma Aldrich), 100ng/ml cholera toxin (Sigma Aldrich) and 2% (v/v) of Cultrex Reduced Growth Factor Basement Membrane Extract (Type 2, Pathclear, Biotechne). The media was changed every 3 days for the Cal-51 and every 4 days for the MC10A cells.

2.8 BLOCKING OR STIMULATION OF THE CFTR ION CHANNEL AND NA^+/K^+ PUMP

Ouabain is a substance derived from the plant Strophanthus gratus. It inhibits Na^+/K^+ pump activity since it binds with great affinity to the extracellular domain of the α-subunit, the catalytic unit of Na, K-ATPase that allows the E1–E2 conformational change for the Na^+ and K^+ transport (Jorgensen 1983, Ou, Pan et al. 2017). The dose-effect ratio and the cytotoxic effect of ouabain differ according to the cell type in which this treatment is applied, and it has not been widely described for MECs. In some breast cell lines, the use of ouabain from 1nM to 100uM has been tested for proliferation assays, reporting IC50 up to 149nM (Khajah, Mathew et al. 2018). However, the inhibition effect of the Na^+/K^+ pump activity in normal MECs has been poorly studied. For this reason 3 different ouabain doses (1 nM, 10 nM and 100 nM) described within an effect on epithelial cells (without reports of toxic effects) were tested (Li, Findlay et al. 2004, Pearson, Hughes et al. 2009, Cabrita, Kraus et al. 2020, Narayanan, Schappell et al. 2020) for an effect in the lumen structure in MECs.

CFTRinh-172 is an allosteric specific inhibitor of the CFTR ion channel that binds to the NBD1 domain, stabilising a pore conformation in which the Cl^- is blocked from the

extracellular side of the cell membrane (Caci, Caputo et al. 2008, Young, Levring et al. 2024). The CFTRinh-172 inhibitor use at 10 µM has been consistently tested in different epithelial cells showing to have an effect on the blocking of the CFTR activity without reports of toxicity (Verkman, Synder et al. 2013, Narayanan, Schappell et al. 2020). Therefore, this concentration was used to inhibit the Cl^- transport in the MECs.

Forskolin is a diterpene that binds at the pseudo substrate site on the adenylate cyclase enzyme and stimulates the conversion of ATP to cAMP and pyrophosphate (Daly 1984). cAMP activates PKA that phosphorylates the R domain of the CFTR ion channel and, together with ATP, permits conformational changes for the active stage of this ion channel (Anderson, Berger et al. 1991, Cheng, Rich et al. 1991, Picciotto, Cohn et al. 1992). Forskolin was reported to have an effect at 10µM in the stimulation of the cAMP production and influence lumen structure in the epithelial such as MDCK cells and AT II cells (Yu, Fang et al. 2007, Cabrita, Kraus et al. 2020, Narayanan, Schappell et al. 2020). Therefore, this drug was used at 10µM.

The CFTR ion channel and Na^+/K^+ pump stimulation or inhibition were carried out in 3D cell culture with primary MECs and cell lines. The mouse primary MECs, EpH4 and CAL-51 cells, were seeded under previously described conditions to form 3D cell structures in BMM (see sections 2.5.1, 2.6.1 and 2.6.2). The drug treatment (Table 2.2) for the primary MECs and for the EpH4 cells was applied for 24h to the cell media on days 2 or 3 after seeding. With the CAL-51 cells, the treatment was applied for 6 days starting on day 3 after seeding.

Table 2.2 Doses of the treatments applied to the cell lines and the primary cells.

Activator/Inhibitor	**Dose**	**Reference of Doses**
Ouabain octahydrate (Sigma-Aldrich)	1nM, 10nM, 100nM	(Khundmiri, Metzler et al. 2006, Pearson, Hughes et al. 2009, Narayanan, Schappell et al. 2020)
CFTR(inh)-172 (Sigma-Aldrich)	10μM	(Verkman, Synder et al. 2013, Cabrita, Kraus et al. 2020, Narayanan, Schappell et al. 2020)
Forskolin (APExBIO)	10μM	(Yu, Fang et al. 2007, Cabrita, Kraus et al. 2020, Narayanan, Schappell et al. 2020)

2.9 MORPHOLOGICAL MEASUREMENTS OF LUMEN FORMATION AND AREA

2.9.1 Mouse primary organoids after drug treatments

For the experiments of lumen maintenance, the lumen area in the organoids or in the EpH4 acini structures was measured before (0h) and after (24h) the stimulation or inhibition of CFTR or Na^+/K^+ pump activity. Images were taken using a light microscope (Leica DMi1) on days 2 and 3 for the treatment applied on day 2 and days 3 and 4 for the treatment applied on day 3. In order to localise and track different structures over time, an adhesive grid (squares of 2mmx2mm) was applied to the base of the 24-well plates before imaging. The area measurement was performed using ImageJ and the free hand selection tool (to select the specific lumen area). Calculation of the percentage of lumen area change was made with the area measurements before and after treatment:

$$\left(\frac{A_2 - A_1}{A_1}\right) 100$$

A1= area before treatment A2= area after treatment

For the experiments of lumen formation, the percentage of lumens reported was determined by counting the total number of 3D cell structures (from the EpH4 cells or primary cells) and their relation with the number of 3D cell structures with a lumen after 24h of treatment.

2.9.2 Morphological measurements for mouse primary cells after CFTR KD

For the CFTR KD experiments in primary MECs, the lumen area of the same organoids was measured before (0h) and 24h or 48h after post-transfection. Calculations of the lumen area change were made according to the formula described above (see section 2.8.1). Images were analysed in ImageJ, and the organoids with an area superior to 24000 units from the ImageJ "analyse tool" or ~826µm^2 were counted as organoids.

The percentage of lumens formed was calculated from the relation of the total number of organoids and the number of organoids with lumen counted.

2.9.3 Morphological measurements of the CAL-51 acini following drug treatment

The CAL-51 cells cultured in BMM were treated with 10µM forskolin for 6 days, after which images were taken on the light microscope (Leica DMi1). Photos of randomly selected sections were taken to compare the 3D cell structures of the control group with the treatment group. The photos were analysed, and the 3D cell structures with an area superior to 20,000 units from the ImageJ "analyse tool" or 688µm^2 were counted as independent 3D cell structures. The relation of the total counting of 3D cell structures with the total number of 3D cell structures with lumen determined the percentage of lumens formed.

2.10 IMMUNOFLUORESCENCE

2.10.1 Acid-etching coverslips

Concentrated nitric acid (70%) (Fisher Scientific) was added to the 13mm coverslips and was incubated at room temperature for 5 minutes. Subsequently, nitric acid was slowly diluted with water and removed from the coverslips. The coverslips were washed in running tap water for 2 hours to remove nitric acid residues. A final wash was done with distilled water and ethanol. The coverslips were stored in absolute ethanol at room temperature.

2.10.2 Immunofluorescence

The mouse primary MECs, EpH4, CAL-51, MCF7, MDA-MB-231, T47D and MCF10A cells were washed with 1X PBS (Thermo Scientific, pH 7.4) (three times) to remove residues from the culture media and were fixed in a solution of 4% ultrapure formaldehyde solution (Polysciences) in PBS or 10% Formalin solution (Sigma) for 10 minutes. Subsequently, the samples were washed with 1X PBS and then permeabilised with a 0.25% (v/v) Triton x-100 (Sigma Aldrich) in 1X PBS for 7 minutes at room temperature. Samples were washed with 1X PBS and subsequently blocked in 10% goat serum (LabTech) or 10% (w/v) BSA (Sigma Aldrich) in 1X PBS for 1 hour at room temperature.

The antibodies or fluorescent dyes (Table 2.3) were applied to cells in a 5% goat serum (LabTech) solution or 5% (w/v) BSA (Sigma Aldrich) in 1X PBS (Thermo Scientific, pH 7.4) for 2 hours at room temperature. The samples were washed with 1X PBS (Thermo

Scientific, pH 7.4) (three times), and excess PBS was carefully removed. Secondary antibodies (Table 2.3) were applied to the samples diluted in 5% (v/v) goat serum solution or 1% (w/v) BSA (Sigma Aldrich) in 1X PBS (Thermo Scientific, pH 7.4) for 2 hours at room temperature. At the end of the incubation, the samples were washed with 1X PBS (Thermo Scientific, pH 7.4) and stained with Hoescht (Invitrogen) at a 1:1000 dilution for 3 minutes at room temperature. Cells were washed with 1X PBS (Thermo Scientific, pH 7.4) (three times) and mounted on slides with ProLong Gold Antifade Mountant (Invitrogen). The mounted samples remained at room temperature overnight and were subsequently stored at 4°C.

The experiments included negative control samples, which consisted of the same reagents, concentrations and steps as the other samples but without the primary antibody solution.

Images were obtained in the Olympus IX73, EVOS fluorescent microscopes, or Zeiss LSM980 Confocal microscope.

Table 2.3 Dyes, Primary and secondary antibodies and their dilution factor.

Antibody/dye	**Dilution factor**	**Brand**
TRITC-phalloidin	1:500	Sigma-Aldrich
Hoechst 33258	1:1000	Sigma- Aldrich
Goat Anti-rat IgG, Rhodamine Red-X	1:500	Jackson Immunolabs
Rat anti-Integrin β1 (monoclonal)	1:100	Merck Millipore
Mouse anti-ZO-1 (monoclonal)	1:200	Invitrogen
Rabbit anti-CFTR (polyclonal)	1:400	Alomone labs
Rabbit anti-ZO-1 (monoclonal)	1:400	Sigma- Aldrich
Goat Anti-rabbit IgG, Alexa fluor 647	1:500	Jackson Immunolabs
Anti-mouse IgG, Alexa Fluor 555	1:400	Abcam
Pig Anti-Keratine K8/K18 (polyclonal)	1:400	PROGENE
Donkey Anti-Guinea pig IgG, Alexa fluor 488	1:500	Jackson Immunolabs
Mouse Anti-Cre Recombinase (monoclonal)	1:100	Sigma-Aldrich
Goat Anti-rat IgG, Cyanine Cy5	1:400	Jackson Immunolabs
Rabbit anti-CFTR (polyclonal)	1:400	Abcam
Donkey Anti-rabbit IgG, Alexa fluor 488	1:400	Abcam
Goat Anti-mouse IgG, Cyanine Cy5	1:400	Jackson Immunolabs

2.11 BACTERIAL TRANSFORMATION AND SELECTION OF LENTIVIRAL PLASMID DNA

The lentiviral plasmids pLVTHM miRNA ITGB1 and PLVTHM scrambled were provided by the Dr Akhtar lab group. Both plasmids were amplified in DH5α Competent Cells (Provided by Dr Akhtar lab group). The bacteria aliquots (50 µl) were thawed on ice for 20 minutes. 500ng DNA of the constructs from pLVTHM miRNA ITGB1 or PLVTHM plasmids was added to each tube and incubated for 15 minutes on ice. The samples were quickly transferred to 42°C for a heat shock for 90 seconds and then placed on ice for 5 minutes. Subsequently, 800µl of sterile Lysogeny Broth (LB) medium containing 10g/L tryptone (Oxoid), 5g/L yeast extract (Sigma Aldrich) and 10g/L NaCl (Prolabo chemicals or Fisher Chemical) was added to the tubes and incubated for 2 hours at 37°C under continuous shaking. After incubation, 100µl of the bacteria solution was seeded on LB agar plates containing 50 µg/ml ampicillin (Sigma Aldrich) and incubated overnight at 37°C. The next day, one colony was taken to grow in a sterile conical flask with 100ml LB medium containing 50µg/ml ampicillin. The conical flask with bacteria was incubated overnight at 37°C under constant shaking. The plasmid DNA was extracted from the bacteria that grew after this last incubation.

2.12 PLASMID DNA EXTRACTION

Plasmid DNA was extracted from bacteria grown in the LB medium with ampicillin (Sigma Aldrich). The plasmid Midi kit 25 (QIAGEN) was used to extract the plasmid DNA, and the protocol followed was according to the manufacturer instructions. The

DNA obtained was diluted in 50µl TE buffer (kit solution), quantified by absorbance in a NanoDrop or Fluorometrically in Qubit Flex Fluorometer (dsDNA BR Assay Kit, Invitrogen) and stored at -20°C.

2.13 LENTIVIRUS PRODUCTION

The lentiviral vectors pLVTHM miRNA ITGB1 and PLVTHM scrambled, and the packaging plasmids (Trono Lab): psPAX2 plasmid (envelope) and PMD2G plasmid (packaging) were used to produce lentiviruses.

Lentivirus production was conducted by transfection of the 293T cells at 70-80% of confluence. A mix of 6µg pLVTHM miRNA ITGB or PLVTHM scrambled vectors, 3µg psPAX2 and 4.5µg pMD2G packeting vectors were prepared. 1mg/ml polyethyleneimine (PEI; JetPEITM reagent; Sigma-Aldrich) of stock solution was added with the DNA vectors mix in a ratio of 2:1. The cells were incubated with the mix of plasmid DNA:PEI overnight, and then fresh media was replaced. Subsequently, the cells were treated with 100µl of 1M sodium butyrate solution (Millipore). 48h after the transfection of the cells, the culture medium in which the cells were cultured was collected and stored at 4°C. New fresh media was added to the transfected cells and collected 24 hours after the last media collection. The media collected was passed through a 0.45 µm filter and ultracentrifuged at 21,000xg for 4 hours at 4°C. The pellet obtained was resuspended in 200µl of DMEM F12 medium and frozen at -80°C.

2.14 VIRUS TITRATION

The lentivirus titration to determine the amount of viral solution necessary to generate an efficient infection and the β1 integrin knockdown in EpH4 cells were done by immunofluorescence. Different volumes (20,40, 60, 80, 100 and 120µl) of the virus solution were added to $5x10^4$ EpH4 cells placed on 24-well plates (with coverslips) containing the standard media to culture this cell line. The lentivirus infection was done when the cells were seeded. The media change was after 12h post-transfection. The cells were occasionally observed under the fluorescence microscope to determine if the fluorescent marker (GFP protein) from the viral construct was present. Cells were fixed as described in section 2.9.2 on day 4, and immunofluorescence was carried out to analyse β1 integrin Knockdown.

2.15 PERMEABILITY ASSAYS

2.15.1 Permeability assays with the mouse mammary epithelial cells

Fresh primary mouse MECs cells derived from β1-integrin fx/fx-K18CreERT mice (described in section 2.1.2) were seeded on polyester membranes of Transwell inserts (12mm, Costar) placed in 24-well plates. The cells were cultured with Ham's F12 media (Lonza) supplemented with 1µg/ml hydrocortisone (Sigma Aldrich), 5ng/ml EGF (Sigma Aldrich), 5µg/ml insulin (Sigma Aldrich), 1% (v/v) of penicillin/streptomycin (Lonza) and 10% (v/v) serum (Biosera) until they formed a confluent monolayer. The

knockout of β1 integrin was made by adding 4-OHT to the cells on day 2. The permeability experiments were done when the cells showed a confluent monolayer (at least 2 days after the +4OHT addition) after assessment under the light microscope, and immunofluorescence confirmed the confluence. 1mg/ml dextran (4KDa FITC, Sigma Aldrich) in complete media was added to the top chamber of the transwell, and after 24 hours of incubation at 37°C, media from the top and bottom chamber was collected and added to 96-well plates. The fluorescence intensity detection of the dextran was made in the EnSight Multimode Plate Reader using a standard curve of 4KDa dextran (from 0-1mg/ml). Dextran concentration was calculated using a polynomial equation (3rd degree) generated from the curve.

2.15.2 Permeability assays with the EpH4 cells

$5x10^4$ EpH4 cells were seeded on the polyester membranes of the transwell inserts (12mm, Costar) placed in 24-well plates. The infection with the pLVTHM miRNA ITGB1 or PLVTHM scrambled lentivirus was carried out on the same cell seeding. The media was changed after 12h post-transfection for fresh complete media. The permeability assay using 1mg/ml dextran (4KDa FITC, Sigma Aldrich) was made when the cells showed a confluent monolayer post-infection. The permeability assay with the dextran was the same procedure used for the permeability assays of the primary cells (see section 2.14.1).

2.15.3 Permeability experiments with the CAL-51 cells

The permeability assays were done with the support of Joely Mynnott. The CAL-51 cells treated with forskolin were done by seeding $2x10^4$ cells on the 0.4µm polyethylene membrane inserts (6.5mm, STEMCELL Technologies), placed in 24-well plates. Cells were maintained in standard media for 2D cell culture (see 2.3.3 section). The permeability assay was made on day 3, changing the media to the 2 chambers with fresh complete media containing 10µM forskolin or DMSO (for the control samples using the same volume as the forskolin was used) and 1mg/ml Dextran (4KDa FITC, Sigma Aldrich) only for the bottom chamber. After 24h, media from the top chambers were collected to detect the dextran fluorescence signal (FITC) using the EnSight Multimode Plate Reader. The concentration of dextran in the media of the top chamber was determined using a standard curve, and the dextran transported was calculated using a polynomial equation of 2^{nd} or 3^{rd} degree.

2.16 TRANSEPITHELIAL ELECTRICAL RESISTANCE (TEER) MEASUREMENTS

TEER measurements were made using the EVOM2 equipment (World precision instruments) to monitor a complete monolayer in the membrane inserts. The TEER measurements were done when the cells cultured on the membrane inserts showed a confluent monolayer on the light microscope. The TEER number related to the confluent monolayer for the EpH4 and primary cells was established when a confluent monolayer was observed under the light microscope. Immunofluorescence was used to confirm the complete monolayer.

The TEER electrodes were disinfected in 70% ethanol for 15 minutes and rinsed with double-distilled sterile water and a blank media. After the washes, electrodes were inserted into each of the wells without touching the membrane of the inserts, and the sample reading in Ohms was detected (Figure 2.1). Three readings per well were done in different sections of the well to verify the resistance number.

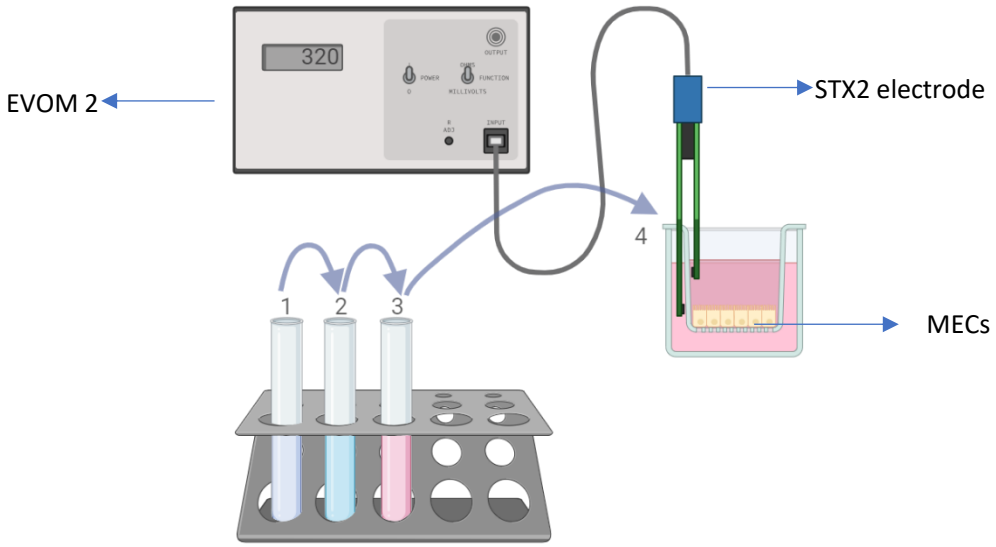

Figure 2.1 TEER measurements to test monolayer confluence. The confluent monolayers (previously observed in the light microscope) on the semipermeable membranes were tested to measure the monolayer trans-epithelial resistance using the EVOM2 equipment. The STX2 electrode was disinfected with ethanol (70%) (1) and washed with double-distilled sterile water (2) and a blank media (3). The STX2 electrode was placed in the wells; the outer electrode between the well and the membrane, and the inner electrode inside the semipermeable chamber, avoiding touching the membrane insert. Illustration was created using Biorender.

Calculations reported were performed as follows:

R blank (average of membranes without cells) - R sample (average of membranes with cells) = R total

Unit area of resistance = R total Ω x πr^2

$=\pi(d/2)^2$

2.17 CFTR KD IN MECS

2.17.1 CFTR KD for lumen formation experiments

Mouse primary MECs were seeded on 2D conditions and fed with Ham's F12 media (Sigma Aldrich) supplemented with 1µg/ml Hydrocortisone (Sigma Aldrich), 5ng/ml EGF (Sigma Aldrich), 5µg/ml Insulin (Sigma Aldrich), 1% (v/v) of penicillin/streptomycin (Sigma Aldrich) and 10% (v/v) serum (BioWhittaker). One day after seeding the cells, they were transfected on 2D conditions in 1:1 DMEN F-12 media (Sigma Aldrich) and Optimen media (Gibco) containing 5pmol of Lipofectamine™ RNAiMAX Transfection Reagent and 120nM of CFTR siRNA (Silencer select, Ambion), 120nM Negative control siRNA (Silencer select, Ambion) or 120nM positive control siRNA (Block-iT Alexa Fluor, Invitrogen). The transfection procedure followed was according to the manufacturer's instructions.

After 48h post-transfection, the MECs were detached using trypsin (Sigma Aldrich) for 3 minutes. Cells were transferred to a 15ml tube, centrifuged at 300xg for 3 minutes, and collected as a cell pellet to seed them on 3D conditions (following the method described in section 2.5.2) to form organoids with or without lumen structures.

2.17.2 CFTR KD for lumen maintenance experiments

Mouse primary MECs were directly seeded on 3D conditions (previously described in section 2.5.2) and transfected on day 6, when the organoids presented lumen

structures. The transfection was done using 5pmol of Lipofectamine™ RNAiMAX Transfection Reagent and 120nM of CFTR siRNA (Silencer select, Ambion), 120nM Negative control siRNA (Silencer select, Ambion) or 120nM positive control siRNA (Block-iT Alexa Fluor, Invitrogen). The siRNA and the transfection reagent were combined and added to the cells according to the manufacturer's instructions. After adding the transfection mix, the plate with cells was incubated for 10 minutes at 4°C. Serum-free media (300µl total) made of 1:1 DMEN F-12 media (Sigma Aldrich) and Optimen media (Gibco) was added to the cells and incubated at 37°C. The analysis of the lumen area was carried out at 0h (before transfection), 24h and 48h post-transfection. For the 48h experiment, the media was changed for DMEM F-12 media (Sigma Aldrich) containing 5µg/ml insulin (Sigma Aldrich), 1µg/ml hydrocortisone (Sigma Aldrich), 5ng/ml EGF (Sigma Aldrich), and 1% of penicillin/streptomycin after 24h post-transfection.

2.18 FORSKOLIN TREATMENT IN CAL-51

The CAL-51 cells were seeded in 3D conditions for 3 days to allow for the formation of 3D cell structures (section 2.7.2). On day 3 post-seeding, the media was replaced with standard media containing 10µM forskolin (APExBIO). The media containing forskolin was changed every 2 days until day 10 of drug treatment. Photos of random sections of 2 different replicates per sample were taken (15 photos per sample in each experiment). The number of acini structures formed is determined as described in section 2.8.3.

2.19 PRODUCTION OF CFTR VECTOR AND GENERATION OF THE NEGATIVE CONTROL VECTOR

The CFTR vector was obtained from Promega (sequence in Appendix I), and the negative vector was generated by deleting the CFTR sequence (Appendix I and Figure 2.1). Specific primers (Table 2.4) that flank the CFTR sequence in the CFTR vector were used to amplify the backbone vector components without the CFTR sequence. The vectors were amplified in DH5α bacteria (NEB®) by transformation. The bacteria were defrosted from -80°C, and 5µl DNA (1-100ng) from the amplification of the control vector or 30ng DNA of the CFTR vector was added to the bacteria aliquots. Immediately after adding the DNA vectors, the aliquots were incubated on ice for 30 minutes, at 42°C for 40 seconds, and finally, incubated for 5 minutes on ice. Super Optimal broth with Catabolite repression (SOC) growth medium was added (up to 1ml) and incubated at 37°C for 1h with shaking (approximately 250rpm). After the incubation, 100µl of cell bacteria solution was taken to spread in LB agar plates containing 50µg/ml ampicillin (Sigma Aldrich) and incubated at 37°C overnight. The next day, one bacteria colony was selected and transferred to a conical flask with LB media containing 50µg/ml ampicillin (Sigma Aldrich) for overnight incubation at 37°C with shaking (approximately 250rpm). The next day, the LB media with bacteria were collected and centrifuged at 3893xg for 30 minutes. The bacteria pellet was used to do the plasmid extraction following the previously described protocol (section 2.11).

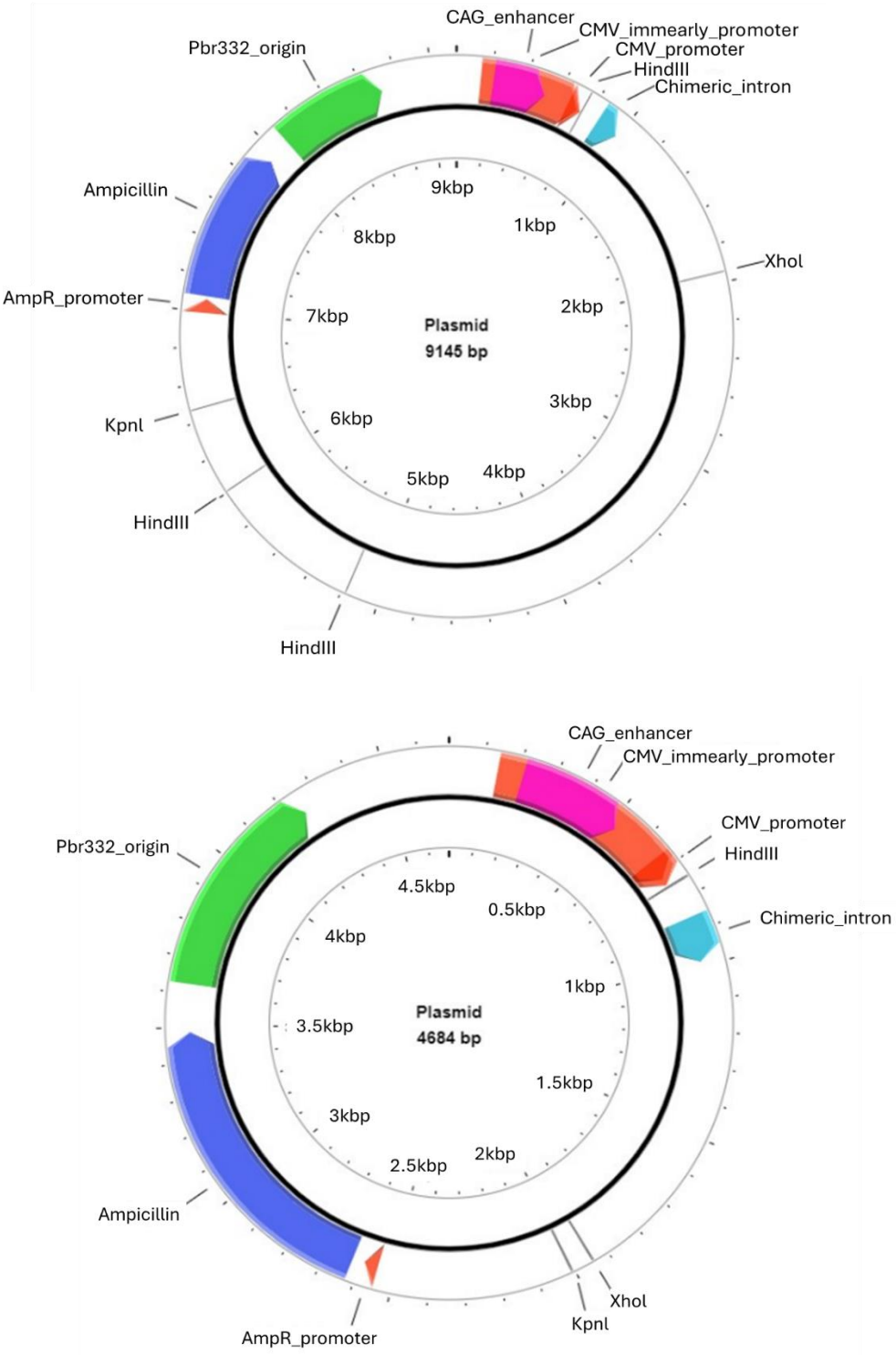

Figure 2.2. Main components of the CFTR vector and the negative control vector. On the top is the CFTR vector containing the CFTR sequence (Appendix I), and on the bottom is the negative control with the CFTR sequence removed. The illustrations were created using PlasMapper 3.0.

Table 2.4 Primers to create the negative control from the CFTR vector.

Primer	**Sequence**
Forward	**TAAACGAATTCGGGCTCG**
Reverse	**CTGAAAGTACAGATCCTCAG**

2.20 RNA EXTRACTION

2.20.1 From cells cultured on 2D conditions

The mouse primary MECs, and the mouse and mammary cell lines cultured on 2D conditions were detached using trypsin (Sigma Aldrich) for 3 minutes. Cells were collected by centrifugation (Allegra X-22R, Beckman Coulter) as a pellet at 1000rpm (193xg) at 4°C. 1ml of TRI reagent (Sigma-Aldrich) was added to the pellet, mixed and transferred to a polypropylene tube. Subsequent steps were carried out in accordance with the manufacturer's instructions.

2.20.2 From cells cultured on 3D conditions

The mouse mammary organoids were collected with cold 1X PBS (Sigma Aldrich) to facilitate Cultrex Basement Membrane Extract (Type 2, Pathclear) dissolution and organoids collection. Subsequently, the mix of PBS, BMM and organoids was centrifuged to obtain an organoid pellet (2 washes with PBS were made). 1ml of TRI reagent (Sigma-Aldrich) was added to the pellet, mixed by pipetting several times and

transferred to a polypropylene tube. Subsequent steps were carried out in accordance with the manufacturer's instructions.

2.21 PROTEIN EXTRACTION

The cells used for protein extraction were seeded according to each experiment described previously. The collection of cells was according to the cell culture used; both methods are described in the following sections.

2.21.1 Protein extraction for cells cultured on 2D conditions

The cells cultured on 2D conditions were trypsinised and collected as a pellet after centrifugation (Allegra X-22R, Beckmen Coulter) at 1000rpm (193xg) at 4°C. Once the pellet was collected, 900µl RIPA buffer (see components in Appendix II) and 100µl of 10X of proteinase inhibitor (Sigma) were added to the pellets, vortexed and incubated on ice for 5 minutes. Centrifugation at 14000xg for 15 minutes was made to obtain the supernatant fraction with proteins.

2.21.2 Protein extraction from the primary organoids

The mammary organoid pellet collection was made by adding cold 1X PBS (Gibco) to the wells with the organoids to facilitate Cultrex Basement Membrane Extract (Type 2, Pathclear) dissolution and organoid collection. Subsequently, the PBS, BMM and

organoids were centrifuged to obtain the organoid pellet (2 washes with PBS were made). 900µl RIPA buffer and 100µl of 10X of proteinase inhibitor (Sigma Aldrich) were added to the organoid pellets, vortexed and incubated on ice for 5 minutes. Centrifugation at 14000xg for 15 minutes was made to obtain the supernatant fraction with proteins.

2.21.3 Protein extraction for the CFTR expression in the membrane and cytoplasmic fractions

The extraction of proteins for the analysis of CFTR expression in the membrane and cytoplasm in the human breast cell lines was conducted with the support of Lisa Ding. The protein extraction was done using the subcellular protein fractionation kit in accordance with the manufacturer's instructions (Thermo Scientific). The cells for each sample were initially collected from 3 wells of 6-well plates at 80%-90% of cell confluence. The cell solution collected was centrifuged (Allegra X-22R, Beckmen Coulter) at 1000rpm (193xg) to obtain a cell pellet. The extracted proteins were stored at -80°C.

2.22 PROTEIN, DNA AND RNA QUANTIFICATION

The protein, DNA and RNA quantification was determined using a Qubit fluorimeter (Invitrogen) in accordance with the manufacturer's instructions (Table 2.5). The plasmid DNA was quantified using a NanoDrop (Thermo Scientific).

Table 2.5 Kits used for the RNA, DNA and protein extraction.

Biomolecule	Name of kit	Brand
RNA	Qubit RNA BR Assay Kit	Invitrogen
DNA	Qubit dsDNA BR Assay Kit	Invitrogen
Protein	Qubit Protein Assay Kit	Invitrogen

2.23 RT-PCR AND QPCR

2.23.1 RT-PCR

100ng RNA was used to do the Reverse Transcription (RT) using the SuperScript IV (Thermo Fisher Scientific). The protocol followed was according to the manufacturer's instructions.

2.23.2 qPCR

qPCR reactions (20µl) were set up using 10µl KAPA SYBR FAST mix (Kapa Biosystems, Inc) 0.25mM forward and reverse primers (Table 2.6), Dnase/Rnase-Free Distilled Water and 1µl cDNA. The cycling parameters used were 95°C for 3 minutes, 40 cycles of amplification at 95°C for 3 seconds, 57°C for 20 seconds and 72°C for 5 seconds (qPCR protocol in Appendix III). This was followed by melting curve acquisition for the specificity of qPCR products. Data were obtained from three independent experiments and had at least 2 technical (PCR) replicates per sample. Negative controls (no template control or no DNA) were included in each qPCR

experiment. The qPCRs were made in the Rotor-Gene (Qiagen), and the relative expression was calculated using data (CT values) obtained from the Q-Rex (Version 1.1.0.4) report.

Table 2.6 Forward and Reverse primers used in the qPCRs.

Primer	**Sequence (5'-3')**
Mouse *Cftr*_Forward	cgctggtgcatacgttaatc
Mouse *Cftr*_Reverse	agaggcagaaagtcatccaaa
Human *CFTR*_Forward	ggcaaacttgactgaactgg
Human *CFTR*_Reverse	tcactgctggtatgctctcc
Mouse *Hprt1*_Forward	aaaggacctctcgaagtgttgg
Mouse *Hprt1*_Reverse	gcgctcatcttaggctttgtat
Human *GAPDH*_Forward	ctgccgtctagaaaaacc
Human *GAPDH*_Reverse	ccaccttcgttgtcatacc
Human *ACTB*_Forward	caccattggcaatgagcggttc
Human *ACTB*_Reverse	acgtggacatccgcaaagacct

2.24 WESTERN BLOT

20µg of protein per sample and 6µl of protein ladder (BlueStar Plus Prestained protein marker) were separated in an 8% sodium dodecyl sulphate (SDS)–polyacrylamide gel electrophoresis (PAGE) (see gel recipe in Appendix IV) at 100V for ~1:40h. The separated proteins were transferred onto PVDF membranes (Millipore) using a semi-dry system (Trans-Blot SD semi-dry transfer cell, Bio-Rad). The membrane was

incubated for 1h in a blocking solution made of 5% (w/v) dried milk (Marvel) diluted in 0.1% (v/v) tween (Prolabo chemicals) in Tris-buffered saline (TBS) buffer (TBST) (see recipe in Appendix V). After blocking, the membrane was incubated overnight with constant agitation with the primary antibody (Table 2.7) diluted in a blocking solution made of 2.5% (w/v) dried milk (Marvel) diluted in 0.1% (v/v) tween (Prolabo chemicals) in TBST. After antibody incubation, 3 washes were done with TBST buffer for 10 minutes (each wash), and secondary antibody (Table 2.6) incubation was done for 1h at room temperature. After secondary incubation, membranes were washed 3X in TBST buffer (10 minutes each). Membranes were incubated in the appropriate secondary antibody (Table 2.7) diluted in TBST. Bands were visualised by chemiluminescence using the western ECL kit (Fast Gene).

Table 2.7 Antibodies used for the WB experiments.

Antibody	**Dilution**	**Supplier**
Rabbit anti-CFTR (polyclonal)	1:500	Alomone labs
Mouse anti-CFTR (monoclonal)	1:500	Bio-techne
Rabbit anti-GAPDH (polyclonal)	1:1000	Santa Cruz
Rabbit anti-B-ACTIN (polyclonal)	1:2000	Abcam
Goat anti-Mouse /HRP	1:1000	Dako
Goat anti-Rabbit /HRP	1:1000	Dako

2.25 STATISTICAL ANALYSIS

For the statistical analysis, the data were first tested for normality distribution by applying the Shapiro-Wilk test. Once the normality distribution was known, parametric or nonparametric tests were used to analyse the data.

Parametric statistical tests were used when the groups to be analysed passed the normality analysis. In contrast, the non-parametric tests were applied when the groups did not pass the normality analysis. The statistical tests used were: the unpaired student's t-test, ordinary one-way ANOVA with (Dunnestt test) and without multiple comparisons, Mann-Whitney and Kruskal-Wallis tests with (Dunn's test) and without multiple comparisons. Each figure legend of results contains the statistical test used for the corresponding analysis.

Statistical significance was analysed using GraphPad PRISM software V 8.4 and 10. Results are expressed with the mean ± Standard Error of Mean (SEM). Data was considered statistically significant, where $P \leq 0.05$.

Chapter 3

3. EXAMINING THE ROLE OF THE CFTR ION CHANNEL AND THE NA^+/K^+ ATPASE IN LUMEN FORMATION AND MAINTENANCE

3.1 INTRODUCTION

The mammary gland is an exocrine gland composed of lobes and lobules forming lactiferous ducts built by epithelial cells. Structurally, the ducts contain an opening inside space free of cells called lumen, whose primary function during lactation is milk transport (Ramsay, Kent et al. 2005). The lumen space is surrounded by a bilayer of epithelial cells, the myoepithelial and luminal cells. The myoepithelial cells represent the outer layer in contact with the BM, while the luminal cells are the inner layer in contact with the luminal space (Biswas, Banerjee et al. 2022).

The lumen space in the mammary gland is formed during embryogenesis (Hogg, Harrison et al. 1983), and from then on, the lumen structure is maintained despite the different developmental and morphological changes that occur during puberty, pregnancy and involution (Oakes, Hilton et al. 2006, Javed and Lteif 2013).

In certain situations, such as the case of breast cancer, the lumen is lost due to its filling with epithelial cells (Gudjonsson, Adriance et al. 2005, Kaushik, Pickup et al. 2016). According to the American Cancer Society, the most common invasive breast cancer is ductal, which represents 75% of breast cancers. Ductal breast cancer progression begins with ductal hyperplasia followed by atypical hyperplasia, characterised by multilayering and proliferation of monomorphic epithelial cells and depolarised cells (Chatterjee and McCaffrey 2014). Further progression can lead to ductal carcinoma in situ and subsequently to metastasis (Figure 3.1). Continuous alteration of the lumen structure and the changes from a single lumen to multilumens

are reflected by the progressive stages of breast cancer (Halaoui, Rejon et al. 2017). Since alterations in the lumen structure characterise breast cancer, understanding what regulates normal lumen maintenance is therefore important. This project addresses lumen formation and maintenance.

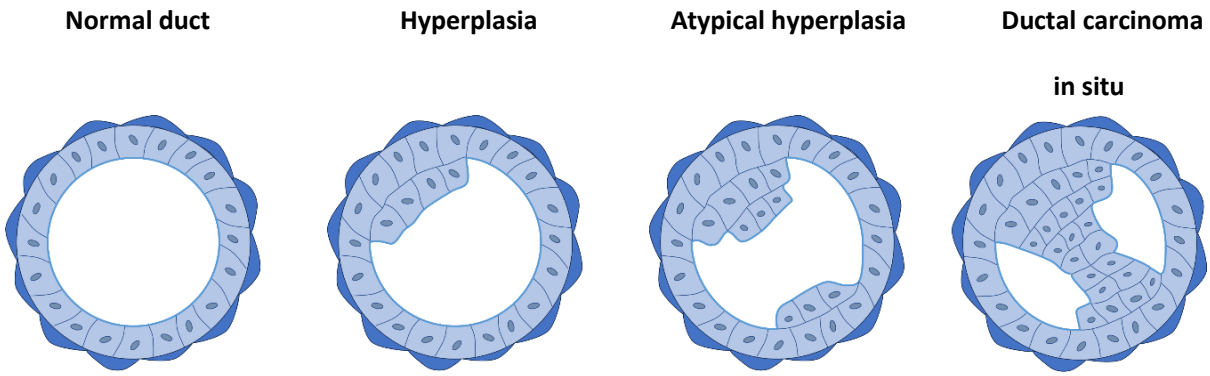

Figure 3.1. Stages of breast cancer progression and lumen structure changes. Image adapted from Chatterjee and McCaffrey 2014. The illustration was self-drawn based on the citations mentioned in this figure legend.

The fluid secretion mechanism explains how a single lumen is formed by hydrostatic pressure created from fluid secretion and its accumulation in a limited area (Li, Findlay et al. 2004, Bagnat, Cheung et al. 2007). In epithelial cells, fluid secretion depends on the transport of ions such as Cl^- and Na^+, which creates an osmotic gradient triggering fluid transport (Almassy, Siguenza et al. 2018). Ion transporters such as ion channels and the Na^+/K^+ pump are the main proteins that control the electrochemical and osmotic gradient in the cell, and their normal expression and activity are essential to maintain secretion and absorption homeostasis in epithelial cells (Palk, Sneyd et al. 2010, Saint-Criq and Gray 2017). CFTR is known to control fluid secretion in epithelial cells through Cl^- secretion from the apical membrane, promoting paracellular and

transcellular fluid transport in conjunction with other ion channel activities (Frizzell and Hanrahan 2012).

The relevance of CFTR and Na^+/K^+ pump activity in fluid secretion has primarily been studied using drugs, including inhibitors and stimulators. For example, CFTRinh-172 is a specific inhibitor for CFTR (Caci, Caputo et al. 2008); ouabain, an inhibitor of the Na^+/K^+-ATPase activity (Schatzmann 1953); and forskolin, a cAMP-raising drug that stimulates CFTR and Na^+/K^+-ATPase activity (Daly 1984, Haws, Nepomuceno et al. 1996). In order to investigate lumen formation and maintenance in MECs, a representative three-dimensional cell culture consisting of BMM was required. This model has similar in vivo BM components such as collagen IV, laminin, entactin, heparin sulphate proteoglycans and growth factors (Vukicevic, Kleinman et al. 1992, Zhao, Chen et al. 2022). The properties of this system allow the establishment of proper cell interactions between the BMM and cells, recapitulating numerous features of the mammary epithelium, leading the cell organisation and polarisation to form structures such as the lumen (Petersen, Ronnov-Jessen et al. 1992, Campbell and Watson 2009).

Although the mammary gland is an exocrine gland, its secretory function beyond lactation is poorly studied. Likewise, the mechanisms of lumen formation in this organ are not well understood; specifically, it is unknown if key regulators of fluid secretion participate in the formation and maintenance of a single lumen. Since fluid secretion is a mechanism of lumen formation in some organs of the zebrafish (Bagnat, Navis et al. 2010, Navis, Marjoram et al. 2013) and in vitro in kidney epithelial cells (Narayanan,

Schappell et al. 2020), the hypothesis for this Chapter is that the **fluid secretion is a mechanism that participates in forming and maintaining a lumen in MECs and it is dependent upon the activity of CFTR and Na^+/K^+-ATPase**. This first chapter aims to determine whether CFTR and Na^+/K^+-ATPase activity regulates lumen morphogenesis and maintenance in mouse mammary epithelial cells. The Objectives for this Chapter are:

- To evaluate the effect of CFTR and Na^+/K^+-ATPase stimulation in lumen formation and lumen area maintenance using forskolin in primary mammary epithelial cells and EpH4 cells cultured in 3D conditions with BMM.
- Determine whether the inhibition of CFTR and Na^+/K^+-ATPase activity with CFTR-inh172 or ouabain in primary mammary epithelial cells and EpH4 cells cultured in 3D conditions with BMM alters lumen formation and area.

3.2 METHODS

3.2.1 Mammary gland dissection and epithelial cell collection

The maintenance and handling of mice were carried out in accordance with the Animals (Scientific Procedures) Act 1986 (and associated practices) of the UK legislation under Project Licence PP1836785. The mice were kept at 22°C with 40-60% and 12h photoperiod in the Biological Services Unit of the Medical School of the University of Sheffield. Mice were killed using the Schedule 1 procedure by a trained and registered practitioner.

The β1-integrin fx/fx: YPF: K14-CreERTM transgenic mice were culled by cervical dislocation and dissected in sterile conditions to obtain the mammary gland tissue. All material for dissection was previously sterilised, and the dissection incision was made from the perianal area to the neck to collect tissue from 5 pairs of mammary glands. The tissue obtained was processed as described in section 2.2. At least 3 mice were used per experiment (n=3).

3.2.2 Lumen tracking

Mouse primary MECs and EpH4 cells were cultured according to the procedure described in sections 2.4.2 and 2.4.1, respectively. For each cell model, three different experiments with three replicates per experiment were performed in order to count the number of lumens formed throughout. The 3D cell structures with lumen counting were

evaluated from photos taken from random sections of the samples. At least 100 3D cell structures of the EpH4 cells or 60 mammary organoids were counted per experiment. An adherent plastic grid was used on the bottom of the plates to facilitate counting the organoids and EpH4 3D cell structures (Figure 3.2).

A)

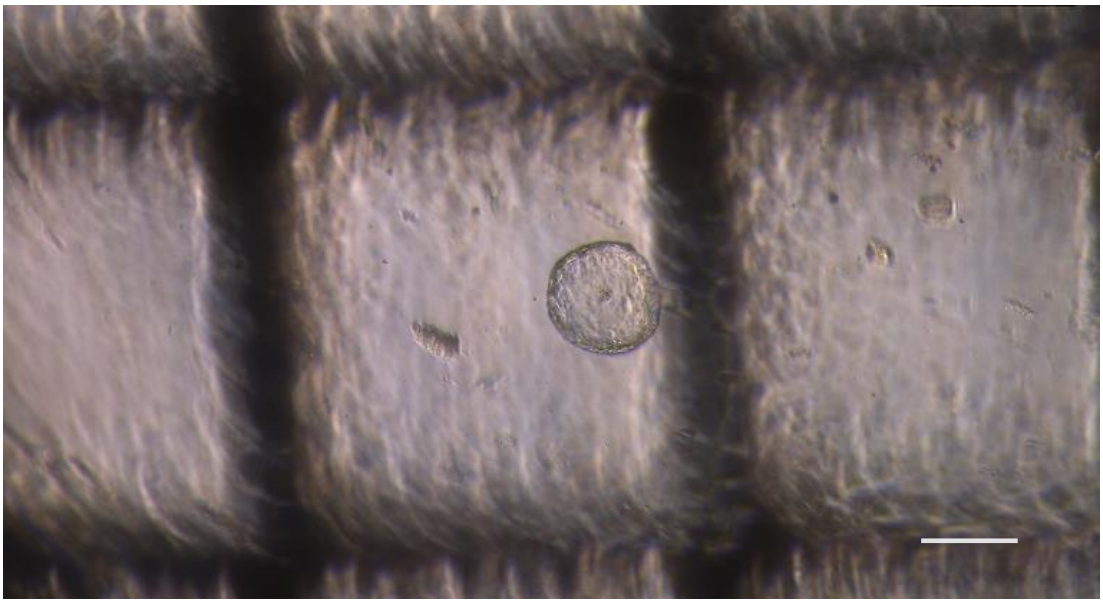

B)

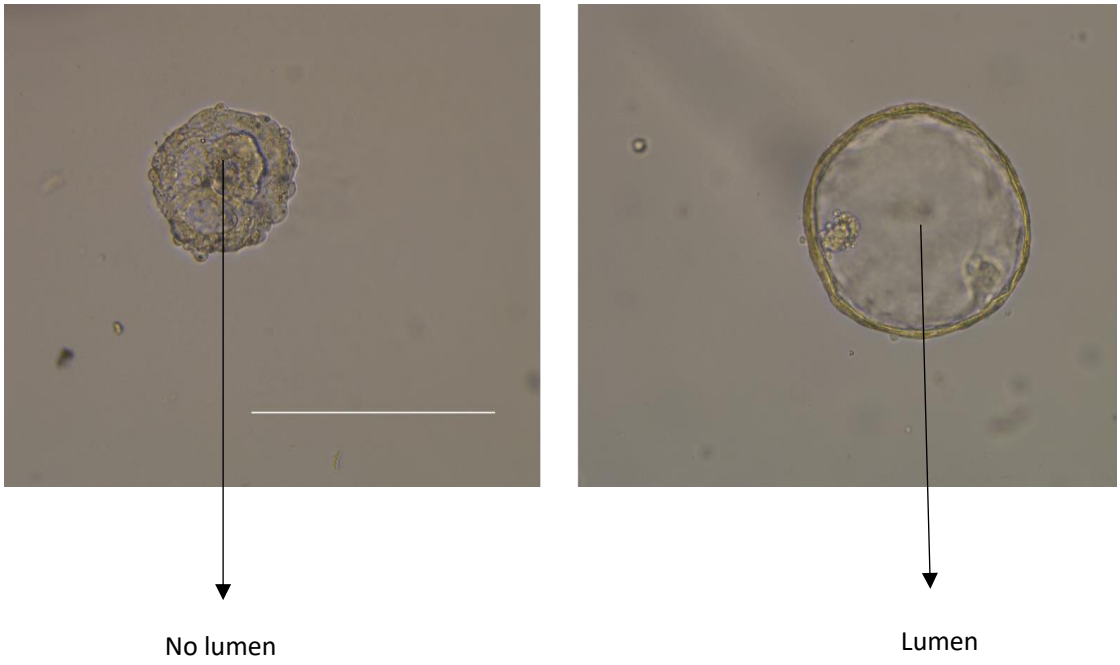

Figure 3.2. Mammary organoids with and without a lumen. A) Example of a mammary organoid located in the light microscope (Leica DMi1) using a plastic grid. Scale bar= 100µm. Microscope magnification= 5X. B) An example of mammary organoids with and without a lumen located in the light microscope (Leica Dmi1). Scale bar= 100µm. Microscope magnification= 20X.

3.2.3 Drug treatments

The mouse primary MECs and EpH4 cells were seeded in 3D conditions to allow lumen formation. The procedure was carried out according to the protocol described in sections 2.5.1 and 2.6.1. The stimulation of CFTR and the Na^+/K^+ pump in cell culture were made using 10µM forskolin. The blocking of CFTR ion channel activity was made using 10µM CFTRinh-172. The Na^+/K^+ pump blocking was made using ouabain at 1nM, 10nM, and 100nM concentration. The drug treatment was applied in the media where the primary MECs or EpH4 cells were cultured for 3-4 days in 3D conditions (see complete description section 2.7). After 24h of treatment, lumen structures were evaluated in both cell models. Three experiments with three replicates were done for both kinds of cells. For the experiments with the EpH4, different cell passage numbers were used for each experiment.

3.2.4 The number of lumens formed and the change in the lumen area

A plastic grid was collocated on the bottom of the plates to count the number of organoids or EpH4 3D cell structures with and without lumen and to localise the same cell structures for lumen area measurements in the light microscope (Figure 3.2A and 3.3). The three replicates of the three experiments were counted independently. Data

were normalised to the percentage of lumens before the treatments. The change in lumen area is presented as an average of independent organoids or EpH4 acini structures measured from 3 different experiments as described in section 2.8.

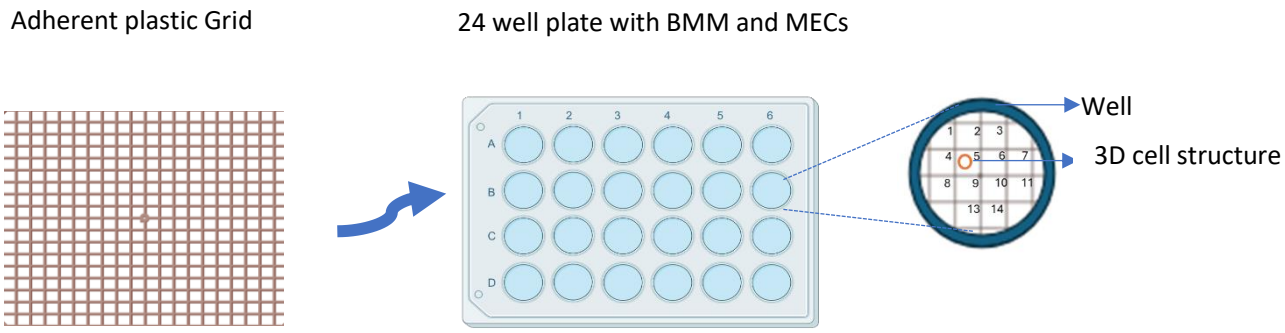

Figure 3.3 Location of 3D cell structures in the 24 well plates. The adherent plastic grid was placed on the bottom part of the 24 well plates, where previously, the MECs were cultured on BMM and formed 3D cell structures. Under the light microscope, the 3D cell structures can be located in the squares of the grid. The illustration was self-drawn.

3.2.5 Staining

The organoids from the drug treatment experiments were used for the F-actin with TRITC-phalloidin (Sigma Aldrich) and nuclei staining Hoechst 33258. The protocol followed is described in section 2.9.2.

3.3 RESULTS

3.3.1 Lumen tracking

The MECs were seeded in 3D conditions with BMM to allow cell organisation and formation of luminal structures. As a first step, the time course of lumen formation was evaluated.

EpH4 cells began to form lumens from day 1 after being seeded on the BMM. The 3D cell structures considered to exhibit a lumen (acini) have a well-defined structure of cells surrounding the contour of a continuous luminal space. Over time, an increase in the percentage of lumens formed was observed (Figure 3.4). The percentage of lumens formed on day three was 18%; on day four, 29%; and on day five, 31%. A cross all days, a combination of 3D cell structures with or without lumen was observed.

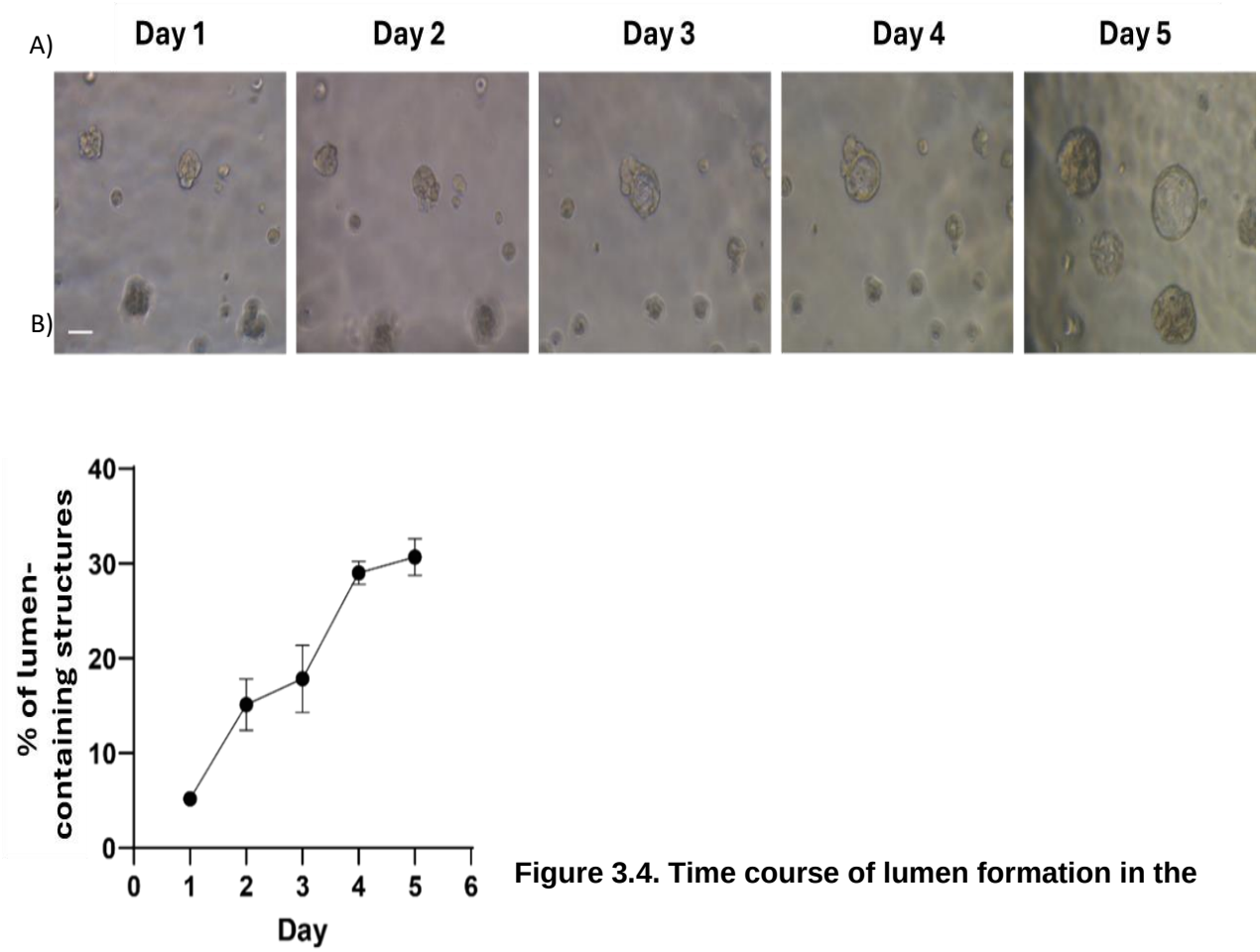

Figure 3.4. Time course of lumen formation in the Eph4 cells. The cells were cultured for 5 days in BMM to allow the formation of acini structures. Photos were taken daily with a light microscope to monitor lumen formation. A) Representative images of lumen development with EpH4 cells. Scale bar=50μm. Microscope magnification= 20X. B) Percentage of acini structures formed in the first 5 days after the cells were seeded. At least 100 3D cell structures per experiment were counted. Data represent three independent experiments (n=3). The graph shows mean ± SEM.

The mouse primary MECs were seeded with BMM to form organoids, and lumen formation was monitored during the 4 subsequent days. On day 1, the organoids were observed as small parts of a self-organised three-dimensional tissue; however, there was no evidence of lumen formation at this time point. On the second day, 18% of the organoids contained a lumen structure; on the third day, 33% and on the fourth day, 44% of organoids contained a lumen (Figure 3.5).

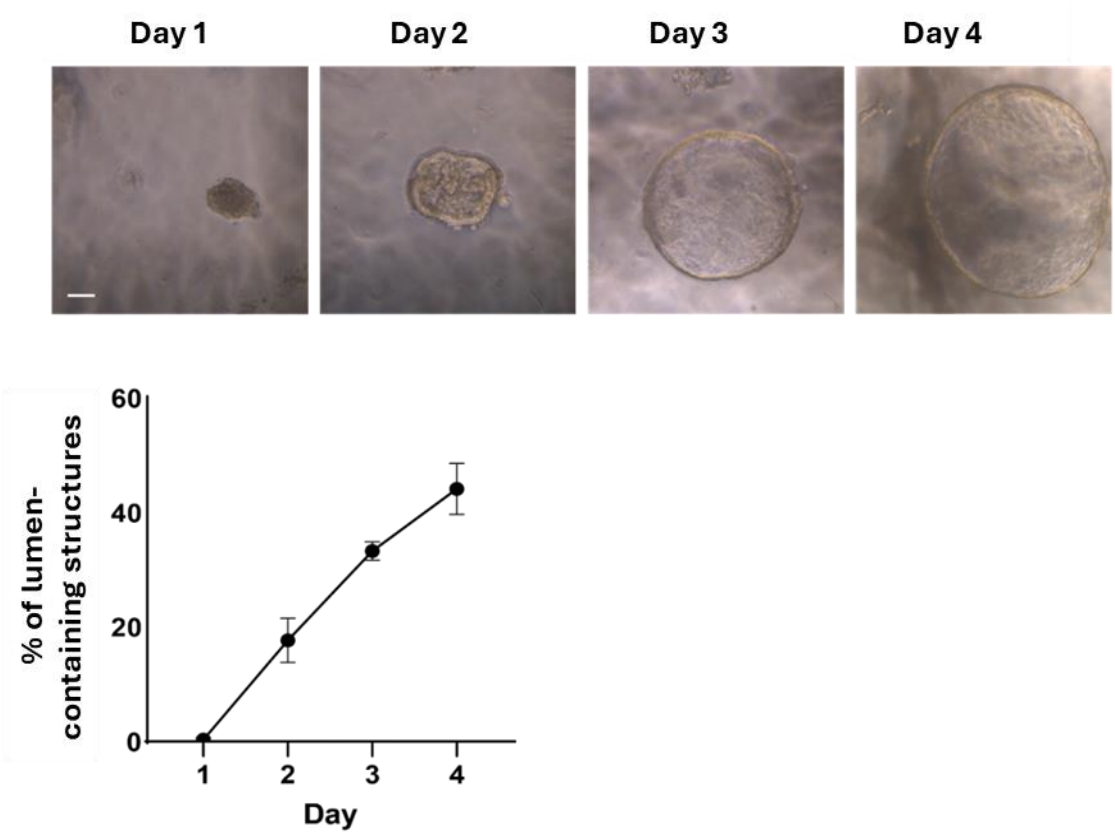

Figure 3.5. Time course of lumen formation in primary MECs organoids. The cells were cultured with BMM for 4 days. Photos were taken daily with a light microscope to monitor the lumen formation. A) Representative images of lumen development in primary mammary organoids. Scale bar = 50µm. Microscope magnification= 20X. B) Percentage of organoids with a lumen formed in the first 4 days after the cells were seeded. At least 60 organoids per experiment were counted. Data represents three independent experiments (n=3). The graph shows mean ± SEM.

Day 2 was the earliest time in which both cultures (EpH4 or primary MECs) showed the presence of lumens structures. On day 3, some lumens previously formed on day 2 were maintained, and some 3D cell structures without lumens of both cell cultures opened from day 2 to 3. On day 4, some lumens formed were maintained, and some lumens were formed from days 3 to 4. As lumen development occurs during the first days of cell culture, the earliest days (2 and 3), with both features of lumen formation and maintenance, were chosen to interrogate the effect of CFTR and Na^+/K^+ ATPase activity on lumen formation as well as their effect on the lumens already formed. The treatments were applied on days 2 and 3, and the drug effect was analysed on days

3 and 4. In addition, the study of the drug treatment effect on lumen structure at two different times provides information about the reproducibility of the drug effect on lumens, independently of the time applied.

3.3.2 Lumen formation

The alteration of the activity of CFTR and Na^+/K^+ pump to evaluate lumen formation was evaluated using forskolin, ouabain and CFTRinh-172. As the drugs were dissolved in DMSO and water, it was first tested if the same volume of these diluents caused an effect on the lumen formation in our model. The results show that on both days (3 and 4), the % of EpH4 acini structures or primary organoids with lumen did not differ between cultures exposed to these components (Figure 3.6).

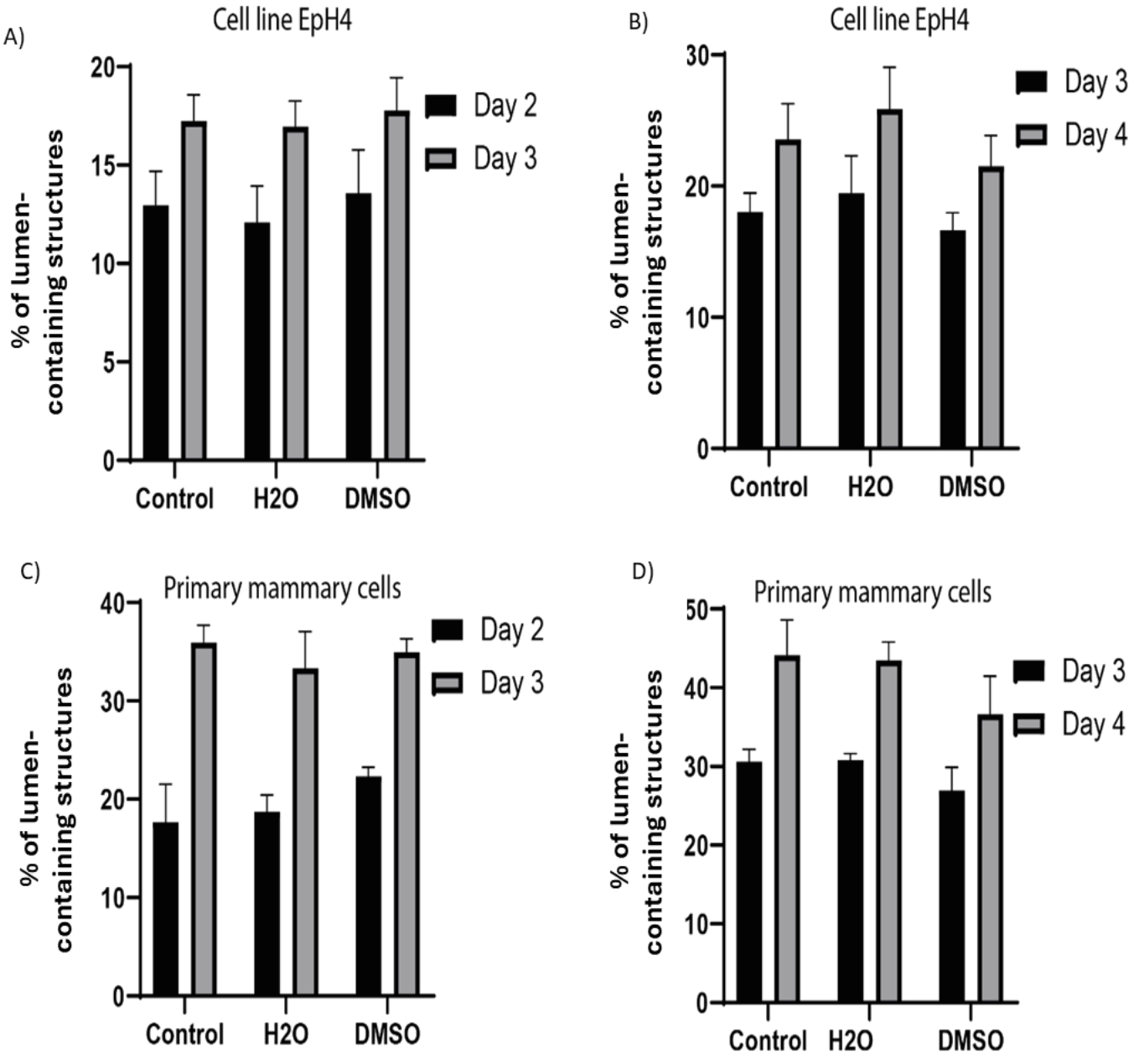

Figure 3.6. Percentage of lumens formed in different control conditions in EpH4 cells and primary MECs. The cells were cultured in BMM, and 1% water or DMSO was added to the cell culture media on days 2 or 3 after the cells were seeded. A) and B) Percentage of lumens formed with the EpH4 cells on days 3 and 4, respectively. C) and D) Percentage of lumens formed with the primary MECs on days 3 and 4, respectively. Data shows the n=3. Each n represents an independent experiment and is made up of a count of at least 40 3D cell structures per group. The data shows mean ± SEM. An ANOVA statistical analysis was performed for each graph to compare the groups after the diluents were applied, and a $P > 0.05$ was obtained.

3.3.2.1 EPH4 CELLS CULTURED ON 3D CONDITIONS WITH BMM

Once the volume of the vehicle substances was shown not to significantly affect outcomes, the experiments involving the drug treatments were applied. Forskolin, ouabain, or CFTRinh-172 were added to the complete media on days 2 or 3, and an evaluation of lumen formation was made. Analysis of the percentages of lumen formation was done before and after the treatments (Figures 3.7A and C), and the percentage of these changes in lumen formation of each treatment group was compared to the control group (Figures 3.7B and D).

The forskolin effect in the EpH4 cells on day 3 showed a significant difference (*P<0.05)*, increasing the number of lumens formed (Figure 3.7A) by 136.9% to the control (Figure 3.7B). The ouabain treatment applied on day 2 and evaluated on day 3 did not inhibit lumen formation in EpH4 cells, with any of the drug concentrations used. The samples treated with 1nM ouabain dose present lumen formation (Figure 3.7 A). CFTRinh-172 treatment affected the number of new and existing lumens by 85.16%; 34.23% in new lumens and reducing the existing lumens by 50.93% (P<0.01) (Figure 3.7 A). These results indicate that forskolin and CFTR-inh172 have an effect on lumen formation in the 3D EpH4 cell structures when the drugs are applied in the media on day 2 and analysed on day 3.

When treatments were applied on day 3 and evaluated on day 4, similar results were observed in the forskolin samples. The lumen formation increased significantly (44.2%; P<0.05). All the ouabain doses and the CFTRinh-172 inhibitor, had an effect

decreasing lumen formation (Figure 3.7C and D). With Ouabain 1nM, 10nM and 100nM doses, lumens were reduced by 41.7% (*P<0.05*), 73.55% (*P<0.01*) and 81.1% (*P<0.01*) compared with the control (Figure 3.7D). CFTRinh-172 treatment reduced the number of lumens by 111.15% compared with the control (P<0.001) (Figure 3.7D). These results indicate that the indirect stimulation of the Na+/K+ pump and CFTR ion channel by forskolin applied on day 3 and evaluated on day 4 increased the lumen formation in 3D cell structures formed by EpH4 cells. Opposite to this effect, the three different ouabain doses and the CFTRinh-172 decreased the lumen formation after blocking the Na+/K+ pump and CFTR ion channel activity, respectively.

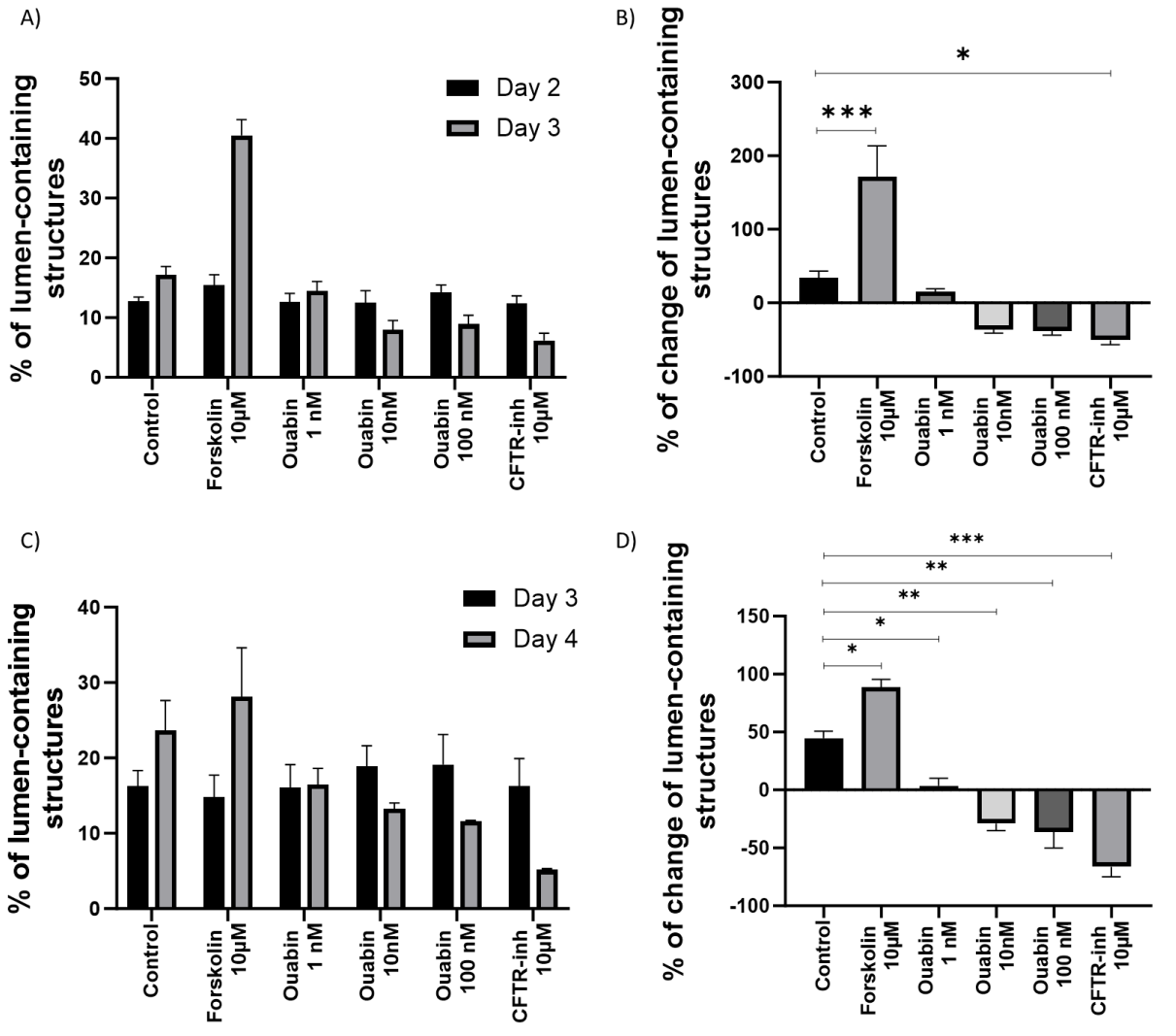

Figure 3.7. Drug effect on the percentage of lumens formed with EpH4 cells cultured on 3D conditions with BMM. Drugs were added on days 2 or 3, and acini structures were counted before and after 24h of treatment. The control group represents the mean of the water and DMSO control group. A) and C) show the percentage of acini structure before and after the treatments. The graph shows mean ± SEM. B) and D) show the percentage change in the number of acini structures after the treatments on days 3 and 4. The graph shows mean ± SEM. Data shows the n=3 for A) and B) and n=2 for C) and D). Each n represents an independent experiment and is made up of at least 50 3D cell structures per group. A Dunnett's multiple comparisons test was used to compare the control group with each treatment group. *$p < 0.05$; **$p<0.01$; *** $p< 0.001$.

3.3.2.2 PRIMARY MECS CULTURED IN 3D CONDITIONS WITH BMM

The same drug doses and treatment days described in the 3.3.2.1 section for the EpH4 cells were applied to the primary MECs in 3D cell culture conditions. Analysis of the percentages of lumen formation was done before and after the treatments (Figures 3.8A and C), and the percentage of these changes in lumen formation of each treatment group was compared to the control group (Figures 3.8B and D).

The results show that on day 3, forskolin increased the number of acini structures (Figure 3.8A) by 77.33% compared with the control (Figure 3.8B), however this change is not statistically significant (*P=0.12*). 10nM and 100nM ouabain doses inhibited the formation of new lumens (Figure 3.8A), showing significant differences (*P<0.05* and *P<0.01)* (Figure 3.8B). The most significant effect with ouabain treatment was observed with the 100nM dose. This not only cause inhibition of lumen formation, but it also decreased the previous lumens formed by 14.67% (Figure 3.8B). CFTR activity inhibition had a substantial effect (P<0.001) on the inhibition of the formation of new lumens. In addition, this treatment also showed a reduction by 96.3% of the lumens previously formed on day 2 (Figure 3.8B). These results show that the inhibitors

ouabain (10nM and 100nM) and CFTRinh-172 significantly affect the lumen formation when applied to primary mammary organoids on day 2.

On day 4, forskolin increased the number of organoids with lumens by 125.33% compared with the control (*P<0.05*) (Figures 3.8A and B). The treatments with the 1nM *(P=0.82)*, 10nM *(P=0.25)* and 100nM *(P=0.37)* ouabain doses did not show significant changes in lumen formation. The number of organoids with lumen before the ouabain treatments was conserved (Figure 3.8C). The inhibition of CFTR activity reduced (*p<0.001*) the lumen formation compared with the control by 193% (Figure 3.8C). CFTRinh-172 reduced the previous lumens counted before the treatment by 97% (Figure 3.8D). These results show that the number of lumens increased or decreased after the forskolin and CFTRinh-172 treatments were applied on day 3 to the media where primary mammary organoids are cultured on 3D conditions.

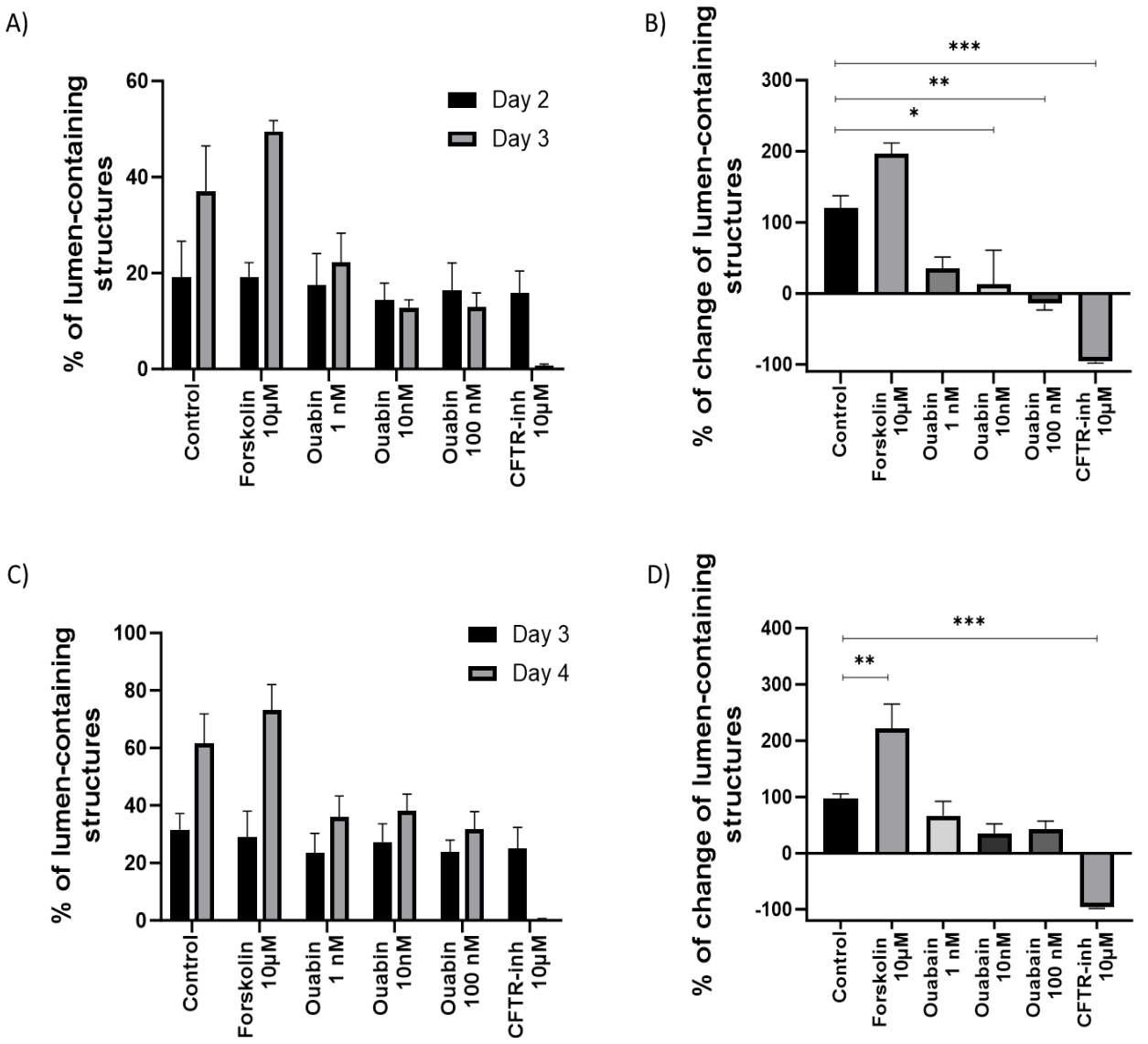

Figure 3.8. Drug effect on the percentage of lumens on primary organoids on days 3 and 4. Drugs were added on days 2 or 3, and lumens were counted before and after 24h of treatment. A) and C) show the percentage of organoids with lumens before and after the treatments. The graph shows mean ± SEM. B) and D) show the percentage change of organoids with lumens after the treatments on days 3 and 4. The graph shows mean ± SEM. Data shows the n=3. Each n represents an independent experiment and is made up of at least 50 organoids per group. A Dunnett's multiple comparisons test was used to compare the control group with each treatment group. **p<0.05; **p<0.01; *** p< 0.001.*

3.3.3 Lumen maintenance

Once the effect of the CFTR and Na^+/K^+ pump activity was tested on the number of lumens, the lumen expansion and maintenance were evaluated. To study this, the change of lumen area was measured in the primary MECs and EpH4 acini structures that presented a continuous lumen before the drug treatment. The acini were located before and after 24h of treatment, and their lumen areas were measured and compared.

3.3.3.1 LUMEN IN EPH4 ACINI

The area change was measured in the EpH4 acini structures on day 2 before the drug treatment and on day 3, after the treatment (Figure 3.9A). On day 3, forskolin did not significantly increase the lumen area (Figure 3.9B). Ouabain treatments decreased the lumen area with the highest ouabain dose (100nM). The lumen size decreased by 83% in the acini structures, showing a significant difference compared with the control ($P<0.05$). The treatment for CFTR blocking showed a significant ($P<0.05$) reduction in lumen area of 100%. In this group, no lumen area was observed (Figures 3.9A and B).

On day 4, the forskolin treatment had not effect on the lumen area. The CFTR treatment showed congruence with the result obtained on day 3, since it drastically reduced the lumen area by 97.93% ($P<0.05$). The ouabain doses had no effect on the lumen area (Figure 3.9B).

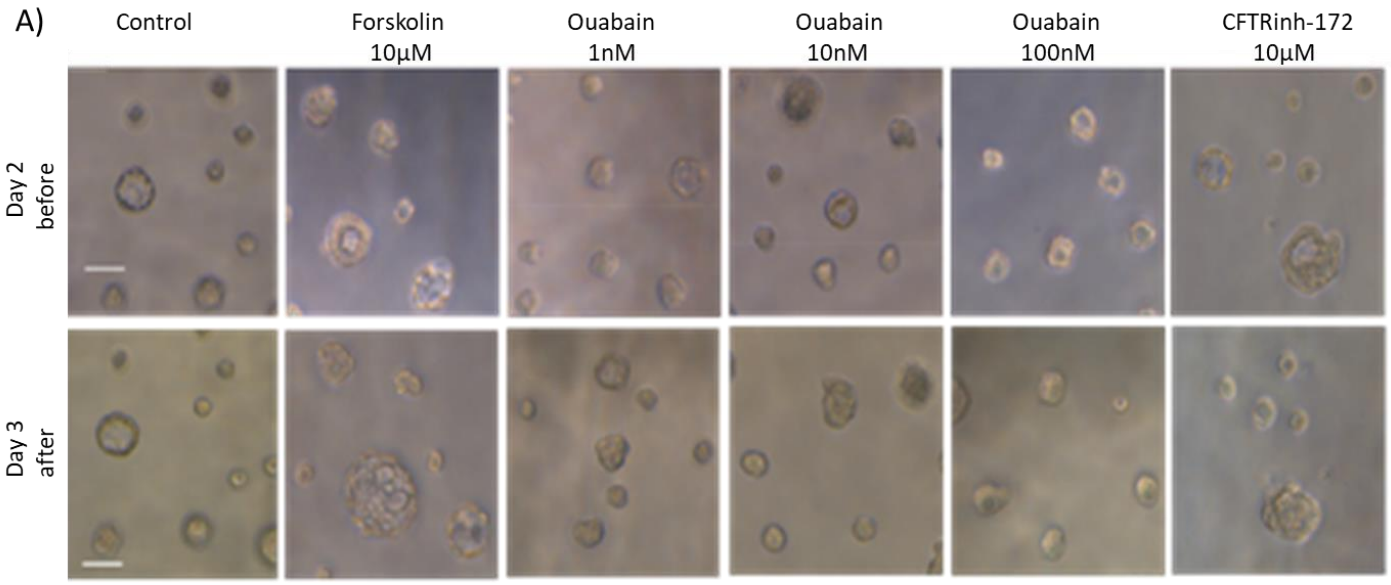
A)
Control
Forskolin 10µM
Ouabain 1nM
Ouabain 10nM
Ouabain 100nM
CFTRinh-172 10µM
Day 2 before
Day 3 after

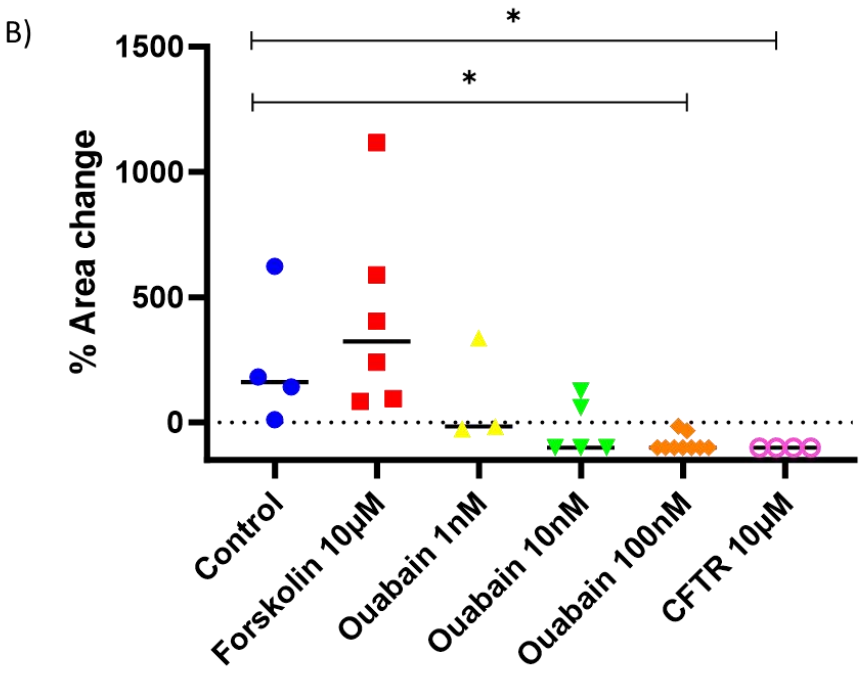
B)
% Area change
1500
1000
500
0
*
*
Control
Forskolin 10µM
Ouabain 1nM
Ouabain 10nM
Ouabain 100nM
CFTR 10µM

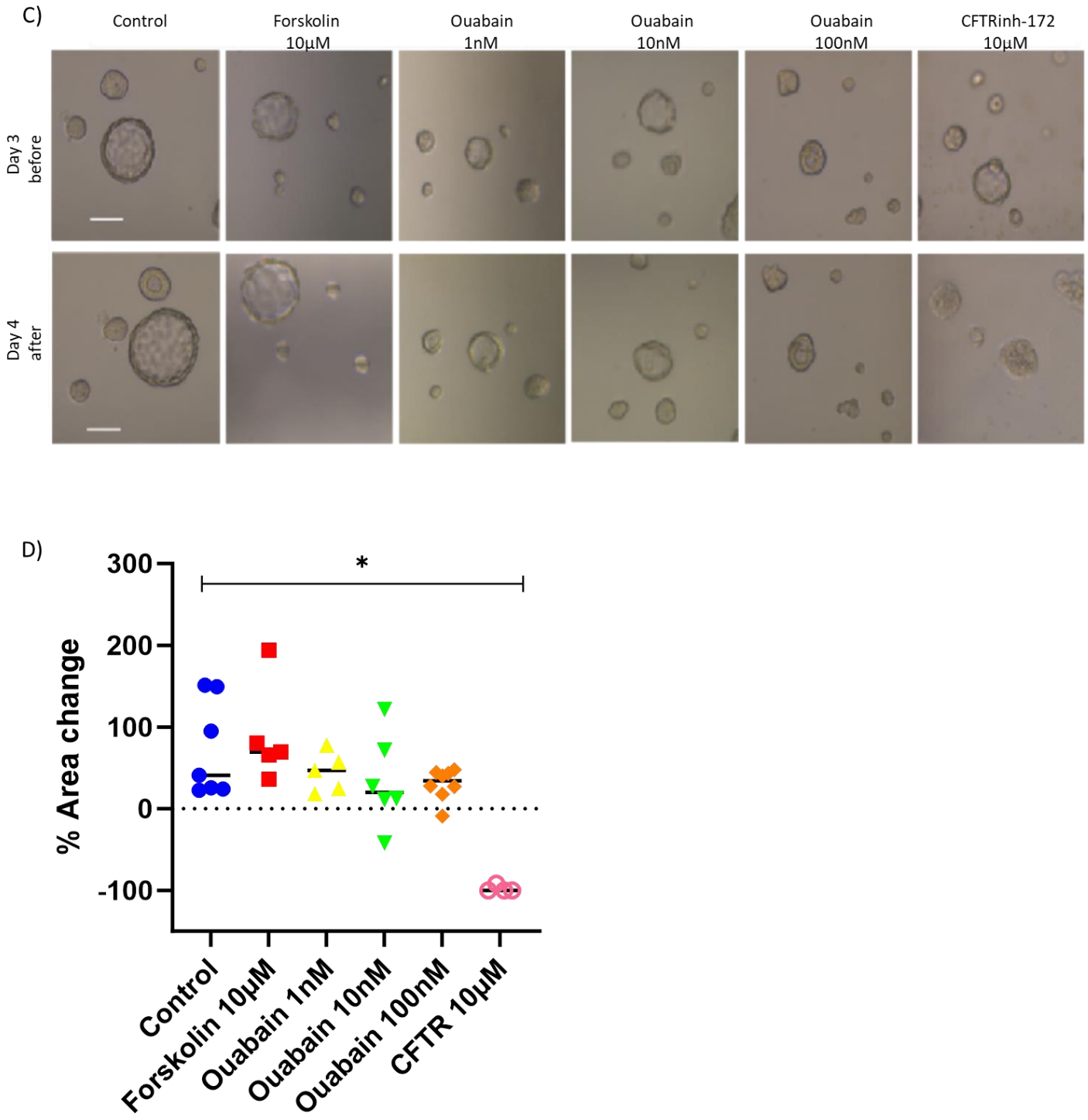

Figure 3.9. Change of lumen area after treatments in the EpH4 cultured in 3D conditions with BMM. Drugs were added to the EpH4 cells cultured in 3D conditions on days 2 or 3. A) and C) Representative EpH4 acini before and after drug treatment. Scale bar= 50µm. Microscope magnification= 20X. B) and D) Graphs show the mean of the percentage of change of lumen area after treatments. Each measurement was normalised with its initial lumen area. At least 3 acini from 3 independent experiments were analysed. A Dunn's multiple comparisons test was used to compare the treatment groups with the control group. **P < 0.05.*

The results of the lumen area evaluation after the drug treatments on days 3 and 4 show that the ouabain (100nM) and CFTRinh-172 decreased the lumen area in EpH4 acini.

3.3.3.2 LUMEN IN PRIMARY ORGANOIDS

The results showed that the lumen area changed by altering the activity of the CFTR and the Na^+/K^+ pump in the mouse mammary organoids. The drug treatments were applied as was done for the EpH4 cells in the 3.3.3.1 section. Figure 3.10A exemplifies the organoid area change before and after applying the treatments on day 2 and the drug effect on day 3. On day 3, the mean area of the control increased by 119.6%, while organoids with forskolin treatment increased to 234.4%. The difference between the increased lumen area of the control group and the forskolin group was 114%; however, it did not show a significant difference (Figure 3.10B). The lumen area of the organoids group treated with 1nM ouabain was not different from the control. Likewise, the mean lumen area of organoids treated with 10nM ouabain was not significantly different from the control. Organoids exposed to 100nM ouabain often exhibited a morphological change from a single continuous area to several small mini areas or micro lumens (Figure 3.10E); in this group, the lumen size was decreased ($P<0.05$). Organoids exposed to the CFTR inhibitor also had a reduction in mean lumen area relative to the control ($P<0.01$). The organoid structure change was evident when observing the lumens filling with cells (Figure 3.10A). The lumens looked completely collapsed after 24h of CFTRinh-

172 treatment. The CFTRinh-172 effect was the most potent, decreasing the area by 100% with the original lumen area (Figure 3.10B).

Organoids on day 4 showed a similar behaviour as they presented on day 3 after treatments (Figure 3.10C). Forskolin increased the original mean lumen area by 253% and 133% more than the control; however, this change is not statistically significant (Figure 3.10D). The mean of the lumen area of the organoids subjected to the inhibition of the Na^+/K^+ pump activity with 1nM and 10nM ouabain doses did not change statistically significantly compared with the control. However, the mean lumen area of the organoids treated with the 100nM dose caused a reduction of 22.1% (*P<0.01).* The CFTR activity inhibition by CFTRinh-172 had the strongest effect on lumen area decrease. Most organoids did not present a lumen structure after 24h of CFTRinh-172 treatment (Figure 3.10C), decreasing the initial lumen area by 92.1% (*P<0.0001)* (Figure 3.10D).

These results show that the CFTRinh-172 and ouabain inhibitors affect the lumen area in mammary epithelial organoids on both days evaluated after the drug treatments (3 and 4).

A)

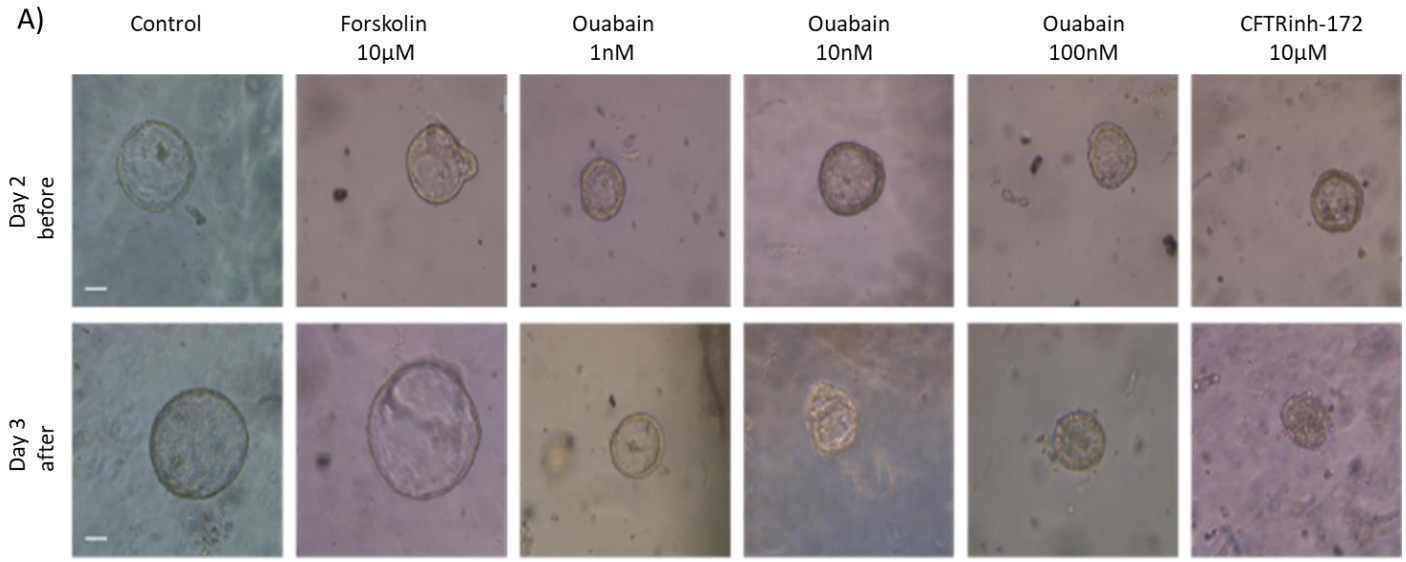
Control
Forskolin 10µM
Ouabain 1nM
Ouabain 10nM
Ouabain 100nM
CFTRinh-172 10µM
Day 2 before
Day 3 after

B)

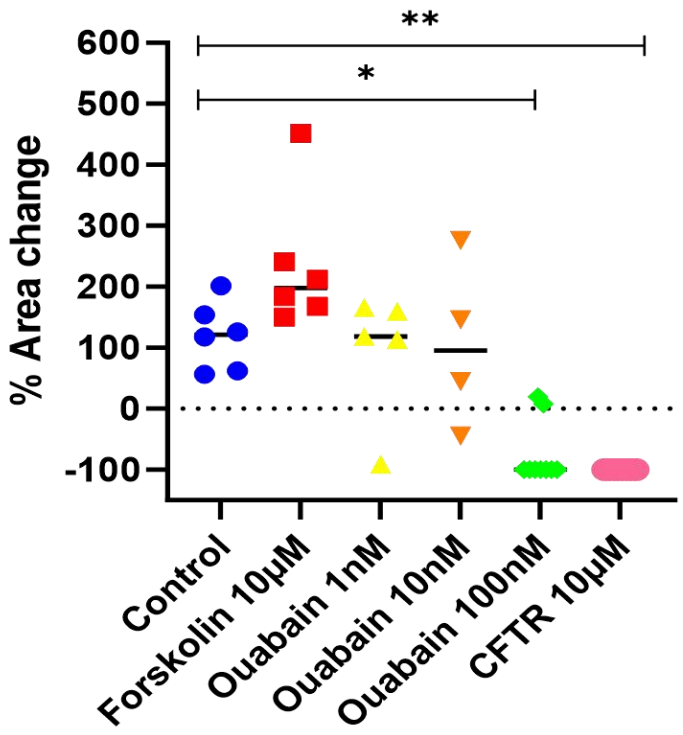
**
*
600
500
400
300
200
100
0
-100
% Area change
Control
Forskolin 10µM
Ouabain 1nM
Ouabain 10nM
Ouabain 100nM
CFTR 10µM

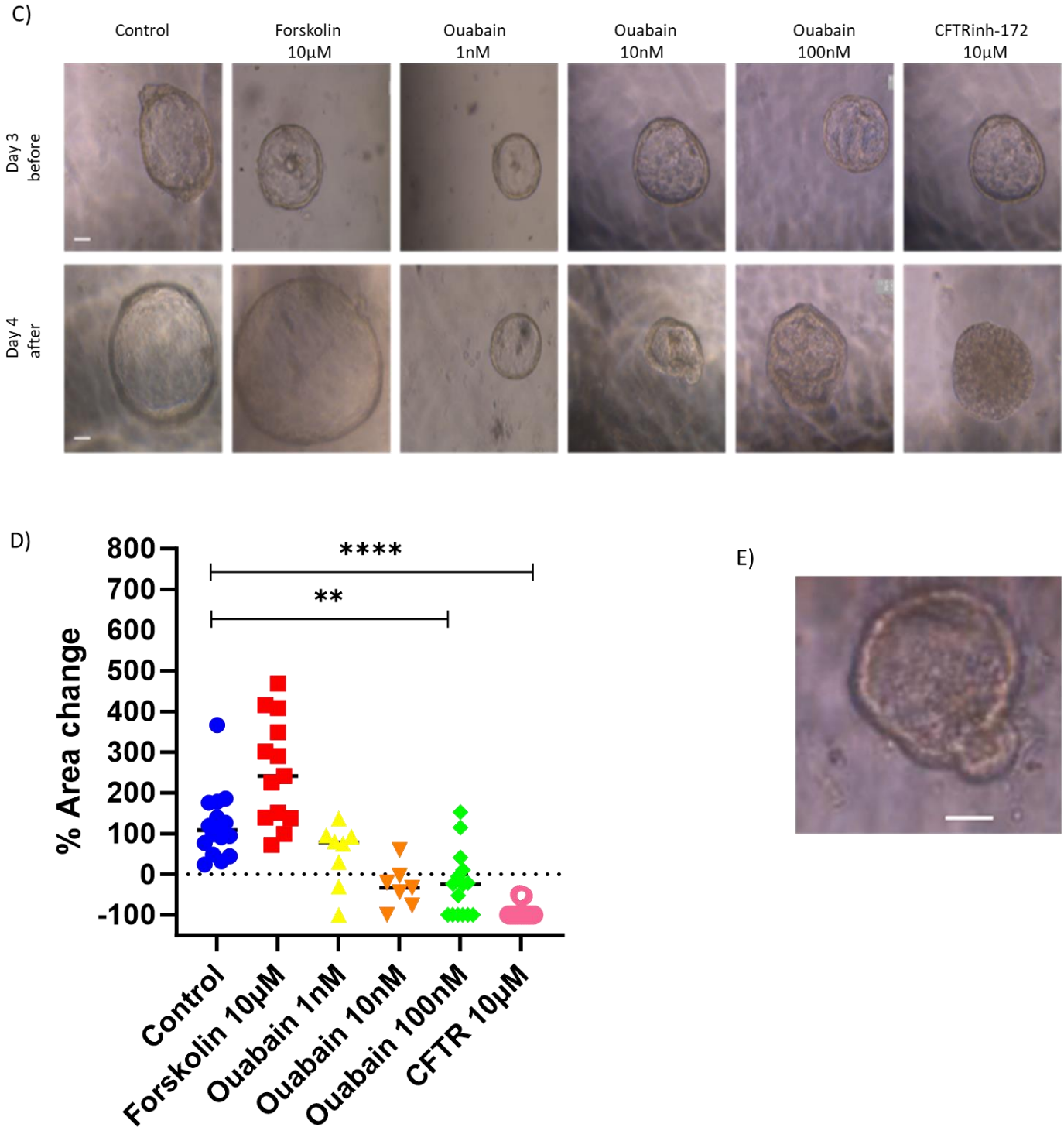

Figure 3.10. Area change of lumens after treatment in primary mammary organoids. Drugs were added on days 2 or 3, and photos of the same organoids were taken with the light microscope before and after treatment to evaluate their lumen area. A) and C) Representative organoids before and after drug treatment. E) Example of organoid with cells in lumen after the 100nM ouabain treatment. Scale bar= 50µm. Microscope magnification= 20X. B) and D) Graphs show the mean of the percentage of change of lumen area after treatments. Each measurement was normalised with its initial lumen area. At least 4 organoids from 3

independent experiments were analysed. A Dunn's multiple comparisons test was used to compare the treatment group with the control group. *$P < 0.05$; **$P<0.01$; ****$P<0.0001$.

Organoids were stained with F-actin to further evaluate the effects of the drugs on morphology. A single continuous lumen was observed in the control and forskolin treated organoids. Some of the organoids exposed to 100nM ouabain showed the presence of cells in the lumen. In the CFTRinh-172 group, most organoids showed a total absence of the lumen and cell uniformity throughout the entire organoid (Figure 3.11).

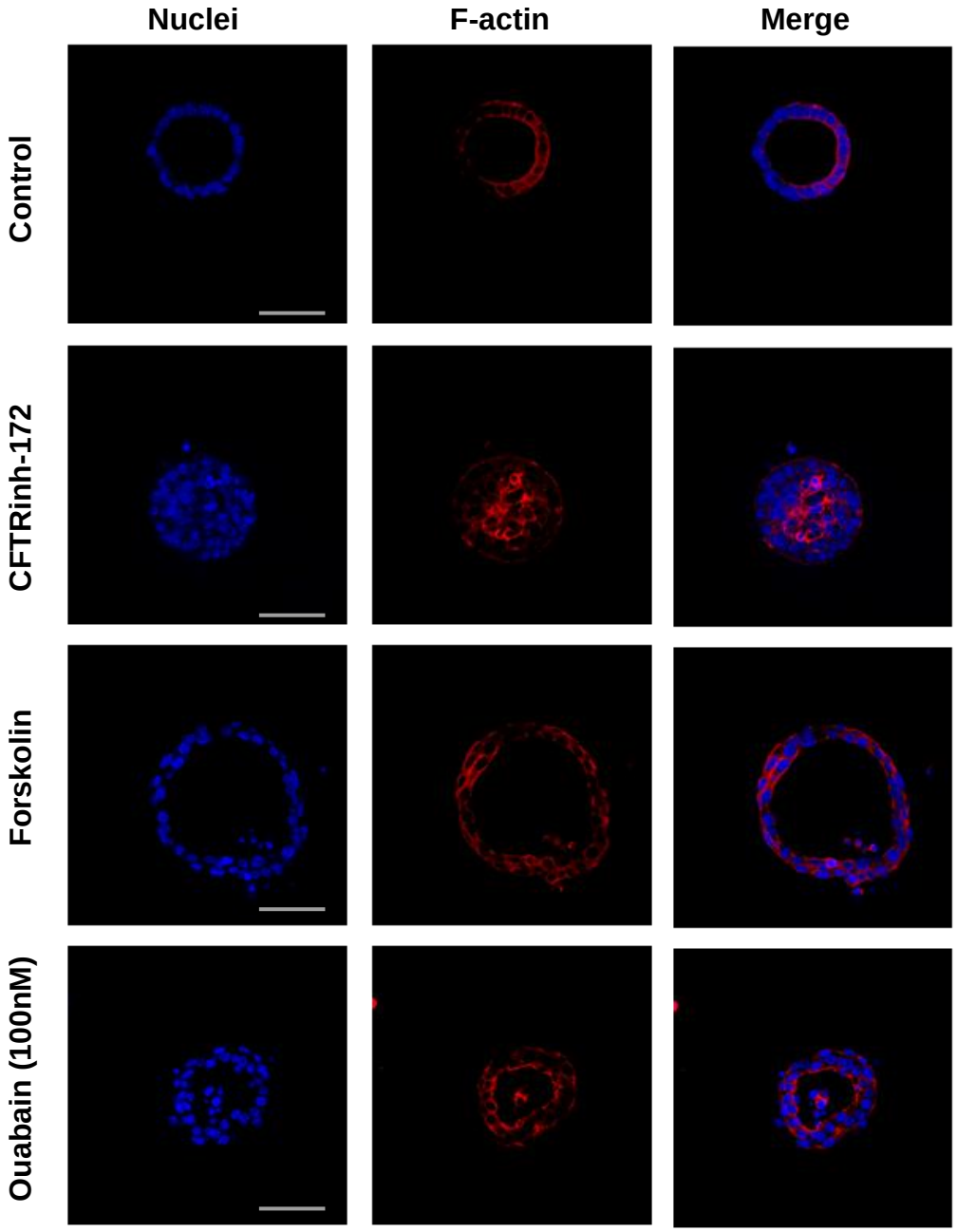

Figure 3.11. Representative organoid structure after treatments. Drugs were added on day 3; cells were fixed 24h after treatments and stained with TRITC phalloidin (red) to localise F-actin. Nuclei are stained with Hoechst (blue). Images were taken with the Zeiss LSM980 confocal microscope. Scale bar= 50µm. Microscope magnification= 40X.

3.4 DISCUSSION

The formation and maintenance of the lumen is an essential biological process in organs composed of a network of ducts, such as the mammary gland. The mechanisms that govern this process have not been fully elucidated. One proposed mechanism for lumen formation is through fluid secretion, which generates a hydrostatic pressure that favours the lumen formation. This mechanism has been described in other biological systems but not in the mammary gland (Bagnat, Cheung et al. 2007, Bagnat, Navis et al. 2010, Barwe, Skay et al. 2012, Rathbun, Colicino et al. 2020). Therefore, this chapter aimed to evaluate the participation of key molecule regulators of fluid secretion, CFTR, and the Na^+/K^+ pump in epithelial cells.

The EpH4 cell line and primary mouse MECs were used to perform the experiments in this chapter. Both cell types were found to be useful models to examine the effects of modulators of fluid secretion and its effects on lumen formation and maintenance. The use of primary cells offers advantages over established cell lines. Primary cells maintain some properties they would normally exhibit in the mammary gland (Richter, Piwocka et al. 2021). In addition, the protocol followed to obtain the MECs from the mammary tissue (Akhtar and Streuli 2013) allows the culture of the two epithelial populations (luminal and myoepithelial) of the mammary gland. Therefore, having the two populations of mammary epithelial cells and their ability to form organoids with tissue-like structures, this model represents a useful research tool for tissue

structures (Sato, Vries et al. 2009, Zhao, Chen et al. 2022). The EpH4 cells are a non-tumorigenic mouse mammary cell line that express luminal markers, such as K18 (Robinson, Karpf et al. 1999, Lee, Huang et al. 2010). The luminal cells are secretory cells in mammary gland tissue during lactation and face the lumen space. In addition, EpH4 cells have been described as a good model for studying lumen formation (Montesano, Soriano et al. 1998). Thus, the EpH4 cell line is a reliable model to study fluid secretion and lumen formation in a specific cell type population.

CFTR is a regulator of the extracellular osmotic gradient and regulates the secretion of fluids in several organs (Saint-Criq and Gray 2017). The importance of this ion channel activity in fluid secretion and lumen expansion after drug treatments have been described *in vitro* and *in vivo* models (Li, Findlay et al. 2004, Bagnat, Navis et al. 2010) but not in MECs. CFTRinh-172 is an allosteric specific inhibitor of the CFTR ion channel that binds to the NBD1 domain, maintaining the closed state of the channel (Caci, Caputo et al. 2008). This interaction between CFTR and CFTRinh-172 decreases Cl^- transport and alters the osmotic gradient. The use of CFTRinh-172 in the MECs in this project impacted lumen formation and maintenance in both cell models used (primary and EpH4 cells). As luminal cells are common in both models, it is assumed that the impairment of CFTR activity in this cell type is sufficient to alter lumen morphogenesis and the structure of previously existing lumens. CFTRinh-172 treatment not only caused a reduction in the lumen area but also caused the lumen space to collapse in most of the Eph4 acini structures and organoids with lumen on all days tested.

The Na^+/K^+ pump regulates the movement of Na^+ and K^+ through cells and their microenvironment, and its activity is shown to be important in the formation and expansion of lumens in the MECs in this study. The ouabain effect on the MECs affected lumen formation and the maintenance of the lumen area, suggesting that the inhibition of the Na^+/K^+ pump activity affects the fluid secretion towards the luminal area. In this study, three different concentrations of ouabain were tested. The 100nM ouabain dose was the only one that showed consistency in affecting lumen formation and maintenance in both cell models, at least in one of the two das tested. This ouabain concentration has been used in kidney acini, having an effect on lumen reduction size (Narayanan, Schappell et al. 2020).

The way ouabain modifies the electrochemical gradient and contributes to the fluid secretion is due to its union with the α subunit of the Na^+/K^+-ATPase. Another described impact of blocking the Na^+/K^+-ATPase activity with high ouabain doses (>300nM) is the stability of the TJs in epithelial cells (MDCK) (Larre, Lazaro et al. 2010). However, at 10nM, ouabain induces TJ sealing in MDCK cells. In epithelial cells existing as a monolayer, 10Mm ouabain induces the disassembly of cell adhesions, causing the cells to detach from each other and from the substrate (Contreras, Shoshani et al. 1999). Therefore, in our experiments, the TJs of the cells subjected to ouabain treatment could change their integrity and adhesive contact with neighbouring epithelial cells. The study of the TJs in our model with MECs post 100nM ouabain treatment could give information about another ouabain effect beyond the electrochemical gradient.

The structural effect of ouabain after 24h was different from that of CFTR inhibition. In particular, with ouabain, some cells in the lumen space were observed (Figures 3.10A, B and E), while with the CFTRinh-172 treatment, most lumens had totally collapsed. The organoids after ouabain treatment exhibited similar structures to those found in organoids before forming a continuous lumen (example: Figure 3.5, day 2 in organoids and figure 3.10E, organoid after ouabain treatment). According to the lumen formation model, the appearance of micro lumens first arises and then expands to a single lumen (Navis and Bagnat 2015). The results show structural similarity at both points, suggesting a structural regression to previous stages of lumen formation post-treatment.

Forskolin stimulates the activity of the adenylyl cyclase enzyme and increases cAMP levels (Seamon and Daly 1981). cAMP indirectly promotes the Na^+/K^+ pump and CFTR ion channel stimulation (Daly 1984, Haws, Nepomuceno et al. 1996). The CFTR and Na^+/K^+ pump stimulation with forskolin significantly increased the number of lumens in at least one of the days studied in both cell models. Although it was observed that forskolin increased the lumen area, it was not statistically significant. Therefore, the forskolin treatment does not affect lumen maintenance in the MECs. The effect of forskolin in lumen formation supports the hypothesis that fluid secretion participates in lumen formation in the MECs. However, it must be considered that forskolin is not a specific drug since, as was previously mentioned, its route of action is through the increase of cAMP, which not only has an effect on the phosphorylation of Na^+/K^+ pump and CFTR subunits but also it is a messenger in several biological processes through its major effector proteins (PKA and EPAC) (Sassone-Corsi

2012, Kilanowska, Ziolkowska et al. 2022). Thus, the forskolin effect observed on the lumen formation or the no effect on lumen area changes needs to be considered as a result of no direct interactions between Na+/K+ pump/forskolin or CFTR/forskolin.

This chapter provides information about the importance of the activity of CFTR and the Na^+/K^+ pump in the lumen formation in primary mouse MECs and the EpH4 cells. The inhibition of the Na^+/K^+ pump activity with ouabain (100nM) alters the lumen formation and maintenance in EpH4 and primary mouse MECs. The specific inhibition of CFTR with CFTRinh172 had a significant effect on the reduction of lumen formation in primary mouse MECs and the EpH4 cells. Furthermore, the existing lumens formed by primary mouse MECs and the EpH4 cells before treatment were lost after the CFTR activity inhibition with CFTRinh-172. The CFTR activity inhibition is consistent in all the experiments, showing the important role of the activity of this ion channel in lumen structures in MECs. Forskolin treatment increased the lumen formation in primary mouse MECs and the EpH4 cells, but it did not show a significant increase or change in the lumen area. Only the inhibition of CFTR activity consistently affected the lumen formation and maintenance in both cell models on both days evaluated (days 3 and 4). For the first time, this result shows the importance of CFTR activity in the lumen formation and maintenance in MECs. Therefore, it would be interesting to delve deeper into the study of CFTR in the MECs since it is a molecule poorly studied in the mammary gland. Specifically, the study of the CFTR expression in the lumen morphogenesis in MECs would confirm the

importance of this molecule in the mammary gland structure and give clues to what may be deregulated in breast cancer.

Chapter 4

4. REQUIREMENT OF CFTR EXPRESSION IN LUMEN FORMATION AND MAINTENANCE IN MECS

4.1 INTRODUCTION

Results from the previous Chapter 3 (Figures 3.6-3.9) suggested that CFTR activity is essential for lumen formation and maintenance. Although CFTRinh-172 is a specific inhibitor of the CFTR ion channel, further validation and verification using complementary techniques are necessary to establish a role for this ion channel in lumen formation and maintenance. Manipulation of gene expression is a commonly used approach to gain insight into gene and protein function. Since gene expression involves several steps, there are extensive points to modify it, for example, within the DNA sequence, chromatin or in the post-transcriptional or translational stages (Schneider-Poetsch and Yoshida 2018). The post-transcriptional stage is often used to study gene function without modifying the DNA. One well-established gene modulation technique used is gene silencing by RNA interference (RNAi), which follows a natural process of mRNA degradation stimulated by the complementarity of sequences between the RNAi with mRNA in the RNA-induced silencing complexes (RISC) (Fire, Xu et al. 1998, Filipowicz, Jaskiewicz et al. 2005). Considering this process, specific synthetic siRNAs can be designed with high specificity for transcript targets and delivered to the cells to carry out a specific mRNA Knockdown (KD) (Hu, Zhong et al. 2020). In this way, a reduction or loss-of-function study of a gene of interest is possible.

CFTR is essential for the homeostasis of some organs and ductal tissue morphogenesis(Tizzano, Chitayat et al. 1993, Tizzano, O'Brodovich et al. 1994, Cohen and Larson 2006, Meyerholz, Stoltz et al. 2010). Deletion or mutations in CFTR

affect the branching morphogenesis of organs such as the trachea(Ornoy, Arnon et al. 1987, Bonvin, Le Rouzic et al. 2008, Meyerholz, Stoltz et al. 2018), gut (Ornoy, Arnon et al. 1987), pancreas(Ornoy, Arnon et al. 1987), lungs (Ornoy, Arnon et al. 1987, Meyerholz, Stoltz et al. 2018) in different species. In CF patients who express a mutated form of CFTR, exocrine glands, such as the pancreas and salivary gland, present physiological abnormalities in the secretion of substances that help the organ function (Sato and Sato 1984, Kopelman, Corey et al. 1988, Noel, Strale et al. 2008). *In vitro*, CFTR expression is indispensable for lumen morphogenesis in acini of intestinal (Dekkers, Wiegerinck et al. 2013, Schwank, Koo et al. 2013), kidney (Schutgens, Rookmaaker et al. 2019) and nasal cells (Liu, Anderson et al. 2020).

Since the role of CFTR in the mammary gland is unknown, and findings from the previous Chapter 3 suggest that CFTR activity is essential for lumen formation and maintenance in MECs, the hypothesis in this Chapter is that **the expression of CFTR plays an essential role in lumen formation and maintenance in MECs.**

The aim of this Chapter is to determine the requirement for CFTR expression in primary mammary epithelial cells in lumen formation and maintenance processes. In order to achieve this aim, the following objectives were undertaken:

- Validate the CFTR KD in mammary epithelial cells after using siRNAs.
- Determine whether the CFTR KD impacts lumen formation in mouse primary organoids derived from mammary epithelial cells.

- Determine whether CFTR KD alters lumen area in mouse primary organoids derived from MECs.

4.2 METHODS

4.2.1 Mammary gland dissection and epithelial cells collection

The maintenance and handling of mice were carried out in accordance with the Animals (Scientific Procedures) Act 1986 (and associated practices) of the UK legislation under Project Licence PP1836785. The mice were kept at 22°C with 40-60% and 12h photoperiod in the Biological Services Unit of the Medical School of the University of Sheffield. Mice were killed using the Schedule 1 procedure by a trained and registered practitioner.

The mice were dissected in sterile conditions to obtain the mammary gland tissue. The dissection incision was made from the perianal to the cervical area to collect tissue from 5 pairs of mammary glands. The tissue obtained was processed as described in section 2.2. Tissue was collected from at least 3 mice per experiment.

4.2.2 Transfections for lumen formation

Reverse and forward transfection techniques were tested during the standardisation process to choose the best transfection procedure for the CFTR KD in the MECs. The reverse transfection was done at the same time as the cell seeding in the plates, while the forward transfection was carried out after one day of cell seeding when the cells were attached to the plate.

Only experiments were done on the positive and control groups during the standardisation. The positive control group was treated with the positive control siRNA Block-iT Alexa Fluor (a non-targeting siRNA labelled with Alexa Fluor 555), and the negative control group was treated with a non-targeting siRNA.

4.2.2.1 REVERSE TRANSFECTION

After mammary gland dissection and collection of the epithelial cell pellet, cells were transfected and cultured on 24 well plates. Reverse transfections were made simultaneously when the cells were seeded. 1:1 DMEN F-12 media (Sigma Aldrich) and Optimen media (Gibco) containing 5pmol of Lipofectamine™ RNAiMAX Transfection Reagent, 120nM of the positive control siRNA (Block-iT Alexa Fluor, Invitrogen) or only transfection reagents (mock transfection; negative control) were added to the seeded cells. The transfection mix was prepared according to the manufacturer instructions.

Cells were incubated with the transfection reagents for 24h, and media was replaced with fresh complete media for 2D primary cells (section 2.16.1), and cells were cultured for one day). Images of random sections of the samples were taken with the light microscope (Leica DMi1) to analyse the cell density after the transfection.

4.2.2.2 FORWARD TRANSFECTION

Primary cells were cultured and transfected on 2D conditions, as described in section 2.16.1. The negative, positive, and CFTR siRNA concentrations used were 120nM. The cells were transfected for 24h, the transfection media was changed for fresh complete media (2D conditions media, section 2.16.1) and cultured for 2 days. Images of random sections of the samples were taken with the light microscope (Leica DMi1) to analyse the cell density after the transfection.

The cells were transferred to 3D conditions and cultured for 4 days. At least 10 images per experiment (10 images for the first experiment and 30 images for the second, third and fourth experiments) of random sections of samples were taken with the light microscope (Leica DMi1) to count the number of organoids (at least 23 per sample group in each independent experiment or 331 in total from all the experiments) with and without lumen. Images were analysed in Image J, and the organoids with an area of >24,000 units (~826μm2) from the “analyse tool” were counted as organoids. The count of organoids was divided into two categories: organoids with or without lumen.

4.2.3 Transfections for lumen maintenance

4.2.3.1 TRANSFECTION OF ORGANOIDS SEEDED ON THE TOP OF BMM

Mouse MECs were seeded and cultured according to the method described in section 2.5.2. The transfection was done on day 6 when the cells cultured formed organoids with a single lumen. The transfection method followed is described in section 2.16.2.

Organoids with a single lumen were localised before and after the transfection, and their area was measured as described in section 2.8.2.

4.2.3.2 TRANSFECTION OF ORGANOIDS EMBEDDED IN BMM

Mouse MECs were cultured with BMM to allow the formation of organoids with lumen, as described in section 2.5.2. On day 4, when organoids presented a single lumen, the transfection was carried out. 5pmol of Lipofectamine™ RNAiMAX Transfection Reagent and 120nM of the Negative control siRNA (Silencer select, Ambion) or 120nM of the positive control siRNA (Block-iT Alexa Fluor, Invitrogen) were combined and added to the cells according to the manufacturer instructions. Serum-free media (500µl total) consisting of 1:1 DMEN F-12 media (Sigma Aldrich) and Optimen media (Gibco) was added to the cells and incubated at 37°C for 24h. The media was changed for DMEM F-12 media (Sigma Aldrich) containing 5µg/ml insulin (Sigma Aldrich), 1µg/ml hydrocortisone (Sigma Aldrich), 5ng/ml EGF (Sigma Aldrich), and 1% (v/v) of penicillin/streptomycin and cells were incubated for further 24h. An evaluation of the transfection was made 48h post-transfection.

4.2.4 Evaluation of transfection

After 48h post-transfection of the mouse MECs, the cells were washed with 1X PBS (Thermo Scientific, pH 7.4) (three times) to remove residues from the culture medium and were fixed in a solution of 10% formalin solution (Sigma) for 10 minutes. The coverslips containing the cells were stained with Hoechst (Invitrogen) at a 1:1000

dilution (in 1X PBS) for 3 minutes at room temperature. Cells were washed with 1X PBS (Thermo Scientific, pH 7.4) (three times) and mounted on slides with ProLong Gold Antifade Mountant (Invitrogen) for further observation.

The transfection signal from the positive control siRNA was detected using the Zeiss LSM 980 Airyscan confocal microscope. For the forward transfection (method chosen for the lumen formation experiments), at least 10 photos of a random field of view within a well (from 3 wells) were taken to evaluate the Alexa Fluor™ 555 siRNA signal (from the positive control) in the cells. The count of positive cells (transfected cells) was carried out manually in ImageJ. The number of positive cells (with red signal) was related to the total number of cells counted in the images. The data is presented as a percentage of positive cells transfected. In addition, 3 replicates of positive control per experiment were included in all the transfection experiments to monitor the transfection.

4.2.5 RT and qPCR

Transfected cells were collected after 24h or 48h post-transfection. RNA was extracted as described previously for the cells in 2D conditions (section 2.19.1) or the organoids in 3D conditions (section 2.19.2). RT and qPCR were carried out according to the procedure described in section 2.22.

For the lumen formation experiments, 3 independent RTs and qPCRs were performed. For the lumen maintenance experiments, 1 RT-qPCR was performed. The qPCRs consisted of 3 replicates per sample.

4.2.6 Fluorescence staining

The BLOCK-iT™ Alexa Fluor™ Red Fluorescent siRNA control allows the detection of the transfection under a fluorescence microscope. Therefore, this siRNA was used as a positive control to determine the efficiency of transfection with the conditions used. After 48h post-transfection, the cells cultured and transfected in 2D conditions or 3D conditions were fixed and stained as described above in section 4.2.4.

CFTR expression was also analysed after 48h post-transfection for the lumen formation experiments. The procedure followed is described in section 2.9.2. Two replicates of at least 2 independent experiments were processed.

Organoids post-transfection were stained for F-actin with TRITC-phalloidin (Sigma Aldrich) and with Hoechst 33258 for nuclei staining. The protocol followed is described in section 2.9.2.

4.2.7 Western blot

To analyse the CFTR protein expression after the CFTR KD by siRNAs in the MECs, the post-transfected cells were collected and processed as described in section 2.20.1 for the cells cultured in 2D and section 2.20.2 for those cultured in 3D conditions. The CFTR protein was detected using the CFTR primary antibody (Mouse anti-CFTR) and the secondary antibody (Goat anti-Mouse /HRP) (Table 2.3). For the lumen formation experiment, three WB were made with proteins extracted from the three independent experiments (n=3).

4.3 RESULTS

4.3.1 Lumen formation

4.3.1.1 CFTR KD IN MOUSE PRIMARY MECS

CFTR expression was modified by siRNAs to further understand the role of this ion channel in lumen formation. A forward transfection approach was performed one day after seeding the primary MECs and acclimatisation in 2D conditions. After transfection, cell morphology was initially compared with the same batch of primary cells that had not been transfected to observe differences in growth. At 24h and 48h post-transfection in serum and antibiotic-free conditions, the cells continued to attach to the plates and showed cell morphology similar to that of the non-transfected cells under the light microscope (Figure 4.1).

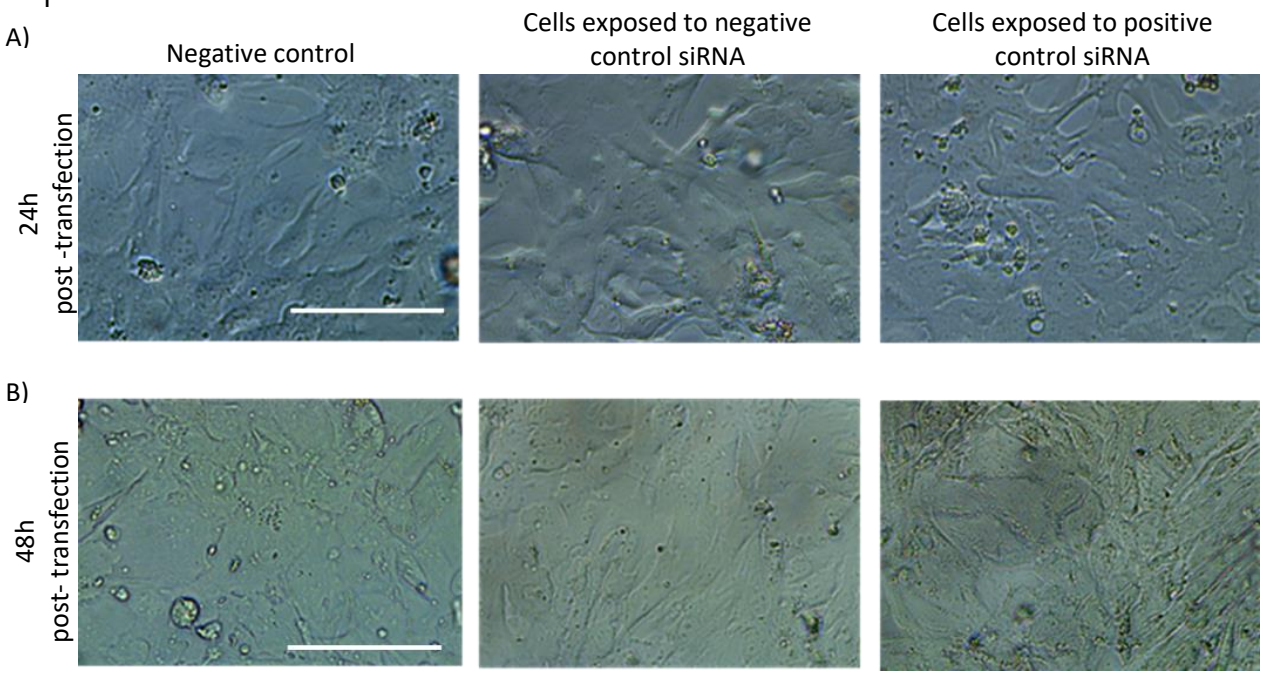

Figure 4.1. Primary mouse MECs following exposure to siRNA. The cells are attached to the plate and show similar cell morphology to the non-transfected cells after A) 24h post-transfection and B) 48h post-transfection. The negative control group represent the samples without transfection reagents. Scale bar= 100µm. Microscope magnification= 20X.

During the standardisation period, reverse transfection (simultaneous transfection with cell seeding) was attempted, and after 48h post-transfection, the majority of the cells were not attached to the plates (Figure 4.2).

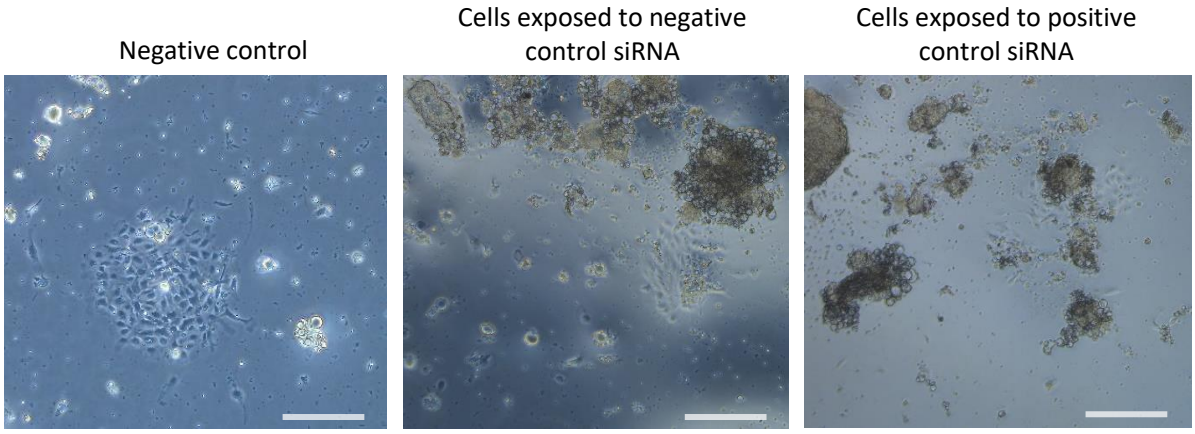

Figure 4.2. Primary MECs 48h after reverse transfection with siRNAs. The negative control group represent the samples without transfection reagents. Scale bar= 100 µm. Microscope magnification= 20X.

Evaluation of the red fluorescent signal (Alexa Fluor™ 555) from the positive control was carried out in the MECs transfected with the forward method, as this transfection method showed higher cell density after transfection. Figure 4.3 shows the red fluorescence signal detected only in the cells transfected with the positive control siRNA. These images indicate that the primary MECs were able to take up the oligo or positive control siRNA in the conditions and concentrations used. The positive cells were counted, and the percentage of transfection was 31.97%.

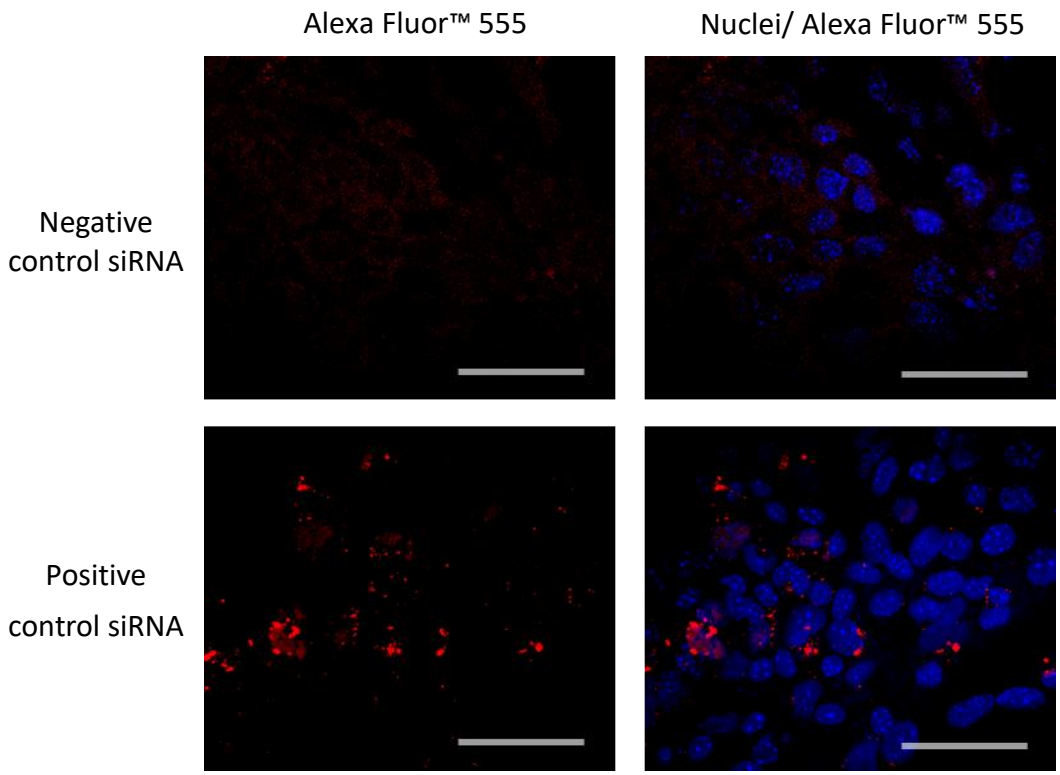

Figure 4.3. 2D Primary MECs transfected with the positive and negative siRNA controls. Images correspond to 48h post-transfected cells. Red signal (Alexa Fluor™ 555) was detected in the cells transfected with the siRNA control, and the blue signal from the nuclei staining with Hoechst. Scale bar=100 μm. Microscope magnification= 40X.

Once it was known that transfection occurred under these conditions, the evaluation of CFTR KD was determined by qPCR. *Cftr* transcript expression was reduced significantly by 42.8% relative to the negative control (cells transfected with the negative control siRNA, a no targeting sequence) (Figure 4.4A) after 48h post-transfection. Protein expression was also reduced compared to the negative control group (cells transfected with the negative control siRNA) by 51.25% (Figure 4.4B and C). These data show that CFTR expression was significantly reduced in primary MECs by the CFTR siRNA on the second day post-transfection (or the third day after seeding the primary cells on 2D conditions).

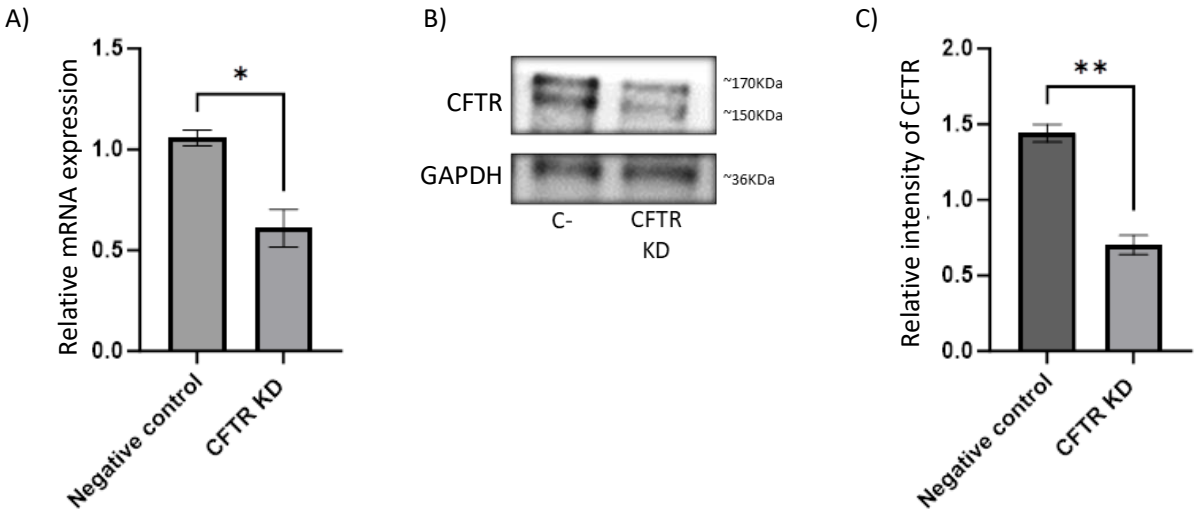

Figure 4.4. CFTR mRNA and protein expression in mouse primary MECs following targeted knockdown with siRNA. A) Expression of *Cftr* 48h after exposure to targeted siRNA in MECs relative to non-targeting siRNA (negative control). Data were normalised to the expression of *Hprt1* (internal housekeeping gene) and expressed as fold change. The graph shows mean ± SEM (n=3). An unpaired student's t-test was used to compare groups. *$P < 0.05$. B) Image of WB with the proteins extracted from primary MECs after 48h post-transfection with either non-targeting siRNA (C-) or siRNA targeting Cftr (CFTR KD). C) Relative intensity of CFTR and GAPDH. The relative intensity of the CFTR protein band is normalised against the band intensity of GAPDH. The graph shows mean ± SEM (n=3). An unpaired student's t-test was used to compare groups. **$P<0.01$.

After seeing a reduction of around 50% of CFTR protein from the WBs, an analysis of CFTR localisation in the cells cultured under 2D conditions was carried out by IF. Zonula Occludens-1 (ZO-1) is a multi-domain protein of the TJs protein complex located at the border apical and basolateral cell membrane. This protein is frequently associated with cell polarity and as an apical marker in epithelial cells (Plachot, Chaboub et al. 2009, Fanning, Van Itallie et al. 2012). Since, the mature form of CFTR is located in the apical membrane (Gregory, Cheng et al. 1990), ZO-1 was used as a reference for the apical localisation of CFTR. In Figure 4.5A, CFTR expression was found to colocalise with ZO-1. However, CFTR protein was also observed within the cytoplasm of the MECs (Figure 4.5B). The IF images show a variation of CFTR

expression in some sections of the CFTR KD samples, showing that the KD does not occur in a homogeneous manner, which is consistent with the previous transfection images that showed that not all the cells were transfected (Figure 4.3). ZO-1 expression was observed in a similar pattern in the negative control and the CFTR KD samples.

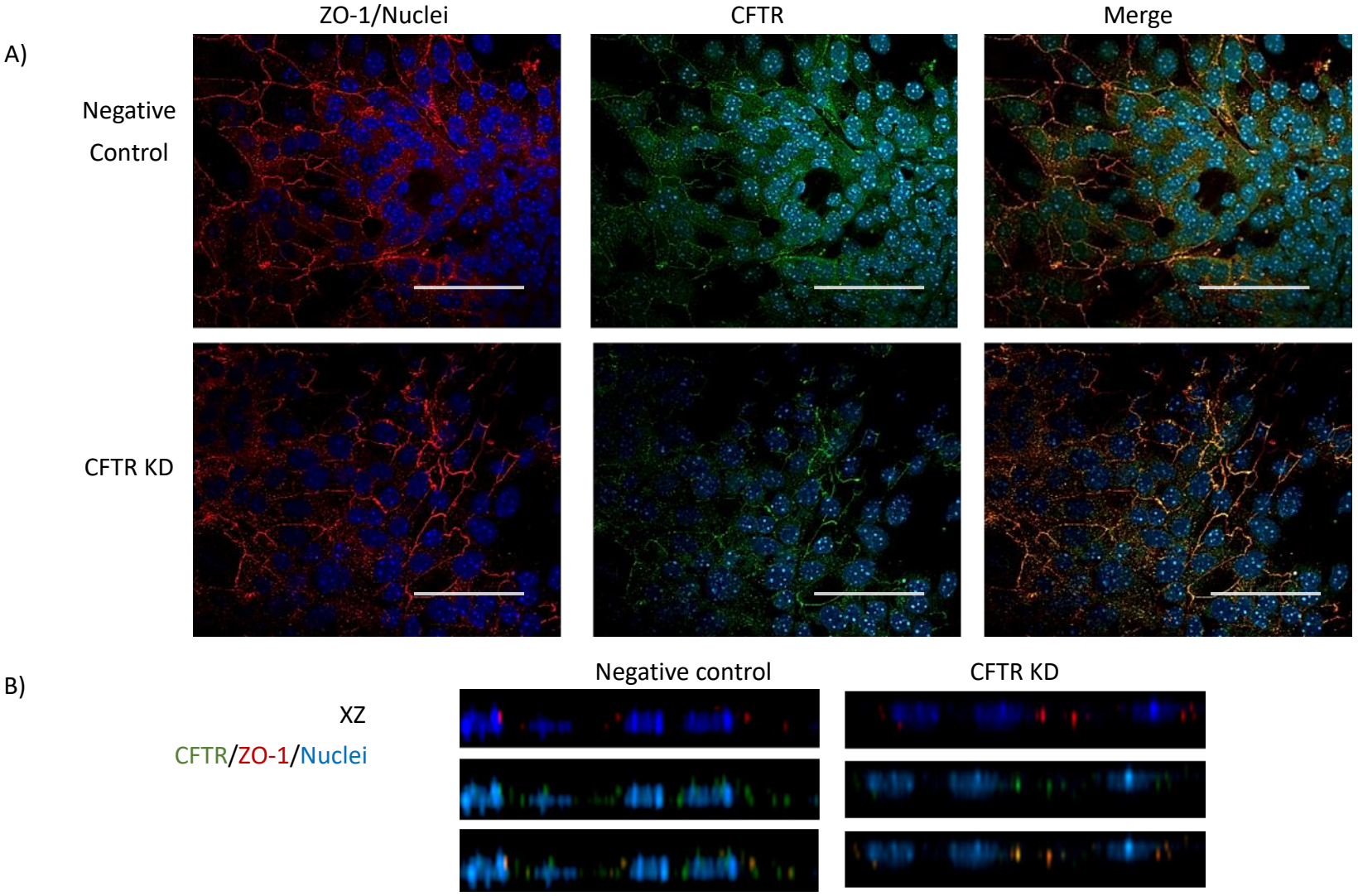

Figure 4.5. CFTR localisation in mouse primary MECs post CFTR KD. A) Representative images after 48h post-transfection in primary cells cultured as a monolayer. Scale bar= 50µm. Microscope magnification= 40X. B) Confocal Z-stack merged images of the mouse primary MECs post CFTR KD. The cross-sectional view shows CFTR expression across the cell. The negative control group represents the samples transfected with the negative control siRNA. Antibodies were used to label ZO-1 (red) and CFTR (green). Nuclei are labelled with Hoechst 33258 (blue).

4.3.1.2 NUMBER OF LUMENS FORMED IN CFTR KD ORGANOIDS

Once the CFTR KD was confirmed in the cells cultured in 2D, transfected CFTR KD cells and transfected control cells were transferred to 3D conditions for a further 4 days to evaluate their capacity to form lumens. Figure 4.6A shows representative images of organoids from the groups treated with either negative control or CFTR siRNAs. The images show that both groups contained organoids with and without a lumen. When these were quantified, there were 23% fewer organoids with lumens in the CFTR KD group compared with the negative control group ($P < 0.05$) (Figure 4.6B).

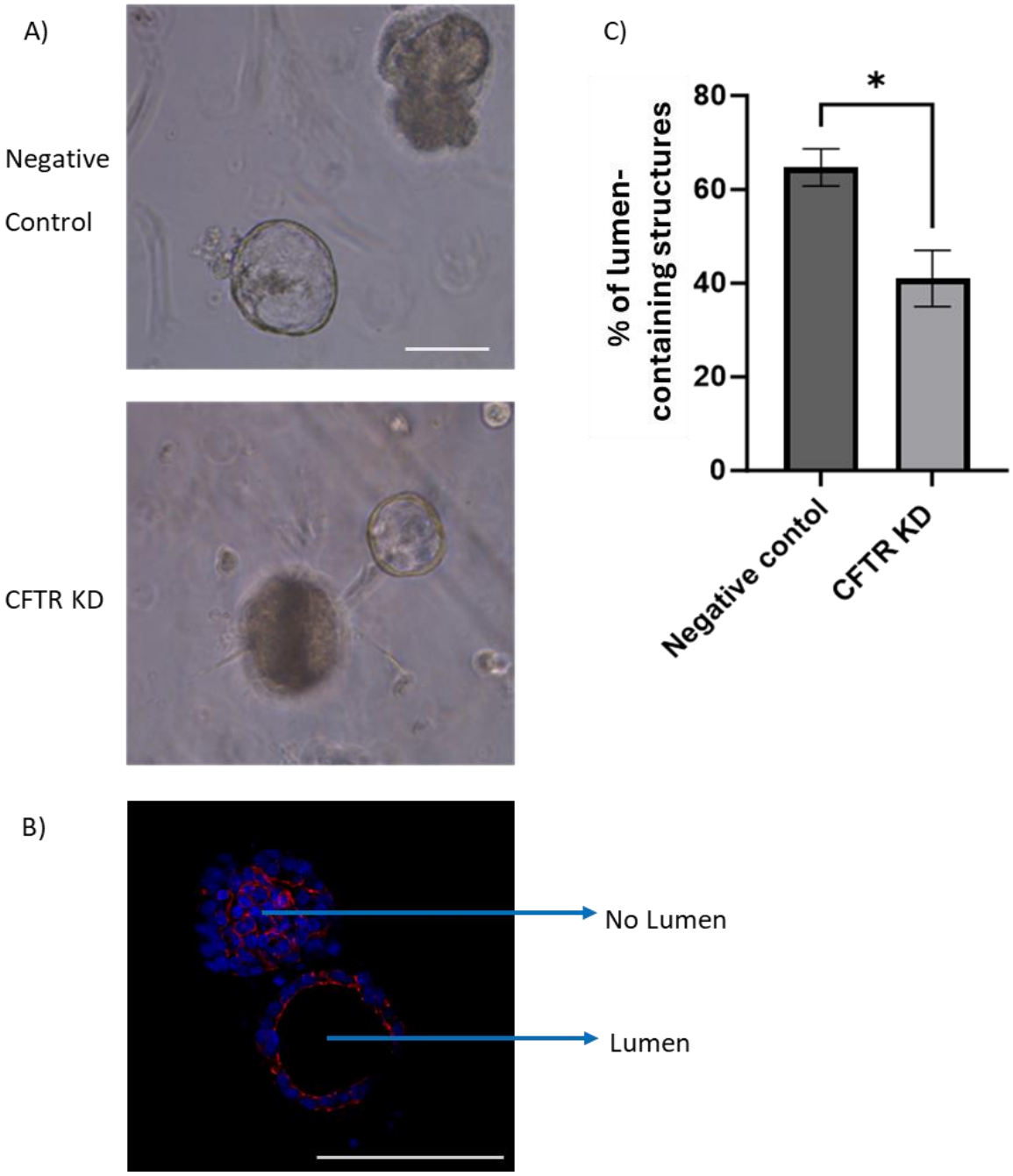

Figure 4.6. CFTR KD and negative control organoids formed with MECs transfected with siRNAs. Representative images of organoids formed from MECs transfected with siRNA and cultured for 4 days in 3D conditions. A) Both samples have a combination of organoids with and without lumens. Scale bar= 100µm. Microscope magnification= 20X. B) Representative image (non-targeting siRNA) showing an organoid with and without a lumen. Cells were labelled with TRITC phalloidin for F-actin (red), and nuclei were stained with (blue). Scale bar= 100µm. Microscope magnification= 40X. C) Percentage of lumens formed in samples transfected with either negative control or CFTR siRNAs. The graph shows mean ± SEM (n=4). Each n represents an independent experiment. 332 and 331 organoids (in total) from at least 10 random sections of the samples from each experiment were counted for the negative control and CFTR KD groups, respectively. An unpaired student's t-test was used to compare groups. *P < 0.05.

4.3.2 Lumen maintenance

4.3.2.1 CFTR KD IN MAMMARY ORGANOIDS

For the transfection in mammary epithelial organoids containing a lumen, two methods were tested according to how the cells were seeded on the BMM: on top or embedded.

Primary MECs were seeded on the top of the BMM or embedded in BMM to allow lumen formation during the first 6 or 4 days, respectively. Lumen-containing organoids were then transfected with the positive control siRNA and analysed 48h post-transfection. Results show that the lumen-containing organoids were evident in negative and positive control siRNA groups in both methods tested (Figure 4.7A and B). This result indicates that the lumen structures in the organoids were maintained after exposure to the transfection procedure and reagents.

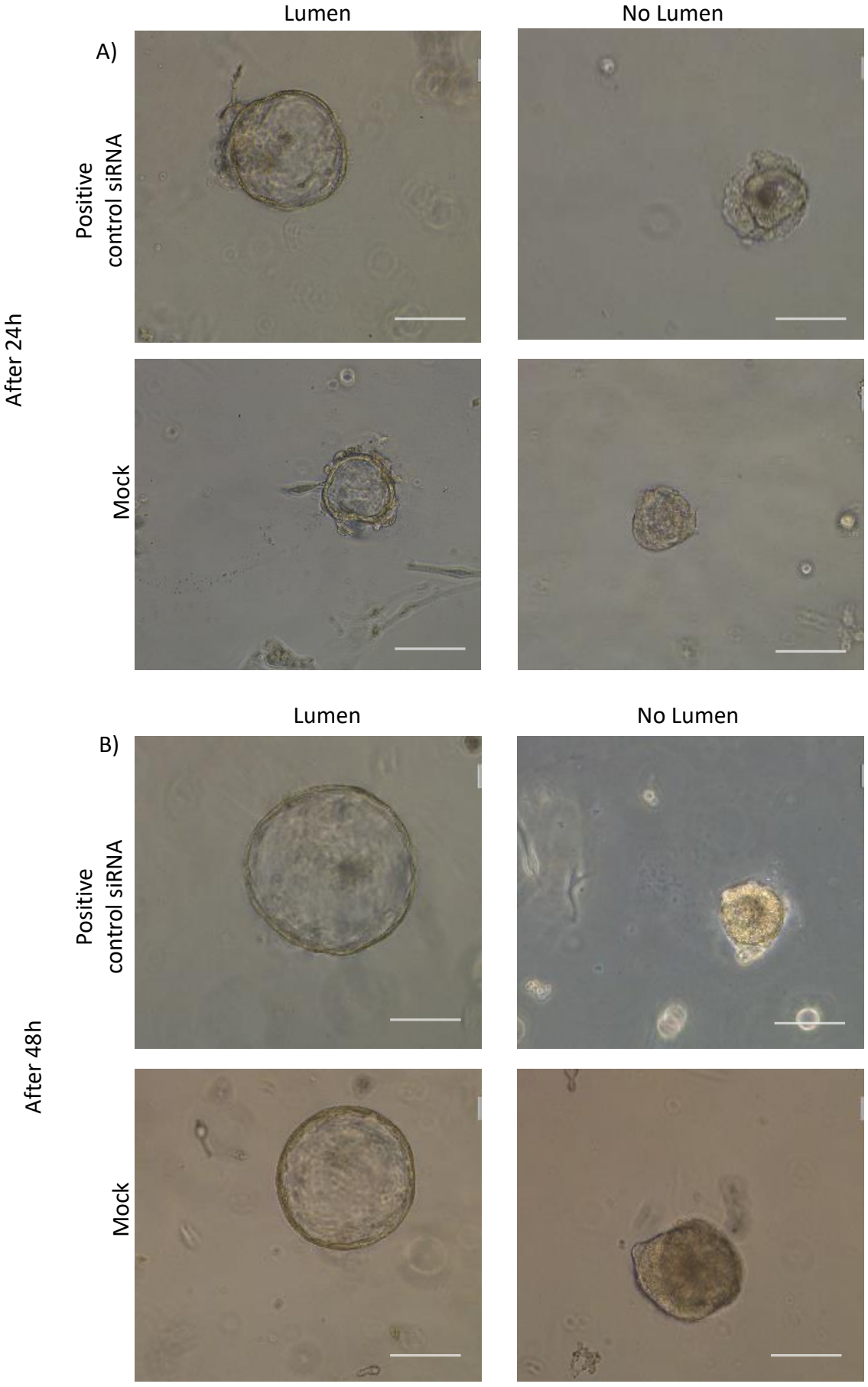
Lumen
No Lumen
A)
Positive control siRNA
Mock
After 24h
Lumen
No Lumen
B)
Positive control siRNA
Mock
After 48h

Figure 4.7. Lumen maintenance in mammary organoids after exposure to control siRNA or transfection reagents. Representative image of organoids with and without lumen A) after 24h or B) after 48h of transfection with the positive control siRNA or mock treatment (only transfection reagents). Scale bar = 100µm. Microscope magnification= 20X.

Subsequently, the transfection was verified by the visualisation and localisation of fluorescent-labelled positive siRNA 48h post-transfection. Two methods were tested based on the seeding of the MECs in the BMM; the cells cultured on the top/surface of the BMM and the cells seeded with the BMM (embedded). In general, the organoids transfected on top of the BMM showed a mix of organoids with the siRNA fluorescent signal in the cells (nuclei) (Figure 4.8B) and others without the signal (Figure 4.8C). Some of the organoids that were positive for the transfection signal did not show fluorescence in all the cells that make up the organoids (Figure 4.8B). The other method tested for transfection of mammary organoids embedded in BMM did not show the fluorescent-labelled positive siRNA in the nuclei of the MECs 48h post-transfection (Figure 4.9). Therefore, the method of organoids seeded on the top of BMM (showing organoids transfected), was selected for the following transfections with the CFTR and negative control siRNAs.

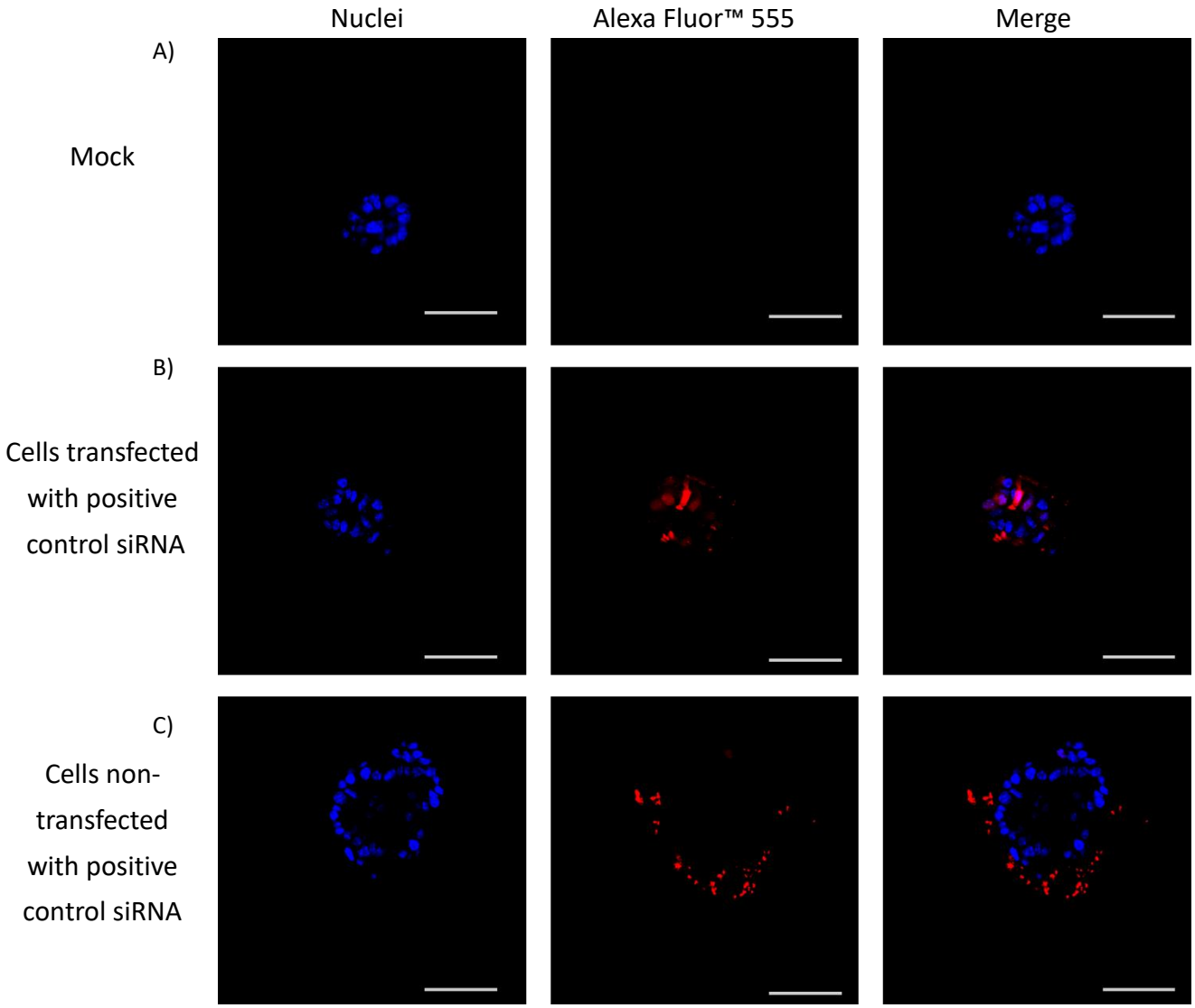

Figure 4.8. Mammary organoids cultured on top of BMM and transfected with positive control siRNAs or transfection reagents. A) Representative organoid from the mock control group (exposed to the same experimental procedure and transfection reagents except for the siRNA). B) Representative organoid from the positive control group (organoids exposed to the transfection reagents and the positive control siRNA). C) Example of an organoid not transfected with the positive control siRNA. The fluorescent-labelled positive siRNA did not colocalise with nuclei (blue). Scale bar= 50µm. Microscope magnification= 40X.

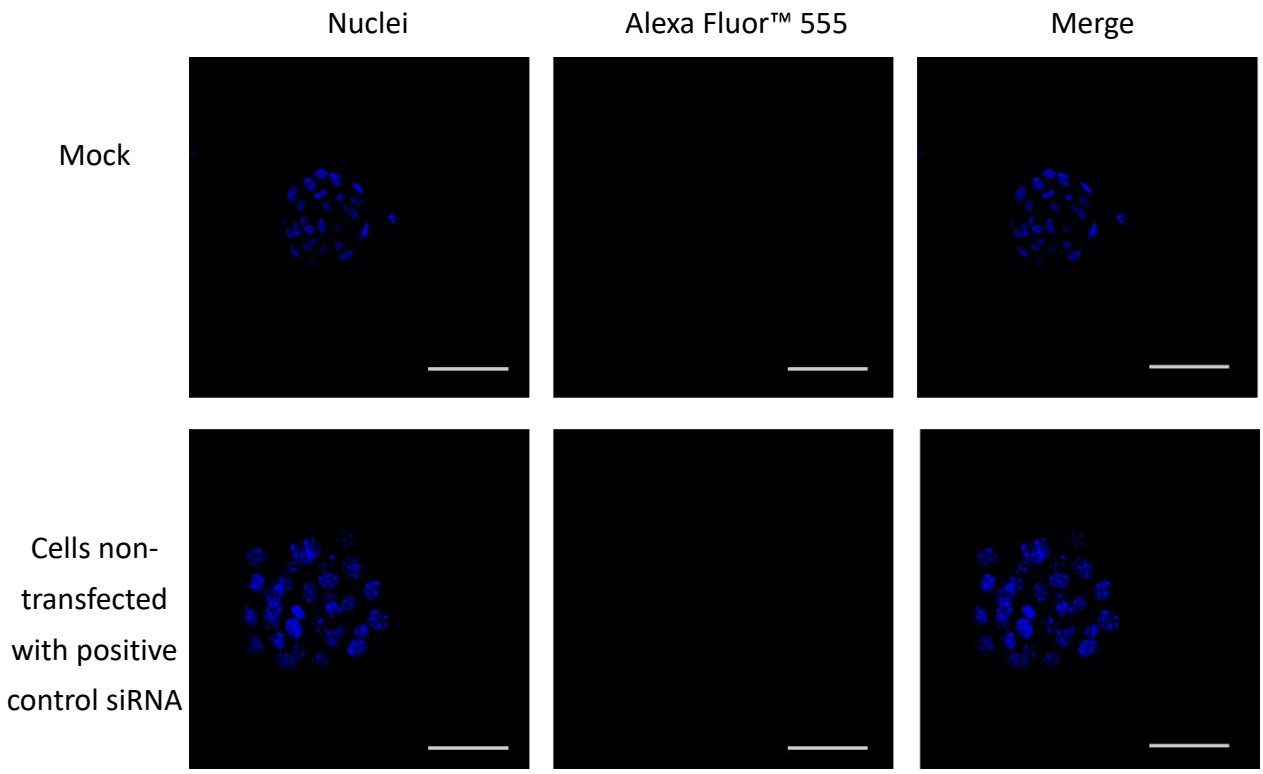

Figure 4.9. Mammary organoids embedded in BMM and transfected with positive control siRNAs or transfection reagents. The organoids were observed 48 post-transfection. A) Representative organoid of the mock transfection group (only transfection reagents). B) Representative organoid exposed to the transfection with positive control siRNA. Fluorescent-labelled positive siRNA was not detected. Scale bar= 50µm. Microscope magnification= 40X.

Once it was confirmed that organoids were able to be transfected with control siRNA, organoids were then transfected with *Cftr*-targeting siRNA and non-targeting control siRNA for analysis of lumen maintenance. The MECs were seeded on the top of the BMM, transfected on day 6 in 3D conditions and collected to analyse the CFTR KD. Organoids were analysed at 24h and 48h post-transfection to determine the optimal time frame for CFTR KD. The results in Figure 4.10 show that *Cftr* expression was reduced by 38.4% after 24h post-transfection and 27.7% after 48 post-transfection.

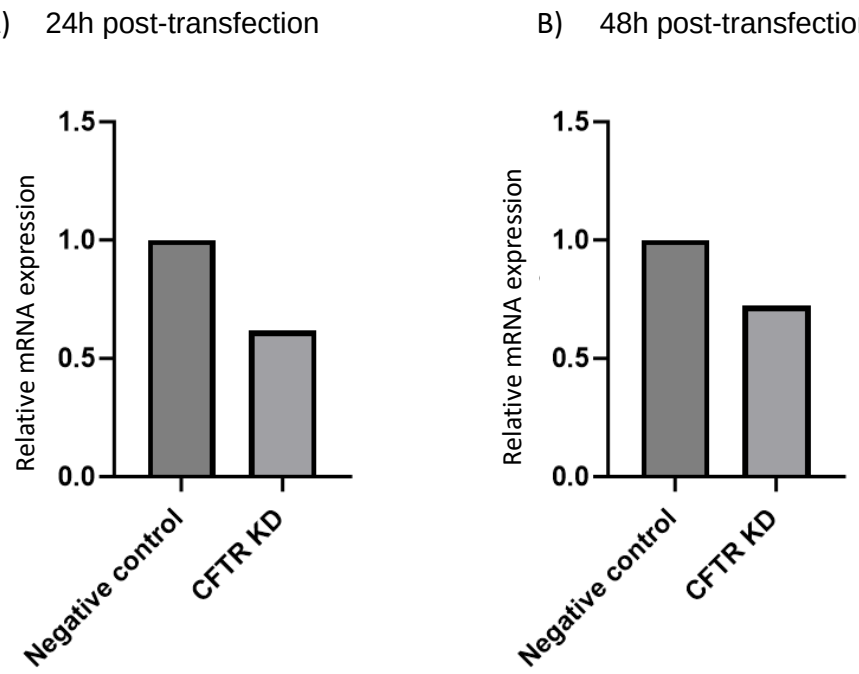

Figure 4.10. *Cftr* expression in mammary organoids post-transfection with non-targeting (Negative control) and Cftr-targeting siRNAs (CFTR KD). A) Relative mRNA expression of *Cftr* after 24h post-transfection and B) after 48h post-transfection. Data were normalised relative to the expression of *Hprt1* (internal housekeeping gene) and expressed as fold change. Data represents an independent experiment (n=1) made of 3 technical replicates.

4.3.2.2 LUMEN AREA IN CFTR KD ORGANOIDS

After transfection with siRNAs lumen maintenance was evaluated by analysing changes in the lumen area post-transfection. The lumen area of organoids was measured before (0h) and after 24h and 48h post-transfection. The changes in the lumen area were compared between the organoids transfected with the non-targeting control and with the organoids transfected with the Cftr-targeting siRNA. The lumen area was significantly reduced in the *Cftr* KD group at 24h and 48h post-transfection ($P<0.0001$ and $P<0.001$, respectively) (Figure 4.11). After 24h post-transfection, 22.8% of the *Cftr* KD organoids no longer exhibited a lumen, and after 48h, the lumen

was totally lost in 37% of the organoids evaluated. The mean lumen area in the negative control increased by 33.4% 24h post-transfection, while the lumen area was reduced in the CFTR KD organoids by 47.3% at the same time point (Figure 4.11A). After 48h post-transfection, the negative control lumen area increased by 37.1% and decreased by 39% in the CFTR KD samples (Figure 4.11B).

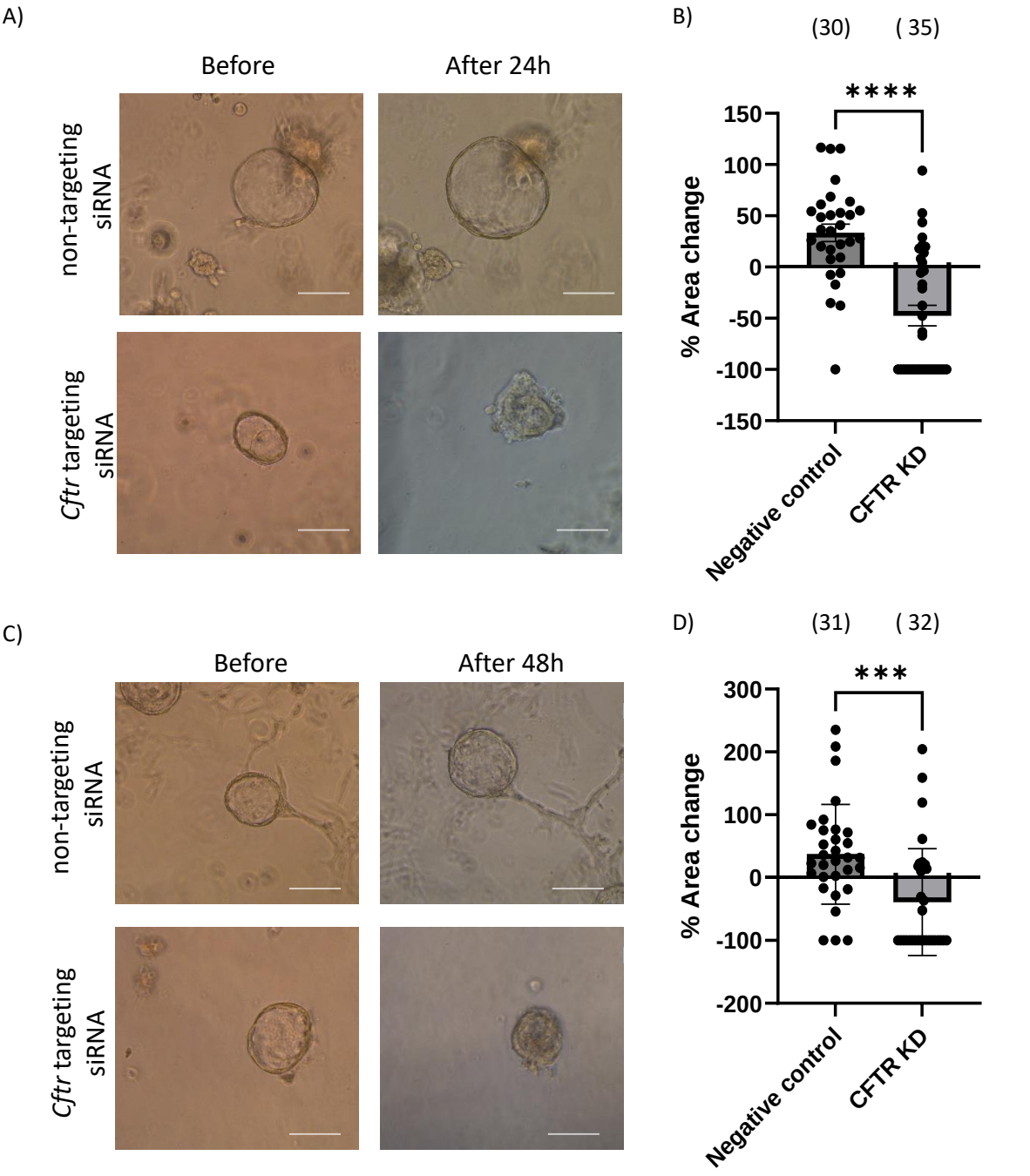

Figure 4.11. Change in the lumen area of organoids after CFTR KD. A) Examples of mammary organoids before and 24h after transfection with non-targeting (Negative control) and Cftr-targeting siRNAs (CFTR KD). Scale bar=100 µm. B) Graph shows the percentage change of lumen area at 24h after transfection. C) Examples of mammary organoids before and 48h after transfection with non-targeting (Negative control) and Cftr-targeting siRNAs (CFTR KD). Scale bar=100 µm. Microscope magnification= 20X. D) Graph shows the percentage change of lumen area at 48h after transfection. Each measurement was normalised with its initial lumen area at time 0h. Data has been pooled from 3 independent experiments, with the number of luminal organoids shown in parentheses above each group; at least 30 organoids were counted. Data shows mean ± SEM. A Mann-Whitney test was used to compare groups. *** *P< 0.001;* ****P=0.0001.*

4.4 DISCUSSION

CFTR is an ion channel that transports chloride and bicarbonate across the apical membrane, and its expression and activity have been described to be important in the morphogenesis of tubular organs with a lumen structure (Tizzano, Chitayat et al. 1993, Tizzano, O'Brodovich et al. 1994, Cohen and Larson 2006, Bonvin, Le Rouzic et al. 2008, Meyerholz, Stoltz et al. 2010, Meyerholz, Stoltz et al. 2018). However, it is unknown whether CFTR plays any role in lumen formation in the context of the mammary gland. Considering the requirement of the mammary gland to maintain a tubular structure with a lumen in normal physiology and how this may be disrupted in breast cancer, this Chapter focused on the role of *Cftr* in lumen maintenance and formation in a mouse mammary epithelial organoid model.

The alteration of *Cftr* gene expression was carried out through the use of siRNAs. This approach was chosen because, in order to study lumen maintenance *in vitro*, normal CFTR activity was required for lumen formation and expansion to occur in MECs (Chapter 3). Once the lumen is formed, modification of CFTR expression is necessary to analyse the role of this factor in lumen maintenance. Modification of the gene expression in a specific stage can be achieved through transfection with siRNAs over a chosen period of time. To be certain of the CFTR KD in the cell model used, a negative control with a non-targeting sequence was included. This control ruled out that the results observed were not affected by the transfection (procedure, toxicity of the siRNA and concentration effects of transfection reagents) procedure but rather by the specificity of the CFTR siRNA.

The results showed that around 32% of the primary MECs were able to be transfected and that this reflected a reduction in the CFTR expression. This low percentage of transfection can be related to the recognised challenges of transfection in primary cells, given that more variables can affect the entry of reagents into the cytoplasm and nucleus of these cells (Gresch and Altrogge 2012). The low transfection efficiency in primary cells has been reported, and the percentage of transfection is dependent on the transfection method and reagents. For example, it has been reported that primary pig tracheal and human tracheal epithelial transfected with lipid-based reagents showed lower transfection efficiency than 25%. However, when the same type of primary cells were transfected using other methods, such as nucleofection, the transfection efficiency increased to over 70% (Maurisse, De Semir et al. 2010). Another method to deliver genetic material to the cells, different from nucleofection and lipid-based reagents, is through viral particles. This method usually reports high cell transduction percentages, even in some cases exceeding the efficiency of the nucleofection method ($25.3 \pm 4.8\%$ transduction efficiency with lentivirus and $16.1 \pm 3.6\%$ transfection efficiency with nucleofection in the H1 hES cells) (Cao, Xie et al. 2010). However, although viruses can offer high efficiency and stable expression, the viral particles can have disadvantages over the other transfection methods, such as immunogenicity and insertional mutagenesis (Butt, Zaman et al. 2022). For this reason and for the high reproducibility of the lipofection method, this was used for the CFTR KD experiments in this Chapter.

The transfection efficiency also depends on the gene expression of the cell type, the culture requirements and how the cells react to the deprivation of these requirements (e.g. serum) during transfection (Kim and Eberwine 2010, Fus-Kujawa, Prus et al.

2021). In this Chapter, the experiments were carried out with mouse MECs extracted from the mammary gland, containing myoepithelial and luminal cells. The complex requirements of both cell types of primary MECs could explain the low-efficiency transfection rate obtained (~32% for the forward transfection) in the experiments; nevertheless, the data analysis showed that CFTR expression was significantly reduced in the lumen formation experiments.

The reduction of CFTR expression in lumens was also verified by IF, as well as the localisation of this protein in mouse primary MECs. Although CFTR is an apical protein, it was also evident within the cytoplasm in MECs. This could be explained because CFTR is a protein that undergoes post-translational modifications before reaching the apical membrane (Bertrand and Frizzell 2003). Three different glycosylated variants of CFTR have been described: non glycosylated CFTR (127 kDa), core glycosylated CFTR (131 kDa), and CFTR with complex glycosylation (160KDa) (Gregory, Cheng et al. 1990). Moreover, to reach the membrane destination, the mature transmembrane CFTR protein is further processed through a secretion pathway. CFTR can be detected in the endoplasmic reticulum, Golgi apparatus (Ward and Kopito 1994) and in transit by the endocytic pathway through travelling vesicles (Bradbury, Cohn et al. 1994, Bradbury, Clark et al. 1999). The endosomes can send CFTR to the membrane again via recycling endosomes or for degradation in the lysosomes (Bertrand and Frizzell 2003, Ameen, Silvis et al. 2007, Kreda and Gentzsch 2011). This internalisation of CFTR from the membrane can occur by 50% in epithelial cells (T84 cells) (Prince, Tousson et al. 1993). Therefore, the cytoplasmatic expression of CFTR detected by the IF can come from these cell compartments previously mentioned.

Reduced expression of CFTR was demonstrated to have an effect on lumen formation by 36% in CFTR KD samples. This result supports findings in Chapter 3, where the specific inhibition of CFTR activity also reduced the formation of lumens. Therefore, modification of CFTR activity and expression has a measurable impact on lumen formation in our MEC model. These findings are consistent with what has been reported in the literature, where alteration of *CFTR* expression (deleted or mutated) affects the morphogenesis of tubular organs with lumen structures such as trachea (Ornoy, Arnon et al. 1987, Bonvin, Le Rouzic et al. 2008, Meyerholz, Stoltz et al. 2018), gut (Ornoy, Arnon et al. 1987), pancreas (Ornoy, Arnon et al. 1987), lungs (Ornoy, Arnon et al. 1987, Meyerholz, Stoltz et al. 2018) in different species. In addition, the importance of CFTR expression for lumen morphogenesis *in vivo* has been demonstrated. Navis et al. 2013 observed that *cftr* mutants have an absent lumen formation in Kupffer's vesicle in zebrafish, while the wild type presented a lumen (Navis, Marjoram et al. 2013). In vitro, the epithelial MDCK cells were modified to express either the most typical CF mutation (F508del-*CFTR*) or the normal CFTR expression to evaluate lumen formation. The result showed that normal *CFTR* expression was necessary to form cysts with a lumen space (Li, Yang et al. 2012). Thus, the normal expression of CFTR seems to be essential for lumen formation in vivo and in vitro in different biological systems.

Lumen maintenance was also affected after transfection with CFTR siRNA. The CFTR KD verification showed reduced expression of *Cftr* mRNA. Due to time constraints, further repeats of the CFTR KD verification in the organoids could not be completed since the collection of the organoids plated on the BMM was difficult to extract, and the few organoids collected gave low RNA concentrations that led to problems with

further processing. However, it was verified through the positive control siRNA that transfection occurred in the organoids. Furthermore, CFTR KD led to a reduction in lumen area relative to control.

After the CFTR KD, the area did not increase as the control did, in fact, the lumen area decreased in comparison with its original area (before the reduction of *Cftr* expression). These results show that CFTR expression is necessary not only for lumen formation but also for lumen maintenance in the MECs. Our results are coherent with the findings reported by other laboratory groups about the relevance of CFTR expression and activity in lumen formation and lumen size in primary epithelial cells cultured in similar conditions (BMM or collagen). (Dekkers, Wiegerinck et al. 2013, Schwank, Koo et al. 2013, Schutgens, Rookmaaker et al. 2019, Liu, Anderson et al. 2020). Dekkers et al. observed a rapid expansion of the organoid size and lumen in intestinal organoids from wild-type mice (expressing CFTR) cultured in BMM and treated with forskolin. In comparison, intestinal organoids without CFTR expression (Cftr−/− mice) treated with forskolin did not increase in size (Dekkers, Wiegerinck et al. 2013). Also, Liu et al. 2020, measured the luminal area of primary nasal epithelial organoids from non-CF healthy and with CF subjects cultured in BMM. They found a significant difference between the lumen area in non-CF and CF organoids; the lumen area of the CF organoids was smaller than the lumen area of the non-CF organoids (Liu, Anderson et al. 2020). Thus, the organoid lumen area and increase are dependent on the normal CFTR expression in other epithelial cells, and given the findings in this Chapter, there is now some evidence in support of a key requirement for CFTR in our MEC model.

For the lumen formation objective, the transfection with siRNAs was applied to cells in 2D conditions, and the evaluation of gene reduction was made with cells collected from a monolayer, while for the lumen maintenance, insufficient numbers of repeats were completed due to the challenges around the collection of the cells from 3D conditions, reducing the amount of biological material that could be obtained, as organoids were attached or partly embedded in BMM. It should be considered to repeat experiments to obtain the n=3 for relative mRNA expression and include analysis for the protein expression level, such as WB or IF, for the detection of CFTR after transfection.

In conclusion, this Chapter provides information about the CFTR expression and its relationship with a lumen structure in mammary epithelial organoids. The CFTR expression was reduced in mouse primary MECs post-transfection with specific siRNAs to the CFTR mRNA sequence. The reduction of CFTR expression in MECs significantly decreased the number of lumens formed in organoids derived from mouse mammary tissue. The lumen area in mammary organoids was also reduced after the CFTR KD in the mouse primary MECs. These results reinforce the previous results obtained in Chapter 3, demonstrating that CFTR activity and expression are important for lumen structure in MECs.

The importance of this finding gives rise to the deeper study of the role of CFTR in the developmental biology of the mammary gland, as well as the study of this protein in breast cancer since lumen space reduction is one of the main characteristics shared

in breast cancer development (Gudjonsson, Adriance et al. 2005, Kaushik, Pickup et al. 2016).

Chapter 5

5. CFTR EXPRESSION IN BREAST CANCER CELL LINES

5.1 INTRODUCTION

The mammary gland is an organ that is structurally made up of a connection of hollow ducts with a luminal space surrounded by polarised epithelia. The maintenance of the epithelia is essential for the homeostasis of this organ. Loss of the lumen space due to filling with epithelial cells is one of the main characteristics of breast cancer (Gudjonsson, Adriance et al. 2005, Kaushik, Pickup et al. 2016, Halaoui, Rejon et al. 2017).

A valuable model for studying mammary gland structures involves 3D cell culture using a BMM. The MECs can form organised and polarised cell structures containing a central lumen mimicking a mammary-like structure (Clevers 2016). However, most breast cancer cells are unable to form a lumen structure *in vitro*. Alterations in gene expression (Nguyen and Shively 2016), microenvironment (Patil, D'Ambrosio et al. 2015) or the polarisation process(Petersen, Ronnov-Jessen et al. 1992) are some of the reasons attributed to the inability of these cells to form lumens; however, the role of CFTR in lumen formation process in breast cancer cells is currently unknown.

CFTR expression is reported to be reduced in breast cancer tissue relative to healthy tissue (Zhang, Jiang et al. 2013, Liu, Dong et al. 2020). In addition, in one study, CFTR expression was localised to the cytoplasm rather than in the apical membrane (Figure 5.1). Moreover, ectopic overexpression of CFTR in the breast cancer cell line MDA-MB-231, increases the expression of E-cadherin and decreases cell invasion and migration *in vitro* and metastasis *in vivo* (Zhang, Jiang et al. 2013).

The function of a protein is usually investigated by experimentally expressing the corresponding gene of interest in a model system. *In vitro*, ectopic gene expression in mammalian cells usually occurs through different types of expression systems that allow stable and transient expression. cDNA or ORF in an expression vector is the most common way to overexpress a gene. To achieve stable expression, the exogenous genetic material (DNA) transfected into the cell is incorporated into the genomic DNA. In contrast, in transient expression models, the exogenous genetic material (DNA or RNA) is not integrated into the genome, so its expression is temporary and limited (Kim and Eberwine 2010). Despite the different approaches, both methods can successfully express the desired protein in mammalian cells. The advantages and disadvantages must be evaluated concerning the experimental design, gene, vector size and the type of cells to work on (Recillas-Targa 2006, Kim and Eberwine 2010, Fus-Kujawa, Prus et al. 2021). Since the previous Chapters 3 and 4 showed that CFTR activity and expression are essential for forming and maintaining a lumen in healthy mouse MECs, the transient transfection using a DNA vector containing the ORF of CFTR was chosen for use in breast cancer cells.

Another way to study protein function is by its stimulation or inhibition. The modulation of ion channel activity has been broadly studied using drugs. They can bind directly to the ion channels to alter their configuration and activity or act indirectly through intermediaries (Camerino, Tricarico et al. 2007). One indirect stimulator of CFTR activity is forskolin, which is a diterpene that binds at the pseudo substrate site on the adenylate cyclase enzyme. Forskolin stimulates adenylate cyclase, raising intracellular cAMP, which activates PKA to phosphorylate the R domain of the CFTR ion channel and, together with ATP, permits conformational changes for the active

stage of this ion channel (Anderson, Berger et al. 1991, Cheng, Rich et al. 1991, Picciotto, Cohn et al. 1992).

Investigating the expression and activity of CFTR in breast cancer is an underexplored area; nevertheless, the relationship between CFTR and breast cancer is beginning to become apparent. An example of this is the increasing incidence of breast cancer cases in patients with CF (Archangelidi, Cullinan et al. 2022, Stastna, Brat et al. 2023). CF patients present mutations in the CFTR gene. The deletion of phenylalanine 508 (ΔF508 CFTR) is the most common mutation, which alters the protein folding and stability and, therefore, its channel function (Du, Sharma et al. 2005). The impaired function of CFTR in CF patients mainly affects organs composed of ducts related to fluid secretion since CFTR plays a fundamental role in this mechanism. (Farrell, Rosenstein et al. 2008, Ostedgaard, Meyerholz et al. 2011, Yu and Sharma 2023). Among the organs composed of tubular structures is the mammary gland, an exocrine gland with a function related to secretion during lactation. This fact lends weight to a potentially important relationship between CFTR function and the recent reports of breast cancer incidence in patients with CF.

The previous chapters showed for the first time that CFTR is essential for lumen formation and maintenance in the MECs. Going beyond the CFTR role in lumen formation and maintenance in normal cells and knowing that breast cancer cells do not form lumens and have low CFTR expression in breast tissue, the hypothesis of this Chapter is that **CFTR expression and/or activity is reduced in breast cancer cell lines and its overexpression or stimulation induce lumen formation.**

The aim of this Chapter is to determine the CFTR expression in human breast cancer cell lines and evaluate the CFTR role in lumen formation in breast cancer cell lines by undertaking the following objectives:

- To analyse the expression of CFTR in a range of breast cancer cell lines *in silico* and experimentally by qPCR and WB.
- To evaluate the cellular localisation of CFTR in breast cancer cells by IF and WB.
- To stimulate CFTR activity using forskolin and evaluate lumen formation in breast cancer cells.
- To develop a CFTR over-expression vector to transfect breast cancer cells and evaluate the ability of these cells to form lumens.

5.2. METHODS

5.2.1 Analysis of CFTR expression in breast cancer cell lines

A search for information on CFTR expression in breast cancer cell lines was conducted in the Gene Expression Omnibus (GEO, https://www.ncbi.nlm.nih.gov/gds) database and The Human Protein Atlas (https://www.proteinatlas.org/).

The Human Protein Atlas data was obtained from the database website selecting the RNA expression of CFTR in breast cell lines. The data presented in the graphs are shown as normalised transcript per million TPM normalised expression values (nTPM).

The data obtained from GEO has accession no. GSE152908. Data was analysed by Dr Sarah Waite. RNA read counts were normalised by RNA length (as per NCBI database) and then by read depth. These normalised RNA read Counts were used to perform differential gene analysis by DESeq2. The normalised RNA read counts were plotted to visually compare CFTR expression between breast cancer and non-tumorigenic breast cell lines.

5.2.2 Cell culture of breast cancer cell lines

5.2.2.1 2D CELL CULTURE

Most of the cell lines were kindly donated by different lab groups from the Department of Oncology and Metabolism at the University of Sheffield. The CAL-51, T47D, and MDA-MB-231 cell lines were obtained from Dr Helen Bryant lab group, the MCF1OA cell line from Dr Chris Toseland lab group, and the MCF7 cell line was from Dr Mark Fenwick lab group. Once the cells were obtained, the passage number did not exceed 15.

For RNA and whole cell protein extraction, cells were split from T-75 flasks, collected as a pellet by centrifugation, resuspended in media, counted, and seeded ($2x10^4$) on 10cm dishes to culture as a monolayer as described in sections 2.3.3 and 2.3.4. The cells were cultured for 3 days, with the media being changed on day 2. On day 3 the cells were detached and collected by centrifugation at 1000rpm (288xg) for protein or RNA extraction. Three replicates were carried out per experiment (n=3) or as indicated in the results.

For the membrane and cytoplasm protein expression experiments, cells were collected as a pellet by centrifugation, resuspended in media, counted, and seeded on 6 well plates to culture them on monolayer as described in sections 2.3.3 and 2.3.4. The media was changed every 2 days. When cells were 80-90% confluent, the cells were detached from the plates by incubation in trypsin for 1 minute prior to using a

scraper to remove the cells from the plate and were centrifuged at 1000rpm (288xg). Three replicates were carried out per experiment (n=3) or as indicated in the results.

For the IF experiments, the cells were seeded ($5x10^6$) on coverslips placed on 24-well plates. The cells were cultured as described in the 2.3.3 and 2.3.4 sections for monolayer conditions. Three experiments with two replicates were carried out.

5.2.2.2 3D CELL CULTURE

The breast cancer cell lines were cultured on the surface (top) of 70µl of solidified (by incubation at 37°C for 15 minutes) Cultrex Reduced Growth Factor Basement Membrane Extract (Type 2, Pathclear, Biotechne) for 11 days to track the 3D cell structures and their ability to form a lumen. The same media for the EpH4 cells cultured in 3D conditions (described in section 2.6.1) was used for all the breast cancer cell lines and changed every 2 days.

For the drug experiments, the CAL-51 cells were seeded on 70µl of solidified (by incubation at 37°C for 15 minutes) Cultrex Basement Membrane Extract, Type 2, Pathclear. The same recipe of media of the EpH4 cells cultured in 3D conditions (described in section 2.6.1) was used to culture the cells. The media was changed every 3 days.

5.2.3 Protein extraction

5.2.3.1 WHOLE CELL PROTEIN EXTRACTION

The protein extraction was made from the different cell lines cultured in 2D conditions on 10cm dishes and collected as described in section 5.2.2.1. Protein extraction and quantification were carried out in accordance with the methods described in sections 2.20.1 and 2.21. Once collected from the cells, the protein samples were maintained on ice prior to further analysis.

5.2.3.2 MEMBRANE AND CYTOPLASMATIC PROTEIN EXTRACTION

The cells used for this protein extraction were cultured and collected as described in section 5.2.2.1. The protein extraction and quantification were made following the methods described in sections 2.20.3 and 2.21. Once collected from the cells, the samples were maintained on ice prior to further analysis.

5.2.4 Western Blot

The proteins extracted and quantified were processed for WB following the procedure mentioned in Section 2.23. Three independent experiments (3 different cell cultures and extractions at different times and passage numbers) were used for these experiments.

5.2.5 Immunofluorescence

The cells were cultured on glass coverslips as described in section 5.2.2.1 and were fixed and stained as described in section 2.9.2. Photos of random sections were taken with the fluorescence microscope (Zeiss LSM980 Confocal microscope). Three experiments with two replicates were carried out.

5.2.6 Drug treatment in CAL-51 cells cultured in 3D conditions with BMM

The CAL-51 cells were cultured as described in section 5.2.2.2. The cells were treated with 10μM forskolin or equivalent volume of DMSO for the control for 6 days. The treatment was applied in media on day 3 after seeding the cells, and the media containing the forskolin was changed every 2 days to the cells cultured on Cultrex Basement Membrane Extract. Two independent experiments with three replicates were carried out. 24 photos of randomly selected sections (from 2 independent experiments) were taken to count the number of 3D cell structures (at least 109 per group). The analysis to determine the number of acini was described in section 2.8.3.

5.2.7 CFTR overexpression

5.2.7.1 VECTORS

The vector containing the human CFTR sequence and the negative control vector (without CFTR sequence) are detailed in section 2.18. The negative vector was

created from the CFTR vector (HaloTag® human ORF in pFN21A, Promega). The production process for the negative vector consisted of the design of primers that flank the region to be deleted in the vector using the NEBase Changer software. The PCR was made to exclude the CFTR ORF, and the products generated were processed using the Q5 Site-Directed Mutagenesis Kit, following the manufacturer's instructions for the phosphorylation and ligation and the digestion of the plasmid template. The new plasmids obtained were stored at -20 °C for their amplification in bacteria.

5.2.7.2 BACTERIAL TRANSFORMATION AND OBTENTION OF THE AMPLIFIED PLASMID IN BACTERIA

The plasmids and bacteria were slowly defrosted on ice and used for bacterial transformation. The method followed is described in section 2.18.

The plasmid DNA was obtained once the bacteria transformation and amplification were done, as described in section 2.11. Finally, the DNA extracted from bacteria was quantified using the NanoDrop (Thermo Scientific). The plasmid DNA was stored at -20 °C in small aliquots for future experiments.

5.2.7.3 RESTRICTION DIGESTS AND ANALYSIS

Enzyme restriction digests were done to make specific cuts in the plasmid DNA sequence. The *in silico* amplified negative control vector sequence (Appendix I) was used to determine the restriction sites and the enzymes (listed in Table 5.1) that can

cut the vector and predict the fragments generated using the NEBcutter program. The enzymes described in Table 5.1 were used according to the manufacturer's instructions.

Table 5.1 Restriction enzymes used to cut specific sites in the plasmids.

Enzyme	Brand	Site
HindIII	New England Labs	5' A▼A G C T T 3' T T C G A▲A
XhoI	New England Labs	5' C▼T C G A G 3' G A G C T▲C
KpnI	New England Labs	5' G G T A C▼C 3' C▲C A T G G

The resulting products from the restriction digest were analysed by size in (bp) in an electrophoresis gel (1% agarose) using a full ranger DNA ladder (NORGEN BIOTEK CORP, 100pb) as a reference.

5.2.8 Permeability assays with the CAL-51 cells

$2x10^4$ CAL-51 cells were seeded on semi-permeable membranes with pores of 0.4µm. The cells were cultured for 3 days in standard media for 2D cell cultures of the breast cancer cells (section 2.3.3). The forskolin was applied on day 3 following the procedure described in section 2.14.3.

5.3 RESULTS

5.3.1 mRNA CFTR expression in breast cancer cells

Initially, CFTR expression was investigated in a range of breast cancer cell lines by analysing information from a database. Data from the Human Protein Atlas shows that *CFTR* expression was detected in 8 of 62 cell lines evaluated. The MFM-223 (Triple negative), ZR75-1 (Luminal A), CAL-51 (Triple negative), AU565 (HER2 positive), CAL-85-1 (Triple negative), HCC1954 (HER2 positive), MDA-BM-157 (Triple negative) and MDA-MB-415 (Luminal A) are the cells that express *CFTR* (Figure 5.1A). The five breast cancer cell lines with a comparatively higher level of expression are MFM-223, CAL-51, ZR75-1, AU565 and CAL-85-1.

Another analysis of *CFTR* expression was performed with data obtained from the GEO database (no. GSE152908). Sixty-three breast cancer cell lines were included in the data analysis, of which only 28 expressed *CFTR*. The comparison between the normalised CFTR transcript values of the non-tumorigenic breast cells and breast cancer cell lines is shown in Figure 5.1B. Compared with the non-tumorigenic, *CFTR* expression in breast cancer cells showed no significant difference. Seven non-tumorigenic breast cell lines were included in the data analysis; however, only 184B5 was shown to express *CFTR*. The five breast cancer cell lines with a comparatively higher expression level are HCC1569, HCC1187, MDAMB361, HCC1954 and CAL-51. MDAMB361 (Luminal B), HCC1187 (Triple negative), and HCC1569 (HER2

positive) breast cancer cell lines express more *CFTR* than the non-tumorigenic 184B5 cell line.

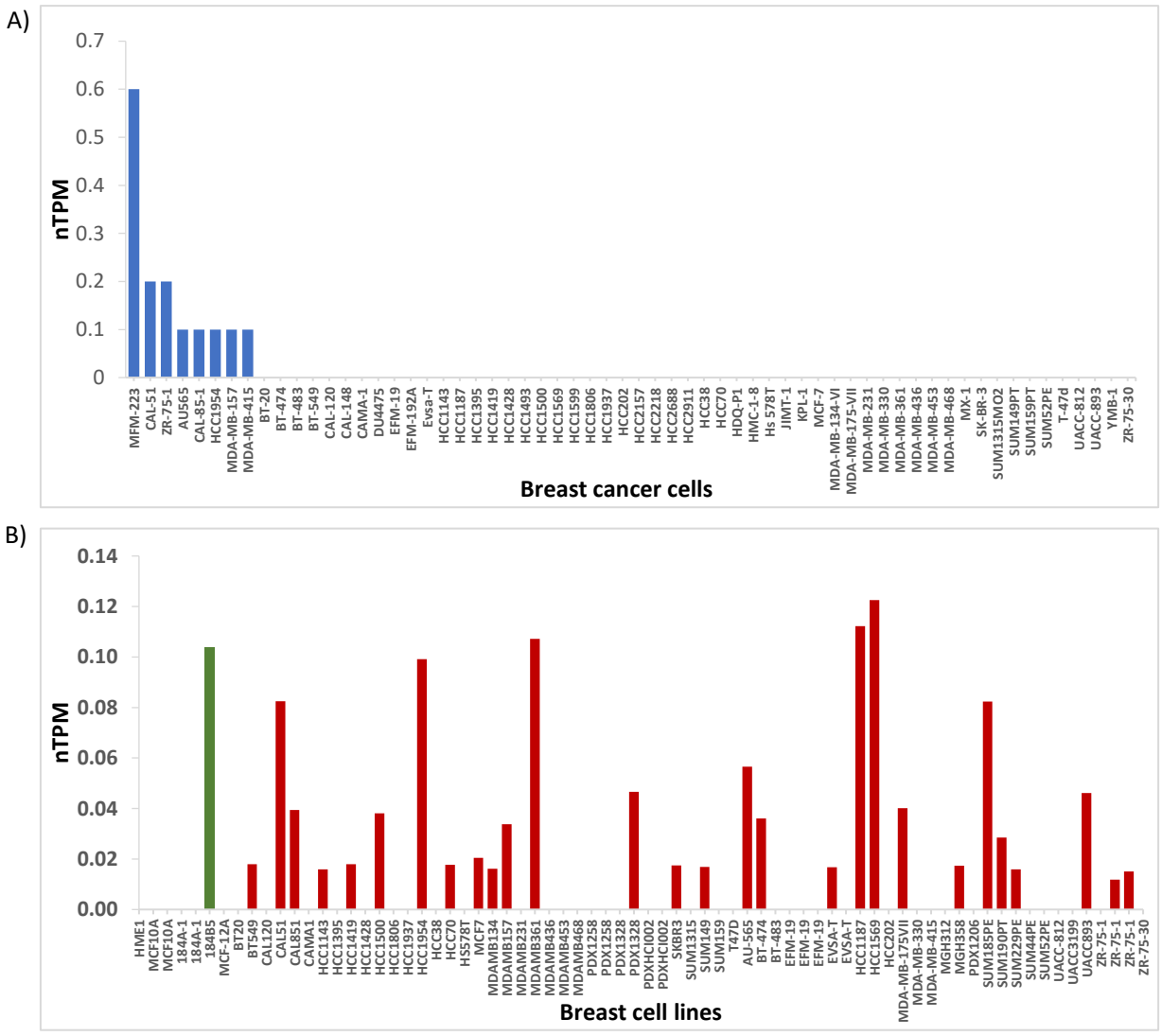

Figure 5.1. *CFTR* expression in a range of breast cell lines. A) *CFTR* profile expression of breast cancer cell lines from Protein Human Atlas database. The data are displayed as normalised transcript per million (nTPM) values. Data collected from the Protein Human Atlas database. B) Comparison of the *CFTR* expression in breast cancer (in red) and non-tumorigenic breast cell lines (in green). Data was obtained from the GEO database (no. GSE152908). The data are displayed as normalised transcript per million (nTPM) values.

Next, an experimental evaluation of *CFTR* expression was carried out to further analyse breast cancer and non-tumorigenic cell lines included in the *in silico* analysis. The CAL-51, MDA-MB-231, MCF7 and T47D breast cancer cell lines and the non-tumorigenic MCF10A cell lines were grown in 2D conditions and processed for RNA extraction and qPCR. MCF10A cells (mammary epithelial cells) were included as a control because they are a well-known cell line that can form lumens (Debnath, Muthuswamy et al. 2003). The qPCR results showed cycles between 22-24 for the reference gene (β -Actin) and cycles between 24-26 for *CFTR*. Analysis for the relative *CFTR* expression to the reference gene (β -Actin) did not show a significant difference between the breast cancer cell lines (CAL-51, MDA-MB-231, CF7 and T47D) and the non-tumorigenic cells (MCF10A) (Figure 5.2).

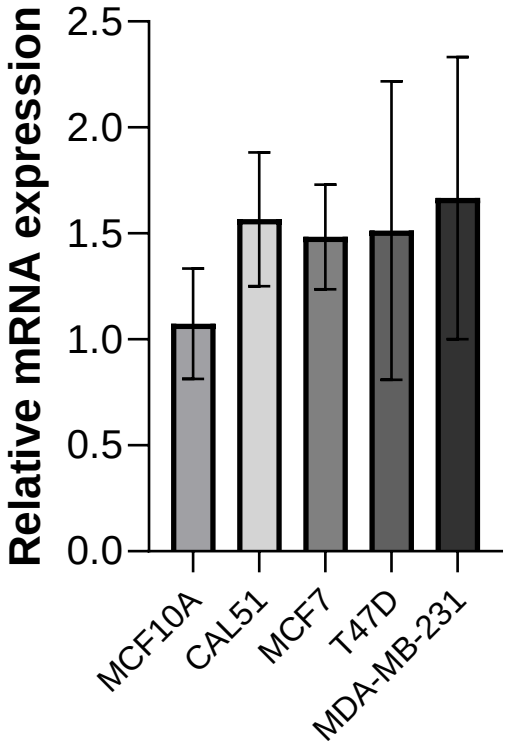

Figure 5.2. *CFTR* expression in breast cell lines. A) Relative mRNA expression of *CFTR* detected by qPCR. Data were normalised relative to the expression of β -Actin (internal housekeeping gene) and presented as fold change. The graph shows mean ± SEM (n=3). A One-way ANOVA was used to compare groups (P>0.05).

Since no changes were found in the expression of the mRNA between the non-tumorigenic cells and the breast cancer cells, and that *CFTR* is a gene that codes for a complex protein that undergoes a maturation process and transport to the plasma membrane, the study of mature CFTR protein was carried out in the cell lines.

5.3.2 CFTR expression in breast cancer cells

To study CFTR protein expression, the cell lines were first seeded in a monolayer, cultured for 3 days and collected to extract their protein fraction. WBs were made using 20µg of protein per sample. Verification of a similar amount of protein used in the WB was analysed (Appendix VI). A band that corresponded to the mature form of CFTR (160-170KDa) was detected in MCF10A cells. CFTR was evident in the MCF10A cells but less obvious in the CAL-51 cells. The rest of the breast cancer cells showed no CFTR mature protein expression (Figure 5.3).

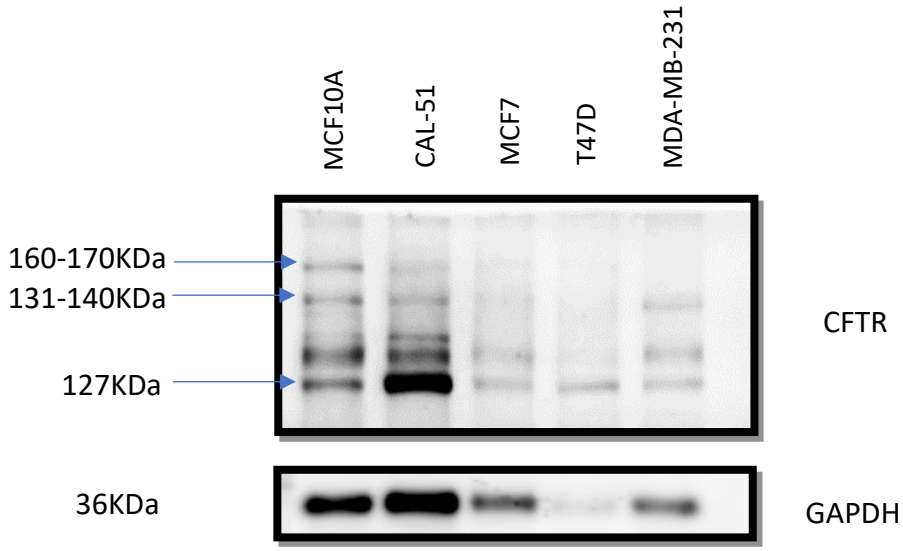

Figure 5.3. CFTR protein expression in breast cell lines. Protein CFTR expression detected by WB in breast cell lines. GAPDH served as a loading control.

Other bands with molecular weights different from the mature CFTR protein form were also detected in the WBs (full/uncropped blots in Appendix VII). Three different molecular weights have been described for CFTR, one at ~127KDa, which is not glycosylated and the other two forms glycosylated of ~131KDa and 160-170KDa (Jacquot, Puchelle et al. 1993, O'Riordan, Lachapelle et al. 2000). To understand more about the bands detected on our WBs and their location in epithelial breast cells, their proteins were extracted from the cytoplasmic and membrane fraction, and the presence of CFTR in these cell compartments was evaluated by WB.

5.3.2.1 CFTR EXPRESSION IN CYTOPLASM

MCF10A and several breast cancer cell lines were cultured on 2D conditions until they showed 80-90% cell confluence for protein extraction and CFTR evaluation by WB. In the cytoplasmic protein fraction, CFTR was detected with the molecular weights of ~160-170kDa (Figure 5.4A), ~130KDa (Figure 5.4B) and a band between the 93KDa-130KDa (Figure 5.4C), in all the breast cell lines. The protein intensity of the known glycosylated forms of CFTR bands was quantified and compared between the groups (Figure 5.4 D, E and F). No significant differences were found.

A) Molecular weight corresponding to the complete glycosylation CFTR protein form (160-170KDa)

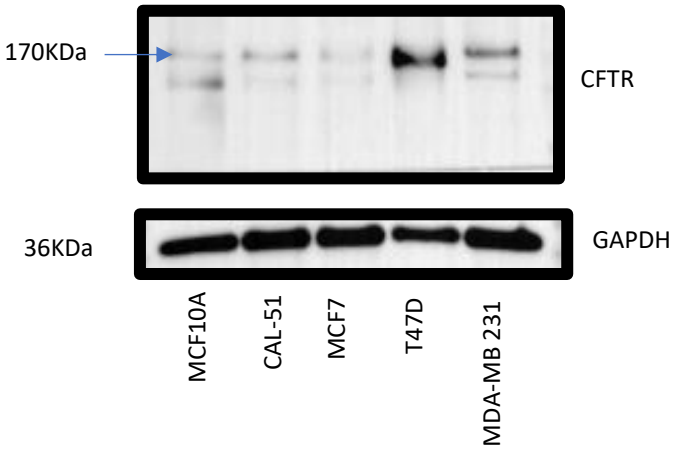

D)

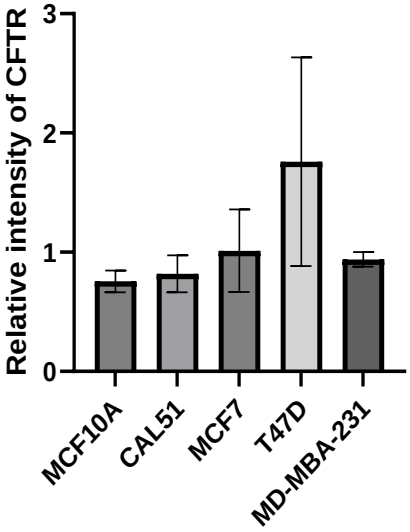

B) Molecular weight corresponding to the core glycosylation CFTR protein form (130KDa)

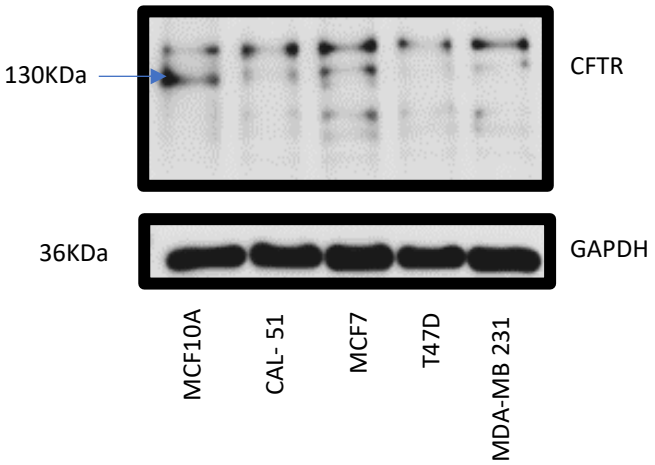

E)

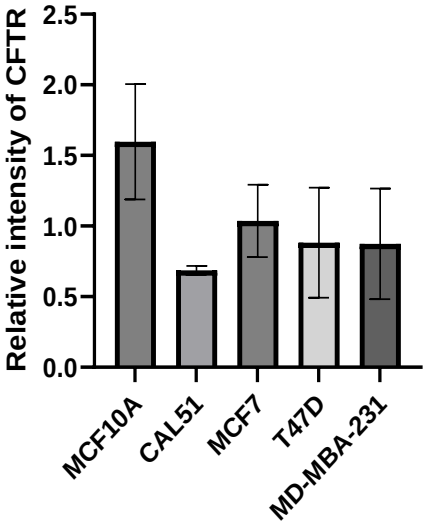

C) Molecular weight corresponding to the non-glycosylation CFTR protein form (~127KDa)

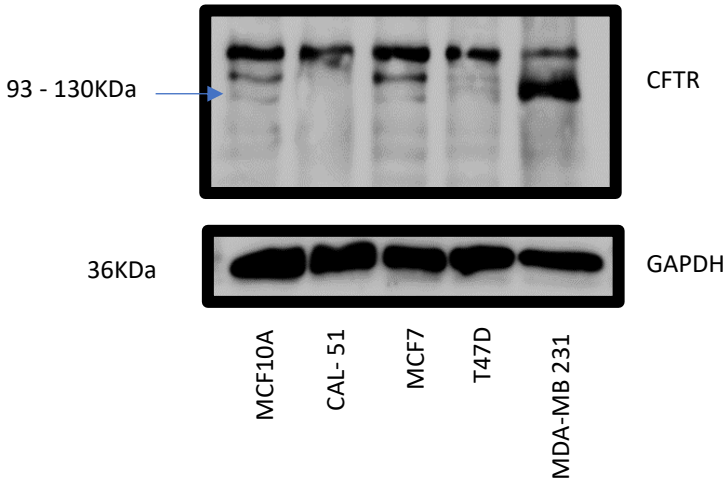

F)

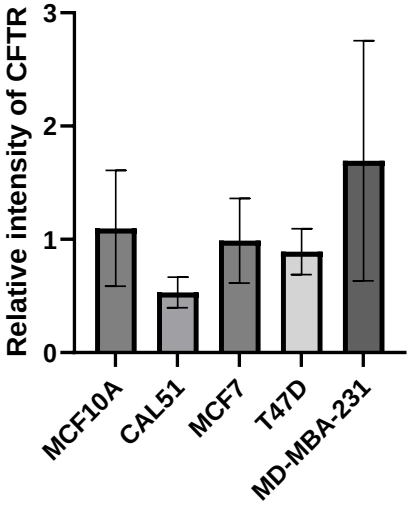

Figure 5.4. Expression of CFTR protein in the cytoplasmic fractions of MCF10A and breast cancer cells. A), B) and C) Representative WBs for detecting the ~170KDa, ~130KDa and 93-130KDa CFTR forms in the cytoplasmic protein fraction. D), E), and F) Relative intensity protein level of CFTR. The relative intensity of CFTR is defined as the intensity of the CFTR protein band normalised against the intensity band of GAPDH. The graph shows mean ± SEM (n=3 from independent experiments). A One-way ANOVA was used to compare groups (*P*>0.05).

Moreover, there were no differences in expression when the total protein (the 3 different molecular weights) in the cytoplasm of the breast cell lines combined (Figure 5.5).

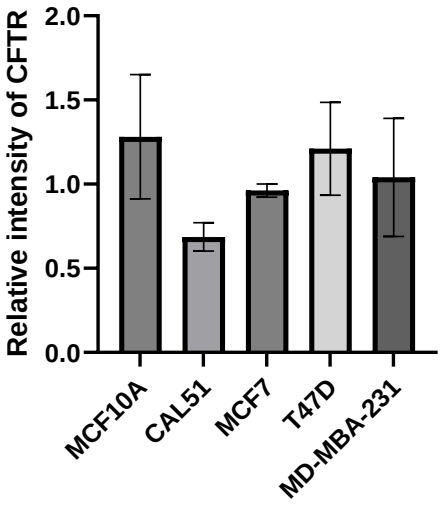

Figure 5.5. Total expression of CFTR in the cytoplasmic fractions of MCF10A and breast cancer cells. Total relative intensity protein level of CFTR expression (160-170kDa, ~130KDa and 93KDa-130KDa) detected in the cytoplasmic fraction. The relative intensity of CFTR is defined as the intensity of the CFTR protein band normalised against the intensity band of GAPDH. The graph shows mean ± SEM (n=3 from independent experiments). Data shows the n=3. Each n represents proteins from independent experiments. A One-way ANOVA was used to compare groups (*P*>0.05).

5.3.2.2 CFTR EXPRESSION IN THE MEMBRANE

In the membrane fraction, CFTR was detected with the ~160-170KDa molecular weight in the MCF10A cells. By comparison, the same band was not detectable in the membrane fraction of the breast cancer cells (5.6A).

Another molecular weight close to the weight corresponding to the mature CFTR protein form is observed in the MCF7, T47D and MDA-MB-231 cells (Figure 5.4B). These bands present a higher molecular weight than 170KDa, and their expression is consistent in all WBs (full/uncropped blots in Appendix VIII).

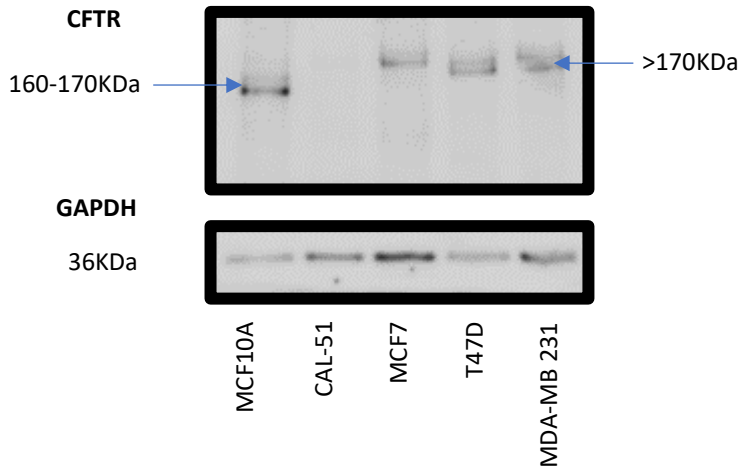

Figure 5.6. Expression of CFTR protein in the membrane fractions of MCF10A and breast cancer cells. Representative WB images shown n=3. CFTR protein detection in the membrane protein fraction of breast cancer cell lines: in the left the arrow points the 160-170KDa molecular weight, and on the right, the >170KDa molecular weight. GAPDH is used as a loading control.

5.3.2.3 CFTR EXPRESSION IN CYTOPLASM AND MEMBRANE

The previous results showed that the molecular weight corresponding to the mature CFTR form (160-170KDa) is expressed simultaneously in the cytoplasm and

membrane only in the MCF10A cells (Figures 5.4A and 5.6A). Because CFTR is a protein that is functionally found in the apical membrane with a molecular weight corresponding to 160-170KDa, and in the WB, it was also detected in cytoplasmic protein fraction, we sought to compare the expression levels in both compartments (Figure 5.7). This relationship can give us an idea of the trafficking of the mature protein from the cytoplasm to the membrane in the MCF10A cells. The mature form of CFTR (160-170KDa) has more expression in the membrane than in the cytoplasm ($P < 0.05$). Trying to visualize the global expression of CFTR in the non-tumorigenic MCF10A cells (which were the only ones that presented the molecular weight corresponding to the mature expression of CFTR in the cytoplasmic and membrane protein fraction), the expression of the precursor and mature forms (160-170kDa, ~130KDa and 93KDa-130KDa) of CFTR in the cytoplasm was compared with the expression of the mature and theoretically functional (160-170KDa) CFTR protein in the membrane protein fraction. Similar levels of protein intensities were detected in both cell compartments, and no significant differences were found (Figure 5.7B).

Finally, to determine the total CFTR protein expression related to the glycosylated state (160-170kDa, ~130KDa and 93KDa-130KDa), the intensity levels of CFTR proteins from the membrane and cytoplasm were added and compared between the different cell lines (Figure 5.7C). No significant differences were found between the groups.

A) CFTR protein expression (160-170KDa) in membrane and cytoplasmic protein fractions in MCF10A Cells.

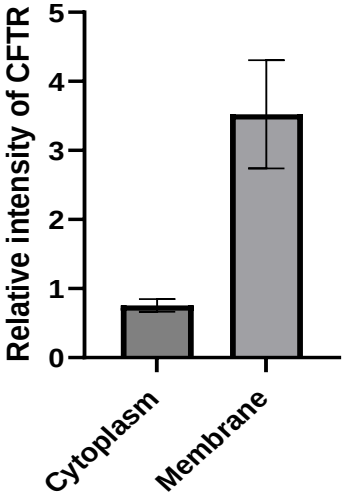

B) CFTR protein expression (160-170kDa, ~130KDa and 93KDa-130KDa) in cytoplasm protein fraction and CFTR protein expression (160-170KDa) in membrane protein fraction in MCF10A cells.

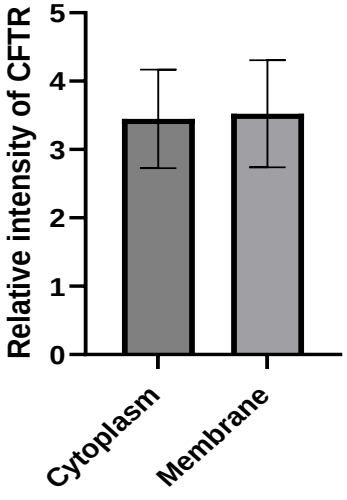

C) CFTR protein expression (160-170kDa, ~130KDa and 93KDa-130KDa) in cytoplasm and membrane protein fractions in breast cells.

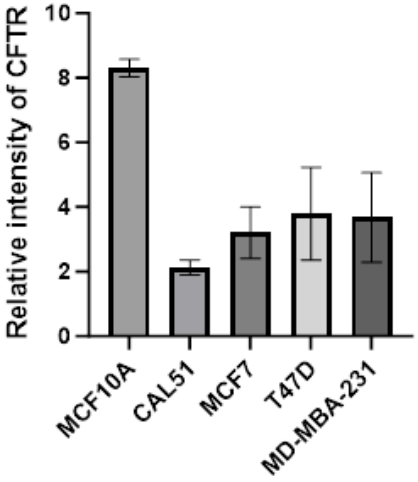

Figure 5.7. Expression of CFTR protein forms in membrane and cytoplasm fractions in MCF10A and breast cancer cell lines. A) Comparison between the mature CFTR protein expression (160-170KDa) in membrane and cytoplasmic fractions in non-tumorigenic MCF10A cells. An unpaired student's t-test was used to compare groups. **P*< 0.05. B) Comparison between the combined expression of CFTR (160-170kDa, ~130KDa and 93KDa-130KDa) in the cytoplasm with the expression of mature CFTR (160-170KDa) in the membrane of MCF10A cells. An unpaired student's t-test was used to compare groups. C) Total protein level of CFTR forms (160-170kDa, ~130KDa and 93KDa-130KDa) from both

cytoplasmic and membrane fractions in all breast cell lines. All data shows n=3 from independent experiments. Each n represents proteins from independent experiments. Kruskal-Wallis test was used to compare groups.

5.3.3 CFTR localisation

The only cell line that presented the mature molecular weight of CFTR protein in the protein membrane fraction was the MCF10A. Therefore, experiments for protein localisation by IF were carried out. It was evaluated whether the expression of CFTR shown in the WB with the proteins from membrane fraction could be detected by IF in the apical membrane of MCF10A cells. Likewise, determine if the >170KDa CFTR proteins in the WB with breast cancer cell proteins have an apical expression pattern and compare it with the CFTR expression in MCF10A. As was described in Chapter 4 (page 126), ZO-1 is a TJ protein, which is associated with the apical membrane location. Therefore, it was also used as a reference for detecting CFTR in the apical membrane when the ZO-1 signal was present. IF showed that MCF10A cells express CFTR in the apical membrane and mostly colocalising with ZO-1 (Figure 5.8). Similarly, IF shows that CFTR was also localised to the membrane of breast cancer cells. Only in some areas is CFTR expression observed in the membrane of some breast cancer cells, but not uniformly as in the MCF10A and MDA-MB-231 cells. The ZO-1 expression is mainly observed in the periphery of the cells in all cell lines except for the T47D. However, some differences are observed; the MDA-MB-231, for example, presents a clear signal of the ZO-1 protein in comparison with the rest of the cell lines.

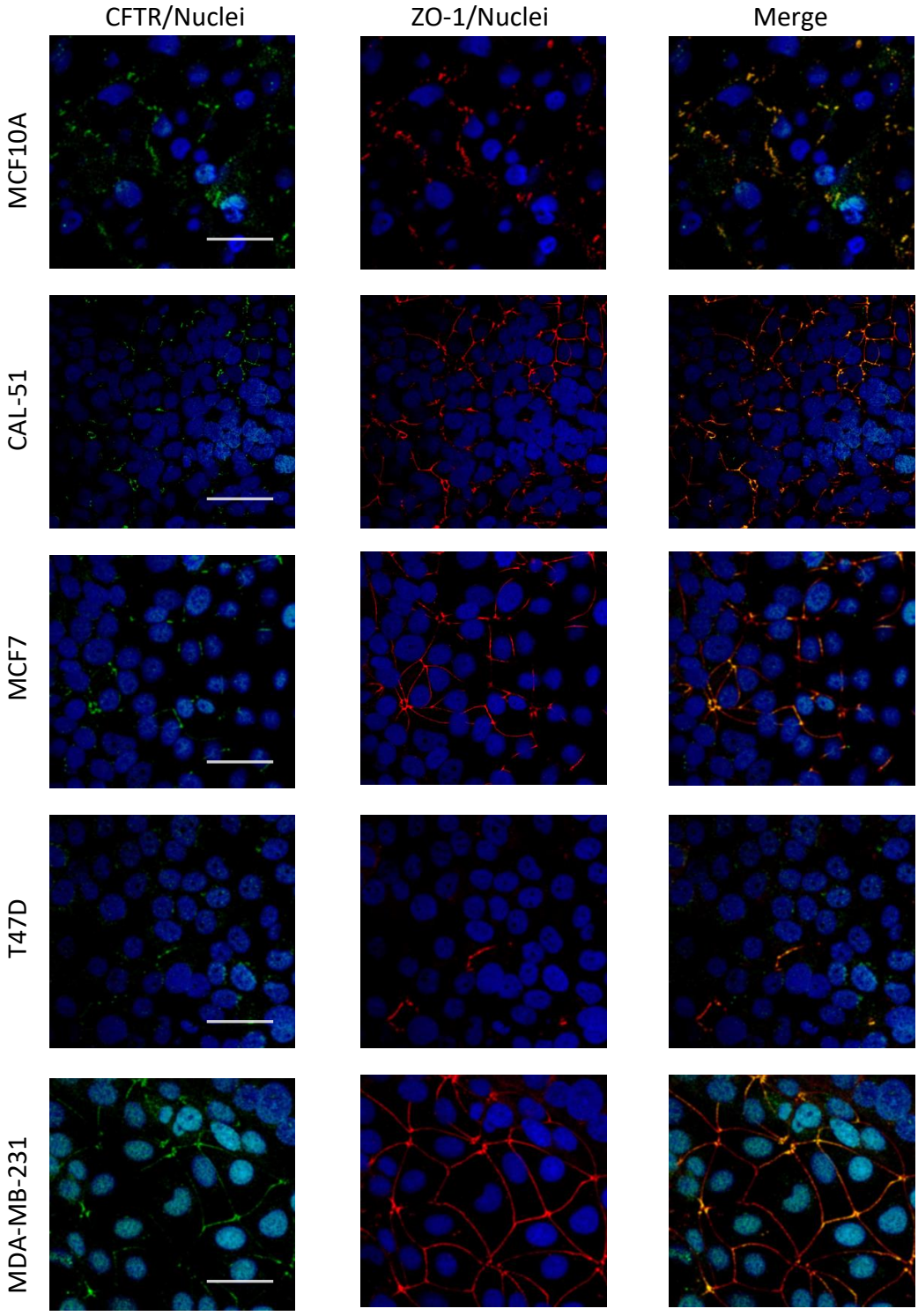

Figure 5.8. CFTR apical expression in breast cell lines. Representative images of CFTR expression and localisation in the non-tumorigenic cell line MCF10A and in the CAL-51, MCF7, T47D, and MDA-MB-231 breast cancer cell lines. Antibodies were used to label CFTR (green) and ZO-1 (red). Nuclei (blue) are stained with Hoechst. Scale bar=50µm. Microscope magnification= 40X.

5.3.4 Evaluation of lumen formation in breast cancer cells

It is known that MCF10A can form 3D cell structures with lumen structures (acini) (Debnath, Muthuswamy et al. 2003) and that cancer cells fail to form cellular structures with a lumen *in vitro* (Kenny, Lee et al. 2007). Firstly, lumen formation was evaluated experimentally in the MCF10A cells (Figure 5.9A).

The evaluation of lumen formation in the breast cancer cells was carried out by growing the cells on BMM over 11 days. Although the same cell density was seeded and the same media and conditions were used, the 3D cell structures that developed exhibited different sizes and shapes between the cell lines (Figure 5.9B). The CAL-51 cells formed mainly two shapes of 3D cell structures, some with a round shape and others with amorphous clusters of cells (Figure 5.10A). These different shapes were evident from day 5 (Figure 5.9B). Some of the CAL-51 3D cell structures with a round shape showed a small empty space in the inner part of the cell mass but not a well-defined lumen (Figure 5.10B). All other breast cancer cell lines could not form a single lumen under the conditions used.

Since the CAL-51 cells cultured on 3D conditions with BMM showed morphological signs of early lumen formation after day 11 (Figure 5.10B), it was decided to stimulate cells using forskolin to further evaluate the ability of these cells to form a lumen.

A)

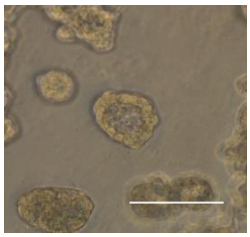

B)

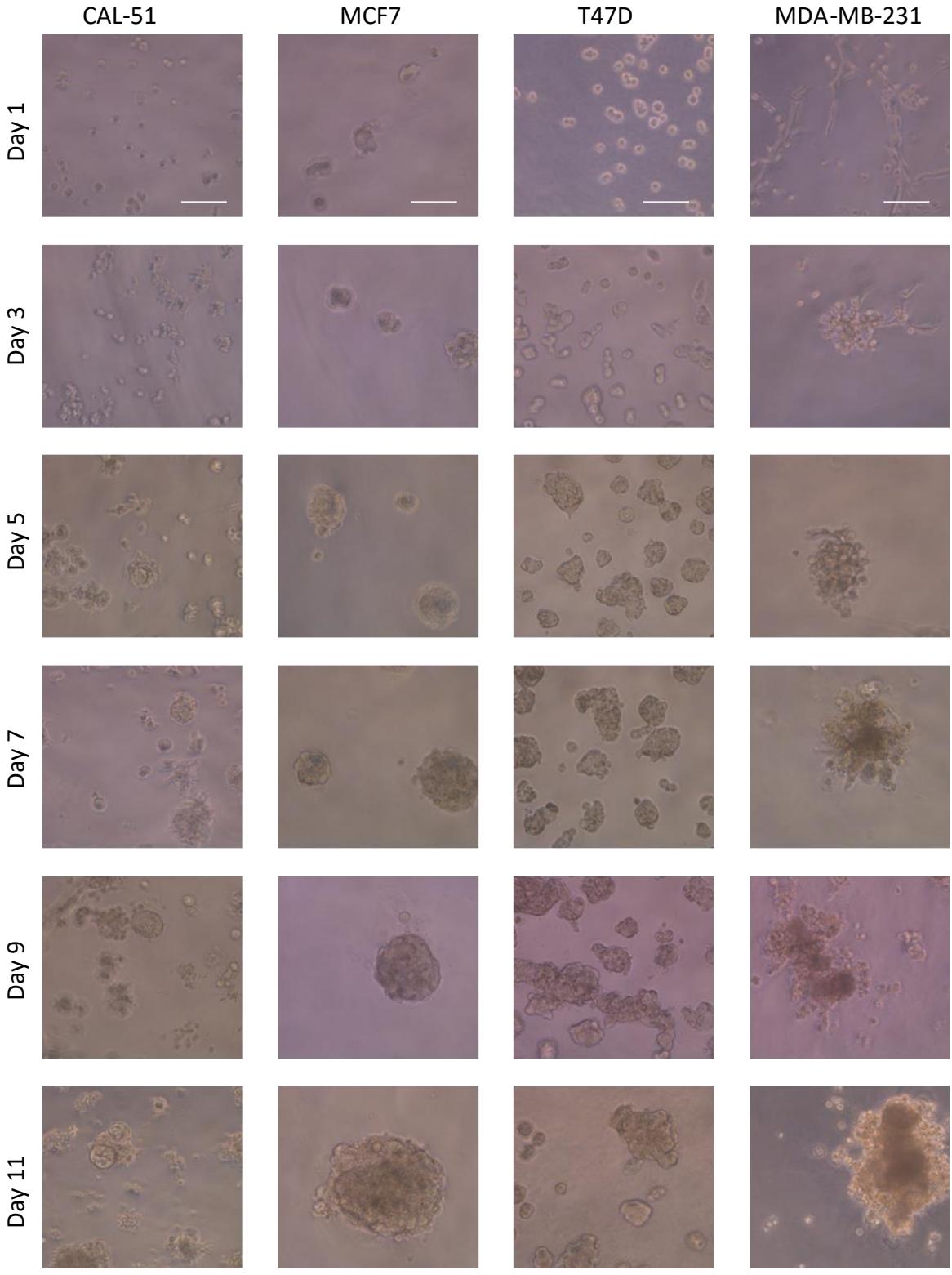

Figure 5.9. Breast epithelial cells seeded on 3D conditions with BMM. A) Lumen structure in the MCF10A acini on day 8. Scale bar= 100µm. Microscope magnification= 20X. B) Representative images of CAL-51, MCF7, T47D and MDA-MB-231 cells cultured on 3D conditions with BMM for 11 days. Scale bar= 100µm.

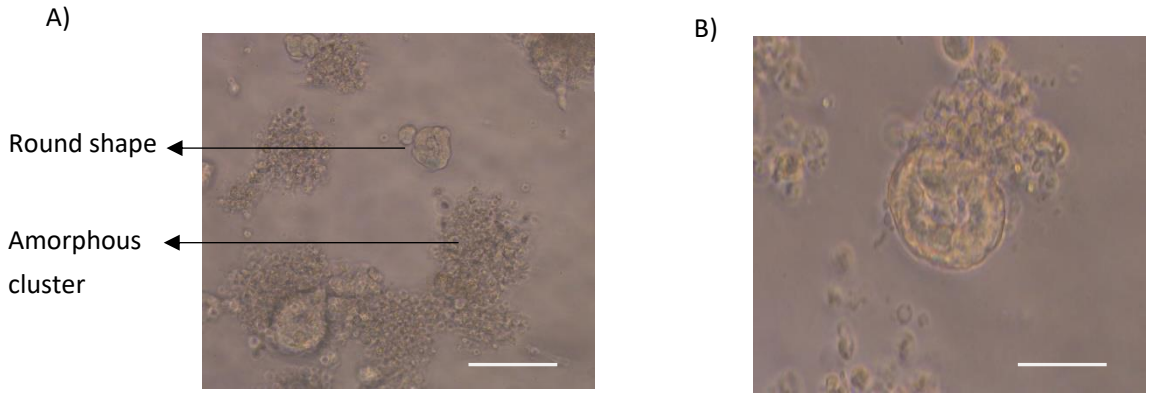

Figure 5.10. CAL-51 cell shapes formed on 3D cell culture with BMM. A) Amorphous cluster of cells and round-shaped. B) Representative photo of a 3D cell structure with a small lumen/microlumens on day 11 after seeding on the top of the BMM the CAL-51 cells. Scale bar= 100µm. Microscope magnification= 20X.

5.3.4.1 CFTR STIMULATION IN CAL-51 CELLS

The CAL-51 cells were grown in 3D conditions to form 3D cell structures, and forskolin treatment was applied in the first three post-seeding days until day 9. Figure 5.8 shows the CAL-51 cells on day 3 prior to the treatment and after treatment on day 9. After 6 days of culture, round and amorphous shapes were evident. Lumens were observed within some of the round-shaped 3D cell structures exposed to forskolin (Figure 5.11).

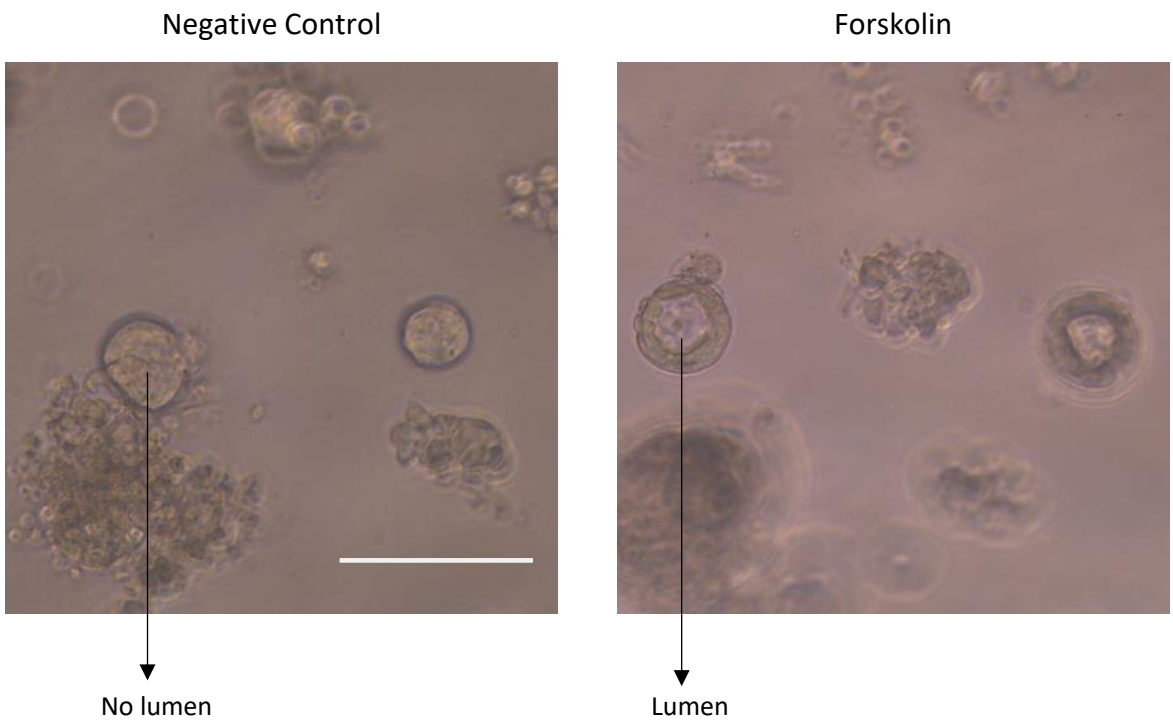

Figure 5.11. Lumen formation in CAL-51 cells after forskolin treatment. A) Example of CAL-51 3D cell structures formed (without a lumen) on day 9 after 6 days of media with DMSO (Negative control). B) Example of CAL-51 3D cell structures formed (with and without a lumen structure) on day 9 after 6 days of media with 10µM forskolin. Scale bar=100µm. Microscope magnification= 20X.

5.3.5 Permeability assays after CFTR stimulation with forskolin

Based on the previous results (see 5.3.4.1 section), where CFTR activity stimulation influenced lumen formation in CAL-51 cells, further experiments were carried out to examine paracellular fluid transport after treatment with forskolin. The CAL-51 cells were seeded ($2x10^4$ cells) on semi-permeable membranes, and FITC-labelled dextran and forskolin were added on day 3 when the cells exhibited a confluent monolayer (Figure 5.12A and B). After 24 hours of forskolin treatment, the dextran transported from one chamber to another chamber was quantified by the absorbance of the fluorescent signal emitted by the labelled dextran. Using a standard curve, the

concentrations of dextran in the chamber compartments of the semi-permeable membranes were calculated (Figure 5.12B). The results show that the dextran transported through the TJs in control is 0.2387mg/ml, while with forskolin treatment, the dextran transported increased to 0.2647mg/ml, finding a difference of 2.1% more dextran transport in the group treated with forskolin (Figure 5.12C). These results indicate that the paracellular fluid transport is increased by 2.3% after the stimulation of CFTR activity with forskolin treatment.

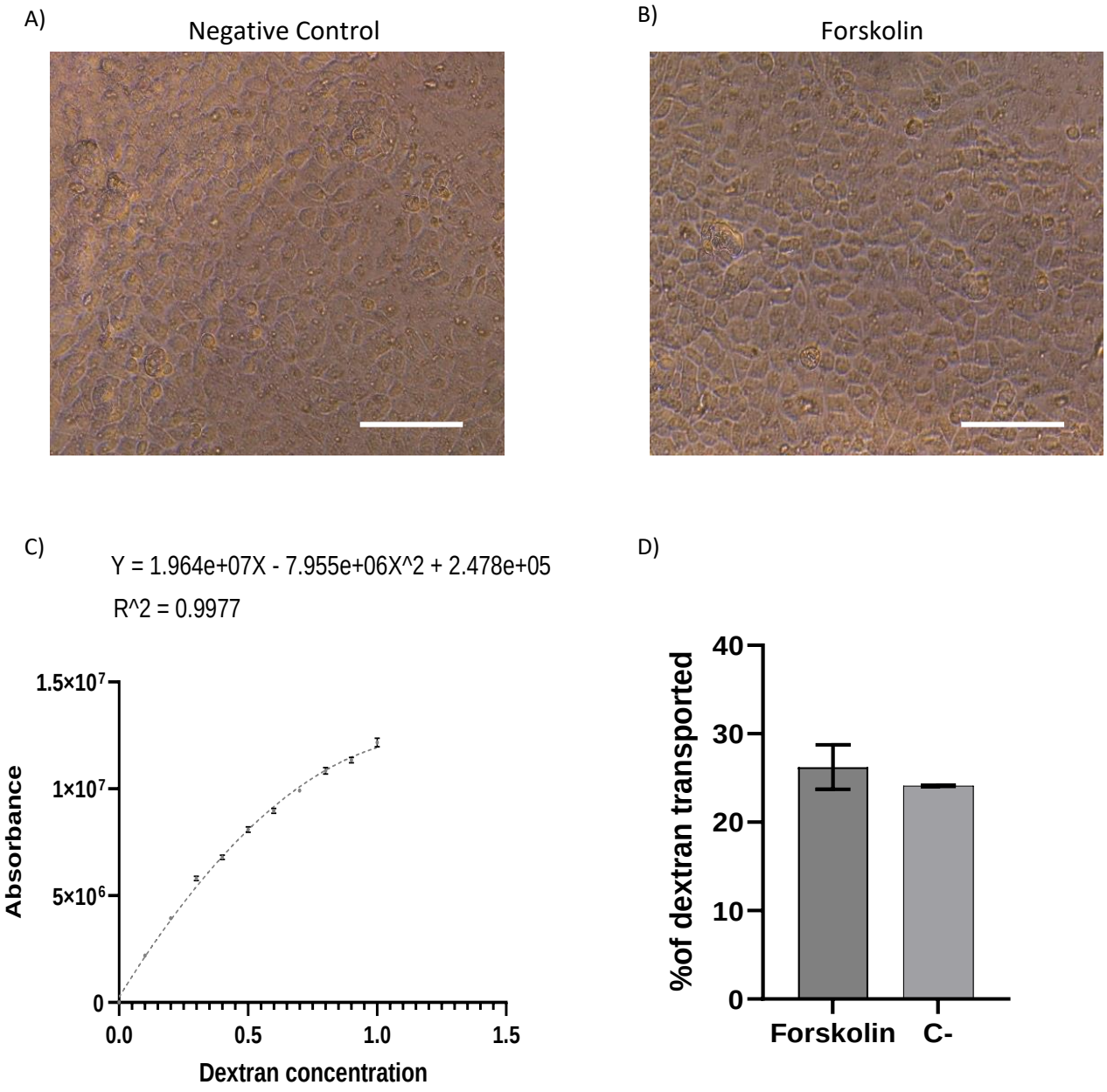

Figure 5.12. Paracellular permeability in the CAL-51 cells. Representative images of the confluent monolayer of CAL-51 cells cultured on semi-permeable membranes after 3 days (before applying the treatment). A) Semi-permeable membrane with CAL-51 cells of the negative control group (DMSO). B) Semi-permeable membrane with CAL-51 cells of the forskolin group (10µM forskolin). Scale bar=100µm. Microscope magnification= 20X. C) Standard curve for the Dextran quantification. The minimum value is the blank media 0mg dextran, and the maximum value is 1mg Dextran in media. D) Percentage of Dextran transported from the bottom chamber to the upper chamber. The graphs show mean ± SEM (n=2 from independent experiments).

5.3.6 Overexpression of CFTR in breast cancer

Previous WB results (Figure 5.3) showed a difference in the mature CFTR protein expression between the MCF10A and breast cancer cells. Among the possible explanations for this event are the mutations in their genome. Therefore, the next objective was to force express the normal CFTR sequence into breast cancer cells and evaluate the lumen phenotype in this model. The vector used was obtained from Promega and contained the sequence that encodes human CFTR (Appendix I and Figure 2.1). The negative vector containing the same backbone except the CFTR sequence was independently generated. The CFTR vector amplified with primers that flank the CFTR sequence produced a 4684pb product without the CFTR sequence (Appendix I Figure 2.1). Subsequently, the vectors were amplified by bacteria transformation and ampicillin selection (an example of bacteria selected in agar plates in Appendix IX). The plasmid DNA extracted from the bacteria was subjected to restriction enzymes to analyse the DNA fragment sizes generated after the specific enzymatic digestion. The products were run on agarose gels and were compared with in silico gels (using NEBcutter program) to verify the DNA sizes according to the vector design. The enzyme digestion with HindIII for the CFTR vector and HindIII, XhoI, and KpnI for the negative control vector show similar DNA fragment sizes in the experimental gels to the ones *in silico* gels (Appendix X). For the CFTR vector, 3 DNA fragments (4428, 829 and 3888pb) were produced after the HindIII digestion (Appendix XB). The negative control showed 2 DNA fragments (3489 and 1195pb) after the digestion with the HindIII/XhoI enzymes and 2 DNA fragments (3423 and 1261pb) with the HindII/KpnI enzymes (Appendix XC and D). The predicted cuts and the experimental gels suggest the vector constructions are correct. Therefore, the next

stages will consist of sequencing the plasmids to verify the complete sequence of the negative control vector generated.

5.4 DISCUSSION

The decrease of luminal space in the mammary gland is a salient feature of breast cancer (Gudjonsson, Adriance et al. 2005, Kaushik, Pickup et al. 2016, Halaoui, Rejon et al. 2017). The reasons why the changes to luminal structure occur have not been completely elucidated. Some studies point to deregulation in the expression of cell adhesion molecules (Kirshner, Chen et al. 2003), oncogene activity such as ErbB2 (Muthuswamy, Li et al. 2001), co-expression of genes related to apoptosis inhibition and activation of proliferation (Debnath, Mills et al. 2002), and polarity (Martin-Belmonte, Yu et al. 2008, Akhtar and Streuli 2013). However, the biological mechanisms that regulate lumen morphology in the mammary gland, such as those that control fluid secretion and hydrostatic pressure in breast cells, have not been well studied. In the previous 2 Chapters, it was showed the importance of the expression and activity of CFTR, one of the main fluid drivers in epithelial cells, in lumen structure formation and maintenance in mouse MECs. Since alterations in lumen structure is one of the main features of breast cancer and CFTR is important for lumen formation and maintenance, this Chapter aimed to study CFTR expression and activity in breast cancer cells. The findings of this study show a difference in the molecular weight of CFTR in the membrane between the non-tumorigenic breast cells and breast cancer cells. Moreover, the activation of CFTR with Forskolin in CAL-51 cells induces lumen formation, further suggesting that CFTR activity is important for a normal mammary gland phenotype.

According to the Human Protein Atlas, most breast cancer cells do not express CFTR. This data is consistent with previous reports on breast cancer tissue from patients, which tend to exhibit reduced expression compared with healthy breast tissue (Zhang, Jiang et al. 2013, Liu, Dong et al. 2020). However, when the other *in silico* analysis of CFTR expression in the breast cancer cell lines was conducted and compared with the CFTR expression in non-tumorigenic breast cell lines, the results did not show a significant difference between these groups. Following this, CFTR expression was evaluated experimentally in some breast cell lines, including MCF10A, CAL-51, MCF7, T47D and MDA-MB-231. Similar to the *in silico* analysis, no significant difference was found when the *CFTR* expression was compared between the breast cell lines by qPCR. This data is at the mRNA level, and the CFTR function is at the protein level. Even if the CFTR protein is translated, it needs proper processing and trafficking to the membrane for its function (Amaral, Hutt et al. 2020).

The protein analysis in the membrane and cytoplasm by WB showed that in the cytoplasm, all cells expressed (in different proportions) three CFTR molecular weights related to known glycosylation variants (Gregory, Cheng et al. 1990). However, only the MCF10A cells in the membrane protein fraction expressed the 160-170KDa CFTR protein, and the breast cancer cells expressed a higher (>170KDa) CFTR molecular weight. Therefore, there are differences in the molecular weight of the CFTR detected in the membrane of the breast cancer and non-tumorigenic breast cells analysed (Figure 5.6 A and B).

The expression of the 160-170KDa CFTR protein, which has the molecular weight corresponding to the fully glycosylated protein trafficked to the surface membrane, was higher in the membrane than in cytoplasmic protein fractions in MCF10A. The total expression of CFTR in the cytoplasm (160-170kDa, ~130KDa and 93KDa-130KDa) and membrane (160-170KDa) was similar (Figure 5.7B) in the MCF10A cells. This last result suggests that all the CFTR proteins detected in the MCF10A cells are divided by similar levels in the cytoplasm and membrane cell compartments on these cells. This result is consistent with the references that show a cytoplasmic CFTR detection in epithelial cells (Ward and Kopito 1994, Bradbury, Clark et al. 1999) and is consistent with our previous data described in Chapter 4, where the CFTR expression is also localised in the cytoplasm of MECs.

The reasons why the detection of a different protein molecular of CFTR between breast cancer and non-tumorigenic cells are diverse. CFTR is a complex protein that requires post-translational processing, correct folding, and correct transport to the membrane for its function (Bertrand and Frizzell 2003, Ameen, Silvis et al. 2007, Kreda and Gentzsch 2011). The post-translational modifications (PTMs) are molecular changes in the proteins that can lead to different molecular weights in the WBs (Riising, Boggio et al. 2008, Wang, Wang et al. 2021). CFTR undergoes different PTMs, such as palmitoylation, sumoylation, phosphorylation, ubiquitination and glycosylation (McClure, Barnes et al. 2016).

The well-known molecular weights for CFTR are associated with glycosylation, leading to the production of 127KDa, 130 KDa and 160-170KDa forms (Gregory, Cheng et al.

1990). As previously mentioned, in the cytoplasm protein fraction, the 160-170KDa band corresponding to the glycosylated mature form was detected in the MC10A and breast cancer cells. This result indicates that all the analysed breast cells can produce the mature CFTR glycosylated protein. Nevertheless, in the membrane, only the MCF10A cells showed a 160-170KDa molecular weight, and the breast cancer cells had a >170KDa molecular weight. Therefore, it is possible that the CFTR protein in the breast cancer cells has another PTM.

One PTM that could slightly increase the molecular weight is ubiquitination. This PTM involves the binding of a ubiquitin to a protein substrate. The ubiquitin consists of 76 amino acids with a molecular weight of 8.5 kDa. An additional mass of ~10KDa in a WB could suggest a monoubiquitination (Vijay-Kumar, Bugg et al. 1987, Nir, Huttner et al. 2015). The function or effect of the monoubiquitination in CFTR has not been fully understood; some studies showed that this PTM is not necessarily related to protein degradation. Instead, it has been associated with a non-destructive signal or stability to the substrate (Braten, Livneh et al. 2016, Yang, Schiapparelli et al. 2017). Other reports support the degradation process by this PTM (Rott, Szargel et al. 2011, Dimova, Hathaway et al. 2012). Ubiquitination is an example of the possible explanations for a different molecular weight; however, the exact molecular weight detected in the WB is higher than 170 and lower than 235 KDa. Therefore, more than one ubiquitination or other PTMs can be in that range of weight. The detection of PTM needs other techniques, such as immunoprecipitation or mass spectrometry. These techniques would also be useful to confirm the glycosylation in the molecular weights observed in the WB.

The WBs showed various CFTR expression molecular weights in the membrane and the cytoplasm. Although the mature CFTR protein form (160-170KDa) is only expressed in the membrane fraction of the MCF10A cells in the WBs, in IF all the breast cancer cells expressed CFTR in their apical membranes. The ZO-1 detection was used as a reference for an apical marker. In addition, the colocalization of ZO-1 and CFTR has been reported in other epithelial cells, such as the mouse epididymal cells (Ruan, Wang et al. 2014). Although the ZO-1 protein expression was detected in most of the periphery of the cells (except for the T47D cells), there is an important visible difference between all the breast cell lines. For example, the signal between the MCF10A cells and the MDA-MB-231 cells. The reason for this different expression of ZO-1 could be linked to the fact that these experiments were done with different cell lines with different biological backgrounds and, therefore, may have different expression profiles. In addition, the different genetic and metabolic profiles of the different cell lines influence the proliferation rates, which can be reflected in the cell density, and ZO-1 expression has been reported to be regulated by the cell density in the epithelial MDCK cells (Balda and Matter 2000). Another factor that influences the ZO-1 expression is the polarity of each type of cell. ZO-1 is a TJ component that interacts with some proteins, such as Par3/6, which are required to establish and maintain cell polarity in epithelial cells (Blasky, Mangan et al. 2015). In breast cancer cells, loss of polarity is one of the main features, and downregulation of ZO-1 has been reported in breast tissue (Hoover, Liao et al. 1998). However, the IF experiments aimed to identify the CFTR expression in the membrane, and it was localised in the breast cancer cells with different signals. CFTR protein distribution in the membrane for the MCF10A cells and MDA-MB-231 were more homogeneous than the rest of the cell lines. Nevertheless, it is difficult to know from the IF if the >170KDa CFTR form

detected in the WB is the one that is expressed in the cell membrane (detected by IF) and if this form is functional.

As the breast cancer cells showed some CFTR signal in the membrane, and it is unknown if it is functional, an experiment of CFTR stimulation was done in the CAL-51 cells to study if the stimulation of this protein promotes lumen formation. CAL-51 cells were chosen because they weakly expressed a band corresponding in size to the mature molecular weight of CFTR by WB and showed CFTR in the membrane by IF. In addition, both *in silico* analyses share that the CAL-51 cell line has a comparatively higher level of expression than other breast cancer cells. Interestingly, the CAL-51 cells were able to form lumen structures after 6 days in culture and exposure to forskolin. This result suggests that despite the low expression of CFTR in these cells, its stimulation is enough to modify the 3D cell architecture to induce lumen formation. Although this finding is intriguing, it is important to note that forskolin may promote lumen formation through an independent mechanism due to the effects on the activity of the adenylyl cyclase enzyme and cAMP (Anderson, Berger et al. 1991, Cheng, Rich et al. 1991, Picciotto, Cohn et al. 1992). Thus, the forskolin effect could promote a change in phenotype through other biological routes that require cAMP. Nevertheless, it has been observed that forskolin increases the size of the lumen in primary intestinal organoids and that this effect is dependent on the expression of CFTR. Therefore, there is a relationship between the effect of forskolin on organoid swelling and CFTR activity (Dekkers, Wiegerinck et al. 2013). In addition, considering the findings from Chapters 3 and 4 about CFTR modification and its effect on the lumen structure, the result in CAL-51 cells may indicate that CFTR stimulation can change the lumen phenotype. Further studies are needed to analyse the stimulation

effect of CFTR with forskolin in other breast cancer cells expressing the >170KDa CFTR protein form.

As the lumen formation effect was observed in the CAL-51 cells using forskolin, which does not directly target CFTR, the overexpression of CFTR experiments in the CAL-51 cells would be helpful to confirm its role in recovering the normal lumen phenotype. As a first step towards this, it was aimed to overexpress CFTR protein in breast cancer cells by transfection of a vector containing the human CFTR sequence. Overexpression of CFTR in breast cancer cells will give important information about the potential for different protein molecular weights to be expressed and detected in WB and the overexpression effect of CFTR in lumen formation. Currently, the CFTR vector to overexpress the human CFTR protein was amplified, and it was also generated the negative control vector from the CFTR vector. The negative control vector was generated by site-directed mutagenesis to delete the CFTR sequence and maintain the rest of the vector structure. The next steps are to carry out the sequencing to confirm the vector sequences and, finally, do the transfection experiments in 2D and 3D conditions. Based on findings from this Chapter, particularly those from the CAL-51 cells, the future hypothesis is that the overexpression of CFTR in breast cancer cells induces lumen formation. Overall, the aim will be to evaluate if breast cancer cells can form 3D cell structures with a lumen structure (acini-like structure) after the CFTR overexpression.

Another aspect that would be interesting to consider for future experiments is the study of transcellular fluid transport. According to the mechanism of lumen formation by fluid

secretion, the fluids can exert a mechanical force that pushes to open a single lumen (Bagnat, Cheung et al. 2007, Pearson, Hughes et al. 2009, Narayanan, Schappell et al. 2020). Section 3.5.3 of this Chapter addressed the paracellular fluid transport after adding forskolin treatment to the CAL-51 cells cultured on the semi-permeable membranes. Preliminary results showed a 2.1% increase in paracellular fluid transport after treatment with forskolin compared with the control (only treated with DMSO). No conclusions can be made about the paracellular permeability as it is necessary to increase the N number and conduct a statistical analysis. However, since there was observed a slight difference (2.1% more fluid transport) after the forskolin treatment in the CAL-51 cells, it is thought that transcellular fluid transport possibly had a greater fluid transport than the paracellular pathway evaluated. The transcellular fluid transport is commonly reported in the epithelial cells and is mainly provided by aquaporins (Folkesson, Matthay et al. 1994, Kreda, Gynn et al. 2001). In addition, previous reports show a relationship between CFTR activity and aquaporins for fluid secretion in epithelial cells (pancreas) (Venglovecz, Pallagi et al. 2018). Thus, studying transcellular fluid transport would also provide more information about the forskolin mechanism in fluid secretion and lumen formation in MECs.

In conclusion, this chapter mainly compares the expression and location of CFTR between non-tumorigenic and breast cancer cells. The *in silico* and experimentally analysis of the CFTR expression did not show differences between the non-tumorigenic and breast cancer cell lines. However at the protein level, the mature (fully glycosylated molecular weight) form of CFTR is only detected by WB in the membrane fraction of the MCF10A cells, which are capable of forming lumens *in vitro*. However, by IF, CFTR was detected in the membrane and cytoplasm in all breast cell lines with

different intensity signals. Likewise, this Chapter reports that lumen formation is inducible in the CAL-51 cells after 6 days of forskolin treatment. All these data support the importance of the CFTR role in the lumen formation and maintenance in the MECs.

Chapter 6

6. ROLE OF B1-INTEGRIN IN PARACELLULAR PERMEABILITY

6.1 INTRODUCTION

Lumen formation is a complex mechanism that relies on various processes, such as establishing cell polarity and polarity orientation, which depend on cell-to-cell and cell-to-BMM interactions (Martin-Belmonte, Yu et al. 2008, Akhtar and Streuli 2013). Some mammary epithelial cells can interact with ECM through cell surface receptors, such as integrins, transmitting signals from the extra- and intra-cellular compartments (Katz and Streuli 2007).

β1 integrin is indispensable for polarity orientation in MEC organoids; its absence causes the inversion of the polarity, altering the location of apical components such as the atypical protein kinase C (aPKC), actin and TJs, which affects the definition of the luminal space. The previous laboratory group results showed a required expression of β1 integrin for lumen formation in MECs, specifically for the polarity orientation (Akhtar and Streuli 2013), a previous step for lumen opening. However, whether β1 integrin participates downstream of the polarity orientation in the expansion of a single lumen is unknown.

One proposed mechanism for lumen expansion is through fluid secretion, which creates a hydrostatic force that promotes the lumen opening and expansion (Bagnat, Cheung et al. 2007, Pearson, Hughes et al. 2009). It has been reported that β1 integrin regulates the paracellular permeability in kidney proximal tubule cells by modifying the expression of TJ components (Elias, Mathew et al. 2014). A critical component of the TJs is the ZO-1 proteins, which stabilise their structure and function (Rodgers, Beam

et al. 2013). Based on the above points, the **hypothesis of this Chapter is that β1 integrin regulates lumen expansion downstream of polarity orientation through fluid secretion**.

The main aim of this Chapter is to determine whether β1-integrin expression in primary mammary epithelial cells and EpH4 cells regulates the paracellular fluids that could contribute to the formation of a lumen.

In order to evaluate the role of β1 integrin in fluid secretion, two *in vitro* MEC models were used. The first cell model consists of primary mammary epithelial cells from mouse mammary gland tissue, and the second consists of the EpH4 cells, a mouse mammary epithelial cell line. The objectives of this Chapter are:

- To validate the β1 deletion in primary mouse mammary epithelial cells of the β1-integrin fx/fx-K18CreER transgenic mice.
- Decrease the β1 expression in the EpH4 cells using the miR-IGTB lentivirus.
- Evaluate the paracellular permeability in primary mammary epithelial cells with β1 integrin expression modified using semi-permeable membranes.
- Evaluate the paracellular permeability in EpH4 cells with β1 integrin expression modified using semi-permeable membranes.

6.2 METHODS

6.2.1 Culture of cell lines

HEK 293T and the EpH4 were provided by Dr Akhtar's laboratory. The cells were grown under conditions described in sections 2.3.1 and 2.3.2.

6.2.2 Mouse model

The maintenance and handling of mice were carried out in accordance with the Animals (Scientific Procedures) Act 1986 (and associated practices) of the UK legislation under Project Licence PP1836785. The mice were kept at 22°C with 40-60% and 12h photoperiod in the Biological Services Unit of the Medical School of the University of Sheffield. Mice were killed using the Schedule 1 procedure by a trained and registered practitioner.

8-12 weeks-old pregnant mice of the β1-integrin fx/fx-K18CreER transgenic background were used for the permeability experiments. This mouse model allows the deletion of β1 integrin in luminal cells under the control of the K18-CreER promoter after adding 4-Hydroxytamoxifen (4-OHT) in the culture medium. The epithelial cells from mammary tissue were obtained as described in the 2.2 section. The β1 integrin KO was confirmed by IF.

6.2.3 Immunofluorescence

For the β1-integrin KO verification, the MECs were cultured on previously treated glass coverslips as described in section 2.9.1. The MECs were maintained for at least 2 days with Ham's F12 media (Lonza) supplemented with 1µg/ml Hydrocortisone (Sigma Aldrich), 5ng/ml EGF (Sigma Aldrich), 5µg/ml insulin (Sigma Aldrich), 1% (v/v) of penicillin/streptomycin (Lonza) and 10% (v/v) serum (Biosera) for the control samples and with the same media as the control but with 4-OHT for the β1-integrin KO samples. Two replicates were carried out per experiment (n=2).

For the permeability experiments, the primary MECs or EpH4 cells were cultured on the semi-permeable membranes as described in sections 2.14.1 and 2.14.2. The membranes were cut from the base of the chambers, and the staining was performed on the membranes following the standard protocol for IF described in section 2.9.2. Two replicates were carried out per experiment (n=2).

The cells were fixed and stained as described in section 2.9.2. Photos of randomly selected sections of the samples in coverslips were taken under the fluorescence microscope (Olympus IX73 or EVOS microscope). Images were processed using FIJI Image J software.

6.2.4 Lentivirus production

The lentiviral plasmids pLVTHM miRNA ITGB1 and PLVTHM scrambled (Rooney, Wang et al. 2016) were provided by Dr Akhtar's lab group. The plasmids were amplified in DH5α Competent Cells by bacterial transformation as described in section 2.10. The plasmid DNAs were extracted as described in section 2.11.

The lentivirus production was done using the plasmids in the HEK 293T cells following the method described in Section 2.12.

6.2.5 Lentivirus titration

The lentivirus was collected and dissolved in blank media and was used at a range of concentrations to infect EpH4 cells, as described in section 2.13. Cells were stained with 1:1000 (in 1X PBS) Hoechst 33258 (Invitrogen), and photos of at least 5 sections of the EpH4 samples were taken with the fluorescent microscope (EVOS). Calculations of the percentage of infection were made, counting the total number of GFP-positive cells relative to the total number of cells.

6.2.6 Permeability assays

Fresh MECs from pregnant mice (between 15-18 days; at least 3 mice per experiment) or EpH4 cells were seeded on semi-permeable membranes as described in sections 2.15.1 and 2.15.2.

The permeability experiments were done when the cells showed a confluent monolayer in the bright field microscope. IF detecting the ZO-1 suggested the formation of TJs and the cell confluence over the semi-permeable membranes. Also, transepithelial electrical resistance measurements were carried out to detect the cell confluence in both cell models in accordance with the procedure described in section 2.15. The permeability assay was carried out when the cell monolayer in the semi-permeable membranes was confluent. 1mg/ml of 4KDa Dextrans labelled with FITC (Sigma Aldrich) was added to the top chamber, and the dextran transported was evaluated after 24h. The dextran transported from one chamber to another chamber was detected by absorbance of the fluorescent signal emitted by the dextran, and the quantification was carried out using a standard curve (0-1mg/ml) and its equation.

6.3 RESULTS

6.3.1 Paracellular permeability in primary MECs

6.3.1.1 VERIFICATION OF B1 INTEGRIN DELETION IN LUMINAL CELLS

In order to evaluate the role of β1 integrin in lumen formation by the fluid secretion mechanism, the manipulation of β1 integrin was made using a mouse model that allows the deletion of this protein *in vitro.* The transgenic mice model (β1-integrin fx/fx-K18CreER) allows the tissue-specific KO of β1 integrin by the Cre/lox system. The addition of 4-OHT to the media causes the translocation of CreERT (in the K18 cells) from the cytoplasm to the nuclei. It triggers the recombination of the β1 integrin sequence flanked by the loxP sites to cause the deletion of the β1 integrin sequence and then the KO. Verification of β1 integrin deletion in luminal cells (K18 cells) and the Cre translocation to the nuclei was confirmed by IF.

The mouse primary MECs were seeded and cultured on coverslips in conditions supplemented with 4OHT to induce KO. Cultured cells were fixed and stained with anti-K18, SMA and β1 integrin antibodies. Figure 6.1A and B show the specific deletion of β1 integrin in the K18 cells (luminal). The positive cells to SMA antibody, which are primarily myoepithelial cells, show β1 integrin expression. Figure 6.1 B shows the Cre expression in the nuclei in the KO cells after the addition of 4OHT. These results confirm that the translocation of Cre occurs after the addition of 4OHT to induce the β1 integrin KO in the luminal (K18) cells. The protein deletion of β1 integrin can be

confirmed as the cells with Cre expression in the nuclei do not have β1 integrin expression.

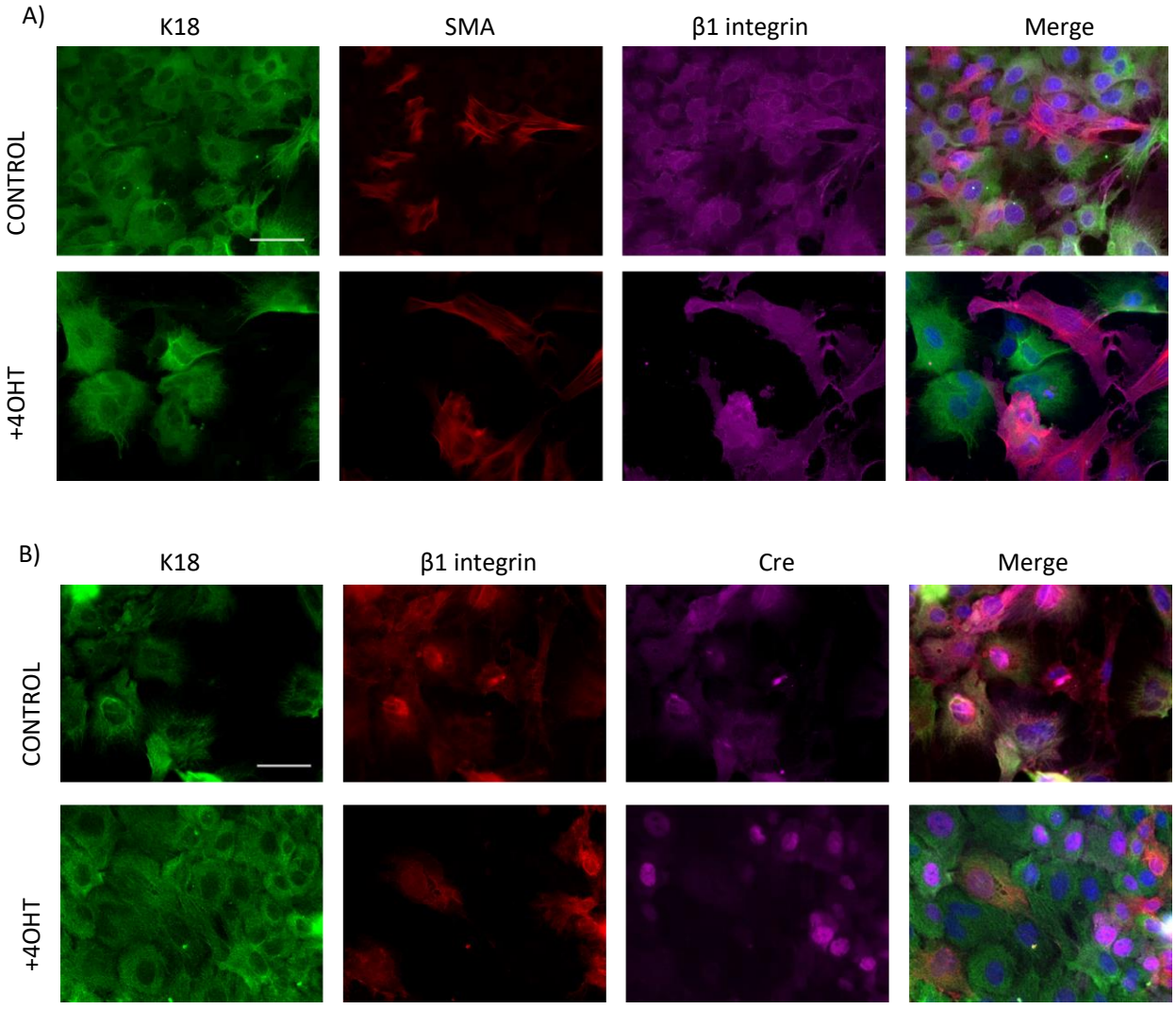

Figure 6.1. β1 integrin KO in mouse primary MECs. A) Representative images of the control samples expressing β1 integrin and +4OHT samples with β1 integrin deleted after (48-72h) 4OHT addition to the media. In green are the luminal cells; in red are the myoepithelial cells; in purple are the β1 integrin positive cells; and in blue the nuclei. Scale bar= 100µm. B) Cre translocation to the nuclei. Representative images of Cre expression in the nuclei after (48-72h) of 4OHT addition in vitro. In green are the K18 positive cells; in red are the β1 integrin positive cells; in purple are the Cre positive cells; and in blue the nuclei. Scale bar= 100µm. Microscope magnification= 40X.

6.3.1.2 PERMEABILITY ASSAYS IN PRIMARY MECS

Once the β1 integrin deletion in the K18 cells was confirmed, the conditions for the standardisation of the permeability experiments were set up. Since the paracellular transport occurs through the TJs, a negative control group for the TJs (disrupted TJs) was also included in the permeability experiments. The cells of this group were cultured on low Ca^{+} media, which affects the formation of the TJs (Zheng and Cantley 2007). MECs from mammary mouse tissue were seeded on semi-permeable membranes and cultured until a confluent monolayer was observed in the disrupted TJs, β1 integrin and β1 integrin KO samples under the bright field microscope at the same time point (Figure 6.2A, B and C). The results show that most parts of the semi-permeable membrane show a monolayer, although there are some regions where clumps of cells from mammary tissue are evident (Figure 6.2D).

Since clumps of cells were detected on the transwells, further optimisation experiments were carried out to improve monolayer formation. The fresh primary cells from the mammary gland were seeded on culture dishes for 5 days to expand the small pieces of tissue to a monolayer, and the cells were then transferred to the semi-permeable membranes. However, some clumps of cells were still evident after this process (Figure 6.2E). Although the sizes of the clumps observed were smaller than the ones observed when the cells were directly seeded on the membranes, the effect of the cell clumps on the monolayer for the further permeability assays was unclear.

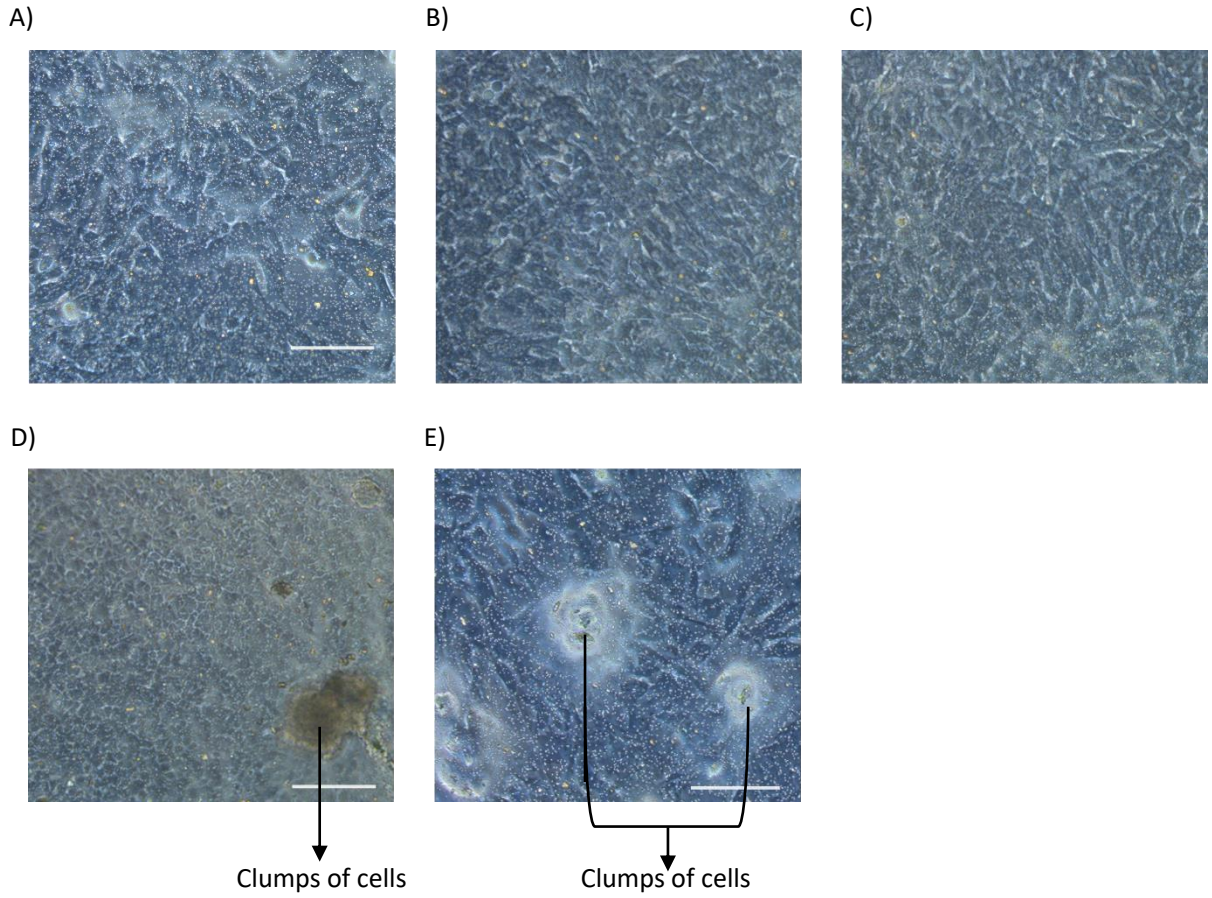

Figure 6.2. Confluent cell monolayer on the semipermeable membranes. A) Representative images of the monolayer formed by fresh primary cells seeded directly on the semi-permeable membranes for the three sample groups: A) Disrupted TJs, B) β1 integrin and C) β1 integrin KO. Scale bar 100µm. D) and E) Examples of clumps of cells formed in a monolayer of primary cells cultured on the semi-permeable membranes. D) After direct cell collection and seeding of the mammary tissue on the semi-permeable membranes, and E) after an intermediate passage prior to seeding on semi-permeable membranes. Scale bar=100µm. Microscope magnification= 20X.

TEER measurements were included in the experiments as part of the standardisation process as an extra step to verify the confluent monolayer and its integrity on the semi-permeable membranes. Once the membranes showed cell confluence under the light microscope, a TEER measurement was associated with this condition. Measurements between 200-360Ω were associated with no confluent monolayer/disrupted monolayer, and over 400Ω were related to a confluent monolayer in primary cell

culture (Figure 6.3). For other experiments, the confluent monolayers detected under the light microscope did not show the TEER values associated with the monolayer. For example, the primary cells reseeded on the membranes did not reach the TEER monolayer measurement (Appendix XI).

Once a confluent primary cell culture was obtained (by microscope and TEER values) on the semi-permeable membranes, an evaluation of the paracellular permeability was done. The dextrans were dissolved in culture media and applied at a final concentration of 1mg/ml in the top chamber for the 3 different groups of samples. After 24h of the dextran addition, cell media from the bottom chamber was collected and evaluated to calculate the dextran present in this chamber. Since the dextran is fluorescently labelled with FITC, its detection was done using a spectrophotometer plate reader and quantification by a standard curve (Figure 6.4A). The samples containing the disrupted TJs showed a dextran concentration of 17.27µg/ml, and the samples with and without β1 integrin expression were 9.19 µg/ml and 10.29 µg/ml, respectively (Figure 6.4B). This preliminary result (n=1) shows that the highest permeability is given in the sample group with the TJs disrupted. The lack of Ca+ in the media compromises the integrity of the TJs, which represents a barrier between the cells for paracellular fluid transport. Therefore, the fluid transport observed was higher in this group than in the other sample groups. The lack of expression of β1 integrin in the luminal MECs could be increasing the paracellular permeability. This preliminary result shows a difference of 1.1 µg/ml (or 1.65 µg of dextran transported) between the β1 integrin KO and its negative control with the β1 integrin expression. (Figure 6.4C).

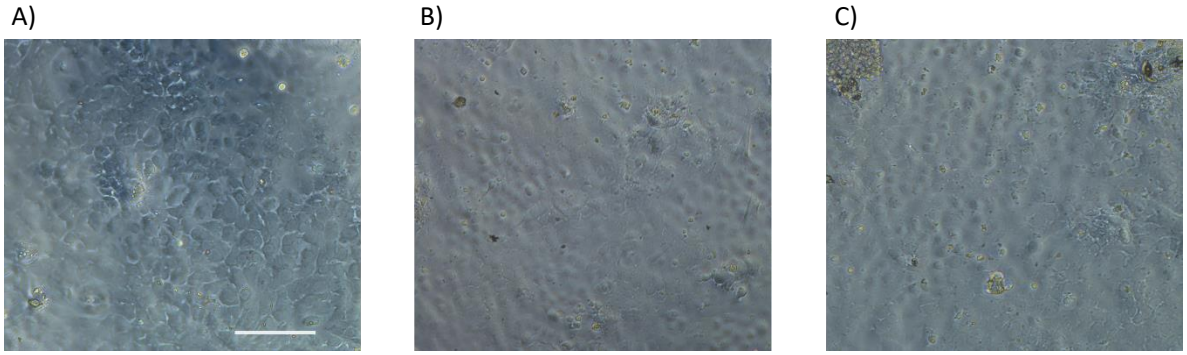

Figure 6.3 Association of TEER measurements with confluent monolayer. Representative images of confluent monolayer and its transepithelial resistance numbers of A) Disrupted TJs, B) β1 integrin and C) β1 integrin KO samples. Scale bar=100µm. Microscope magnification= 20X.

A)

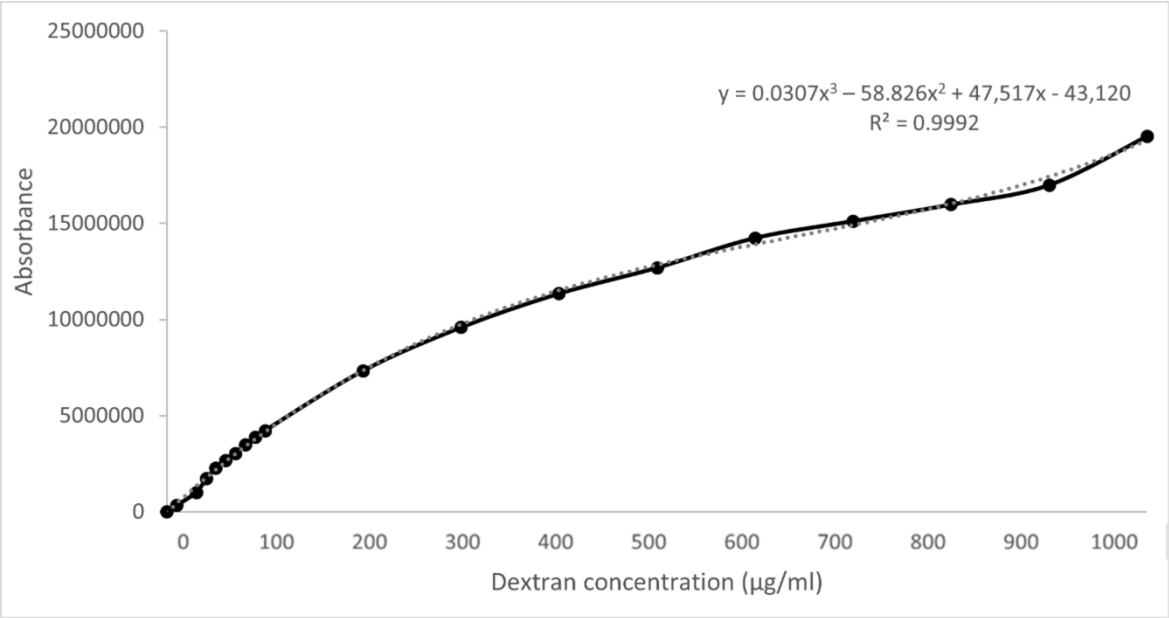

B)

Sample	Dextran concentration (ug/ml) in bottom chamber
Disrupted TJs	17.27
β1 Integrin	9.19
β1 Integrin KO	10.29

C)

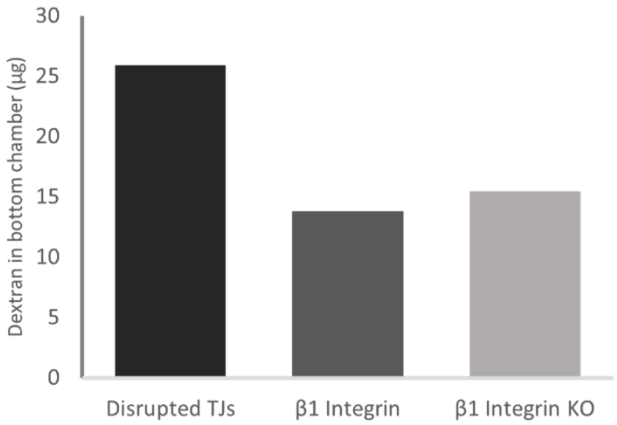

Figure 6.4 Permeability assay with the primary MECs. A) Standard curve for the dextran quantification from 0-1mg/ml. B) Dextran concentration detected in the bottom chamber. C) Micrograms of dextran detected in the bottom chamber.

After the permeability assay, the cells on the membranes were stained for two different proposes; the first was to evaluate the monolayer and its integrity (by ZO-1 expression) across the membrane, and the second was to confirm the expression or deletion of β1 integrin. ZO-1 expression was detected uniformly in most of the cells of the β1 integrin and β1 integrin KO samples, but in the disrupted TJs samples, some areas with gaps or without ZO-1 signal were observed. This result reflects that in the group of the TJs disrupted, the lack of Ca^{+} compromised the integrity of the TJs, affecting the expression of the ZO-1 protein (one of the protein complexes of the TJs) (Figure 6.5). The staining for the detection of β1 integrin protein expression shows that it is detected in the cells of the control groups (without 4OHT), while in the β1 integrin KO group (+4OHT), only some cells expressed β1 integrin (Figure 6.5). As the IF was done in the semipermeable membranes used for the permeability experiments, the staining results show that the permeability experiments were carried out in the desired conditions, with and without β1 expression in some cells in the negative and β1 integrin KO groups, and no homogenous ZO-1 expression in the TJs disrupted group.

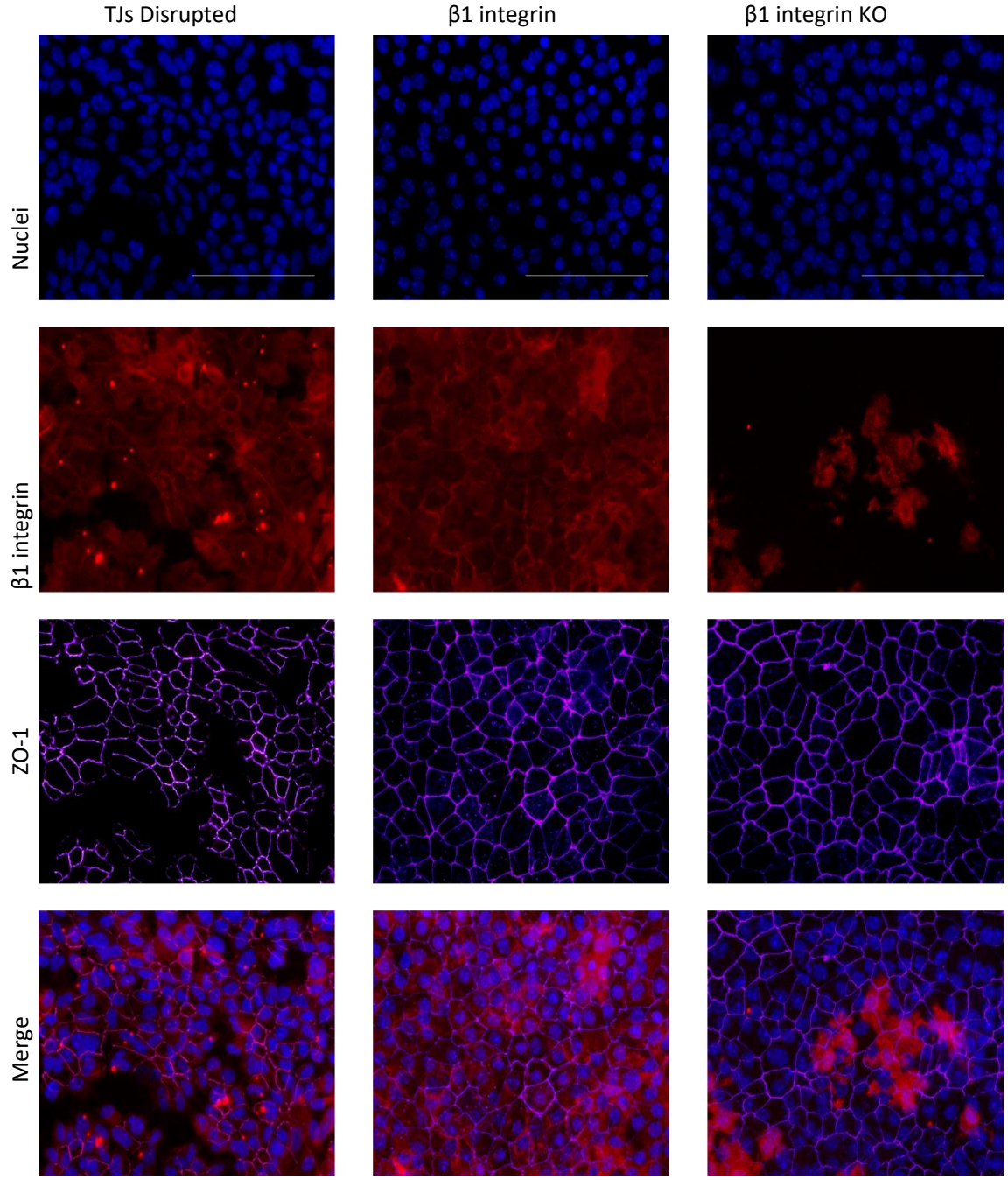

Figure 6.5. IF localisation of ZO-1 and β1 integrin in mouse primary MECs following permeability testing. Antibodies were used to label ZO-1 (purple) and β1 integrin (red). Nuclei are labelled with Hoechst 33258 (blue). Scale bar= 100µm. Microscope magnification= 20X.

6.3.2 Paracellular permeability in the EpH4 cells

6.3.2.1 VERIFICATION OF B1 INTEGRIN KD IN EPH4 CELLS

The EpH4 cells, a non-tumorigenic epithelial cell line isolated from the mammary glands of a mouse, was another cell model investigated. Permeability was evaluated in the EpH4 cells by seeding on semi-permeable membranes as per the primary cells. To modulate β1 integrin, cells were transfected with the miR-ITGB1 lentivirus or corresponding control lentivirus containing a scrambled (non-specific) sequence (Figure 6.6).

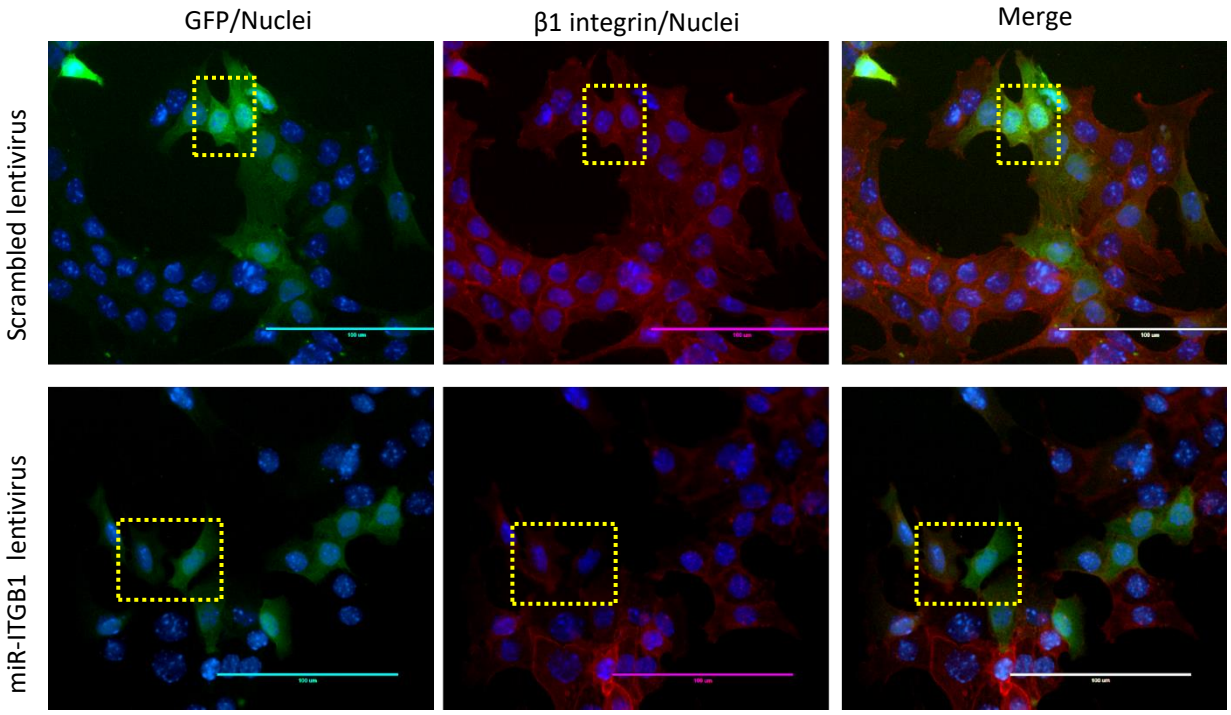

Figure 6.6. β1 integrin expression in the EpH4 cells post 4 days of lentivirus infection. Representative images of infected cells with the miR-ITGB1 and control lentiviruses, which both express GFP (green). The β1 integrin (red) was detected to evaluate β1 integrin KD. Nuclei (blue) stained with Hoechst 33258. Scale bar= 100 µm. Microscope magnification= 20X. The cells framed in the yellow section highlight a clear example of infected cells and their decreased expression of β1 integrin in the miR-ITGB1 group, and no decreased β1 integrin expression in the negative control group.

Prior to assessing permeability, transfection efficiency was evaluated using a range of virus titrations (20-120µl), and after 4 days post-transfection, the infected cells were quantified using the GFP reporter. Figure 6.7 shows the percentage of infection with the miR-ITGB1 and control lentivirus. With 20µl of scrambled lentivirus, 81% of cells were infected, 89% with 40µl and 93% with 60µl of lentivirus volume (Figure 6.7A). The other higher volumes were not evaluated, as many of the cells lost contact with coverslips (Appendix XII). Similarly, infection with the highest volumes of miR-ITGB1 lentivirus disrupted cell attachment; thus, only the cells infected with 20, 40 and 60µl of lentivirus were quantified. With 20µl of the miR-ITGB1 lentivirus, 85% of EpH4 cells were infected, 87% with 40µl and 93% with 60µl (Figure 6.7B).

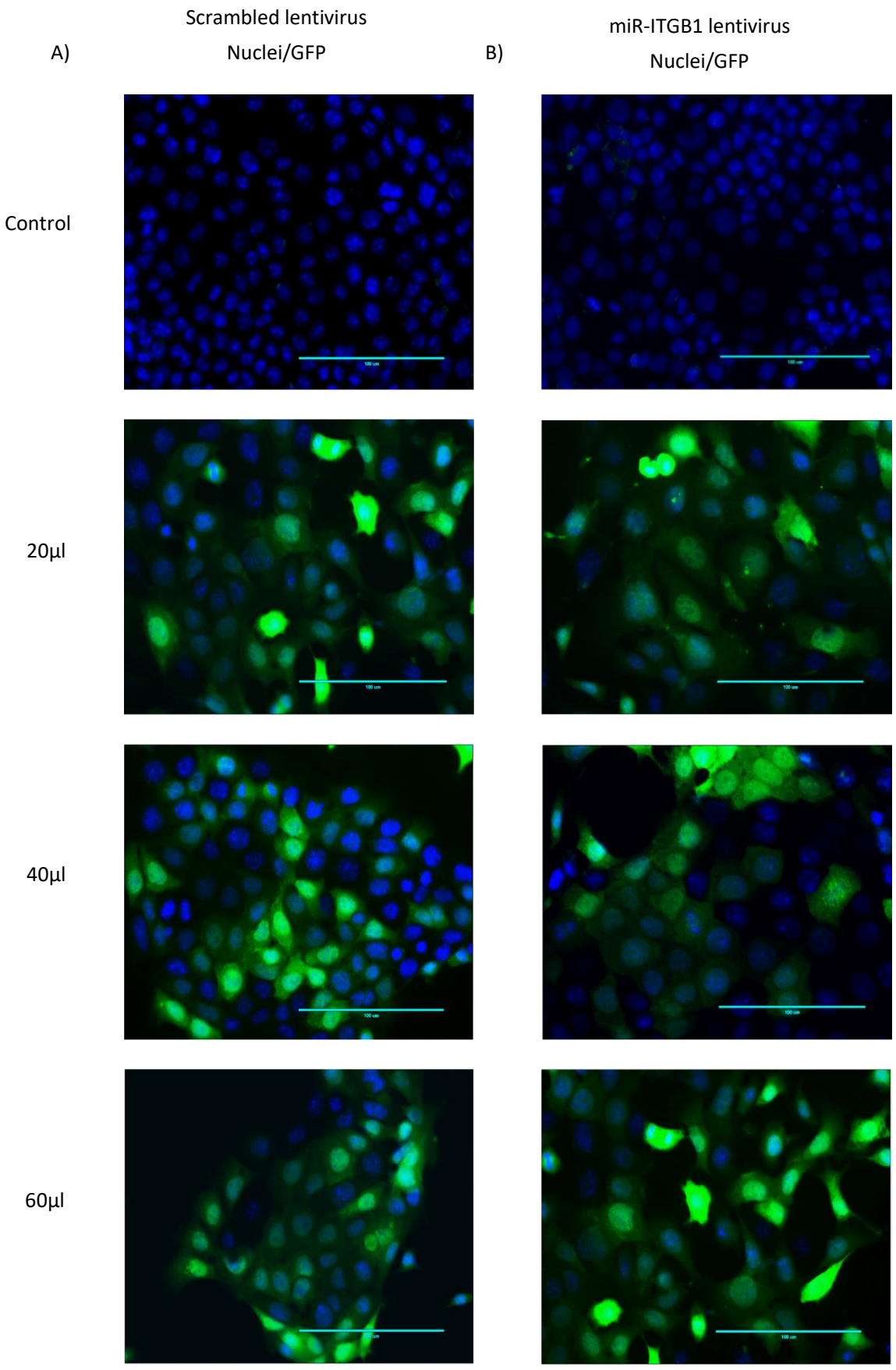
A)
Scrambled lentivirus
Nuclei/GFP
B)
miR-ITGB1 lentivirus
Nuclei/GFP
Control
20µl
40µl
60µl

C)

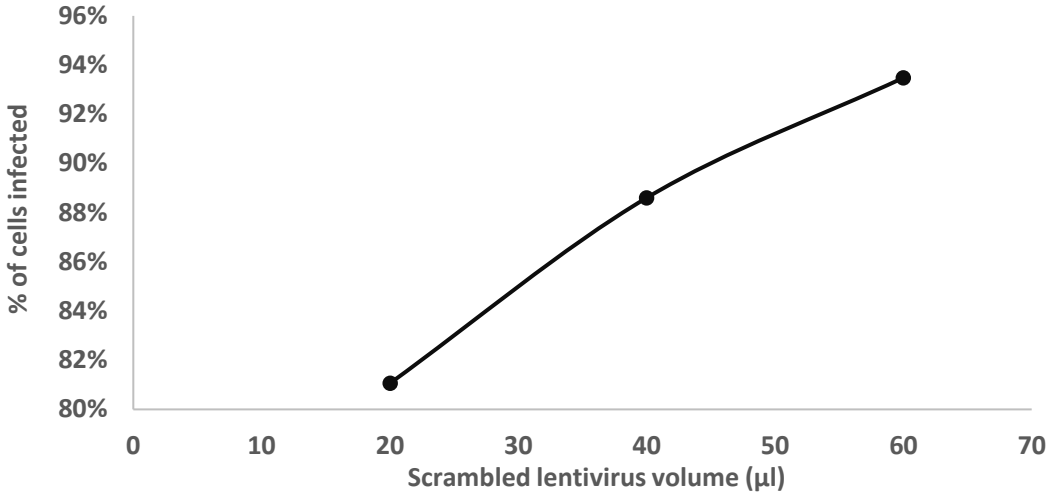

D)

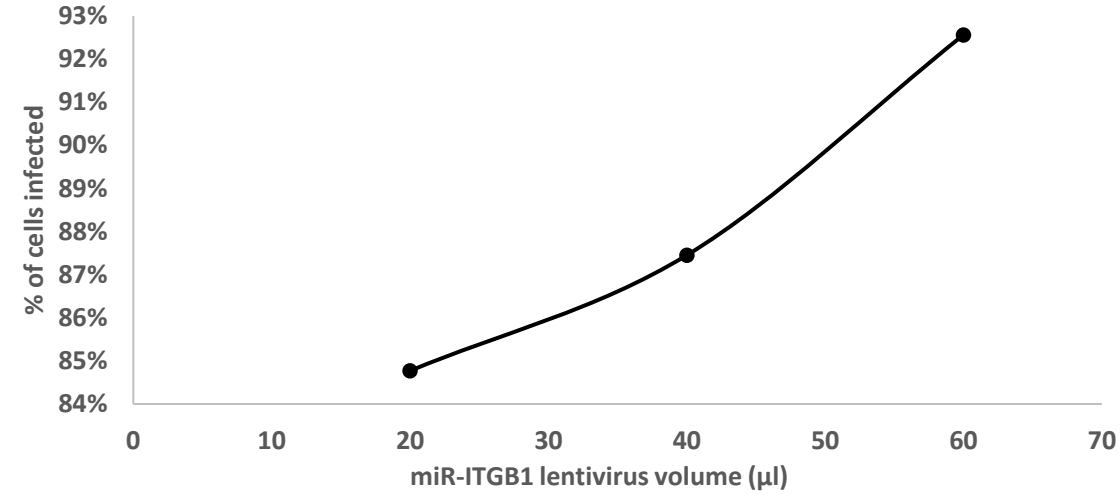

Figure 6.7 Percentage of cells infected with scrambled or miR-ITGB1 lentivirus. The infected cells express the GFP (green). Nuclei (blue) stained with Hoechst 33258. A) Representative photos of the EpH4 cells infected with different scrambled lentivirus volumes. B) Representative photos of the EpH4 cells infected with different miR-ITGB1 lentivirus volumes. C) Quantification of the percentage of cells infected with different scrambled lentivirus volumes. D) Quantification of the percentage of cells infected with different miR-ITGB1 lentivirus volumes. At least 300 cells were counted per group. Scale bar= 100µm. Microscope magnification= 20X.

6.3.2.2 PERMEABILITY ASSAYS IN EPH4 CELLS

The preliminary TEER measurements for the confluent EpH4 cell monolayer were established by microscopy analysis (Figure 6.8A and 6.9B). However, the TEER

measurements after transfection did not always reach the monolayer resistance values (>320Ω) (Figure 6.9C). Therefore, until this point of standardisation, the criteria used for a confluent monolayer were only based on the observation of a complete monolayer under the light microscope and its confirmation by IF.

Since the transfection efficiency of EpH4 cells was greater than 80% at the lowest titration (20µl) (Figure 6.7), and a complete monolayer was observed under the light microscope (Figure 6.8C), the permeability experiments were undertaken. EpH4 cells were cultured on semi-permeable membranes and infected with 20µl of lentivirus solution. The dextran was applied at a final concentration of 1mg/ml to the upper chamber, measured after 24h in the bottom chamber, and calculated using the standard curve (Figure 6.9A). The dextran concentration was 333µg/ml for the control samples (containing only the transfections reagents), 391µg/ml for the lentivirus control samples (scrambled miRNA mimic) and 318µg/ml for the miR-ITGB1 lentivirus samples (Figure 6.10B). The difference in µg between the cells with β1 integrin and the KD β1integrin samples was -109µg of dextran (Figure 6.10C).

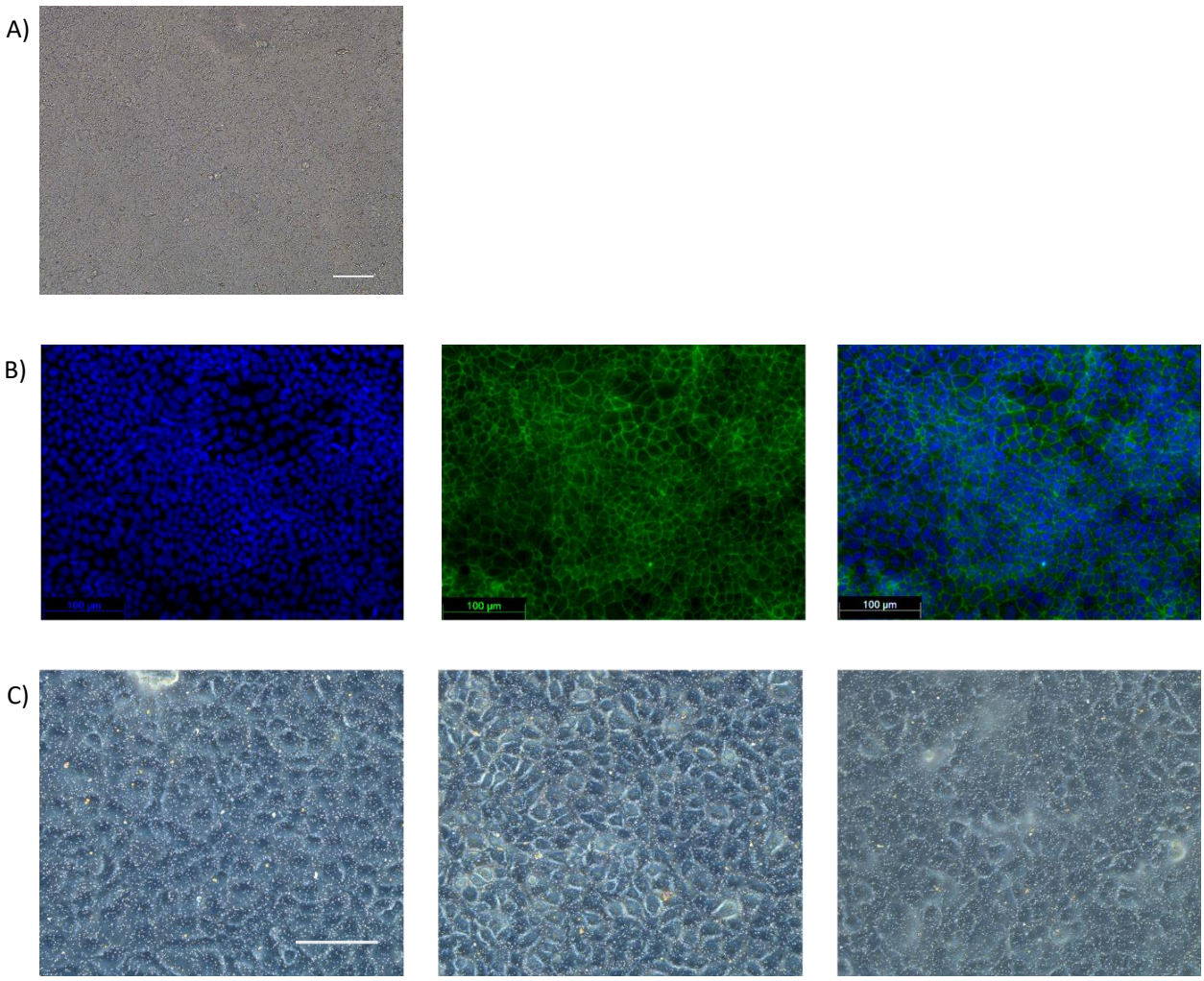

Figure 6.8. EpH4 confluent monolayer on the semipermeable membranes. A) Representative image of a confluent EpH4 cell monolayer with resistance measurements around 320Ω. Scale bar= 100µm. Microscope magnification= 10X.B) IF using antibodies to detect ZO-1 (green) in EpH4 cells grown on semi-permeable membranes (TEER > 320Ω). Nuclei (blue) labelled with Hoechst 33258. Scale bar= 100µm. Microscope magnification= 10X. C) Representative images of cells exposed to (i) transfection reagents (187Ω), (ii) scrambled lentivirus (164Ω) and (iii) miR- ITGB1 lentivirus (171Ω). Scale bar= 100µm. Microscope magnification= 20X.

After the permeability assay, a verification of lentivirus infection and ZO-1 expression was carried out in the cells seeded on the semi-permeable membranes (Figure 6.10). GFP expression was detected in most EpH4 cells exposed to lentivirus, indicating a high degree of uptake. The ZO-1 expression was similar in all the sample groups.

These preliminary results established the standardisation part of the permeability assays for future experiments.

A)

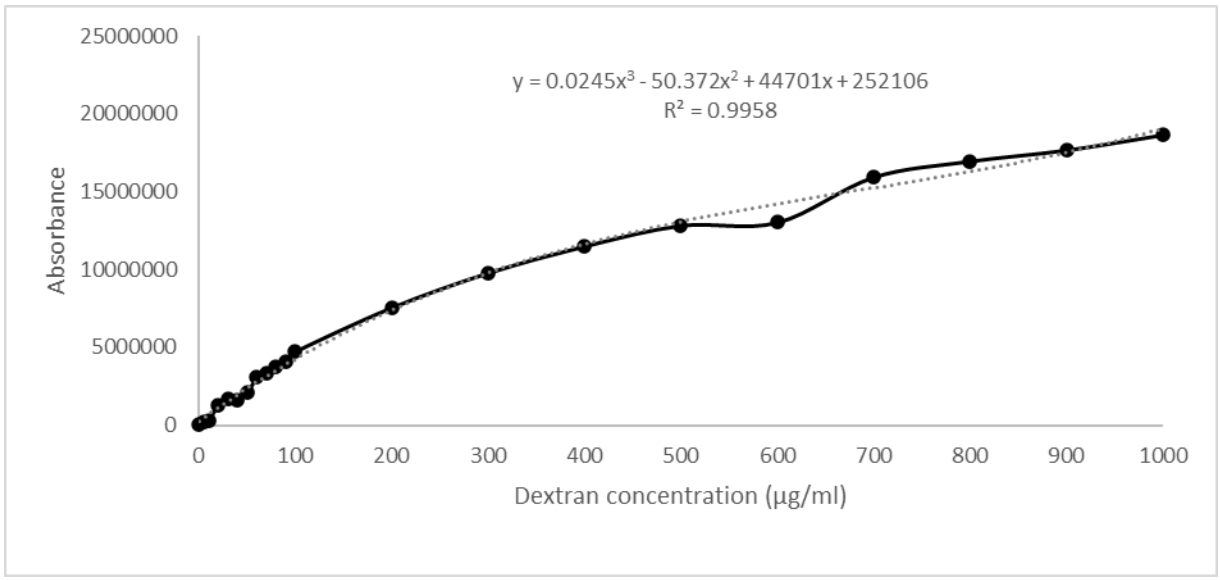

B)

Sample	Dextran concentration (µg/ml) in bottom chamber
Transfection	333.84
Lentivirus	391.50
miR-TGB1	318.22

C)

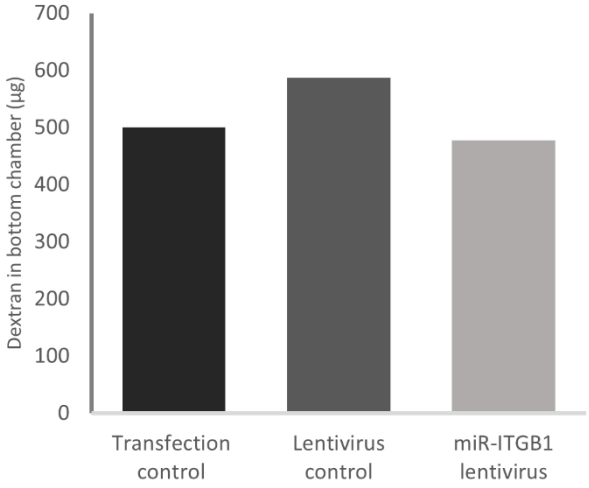

Figure 6.9. Permeability assay with the EpH4 cells. A) Standard curve for the dextran quantification from 0-1000µg/ml. B) Dextran concentration detected in the bottom chamber. C) Micrograms of dextran were calculated in the bottom chamber.

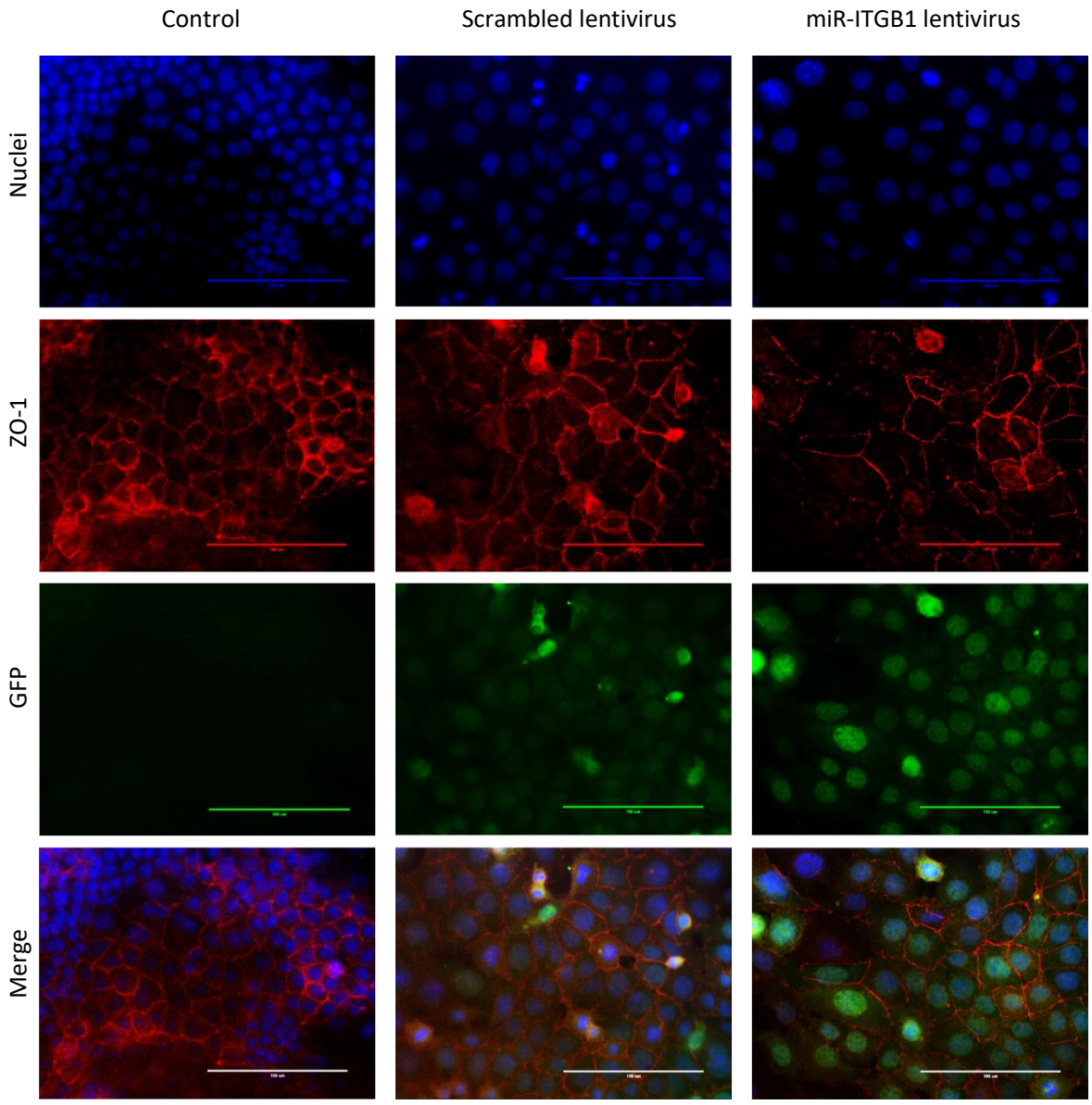

Figure 6.10. EpH4 cells stained in the semi-permeable membranes after the permeability assay. Cells were exposed to transfection reagents only (control), scrambled or miR-ITGB1 lentivirus. Detection of lentivirus infection is indicated by GFP (green) expression. Cells were stained with antibodies against ZO-1 (red) and Hoechst 33258 for nuclei (blue). Scale bar=100μm. Microscope magnification= 20X.

6.4 DISCUSSION

This study aimed to evaluate the deletion of β1 integrin in luminal mouse primary epithelial cells and carried out the KD of β1 integrin in the EpH4 cells and subsequently investigated the paracellular permeability on these cells. To be able to evaluate the role of β1 integrin in MECs, the modification of its expression in 2 different cell models was established. Therefore, the first part of this study consisted of the modification of the β1 integrin expression in both the Eph4 and primary MECs obtained from the mouse mammary glands. Specifically, a lentivirus vector was used to reduce the β1 integrin expression in the EpH4 cell lines, and transgenic Cre-loxP mice with an inducible promotor were used to delete β1 integrin expression in K18 primary MECs. In both models, experiments were undertaken to evaluate permeability across a monolayer. In general, the preliminary results showed that the KO (in the K18 cells) or KD of β1 integrin occurs in the MECs. Likewise, most of the conditions for future permeability experiments in both cellular models were established.

The transgenic mouse model allowed the deletion of β1 integrin in the luminal cells after the addition of 4-OHT. These mice contain an inducible CreER under the control of the K18 promoter, which is expressed in the luminal cells. The addition of 4-OHT in cell culture causes the translocation of CreER protein from the cytoplasm to the nuclei and triggers the recombination of the β1 integrin sequence flanked by the loxP sites, deleting the β1 integrin sequence in K18 epithelial cells (luminal cells). Experimentally, the β1 integrin deletion is relatively easy; however, the biggest challenge with the primary cells is to efficiently and consistently achieve a complete monolayer across

the semi-permeable membrane. The cell culture often exhibited clumps of cells derived from the dissection of mammary tissue. These small pieces of tissue were not able to expand as a monolayer. Although the control samples also presented similar culture distribution, it is likely these clumps of cells in some parts of the semi-permeable membrane can have an impact on paracellular fluid transport, reducing the accuracy of the technique. Another challenge faced with the primary cell culture was the TEER measurements due to not always presenting the same resistance values in different experiments. The exact control of the cell density or the number of cells seeded on the semi-permeable membranes was not applied in the experiments since the number of cells seeded depended on each mouse prep and tissue obtained. For example, some tissues contained more adipose tissue. Even though the final density (confluent monolayer) was one of the parameters used for the permeability assays, more standardisation is required for the initial cell density to obtain more homogenous results in monolayer and over time (days of culture).

Another important point to consider in the permeability assays with the primary MECs is that the cell population is mostly composed of myoepithelial and luminal cells. The transgenic mouse model used in the experiments only made the β1 deletion in the luminal cells. Thus, permeability results could reflect the permeability of cells with and without β1integrin expression. In addition, the permeability assay in the semi-permeable membranes using dextran is dependent on the TJs formed by the cells. As mentioned, the experiments included a mixture of myoepithelial and luminal cells, and the junctions between these cells are different. The TJs are formed between the luminal cells but not the myoepithelial cells (Pitelka, Hamamoto et al. 1973). Therefore, the monolayer formed by the MECs is not homogeneous in the distribution of TJs, so

the permeability will likely be impacted. The detection of ZO-1 by IF was carried out in the cells used for the permeability assays to evaluate the presence of TJs in the monolayer. ZO-1 is a TJ-associated molecule critical for the formation of the TJs (McNeil, Capaldo et al. 2006, Umeda, Ikenouchi et al. 2006). Some sections of the monolayer formed by primary MECs reflected ZO-1 expression, and others did not (Appendix XII). Hence, the transgenic mice used for this experiment and/or the combination of both cell populations on the semi-permeable membranes could not be the best experimental model to answer the β1 role in permeability.

The preliminary result of the permeability assay in the primary cells showed a higher permeability in the β1integrin KO samples compared with its control. The β1 integrin KO samples had 1.64µg of dextran more than the β1 samples. However, no conclusions can be made with this preliminary result, as is required to complete the standardisation and have a representative N number.

The standardisation of the permeability assays in the EpH4 cells involved the use of lentivirus previously verified for the laboratory group to make the β1 integrin KD. To achieve effective KD, the virus infection must occur in a high proportion of the cells. Thus, after generating the lentiviruses, a titration was done to analyse the volume required to obtain around 80% of infection. The results showed that the infection occurs in more than 80% of the cells with 20µl of virus solution. However, previous attempts at the results presented in this Chapter did not show a percentage of 80% or similar percentages of infection in the sample groups in the same experiment (Appendix XIII) after using the virus titration calculations. These changes could have

originated from the way the virus titration was analysed. In this project, the virus titration was analysed by manually counting GFP-positive cells. Therefore, this may be exposed to human counting error and areas with a higher or lower percentage of infection that reduce the certainty of a result (although different random areas were counted). For that, other techniques can be used in future experiments for virus titration counting. An example of an alternative technique is flow cytometry, which has been used to quantify the GFP-positive cells after virus infection (Lu, Zhou et al. 2014, Pivert, Lefeuvre et al. 2021). This technique can reduce human error and increase the accuracy of the results. In addition, by sorting, the technique allows the selection of the infected cells (Wang, Liu et al. 2019), which could be an invaluable approach to seed only the GFP cells in the permeability experiments.

The TEER measurements need to be standardised for the EpH4 cells since the preliminary data showed that the integrity resistance changed after adding the transfection reagents for the lentivirus infection.

In conclusion, this Chapter aimed to determine the participation of β1 integrin in the transport of paracellular fluid in two different cellular models; the Eph4 cells and the mouse primary MECs. The KD of β1 integrin in the EpH4 cells by the infection with the miR-IGTB lentivirus and the KO of β1 integrin expression using the β1-integrin fx/fx-K18CreER transgenic mice were demonstrated. In the primary cells, it was show by IF that the deletion of β1 integrin was achieved specifically in the luminal (K18) cells. In EpH4 cells, it was demonstrated that lentivirus infection occurs in more than 80% by the expression of the GFP protein and that β1 integrin expression was reduced in

some infected cells. These results are part of the first objective established in this Chapter; however, the permeability experiments still need to be completed. Further experiments are needed to conclude the role of β1 integrin in paracellular fluid transport in MECs.

Chapter 7

7. FINAL DISCUSSION

7.1 Introduction

Structurally, the mammary gland consists of a branched tubuloalveolar system leading to the nipple. The ducts consist of a luminal space surrounded by a bilayer of luminal and myoepithelial cells (Biswas, Banerjee et al. 2022). The luminal epithelial cells express keratins 8 and 18 and line the ducts that terminate at the nipple. The myoepithelial cells express smooth muscle actin and keratins 5 and 14 and are in the outer layer of the epithelial bilayer in direct contact with BM (Pechoux, Gudjonsson et al. 1999).

The formation of the lumen in the mammary gland occurs during the embryogenesis stage, and the structure of this luminal space is conserved throughout life despite the drastic changes that this organ experiences during puberty (Javed and Lteif 2013, Ingthorsson, Briem et al. 2016), pregnancy and lactation (Oakes, Hilton et al. 2006, Sternlicht, Kouros-Mehr et al. 2006), and involution after lactation (Watson 2006). The maintenance of the lumen structure is related to the homeostasis of the mammary gland. Loss or alteration of this structure due to cell filling (no dying cells), is commonly associated with breast cancer (Gudjonsson, Adriance et al. 2005, Kaushik, Pickup et al. 2016). One of the main characteristics of ductal breast cancer from its early stage is the proliferation of monomorphic epithelial cells and some depolarised cells, leading to multilayering (Chatterjee and McCaffrey 2014)(Figure 3.1). Being the lumen alteration a histological characteristic shared in some types of breast cancer, it was thought that the approach of lumen study could provide important information about the molecules necessary for the regulation of the tissue architecture in the mammary gland and obtain clues about what is deregulated in breast cancer.

Thus, this research aimed to study the key molecules regulating the mammary gland lumen structure to subsequently evaluate these factors in breast cancer. The lumen study in this work was essentially divided into two parts: formation and maintenance. The lumen formation was approached by modifying the activity of molecules related to fluid secretion in epithelial cells since fluid secretion is one of the recently described mechanisms for lumen formation (Navis and Bagnat 2015). Since the CFTR ion channel and the Na^+/K^+-ATPase are essential for ion transport in cells and fluid secretion, its modification by ouabain, CFTRinh-172 and forskolin was carried out in MECs. It was shown that CFTR and Na^+/K^+-ATPase activities had an impact on the lumen formation and its maintenance in MECs (Figure 7.1). The most significant impact on the lumen was observed with CFTR activity modulation. Therefore, a substantial part of the thesis focused on studying the role of CFTR in the lumen structure of mouse primary MECs and human breast cell lines. The general discussion about the results is considered in the following subsections.

7.2 Key regulatory molecules of fluid secretion and lumen formation in MECs

Fluid pressures have been described as one of the key control forces driving morphogenesis in tubular organs of different species (Alcorn, Adamson et al. 1977, Bagnat, Cheung et al. 2007, Alvers, Ryan et al. 2014). The secretion of fluid and its accumulation in a limited area exerts a hydrostatic pressure, which modulates tissue structure. Fluid secretion has been described as one of the mechanisms involved in the formation of a single lumen *in vivo* in zebrafish (Bagnat, Cheung et al. 2007, Bagnat, Navis et al. 2010) and *in vitro* in models of primary prostatic cells and Madin-

Darby canine kidney (MDCK) cells (Bagnat, Cheung et al. 2007, Pearson, Hughes et al. 2009, Narayanan, Schappell et al. 2020). However, this mechanism for lumen formation has not been described in the mammary gland.

Since fluid secretion is a mechanism described for lumen formation and response to osmotic gradients (Frizzell and Hanrahan 2012), the first experiments in this project were about the modulation of the activity of Na^+/K^+-ATPase and CFTR. Na^+/K^+-ATPase was blocked with ouabain and stimulated with forskolin. CFTR was blocked or stimulated with CFTRinh-172 or forskolin, respectively. The data showed that both transporter's activities are essential for lumen formation and maintenance in the EpH4 cells and the primary MECs when they are blocked (Figures 3.7 and 3.8). The treatment with ouabain and CFTRinh-172 decreased the percentage of lumen formation compared to the control. This result is relevant for the morphogenesis of lumen in mammary epithelial cells. No previous data have reported the role of CFTR and Na^+/K^+-ATPase in lumen formation in MECs.

The lumen maintenance was the other part of the study of CFTR and Na^+/K^+-ATPase activity in this project. This segment was approached from the lumen area measurements before and after treatments. In primary mammary organoids, the CFTR-inh172 and Ouabain (100nM) decreased the lumen area. The most noticeable effect on the lumen structure was after the CFTRinh172 treatment, which collapsed the lumen area in most organoids (Figure 3.10). Forskolin did not significantly alter the lumen area compared with the control in primary mammary organoids. In the EpH4 acini, the lumen area with forskolin did not show significant differences with the control;

however, the inhibitory effect with ouabain and CFTRinh-172 showed a significant area decrease (Figure 3.9). The most evident effect was when the CFTR was blocked. Most of the lumens were totally lost in this group of samples.

The drug used for CFTR inhibition is a specific drug that binds to the NBD1 domain, maintaining the closed state of the channel (Caci, Caputo et al. 2008). That means that the effect observed in the lumen is mainly caused by CFTR inhibition and that the formation, expansion, and maintenance of the lumen depends on the CFTR activity. The relationship between reduced CFTR activity and lumen structure has been described in other biological models, such as the intestine of zebrafish *in vivo* (Bagnat, Navis et al. 2010) and in Caco-2 (colorectal adenocarcinoma cells) and MCDK (Madin-Darby canine kidney cells) cells *in vitro* (Narayanan, Schappell et al. 2020, Lobert, Skardal et al. 2022). In this thesis, the CFTR activity effect in lumen formation and lumen maintenance *in vitro* in MECs was tested (Figure 7.1 A, B, D and E).

With regards to lumen maintenance, it was observed that the morphology of the organoids with a lumen and the EpH4 acini changed drastically from having a lumen to having no lumen after the inhibition of the CFTR activity. This phenotype of mammary epithelial cells lacking a lumen is typically observed in transformed cells derived from breast cancer cells. Alterations in gene expression (Nguyen and Shively 2016), microenvironment (Patil, D'Ambrosio et al. 2015) or the polarisation process (Petersen, Ronnov-Jessen et al. 1992) are some of the reasons accounting for the lack of lumen formation in breast cancer cells. These differences in structural

morphologies of the lumen and no lumen in normal and breast cancer cells gave us a particular interest in studying CFTR in breast cancer for future experiments.

In general, the relevance of the Na^+/K^+-ATPase and CFTR findings reinforces the idea that fluid secretion is a mechanism that participates in single-lumen formation for tubular organs, and for the first time, this thesis showed evidence of it in a model of MECs. Likewise, it was shown that the activity of Na^+/K^+-ATPase and CFTR in EpH4 cells and primary MECs is necessary for lumen formation and its maintenance.

7.3 CFTR expression is necessary for lumen formation and maintenance in normal MECs

Although CFTRinh-172 has been described as a specific inhibitor of CFTR and the concentration used (10 µM) in our experiments was based on previous reports where an effect on CFTR has been observed without reports of toxicity (Cabrita, Kraus et al. 2020, Narayanan, Schappell et al. 2020), it was decided to confirm the role of CFTR in lumen formation and maintenance in MECs using other molecular techniques.

The use of specific siRNAs to target mRNA allowed us to decrease the CFTR expression in primary MECs. The CFTR KD was evaluated at mRNA and protein levels when the cells were transfected on 2D conditions and before being transferred to 3D conditions to assess lumen formation. The data obtained demonstrates that the CFTR expression was significantly decreased in the conditions used (Figure 4.4). The MECs with reduced expression of CFTR seeded on 3D conditions allowed us to

evaluate the effect of the decreased expression of this protein during lumen formation. A significant reduction in lumen formation was observed after the CFTR KD (Figure 4.6C). For the evaluation of lumen maintenance, the experimental design consisted of allowing the lumen formation first and then assessing the effect of the reduction of CFTR expression. Once the organoids with lumens were localised and their area was measured, the CFTR KD was carried out. Before the evaluation of CFTR KD, it was confirmed that transfection occurred in the primary organoids since they were partially embedded in BMM, which made the transfection and organoid collection challenging. Despite this, the collection of organoids was achieved, and the analysis of CFTR expression showed that the reduction was 38% (Figure 4.10A). The CFTR KD showed that the maintenance was affected in the two periods of time evaluated (24 and 48h post-transfection) (Figure 4.11). Therefore, the results obtained after CFTR KD show that CFTR expression is essential for the lumen structure in MECs and reinforces the role that CFTR plays in lumen formation and maintenance (Figure 7.1 C and F).

The findings produced by the modification of the activity and expression of CFTR in MECs have an impact on the area of developmental biology of the mammary gland. These results provide knowledge to understand the development and maintenance of tubular structures with a lumen. It has been described that this *in vitro* model allows the recapitulation of many aspects of function and structure during morphogenesis *in vivo*, including lumenogenesis (Lee, Seijo-Barandiaran et al. 2022). In this work, our *in vitro* model with BMM recapitulates conditions similar to those of the cells forming a luminal structure in the mammary gland, proving that the development of a lumen depends on the expression and activity of CFTR. Besides, these results support the

idea that the fluid secretion mechanism participates in the lumen formation since CFTR transports Cl^- and mediates the osmotic gradient.

The results of this work could also incite greater interest in research about the functioning and anatomy of the mammary glands of patients with CF. Histologically, the mammary gland in CF patients has been described with some changes, such as lobular atrophy (Garcia, Galindo et al. 1998). However, few studies have looked at the mammary glands of CF patients since most studies focus on vital organs such as the lungs.

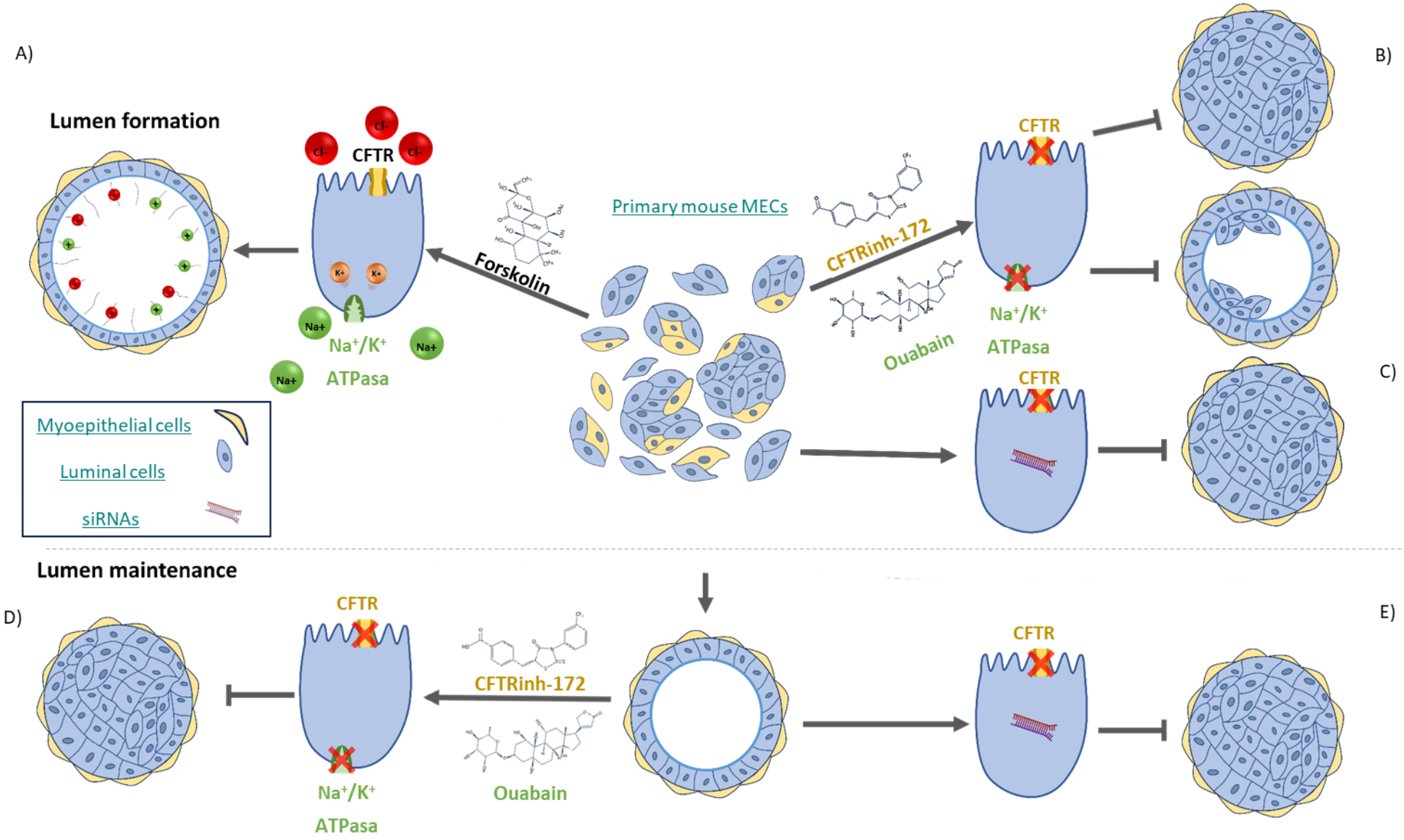
A)
Lumen formation
Cl-
Cl-
Cl-
CFTR
K+
K+
Na+
Na+
Na+
Na+/K+
ATPasa
Forskolin
Primary mouse MECs
CFTRinh-172
Ouabain
CFTR
Na+/K+
ATPasa
B)
C)
CFTR
Myoepithelial cells
Luminal cells
siRNAs
Lumen maintenance
D)
CFTR
CFTRinh-172
Ouabain
Na+/K+
ATPasa
CFTR
E)

Figure 7.1. Summary of CFTR function and effect on lumen formation and maintenance in MECs. Primary cells were obtained from the mouse mammary gland and cultured on BMM to allow the formation of mammary organoids. A), B) and C) Represent the experiments carried out and results obtained from lumen formation in MECs. D) and E) Represent the experiments carried out and results obtained from lumen maintenance experiments in MECs. A) Lumen formation is increased in MECs with the stimulation of Na^+/K^+-ATPase activity and CFTR ion channel with forskolin. B) Lumen formation is decreased in MECs by blocking Na^+/K^+-ATPase and CFTR with ouabain or CFTRinh-172. C) Lumen formation is decreased after reducing CFTR expression with siRNAs in MECs. D) Lumen structure is disrupted after the Na^+/K^+-ATPase and CFTR blocking with ouabain or CFTRinh-172 in MECs. F) Lumen structure is disrupted after reducing CFTR with siRNAs in MECs. The illustration was self-drawn.

7.4 CFTR in breast cancer

After confirming the importance of the activity and expression of CFTR for lumen structure in normal cells of the mouse mammary gland, it was sought to determine the relationship between the expression of this gene in breast cancer cells and their failure ability to form structures with a lumen. Studies were initially searched in relation to the expression of CFTR in breast cancer, and it was found that expression is relatively limited in breast cancer tissue in comparison to healthy tissue (Zhang, Jiang et al. 2013, Liu, Dong et al. 2020). Something that could be attributed to the reduced expression of CFTR is its methylation, which is higher in breast cancer samples compared to healthy samples (Liu, Dong et al. 2020). In addition, in healthy tissue samples, CFTR was localised to the apical membrane of luminal cells, whereas a cytoplasmic expression pattern was reported in breast cancer samples (Liu, Dong et al. 2020).

Knowing that the breast cancer cell lines are unable to form lumen structures (Petersen, Ronnov-Jessen et al. 1992), this characteristic was confirmed in the 3D

culture system used in this thesis (Figure 11.7). Further evaluation of the CFTR expression *in silico* and experimentally by qPCR and WB was carried out in some human breast cell lines. There was no difference in the CFTR expression between the CAL-51, MCF7, T47D and MDA-MB-231 breast cancer cell lines when compared to the MCF10A non-tumorigenic cells. Since the analysis of CFTR expression was performed in cells cultured in 2D conditions, it is possible that this can influence CFTR and, therefore, not reflect expression under 3D conditions. It has been shown in other studies that the same type of cell changes its expression when it is cultured in 2D or 3D (Wang, Weaver et al. 1998). Therefore, it would be important to analyse the CFTR expression of breast cancer cells cultured in 3D conditions with BMM.

An important difference between breast cancer and non-tumorigenic cells was found in this thesis when the CFTR protein expression was analysed by WB. The breast cancer cells do not present the molecular weight of the mature/functional form of CFTR (160-170 KDa). They expressed a higher molecular weight (>170KDa) in the membrane fraction (Figure 5.4). This intriguing result led us to assess whether the expression of this protein could be localised by IF in the apical membrane. The results indicate that CFTR is expressed in the apical membrane in the breast cancer cells and in the MCF10A cells. However, the CFTR detected in apical membranes does not necessarily mean it is functional. There are still many questions to be approached about the >170KDa CFTR protein form in breast cancer cells, such as its functionality, the molecular difference with the 160-170KDa of the MCF10A cells, and the processing of CFTR in breast cancer cells, among other questions.

There are several reasons why >170KDa CFTR form could have a higher molecular weight than 160-170KDa, such as PTMs. One well-known PTM of CFTR is glycosylation, which is necessary for the transport and function of CFTR in the membrane (Gregory, Cheng et al. 1990). Although glycosylation is one of the best-known PTMs for CFTR, it may also have others, such as palmitoylation, sumoylation, phosphorylation, ubiquitination and glycosylation (McClure, Barnes et al. 2016). However, to know if there is another PTM in the >170KDa CFTR, other techniques, such as immunoprecipitation or mass spectrometry, are required. Another explanation for a different molecular weight in proteins could be attributed to genetic mutation. Mutations in CFTR can also lead to different PTMs. For example, CFTR is ubiquitinated when there is a deletion of phenylalanine at position 508 (F508del) (Riordan 2008). This mutation creates a misfolding of the CFTR ion channel and its instability in the membrane. In response, a quality control procedure of proteins, such as ubiquitination, is carried out in the membrane to internalise the CFTR protein to the routes of recycling or degradation (Okiyoneda, Barriere et al. 2010). Therefore, more studies are required in this area (discussed in the subsection of future work).

An intriguing result obtained in this project was the lumen formation in the CAL-51 cells after forskolin treatment (Figure 7.2). These cells were not able to form a lumen structure in standard 3D conditions; however, after the prolonged addition of forskolin, the cells formed a well-defined single lumen (Figure 5.9). The change of morphology with a lumen represents an opportunity to understand the mechanism that allows the reversion of no lumen to lumen after the forskolin effect in breast cancer cells. Research on this mechanism would give us clues about potential dysregulation in

breast cancer cells. As previously mentioned, forskolin stimulates CFTR activity indirectly by raising the cAMP levels, which can indirectly affect another biological process. However, it was demonstrated that the lumen increase in intestinal organoids is dependent on CFTR (Dekkers, Wiegerinck et al. 2013).

Linking the CAL-51 cell results with those observed in normal mouse cells where lumen formation is dependent on the activity and expression of CFTR, the following hypothesis was about the necessary CFTR activity for lumen formation in CAL-51 cells. For this reason, future experiments about gene loss and gain of CFTR (described in the subsection of future work) could address the importance of CFTR in recovering the normal phenotype-like of a lumen structure. The implications of this result would have an impact on breast cancer biology. Understanding the forces and molecules involved in the lumen formation and maintenance could provide valuable information about the organisation of the mammary gland and, with it, a better understanding of the processes that accompany breast cancer development, such as filling the luminal space by cancer cells.

Another possible impact area of this study is in CF and breast cancer. The growing information on the involvement of CFTR in breast cancer (Stastna, Brat et al. 2023) and other types of cancer in lumen-containing organs such as the intestine, pancreas, prostate, and lung (Zhang, Wang et al. 2018) suggests that CFTR could be playing a determining role in the homeostasis of the mammary gland.

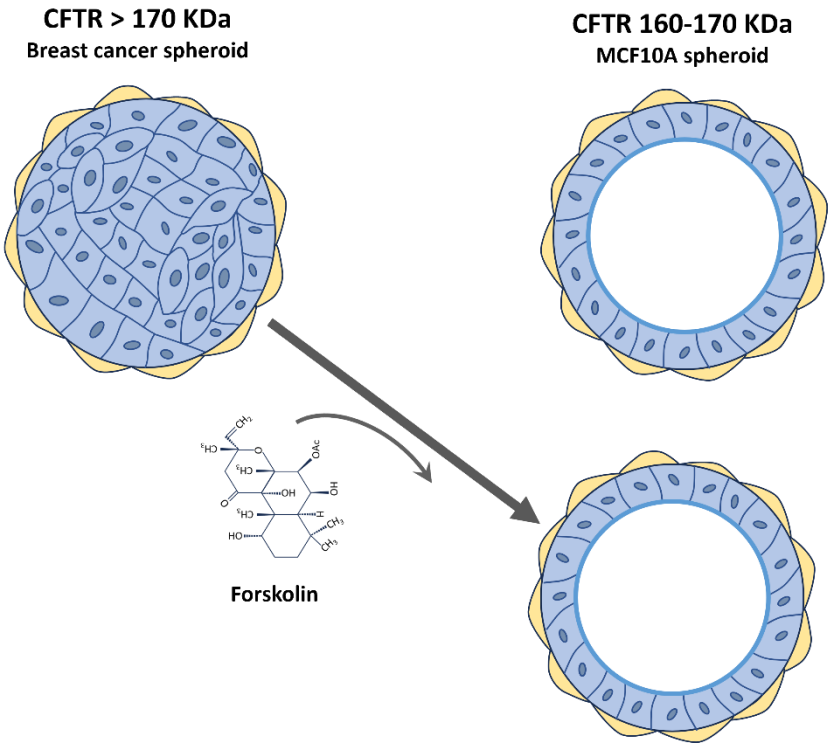

Figure 7.2. Lumen formation after forskolin treatment in CAL-51 cells cultured in 3D conditions with BMM. The breast cancer cells, including the CAL-51 cells, are unable to form acini compared with the non-tumorigenic MCF10A cells. CFTR protein detected in the membrane of breast cancer cells (>170 KDa) differs from the CFTR detected in the membrane of the MCF10A cells (160-170 KDa). Stimulation of Na^+/K^+-ATPase and CFTR ion channel with forskolin promotes lumen formation in 3D cell structures without a lumen formed for CAL-51 cells. The illustration was self-drawn.

7.5 Lumen formation and regulation of fluid secretion by β1 integrin

Previous results of the research group showed the necessary expression of β1 integrin in MECs for lumen formation. It was described that the interaction of MECs with BM through β1 integrin is essential for intercellular signalling of ILK, which allows the positioning of microtubules along the apicobasal axis to orient the cells appropriately towards the lumen as they are formed (Akhtar and Streuli 2013). Based on this, it was

decided to investigate the role that β1 integrin has in lumen formation beyond the polarity orientation. As one of the mechanisms described for single lumen formation is the secretion of fluids, it was therefore evaluated whether β1 integrin had a role in the secretion of fluids in the MECs. The data presented in this thesis related to the β1 integrin research question was obtained from standardisation experiments and preliminary results. The modification of β1 integrin expression was achieved by infection with a lentivirus that allowed the β1 KD and a transgenic mouse that allowed the β1 integrin KO in MECs. During the experiments, some parameters for the permeability experiments were set up for future experiments. However, it will be important to consider some points in the experimental design and limitations in the techniques used. Some of these limitations will be approached in the next section.

7.6 Limitations and future work

This section of the thesis highlights some limitations during the experiments and possible strategies to overcome these limitations. In addition, future work is proposed based on the results obtained in this project. This information is summarised in the following bullet points:

- This project, showed the necessary CFTR expression and activity for lumen formation and maintenance in normal mouse MECs. The first experiments used the specific inhibitor CFTR-inh172 and the stimulator forskolin to block or stimulate the CFTR activity, respectively. The forskolin effect over lumen formation increased the lumen formation; however, the forskolin effect in the

lumen area did not differ from that of the control. One limitation in these experiments is the lack of specificity of forskolin for the CFTR ion channel. To cover this limitation, other technical approaches, such as the CFTR KD, were also used to evaluate only the CFTR effect on lumen structure and maintenance. Nevertheless, it would be useful to test other CFTR stimulators to confirm these previous results or, alternatively, increase the CFTR expression and evaluate lumen formation and maintenance.

- The confirmation of the role of CFTR in lumen structure in MECs was evaluated by doing the CFTR KD using siRNAs. The transfection of these molecules decreased the CFTR expression in the primary MECs and, therefore, responded to research questions about its expression role in lumen formation and maintenance. However, transfection has a limitation related to low transfection efficiency in primary cells. This condition was especially observed when the MECs were cultured in the 3D conditions and then transfected. Not all the cells studied in the experiments were successfully transfected. For this reason, future experiments in 3D conditions approaching the CFTR expression role can be done with a cell model that allows the CFTR KO *in vitro*.

- The stimulation or inhibition of the CFTR and Na+/K+ pump activity by the use of drugs alters lumen formation and maintenance. This result supports the hypothesis that fluid secretion is a mechanism that controls the lumen formation and maintenance in MECs. However, more experiments are required to confirm that fluid secretion generates the hydrostatic pressure that drives lumen

formation and maintenance. Future experiments where the hydrostatic pressure can be measured after the addition of drugs can be carried out using a micropipette connected to a pressure transducer, as reported by Narayanan et al., 2020.

- The effect of CFTR KD in decreasing the lumen formation in normal cells was related to the inability of breast cancer to form lumens. Evaluation of CFTR expression was carried out in cells cultured in 2D conditions. One of the possible limitations of these results is that only the profile expression of CFTR in 2D conditions was studied. Since the gene profile expression of the cells can change from 2D to 3D conditions (Hasler, Wang et al. 1998), further studies are required to evaluate the CFTR expression in non-tumorigenic and breast cancer cells cultured in 3D conditions with BMM.

- In breast cancer cells, the expression of CFTR in the membrane differs from the MCF10A cells at the protein level detected by WB. In breast cancer cells, CFTR presented a molecular size >170 KDa, while the CFTR detection in the MCF10A cell was 160-170 KDa in the membrane. One of the limitations of using only antibodies against CFTR by WB is that it was not possible to detect the molecular differences between the CFTR expressed in the membrane of the breast cancer cells and the MCF10A cells. Therefore, further experiments are needed to analyse the molecular differences between these proteins. As a PTM is a possible explanation for the different molecular weights detected in breast cancer cells, mass spectrometry or immunoprecipitation are potential techniques to use for further experiments.

- It has been reported that breast cancer cells can not form lumen structures (Petersen, Ronnov-Jessen et al. 1992), and this was also confirmed in our results. The forskolin treatment applied to the CAL-51 cells cultured in 3D conditions promoted lumen formation. Ongoing experiments are being carried out to increase the number of experiments. Likewise, evaluation of the forskolin effect in lumen formation with other breast cancer cell lines will be useful to validate the role of CFTR in lumen formation in breast cancer cells.

  Further experiments can be carried out to confirm that the effect of forskolin in the lumen formation came from the stimulation of CFTR in the CAL-51. An option to support the forskolin effect in the CAL-51 cells is to apply CFTRinh-172 treatment to previously treated (with forskolin) CAL-51 cells forming a lumen. CFTRinh-172 is a specific inhibitor, and therefore, if the lumen is altered, it would confirm that the forskolin effect in the lumen is CFTR-dependent. Another possible experiment is to delete or decrease CFTR expression in CAL-51 cells and apply the forskolin treatment to evaluate the ability to form a lumen structure. However, since CFTR expression is the protein to be assessed in lumen formation, it would be more convenient to study the effect of its expression and activity in lumen formation using CFTR KO mouse models as well as in samples from patients with breast cancer.

- Based on the different CFTR protein forms found in the membrane of the breast cancer cells (Figure 5.6) and the results obtained from the indirect stimulation of CFTR with forskolin in the CAL-51 cells (Figure 5.11), experiments to

overexpress CFTR in breast cancer cells were designed to confirm the CFTR role in lumen formation in human breast cell lines.

The negative control vector has been generated from the CFTR vector. This negative control vector includes all the components of the CFTR vector except the CFTR sequence. Both vectors were amplified, quantified and prepared for the vector sequencing. Therefore, the following steps for this objective are to do the sequencing and verify the correct vector construct as well as the presence of the CFTR sequence in the CFTR vector and the absence of the CFTR sequence in the negative control vector by *in silico* analysis (comparing the sequences obtained with the vector design sequences). Once the correct vector sequences are confirmed, transfections in the CAL-51cell will be conducted. Two different approaches are planned:

1. Evaluate the effect of CFTR overexpression in the lumen formation. The cells will be transfected on 2D conditions and then transferred to 3D conditions to evaluate their ability to form a lumen structure.

2. Evaluate the recovery of a lumen after the overexpression of CFTR. The CAL-51 cells will be seeded under 3D conditions, and once they have formed 3D cell structures (without a lumen), they will be transfected to overexpress CFTR. Subsequently, the capacity of lumen formation will be analysed.

- The role of β1 integrin in fluid secretion was evaluated in two cellular models: primary cells and EpH4 cells using semi-permeable membranes. One of the limitations of the permeability assays using primary cells was that the monolayer culture on the semi-permeable membranes presented clumps of cells that can affect the transport of fluids. Another limitation is that the primary MECs obtained from the mouse mammary glands contain myoepithelial and luminal cells, and their cellular junctions differ between those types of cells, possibly affecting the paracellular transport. In addition, only the luminal cells dissected from the mouse mammary gland have the β1 integrin KO. A possible solution for future experiments is the use of cell sorting. This technique would allow the separation of individual (avoiding the clumps of cells) luminal cells (β1 integrin KO) to be cultured as a monolayer on semi-permeable membranes. In addition, this technique can also be used as a more accurate alternative for virus titration in the EpH4 cells model.

7.7 Conclusion

In summary, the data presented in this thesis showed a novel role of CFTR in forming and maintaining a lumen structure in the mouse primary mammary organoids and EpH4 acini. Modulation of CFTR and Na^+/K^+-ATPase activity with CFTRinh-172, ouabain and forskolin showed that the formation and maintenance of the lumen in MECs depends on their activity. The most evident effect on lumen formation and maintenance was observed by the blocking of CFTR activity with the CFRinh-172 inhibitor (10 μM). For this reason, the rest of the thesis focused on evaluating the role

of CFTR in normal mouse MECs and human breast cell lines. The essential CFTR role in lumen formation and maintenance in normal mouse MECs was confirmed when the CFTR expression was reduced by siRNAs and the lumen structure was altered. The results of these experiments and the results of activity modulation of CFTR with drugs lead to the conclusion that the expression and activity of CFTR are essential for the formation and maintenance of the lumen in MECs. A link with breast cancer cells was made to evaluate the CFTR expression and their inability to form a lumen. The results showed that the non-tumorigenic MCF10A cells express the mature molecular weight (160-170 KDa) of CFTR in the membrane protein fraction but not the breast cancer cells studied in this project (MCF7, CAL-51, MDA-MB-231 and T47D). A different band for CFTR with a molecular weight higher than 170KDa was detected by WB in the membrane protein fraction of the breast cancer cells. In 3D conditions, the breast cancer cells could not form a lumen structure; however, the indirect stimulation of CFTR with forskolin promoted lumen formation in the CAL-51 breast cancer cells. All these results suggest that CFTR has an essential role in the lumen structure formed by MECs.

Understanding the morphogenesis of the lumen in MECs not only expands our knowledge of the developmental biology of the mammary gland but also contributes knowledge to understanding the dysregulations in the structure of the tissue associated with breast cancer. The novel requirement for CFTR in normal MECs for lumen structure and its protein abnormality expression in breast cancer cells could contribute valuable information to apply in translational research in the future.

APPENDICES

I. CFTR and negative control vector sequences.

Vector	Sequence
Control vector (without CFTR sequence)	TCAATATTGGCCATTAGCCATATTATTCATTGGTTATATAGCATAAATCAATATTGGCTATTGGCCA TTGCATACGTTGTATCTATATCATAATATGTACATTTATATTGGCTCATGTCCAATATGACCGCCAT GTTGGCATTGATTATTGACTAGTTATTAATAGTAATCAATTACGGGGTCATTAGTTCATAGCCCATA TATGGAGTTCCGCGTTACATAACTTACGGTAAATGGCCCGCCTGGCTGACCGCCCAACGACCCCC GCCCATTGACGTCAATAATGACGTATGTTCCCATAGTAACGCCAATAGGGACTTTCCATTGACGTC AATGGGTGGAGTATTTACGGTAAACTGCCCACTTGGCAGTACATCAAGTGTATCATATGCCAAGT CCGCCCCCTATTGACGTCAATGACGGTAAATGGCCCGCCTGGCATTATGCCCAGTACATGACCTTA CGGGACTTTCCTACTTGGCAGTACATCTACGTATTAGTCATCGCTATTACCATGGTGATGCGGTTTT GGCAGTACACCAATGGGCGTGGATAGCGGTTTGACTCACGGGGATTTCCAAGTCTCCACCCCATT GACGTCAATGGGAGTTTGTTTTGGCACCAAAATCAACGGGACTTTCCAAAATGTCGTAATAACCCC GCCCCGTTGACGCAAATGGGCGGTAGGCGTGTACGGTGGGAGGTCTATATAAGCAGAGCTGGTT TAGTGAACCGTCAGATCACTAGAAGCTTTATTGCGGTAGTTTATCACAGTTAAATTGCTAACGCAG TCAGTGCTTCTGACACAACAGTCTCGAACTTAAGCTGCAGAAGTTGGTCGTGAGGCACTGGGCAG GTAAGTATCAAGGTTACAAGACAGGTTTAAGGAGACCAATAGAAACTGGGCTTGTCGAGACAGA GAAGACTCTTGCGTTTCTGATAGGCACCTATTGGTCTTACTGACATCCACTTTGCCTTTCTCTCCAC AGGTGTCCACTCCCAGTTCAATTACAGCTCTTAAGGCTAGAGTATTAATACGACTCACTATAGGGC TAGCAAAGCCACCATGGCAGAAATCGGTACTGGCTTTCCATTCGACCCCCATTATGTGGAAGTCCT GGGCGAGCGCATGCACTACGTCGATGTTGGTCCGCGCGATGGCACCCCTGTGCTGTTCCTGCACG GTAACCCGACCTCCTCCTACGTGTGGCGCAACATCATCCCGCATGTTGCACCGACCCATCGCTGCA TTGCTCCAGACCTGATCGGTATGGGCAAATCCGACAAACCAGACCTGGGTTATTTCTTCGACGACC ACGTCCGCTTCATGGATGCCTTCATCGAAGCCCTGGGTCTGGAAGAGGTCGTCCTGGTCATTCACG

	ACTGGGGCTCCGCTCTGGGTTTCCACTGGGCCAAGCGCAATCCAGAGCGCGTCAAAGGTATTGCA TTTATGGAGTTCATCCGCCCTATCCCGACCTGGGACGAATGGCCAGAATTTGCCCGCGAGACCTTC CAGGCCTTCCGCACCACCGACGTCGGCCGCAAGCTGATCATCGATCAGAACGTTTTTATCGAGGG TACGCTGCCGATGGGTGTCGTCCGCCCGCTGACTGAAGTCGAGATGGACCATTACCGCGAGCCGT TCCTGAATCCTGTTGACCGCGAGCCACTGTGGCGCTTCCCAAACGAGCTGCCAATCGCCGGTGAG CCAGCGAACATCGTCGCGCTGGTCGAAGAATACATGGACTGGCTGCACCAGTCCCCTGTCCCGAA GCTGCTGTTCTGGGGCACCCCAGGCGTTCTGATCCCACCGGCCGAAGCCGCTCGCCTGGCCAAAA GCCTGCCTAACTGCAAGGCTGTGGACATCGGCCCGGGTCTGAATCTGCTGCAAGAAGACAACCCG GACCTGATCGGCAGCGAGATCGCGCGCTGGCTGTCGACGCTCGAGATTTCCGGCGAGCCAACCA CTGAGGATCTGTACTTTCAGTAAACGAATTCGGGCTCGGTACCCGGGGATCCTCTAGAGTCGACC TGCAGGCATGCAAGCTGATCCGGCTGCTAACAAAGCCCGAAAGGAAGCTGAGTTGGCTGCTGCC ACCGCTGAGCAATAACTAGCATAACCCCTTGGGGCGGCCGCTTCGAGCAGACATGATAAGATACA TTGATGAGTTTGGACAAACCACAACTAGAATGCAGTGAAAAAAATGCTTTATTTGTGAAATTTGTG ATGCTATTGCTTTATTTGTAACCATTATAAGCTGCAATAAACAAGTTAACAACAACAATTGCATTCA TTTTATGTTTCAGGTTCAGGGGGAGATGTGGGAGGTTTTTTTAAGCAAGTAAAACCTCTACAAATG TGGTAAAATCGAATTCTAATGGATCCTCTTTGCGCTTGCGTTTTCCCTTGTCCAGATAGCCCAGTAG CTGACATTCATCCGGGGTCAGCACCGTTTCTGCGGACTGGCTTTCTACGTAATGGTTTCTTAGACG TCAGGTGGCACTTTTCGGGGAAATGTGCGCGGAACCCCTATTTGTTTATTTTTCTAAATACATTCAA ATATGTATCCGCTCATGAGACAATAACCCTGATAAATGCTTCAATAATATTGAAAAAGGAAGAGTA TGAGTATTCAACATTTCCGTGTCGCCCTTATTCCCTTTTTTGCGGCATTTTGCCTTCCTGTTTTTGCTC ACCCAGAAACGCTGGTGAAAGTAAAAGATGCTGAAGATCAGTTGGGTGCACGAGTGGGTTACAT CGAACTGGATCTCAACAGCGGTAAGATCCTTGAGAGTTTTCGCCCCGAAGAACGTTTTCCAATGAT GAGCACTTTCAAAGTTCTGCTATGTGGCGCGGTATTATCCCGTATTGACGCCGGGCAAGAGCAAC TCGGTCGCCGCATACACTATTCTCAGAATGACTTGGTTGAGTACTCACCAGTCACAGAAAAGCATC TTACGGATGGCATGACAGTAAGAGAATTATGCAGTGCTGCCATAACCATGAGTGATAACACTGCG GCCAACTTACTTCTGACAACTATCGGAGGACCGAAGGAGCTAACCGCTTTTTTGCACAACATGGG

	GGATCATGTAACTCGCCTTGATCGTTGGGAACCGGAGCTGAATGAAGCCATACCAAACGACGAGC GTGACACCACGATGCCTGTAGCAATGGCAACAACGTTGCGCAAACTATTAACTGGCGAACTACTT ACTCTAGCTTCCCGGCAACAATTAATAGACTGGATGGAGGCGGATAAAGTTGCAGGACCACTTCT GCGCTCGGCCCTTCCGGCTGGCTGGTTTATTGCTGATAAATCTGGAGCCGGTGAGCGTGGGTCTC GCGGTATCATTGCAGCACTGGGGCCAGATGGTAAGCCCTCCCGTATCGTAGTTATCTACACGACG GGGAGTCAGGCAACTATGGATGAACGAAATAGACAGATCGCTGAGATAGGTGCCTCACTGATTA AGCATTGGTAATTCGAAATGACCGACCAAGCGACGCCCAACCGGTATCAGCTCACTCAAAGGCGG TAATACGGTTATCCACAGAATCAGGGGATAACGCAGGAAAGAACATGTGAGCAAAAGGCCAGCA AAAGGCCAGGAACCGTAAAAAGGCCGCGTTGCTGGCGTTTTTCCATAGGCTCCGCCCCCCTGACG AGCATCACAAAAATCGACGCTCAAGTCAGAGGTGGCGAAACCCGACAGGACTATAAAGATACCA GGCGTTTCCCCCTGGAAGCTCCCTCGTGCGCTCTCCTGTTCCGACCCTGCCGCTTACCGGATACCT GTCCGCCTTTCTCCCTTCGGGAAGCGTGGCGCTTTCTCATAGCTCACGCTGTAGGTATCTCAGTTC GGTGTAGGTCGTTCGCTCCAAGCTGGGCTGTGTGCACGAACCCCCCGTTCAGCCCGACCGCTGCG CCTTATCCGGTAACTATCGTCTTGAGTCCAACCCGGTAAGACACGACTTATCGCCACTGGCAGCAG CCACTGGTAACAGGATTAGCAGAGCGAGGTATGTAGGCGGTGCTACAGAGTTCTTGAAGTGGTG GCCTAACTACGGCTACACTAGAAGGACAGTATTTGGTATCTGCGCTCTGCTGAAGCCAGTTACCTT CGGAAAAAGAGTTGGTAGCTCTTGATCCGGCAAACAAACCACCGCTGGTAGCGGTGGTTTTTTTG TTTGCAAGCAGCAGATTACGCGCAGAAAAAAAGGATTTCAAGAAGATCCTTTGATCTTTTCTACGG GGTCTGACGCTCAGTGGAACGAAAACTCACGTTAAGGGATTTTGGTCATGAGATTATCAAAAAGG ATCTTCACCTAGATCCTTTTATAGTCCGGAAATACAGGAACGCACGCTGGATGGCCCTTCGCTGGG ATGGTGAAACCATGAAAAATGGCAGCTTCAGTGGATTAAGTGGGGGTAATGTGGCCTGTACCCTC TGGTTGCATAGGTATTCATACGGTTAAAATTTATCAGGCGCGATTGCGGCAGTTTTTCGGGTGGTT TGTTGCCATTTTTACCTGTCTGCTGCCGTGATCGCGCTGAACGCGTTTTAGCGGTGCGTACAATTA AGGGATTATGGTAAATCCACTTACTGTCTGCCCTCGTAGCCATCGAGATAAACCGCAGTACTCCGG CCACGATGCGTCCGGCGTAGAGGATCGAGATCT The sequence is to be confirmed.

CFTR vector	TCAATATTGGCCATTAGCCATATTATTCATTGGTTATATAGCATAAATCAATATTGGCTATTGGCCA TTGCATACGTTGTATCTATATCATAATATGTACATTTATATTGGCTCATGTCCAATATGACCGCCAT GTTGGCATTGATTATTGACTAGTTATTAATAGTAATCAATTACGGGGTCATTAGTTCATAGCCCATA TATGGAGTTCCGCGTTACATAACTTACGGTAAATGGCCCGCCTGGCTGACCGCCCAACGACCCCC GCCCATTGACGTCAATAATGACGTATGTTCCCATAGTAACGCCAATAGGGACTTTCCATTGACGTC AATGGGTGGAGTATTTACGGTAAACTGCCCACTTGGCAGTACATCAAGTGTATCATATGCCAAGT CCGCCCCCTATTGACGTCAATGACGGTAAATGGCCCGCCTGGCATTATGCCCAGTACATGACCTTA CGGGACTTTCCTACTTGGCAGTACATCTACGTATTAGTCATCGCTATTACCATGGTGATGCGGTTTT GGCAGTACACCAATGGGCGTGGATAGCGGTTTGACTCACGGGGATTTCCAAGTCTCCACCCCATT GACGTCAATGGGAGTTTGTTTTGGCACCAAAATCAACGGGACTTTCCAAAATGTCGTAATAACCCC GCCCCGTTGACGCAAATGGGCGGTAGGCGTGTACGGTGGGAGGTCTATATAAGCAGAGCTGGTT TAGTGAACCGTCAGATCACTAGAAGCTTTATTGCGGTAGTTTATCACAGTTAAATTGCTAACGCAG TCAGTGCTTCTGACACAACAGTCTCGAACTTAAGCTGCAGAAGTTGGTCGTGAGGCACTGGGCAG GTAAGTATCAAGGTTACAAGACAGGTTTAAGGAGACCAATAGAAACTGGGCTTGTCGAGACAGA GAAGACTCTTGCGTTTCTGATAGGCACCTATTGGTCTTACTGACATCCACTTTGCCTTTCTCTCCAC AGGTGTCCACTCCCAGTTCAATTACAGCTCTTAAGGCTAGAGTATTAATACGACTCACTATAGGGC TAGCAAAGCCACCATGGCAGAAATCGGTACTGGCTTTCCATTCGACCCCCATTATGTGGAAGTCCT GGGCGAGCGCATGCACTACGTCGATGTTGGTCCGCGCGATGGCACCCCTGTGCTGTTCCTGCACG GTAACCCGACCTCCTCCTACGTGTGGCGCAACATCATCCCGCATGTTGCACCGACCCATCGCTGCA TTGCTCCAGACCTGATCGGTATGGGCAAATCCGACAAACCAGACCTGGGTTATTTCTTCGACGACC ACGTCCGCTTCATGGATGCCTTCATCGAAGCCCTGGGTCTGGAAGAGGTCGTCCTGGTCATTCACG ACTGGGGCTCCGCTCTGGGTTTCCACTGGGCCAAGCGCAATCCAGAGCGCGTCAAAGGTATTGCA TTTATGGAGTTCATCCGCCCTATCCCGACCTGGGACGAATGGCCAGAATTTGCCCGCGAGACCTTC CAGGCCTTCCGCACCACCGACGTCGGCCGCAAGCTGATCATCGATCAGAACGTTTTTATCGAGGG TACGCTGCCGATGGGTGTCGTCCGCCCGCTGACTGAAGTCGAGATGGACCATTACCGCGAGCCGT TCCTGAATCCTGTTGACCGCGAGCCACTGTGGCGCTTCCCAAACGAGCTGCCAATCGCCGGTGAG

	CCAGCGAACATCGTCGCGCTGGTCGAAGAATACATGGACTGGCTGCACCAGTCCCCTGTCCCGAA GCTGCTGTTCTGGGGCACCCCAGGCGTTCTGATCCCACCGGCCGAAGCCGCTCGCCTGGCCAAAA GCCTGCCTAACTGCAAGGCTGTGGACATCGGCCCGGGTCTGAATCTGCTGCAAGAAGACAACCCG GACCTGATCGGCAGCGAGATCGCGCGCTGGCTGTCGACGCTCGAGATTTCCGGCGAGCCAACCA CTGAGGATCTGTACTTTCAGAGCGATAACGCGATCGCCATGCAGAGGTCGCCTCTGGAAAAGGCC AGCGTTGTCTCCAAACTTTTTTTCAGCTGGACCAGACCAATTTTGAGGAAAGGATACAGACAGCGC CTGGAATTGTCAGACATATACCAAATCCCTTCTGTTGATTCTGCTGACAATCTATCTGAAAAATTGG AAAGAGAATGGGATAGAGAGCTGGCTTCAAAGAAAAATCCTAAACTCATTAATGCCCTTCGGCGA TGTTTTTTCTGGAGATTTATGTTCTATGGAATCTTTTTATATTTAGGGGAAGTCACCAAAGCAGTAC AGCCTCTCTTACTGGGAAGAATCATAGCTTCCTATGACCCGGATAACAAGGAGGAACGCTCTATC GCGATTTATCTAGGCATAGGCTTATGCCTTCTCTTTATTGTGAGGACACTGCTCCTACACCCAGCCA TTTTTGGCCTTCATCACATTGGAATGCAGATGAGAATAGCTATGTTTAGTTTGATTTATAAGAAGA CTTTAAAGCTGTCAAGCCGTGTTCTAGATAAAATAAGTATTGGACAACTTGTTAGTCTCCTTTCCAA CAACCTGAACAAATTTGATGAAGGACTTGCATTGGCACATTTCGTGTGGATCGCTCCTTTGCAAGT GGCACTCCTCATGGGGCTAATCTGGGAGTTGTTACAGGCGTCTGCCTTCTGTGGACTTGGTTTCCT GATAGTCCTTGCCCTTTTTCAGGCTGGGCTAGGGAGAATGATGATGAAGTACAGAGATCAGAGA GCTGGGAAGATCAGTGAAAGACTTGTGATTACCTCAGAAATGATTGAAAATATCCAATCTGTTAA GGCATACTGCTGGGAAGAAGCAATGGAAAAAATGATTGAAAACTTAAGACAAACAGAACTGAAA CTGACTCGGAAGGCAGCCTATGTGAGATACTTCAATAGCTCAGCCTTCTTCTTCTCAGGGTTCTTTG TGGTGTTTTTATCTGTGCTTCCCTATGCACTAATCAAAGGAATCATCCTCCGGAAAATATTCACCAC CATCTCATTCTGCATTGTTCTGCGCATGGCGGTCACTCGGCAATTTCCCTGGGCTGTACAAACATG GTATGACTCTCTTGGAGCAATAAACAAAATACAGGATTTCTTACAAAAGCAAGAATATAAGACATT GGAATATAACTTAACGACTACAGAAGTAGTGATGGAGAATGTAACAGCCTTCTGGGAGGAGGGA TTTGGGGAATTATTTGAGAAAGCAAAACAAAACAATAACAATAGAAAAACTTCTAATGGTGATGA CAGCCTCTTCTTCAGTAATTTCTCACTTCTTGGTACTCCTGTCCTGAAAGATATTAATTTCAAGATAG AAAGAGGACAGTTGTTGGCGGTTGCTGGATCCACTGGAGCAGGCAAGACTTCACTTCTAATGGTG

	ATTATGGGAGAACTGGAGCCTTCAGAGGGTAAAATTAAGCACAGTGGAAGAATTTCATTCTGTTC TCAGTTTTCCTGGATTATGCCTGGCACCATTAAAGAAAATATCATCTTTGGTGTTTCCTATGATGAA TATAGATACAGAAGCGTCATCAAAGCATGCCAACTAGAAGAGGACATCTCCAAGTTTGCAGAGAA AGACAATATAGTTCTTGGAGAAGGTGGAATCACACTGAGTGGAGGTCAACGAGCAAGAATTTCTT TAGCAAGAGCAGTATACAAAGATGCTGATTTGTATTTATTAGACTCTCCTTTTGGATACCTAGATG TTTTAACAGAAAAAGAAATATTTGAAAGCTGTGTCTGTAAACTGATGGCTAACAAAACTAGGATTT TGGTCACTTCTAAAATGGAACATTTAAAGAAAGCTGACAAAATATTAATTTTGCATGAAGGTAGCA GCTATTTTTATGGGACATTTTCAGAACTCCAAAATCTACAGCCAGACTTTAGCTCAAAACTCATGG GATGTGATTCTTTCGACCAATTTAGTGCAGAAAGAAGAAATTCAATCCTAACTGAGACCTTACACC GTTTCTCATTAGAAGGAGATGCTCCTGTCTCCTGGACAGAAACAAAAAAACAATCTTTTAAACAGA CTGGAGAGTTTGGGGAAAAAAGGAAGAATTCTATTCTCAATCCAATCAACTCTATACGAAAATTTT CCATTGTGCAAAAGACTCCCTTACAAATGAATGGCATCGAAGAGGATTCTGATGAGCCTTTAGAG AGAAGGCTGTCCTTAGTACCAGATTCTGAGCAGGGAGAGGCGATACTGCCTCGCATCAGCGTGAT CAGCACTGGCCCCACGCTTCAGGCACGAAGGAGGCAGTCTGTCCTGAACCTGATGACACACTCAG TTAACCAAGGTCAGAACATTCACCGAAAGACAACAGCATCCACACGAAAAGTGTCACTGGCCCCT CAGGCAAACTTGACTGAACTGGATATATATTCAAGAAGGTTATCTCAAGAAACTGGCTTGGAAAT AAGTGAAGAAATTAACGAAGAAGACTTAAAGGAGTGCTTTTTTGATGATATGGAGAGCATACCAG CAGTGACTACATGGAACACATACCTTCGATATATTACGGTCCACAAGAGCTTAATTTTTGTGCTAA TTTGGTGCTTAGTAATTTTTCTGGCAGAGGTGGCTGCTTCTTTGGTTGTGCTGTGGCTCCTTGGAA ACACTCCTCTTCAAGACAAAGGGAATAGTACTCATAGTAGAAATAACAGCTATGCAGTGATTATCA CCAGCACCAGTTCGTATTATGTGTTTTACATTTACGTGGGAGTAGCCGACACTTTGCTTGCTATGG GATTCTTCAGAGGTCTACCACTGGTGCATACTCTAATCACAGTGTCGAAAATTTTACACCACAAAA TGTTACATTCTGTTCTTCAAGCACCTATGTCAACCCTCAACACGTTGAAAGCAGGTGGGATTCTTAA TAGATTCTCCAAAGATATAGCAATTTTGGATGACCTTCTGCCTCTTACCATATTTGACTTCATCCAG TTGTTATTAATTGTGATTGGAGCTATAGCAGTTGTCGCAGTTTTACAACCCTACATCTTTGTTGCAA CAGTGCCAGTGATAGTGGCTTTTATTATGTTGAGAGCATATTTCCTCCAAACCTCACAGCAACTCA

	AACAACTGGAATCTGAAGGCAGGAGTCCAATTTTCACTCATCTTGTTACAAGCTTAAAAGGACTAT GGACACTTCGTGCCTTCGGACGGCAGCCTTACTTTGAAACTCTGTTCCACAAAGCTCTGAATTTAC ATACTGCCAACTGGTTCTTGTACCTGTCAACACTGCGCTGGTTCCAAATGAGAATAGAAATGATTT TTGTCATCTTCTTCATTGCTGTTACCTTCATTTCCATTTTAACAACAGGAGAAGGAGAAGGAAGAG TTGGTATTATCCTGACTTTAGCCATGAATATCATGAGTACATTGCAGTGGGCTGTAAACTCCAGCA TAGATGTGGATAGCTTGATGCGATCTGTGAGCCGAGTCTTTAAGTTCATTGACATGCCAACAGAA GGTAAACCTACCAAGTCAACCAAACCATACAAGAATGGCCAACTCTCGAAAGTTATGATTATTGA GAATTCACACGTGAAGAAAGATGACATCTGGCCCTCAGGGGGCCAAATGACTGTCAAAGATCTCA CAGCAAAATACACAGAAGGTGGAAATGCCATATTAGAGAACATTTCCTTCTCAATAAGTCCTGGCC AGAGGGTGGGCCTCTTGGGAAGAACTGGATCAGGGAAGAGTACTTTGTTATCAGCTTTTTTGAGA CTACTGAACACTGAAGGAGAAATCCAGATCGATGGTGTGTCTTGGGATTCAATAACTTTGCAACA GTGGAGGAAAGCCTTTGGAGTGATACCACAGAAAGTATTTATTTTTTCTGGAACATTTAGAAAAA ACTTGGATCCCTATGAACAGTGGAGTGATCAAGAAATATGGAAAGTTGCAGATGAGGTTGGTCTC AGATCTGTGATAGAACAGTTTCCTGGGAAGCTTGACTTTGTCCTTGTGGATGGGGGCTGTGTCCT AAGCCATGGCCACAAGCAGTTGATGTGCTTGGCTAGATCTGTTCTCAGTAAGGCGAAGATCTTGC TGCTTGATGAACCCAGTGCTCATTTGGATCCAGTAACATACCAAATAATTAGAAGAACTCTAAAAC AAGCATTTGCTGATTGCACAGTAATTCTCTGTGAACACAGGATAGAAGCAATGCTGGAATGCCAA CAATTTTTGGTCATAGAAGAGAACAAAGTGCGGCAGTACGATTCCATCCAGAAACTGCTGAACGA GAGGAGCCTCTTCCGGCAAGCCATCAGCCCTTCCGACAGGGTGAAGCTCTTTCCCCACCGGAACT CAAGCAAGTGCAAGTCTAAGCCCCAGATTGCTGCTCTGAAAGAGGAGACAGAAGAAGAGGTGCA AGATACAAGGCTTGTTTAAACGAATTCGGGCTCGGTACCCGGGGATCCTCTAGAGTCGACCTGCA GGCATGCAAGCTGATCCGGCTGCTAACAAAGCCCGAAAGGAAGCTGAGTTGGCTGCTGCCACCG CTGAGCAATAACTAGCATAACCCCTTGGGGCGGCCGCTTCGAGCAGACATGATAAGATACATTGA TGAGTTTGGACAAACCACAACTAGAATGCAGTGAAAAAAATGCTTTATTTGTGAAATTTGTGATGC TATTGCTTTATTTGTAACCATTATAAGCTGCAATAAACAAGTTAACAACAACAATTGCATTCATTTT ATGTTTCAGGTTCAGGGGGAGATGTGGGAGGTTTTTTTAAGCAAGTAAAACCTCTACAAATGTGG

	TAAAATCGAATTCTAATGGATCCTCTTTGCGCTTGCGTTTTCCCTTGTCCAGATAGCCCAGTAGCTG ACATTCATCCGGGGTCAGCACCGTTTCTGCGGACTGGCTTTCTACGTAATGGTTTCTTAGACGTCA GGTGGCACTTTTCGGGGAAATGTGCGCGGAACCCCTATTTGTTTATTTTTCTAAATACATTCAAATA TGTATCCGCTCATGAGACAATAACCCTGATAAATGCTTCAATAATATTGAAAAAGGAAGAGTATG AGTATTCAACATTTCCGTGTCGCCCTTATTCCCTTTTTTGCGGCATTTTGCCTTCCTGTTTTTGCTCAC CCAGAAACGCTGGTGAAAGTAAAAGATGCTGAAGATCAGTTGGGTGCACGAGTGGGTTACATCG AACTGGATCTCAACAGCGGTAAGATCCTTGAGAGTTTTCGCCCCGAAGAACGTTTTCCAATGATGA GCACTTTCAAAGTTCTGCTATGTGGCGCGGTATTATCCCGTATTGACGCCGGGCAAGAGCAACTC GGTCGCCGCATACACTATTCTCAGAATGACTTGGTTGAGTACTCACCAGTCACAGAAAAGCATCTT ACGGATGGCATGACAGTAAGAGAATTATGCAGTGCTGCCATAACCATGAGTGATAACACTGCGG CCAACTTACTTCTGACAACTATCGGAGGACCGAAGGAGCTAACCGCTTTTTTGCACAACATGGGG GATCATGTAACTCGCCTTGATCGTTGGGAACCGGAGCTGAATGAAGCCATACCAAACGACGAGCG TGACACCACGATGCCTGTAGCAATGGCAACAACGTTGCGCAAACTATTAACTGGCGAACTACTTA CTCTAGCTTCCCGGCAACAATTAATAGACTGGATGGAGGCGGATAAAGTTGCAGGACCACTTCTG CGCTCGGCCCTTCCGGCTGGCTGGTTTATTGCTGATAAATCTGGAGCCGGTGAGCGTGGGTCTCG CGGTATCATTGCAGCACTGGGGCCAGATGGTAAGCCCTCCCGTATCGTAGTTATCTACACGACGG GGAGTCAGGCAACTATGGATGAACGAAATAGACAGATCGCTGAGATAGGTGCCTCACTGATTAA GCATTGGTAATTCGAAATGACCGACCAAGCGACGCCCAACCGGTATCAGCTCACTCAAAGGCGGT AATACGGTTATCCACAGAATCAGGGGATAACGCAGGAAAGAACATGTGAGCAAAAGGCCAGCAA AAGGCCAGGAACCGTAAAAAGGCCGCGTTGCTGGCGTTTTTCCATAGGCTCCGCCCCCCTGACGA GCATCACAAAAATCGACGCTCAAGTCAGAGGTGGCGAAACCCGACAGGACTATAAAGATACCAG GCGTTTCCCCCTGGAAGCTCCCTCGTGCGCTCTCCTGTTCCGACCCTGCCGCTTACCGGATACCTGT CCGCCTTTCTCCCTTCGGGAAGCGTGGCGCTTTCTCATAGCTCACGCTGTAGGTATCTCAGTTCGG TGTAGGTCGTTCGCTCCAAGCTGGGCTGTGTGCACGAACCCCCCGTTCAGCCCGACCGCTGCGCCT TATCCGGTAACTATCGTCTTGAGTCCAACCCGGTAAGACACGACTTATCGCCACTGGCAGCAGCCA CTGGTAACAGGATTAGCAGAGCGAGGTATGTAGGCGGTGCTACAGAGTTCTTGAAGTGGTGGCC

	TAACTACGGCTACACTAGAAGGACAGTATTTGGTATCTGCGCTCTGCTGAAGCCAGTTACCTTCGG AAAAAGAGTTGGTAGCTCTTGATCCGGCAAACAAACCACCGCTGGTAGCGGTGGTTTTTTTGTTTG CAAGCAGCAGATTACGCGCAGAAAAAAAGGATTTCAAGAAGATCCTTTGATCTTTTCTACGGGGT CTGACGCTCAGTGGAACGAAAACTCACGTTAAGGGATTTTGGTCATGAGATTATCAAAAAGGATC TTCACCTAGATCCTTTTATAGTCCGGAAATACAGGAACGCACGCTGGATGGCCCTTCGCTGGGATG GTGAAACCATGAAAAATGGCAGCTTCAGTGGATTAAGTGGGGGTAATGTGGCCTGTACCCTCTGG TTGCATAGGTATTCATACGGTTAAAATTTATCAGGCGCGATTGCGGCAGTTTTTCGGGTGGTTTGT TGCCATTTTTACCTGTCTGCTGCCGTGATCGCGCTGAACGCGTTTTAGCGGTGCGTACAATTAAGG GATTATGGTAAATCCACTTACTGTCTGCCCTCGTAGCCATCGAGATAAACCGCAGTACTCCGGCCA CGATGCGTCCGGCGTAGAGGATCGAGATCT

II. RIPA buffer recipe

Reagent	Concentration	Brand
Tris, pH 8.0	50mM	Sigma Aldrich
Triton X-100	1% (v/v)	Sigma Aldrich
Sodium Deoxycholate	0.5% (w/v)	Sigma Aldrich
SDS	0.1% (w/v)	BDH
NaCl	150mM	Fisher Chemicals

III. qPCR protocol

qPCR protocol

Rotor type	72-Well Rotor
Reaction volume	20 µl
Phase	**Description**
Hold	Hold at 95°C, 00:03:00
Cycling(40 repeats)	Step 1: Hold at 95°C, 00:00:03 Step 2: Hold at 57°C, 00:00:20 Step 3: Hold at 72°C, 00:00:05, acquiring on Green
Melt	Ramp from 72°C to 95°C per every 1°C Hold for 5s on next steps, acquiring on Green Melt

Figure 1. qPCR protocol. Report created in the Q-Rex (Version 1.1.0.4) software.

IV. SDS-PAGE Recipe used for protein separation

Reagent	**Volume for 10ml**
H_2O	4.6ml
Acrylamide/bis (30%, 0.8%)	2.7ml
Tris–HCl (1.5M, pH 8.8) ….	2.6ml
Ammonium persulfate (10%)	0.1ml
Tetramethylethylenediamine	0.006ml

V. Recipe of T-TBS Buffer (adjusted to pH 7.6)

Reagent	**Concentration**
Tris Base (Sigma Aldrich)	200 mM
NaCl (Fisher Chemicals)	1500

VI. Ponceau staining of membranes with 20µg of protein

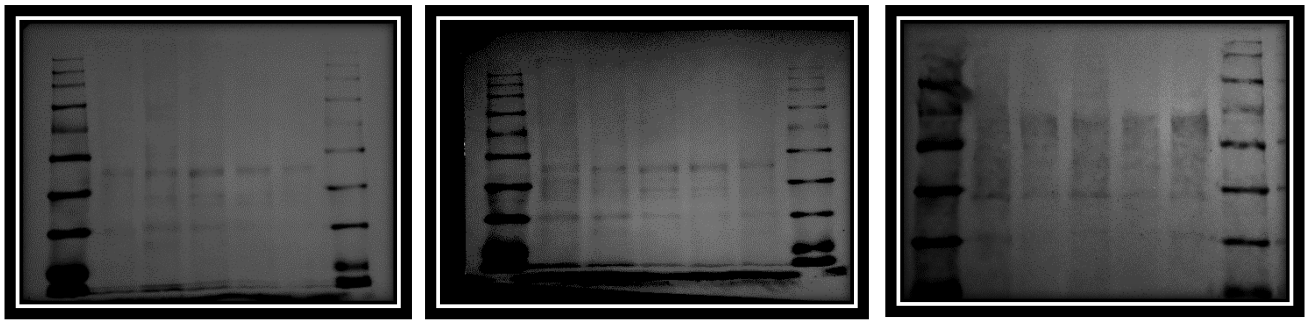

VI.1 Protein staining after protein transference into a membrane. Ponceau staining was made after the transference of proteins in the nitrocellulose membrane. The staining shows similar protein amounts in all the breast cell lines used.

VII. CFTR glycosylated forms

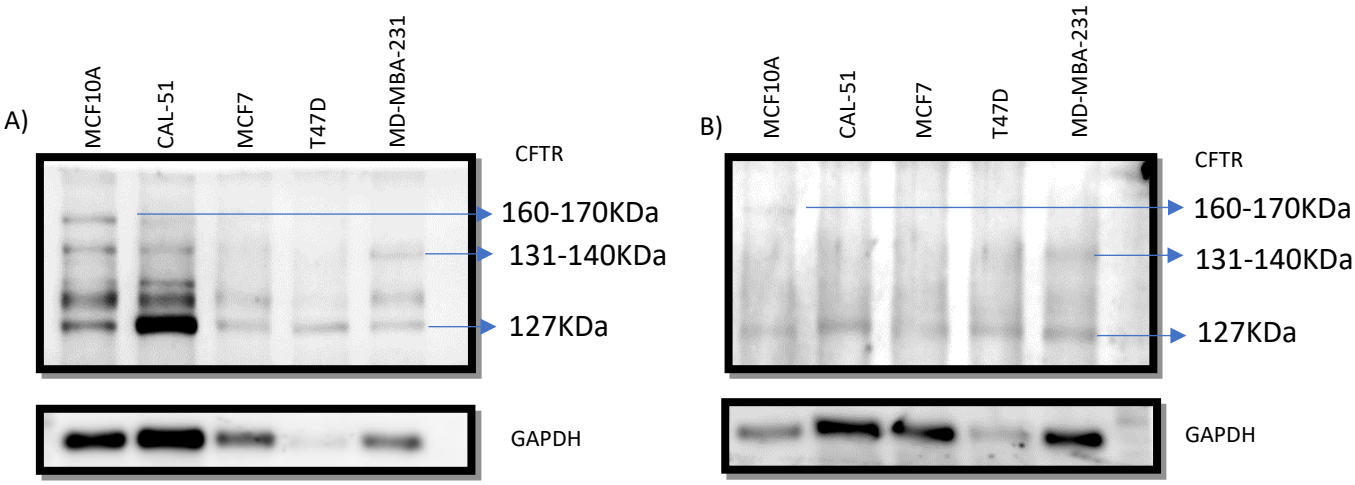

VII. 1. CFTR bands in WB. A) and B) Independent WBs with cell samples from different cell passage number. The Images arrows point out the non-glycosylated CFTR (~127 kDa), core glycosylated CFTR (~131 kDa), and CFTR with complex glycosylation (~160KDa).

VIII. CFTR detection in the cytoplasm and membrane fractions.

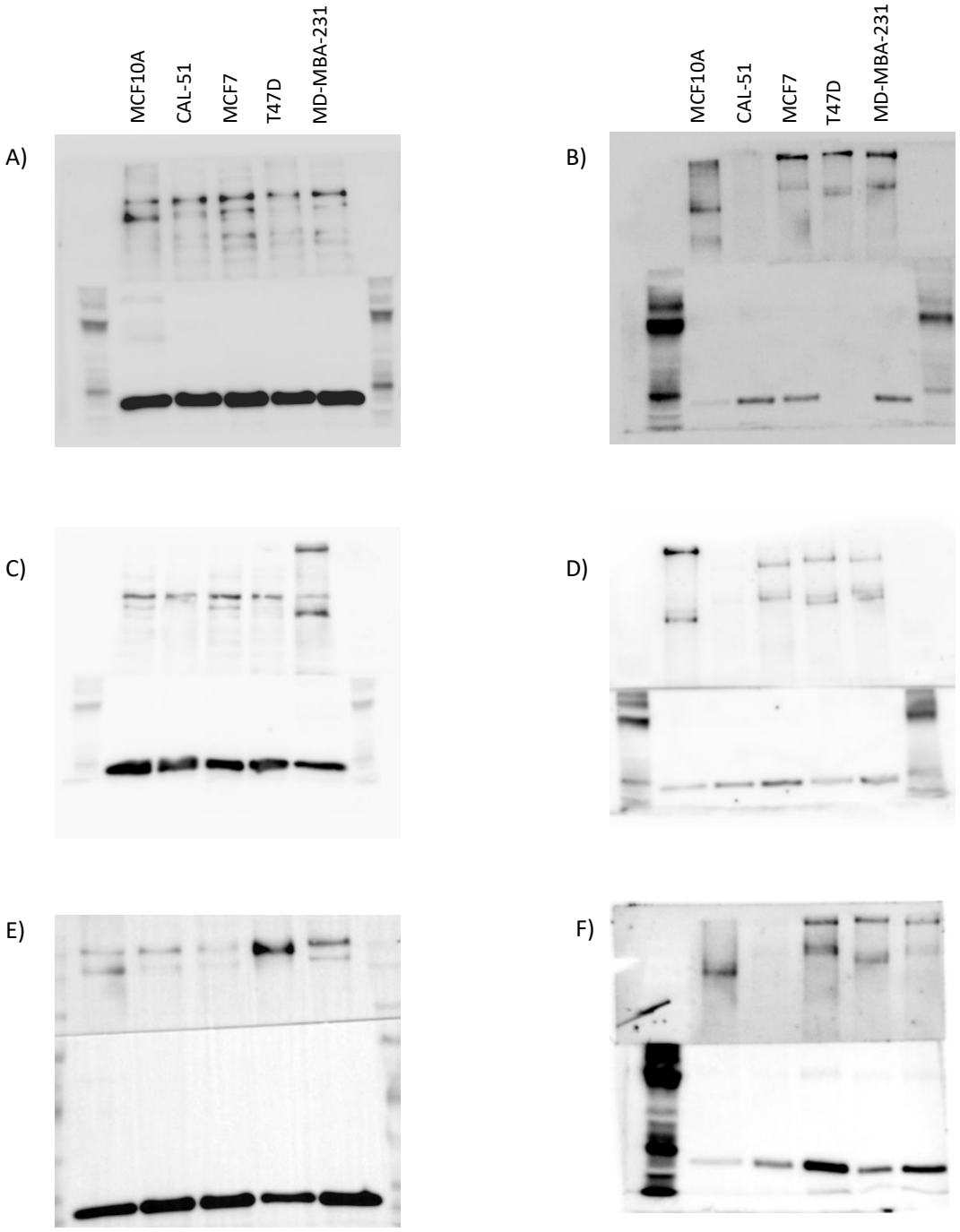

VIII.1. CFTR protein detection in WB. A), C) and E) WBs made with the cytoplasm protein fraction. B), D) and F) WBs made with the membrane protein fraction.

IX. Example of selection of bacteria in agar plates

C- C+ VECTOR

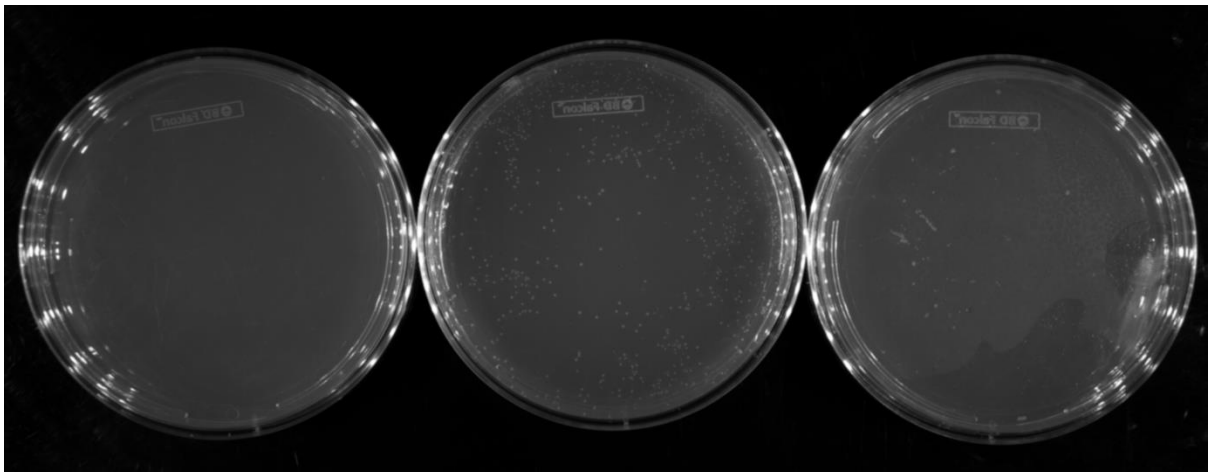

X. Restriction enzyme digestion of the negative control and CFTR vector

A)

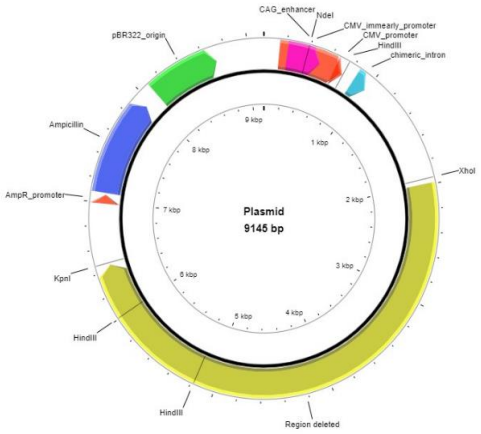

B)

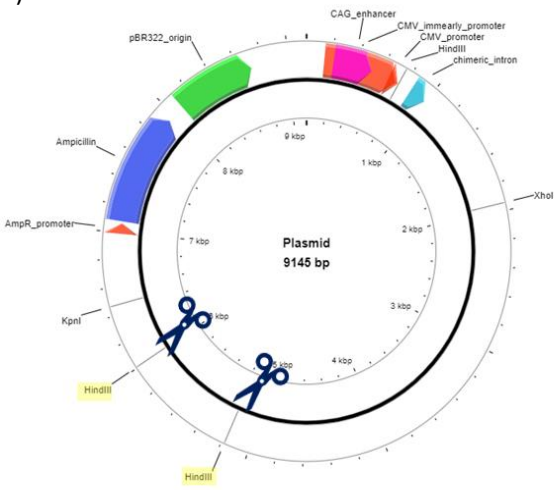

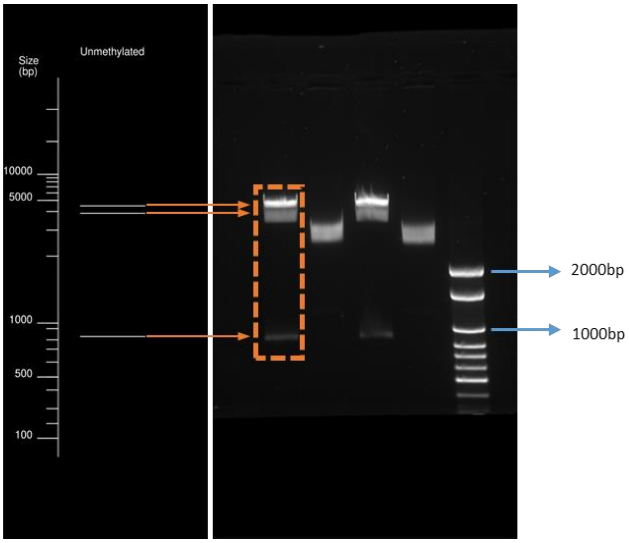

C)

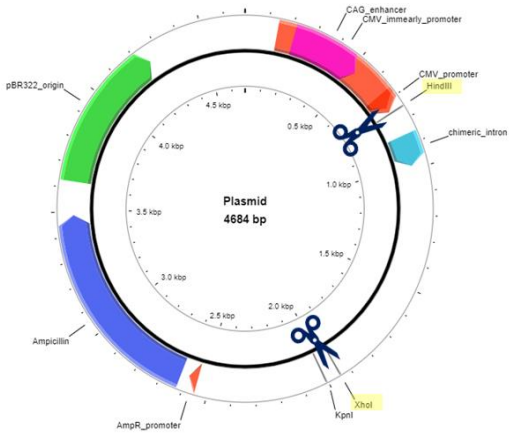

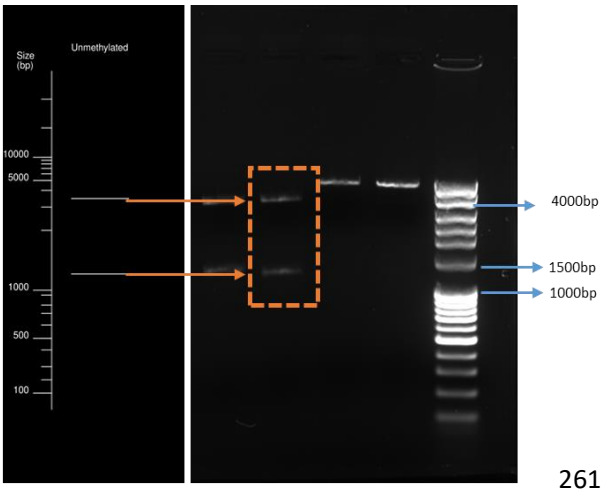

D)

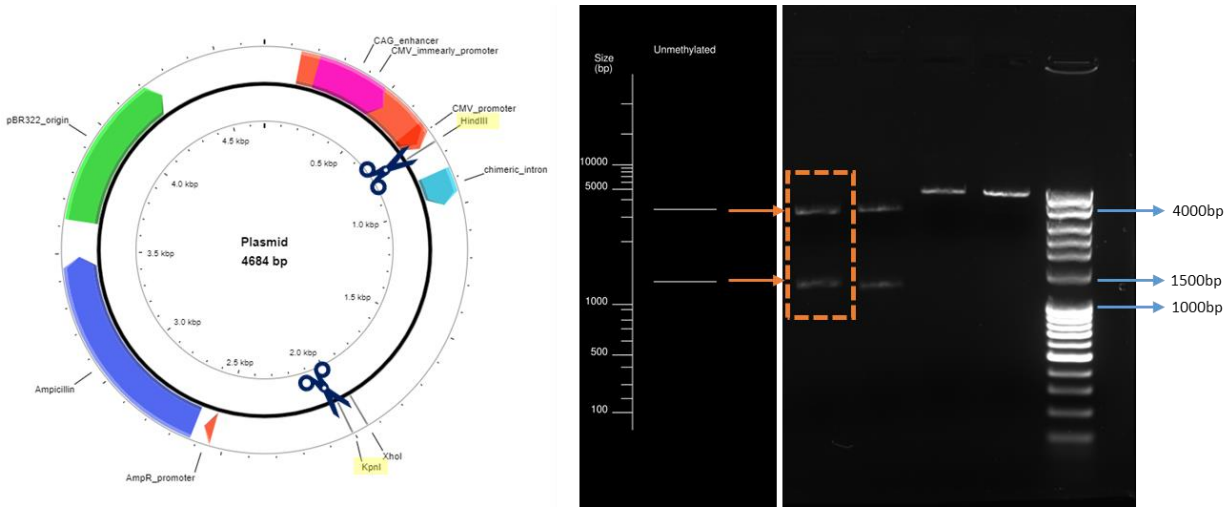

X.1. CFTR and negative control vectors. A) Image illustrating the CFTR vector map and the sequence to be deleted to create the negative control in green. B) The CFTR vector, and C) and D) the negative control vector. In the left part are the vector maps with the restriction sites chosen. On the right side is the in silico and the experimental agarose gel with the DNA plasmid fragments after their restriction digest with the indicated enzymes. The vector maps were created and modified in PlasMapper 3.0. The *in silico* gels were created using NEBcutter program.

XI. Cells reseeded and cultured on semi-permeable membranes

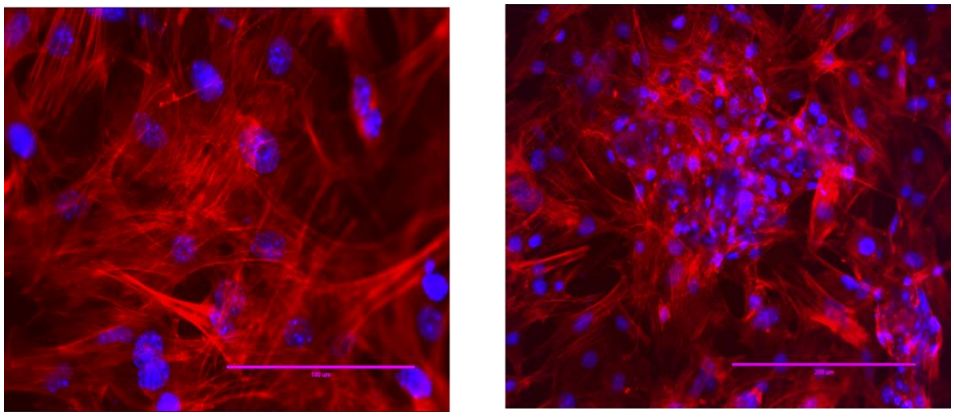

XI.1. Representative images of primary MECs transferred from culture dishes to the semi-permeable membranes (cultured for 4 days). The cell culture on the semi-permeable membranes did not reach 400Ω or over. Cell confluence is observed in A) and B); however, an overlapping of cells is observed, especially in Figure B), which contains a clump of cells. In red are the actin filaments (stained by TRITC-Phalloidin), and in blue are the nuclei. Scale bar= 100µm. Microscope magnification= 20X.

XII. Lentivirus titration in EpH4 cells

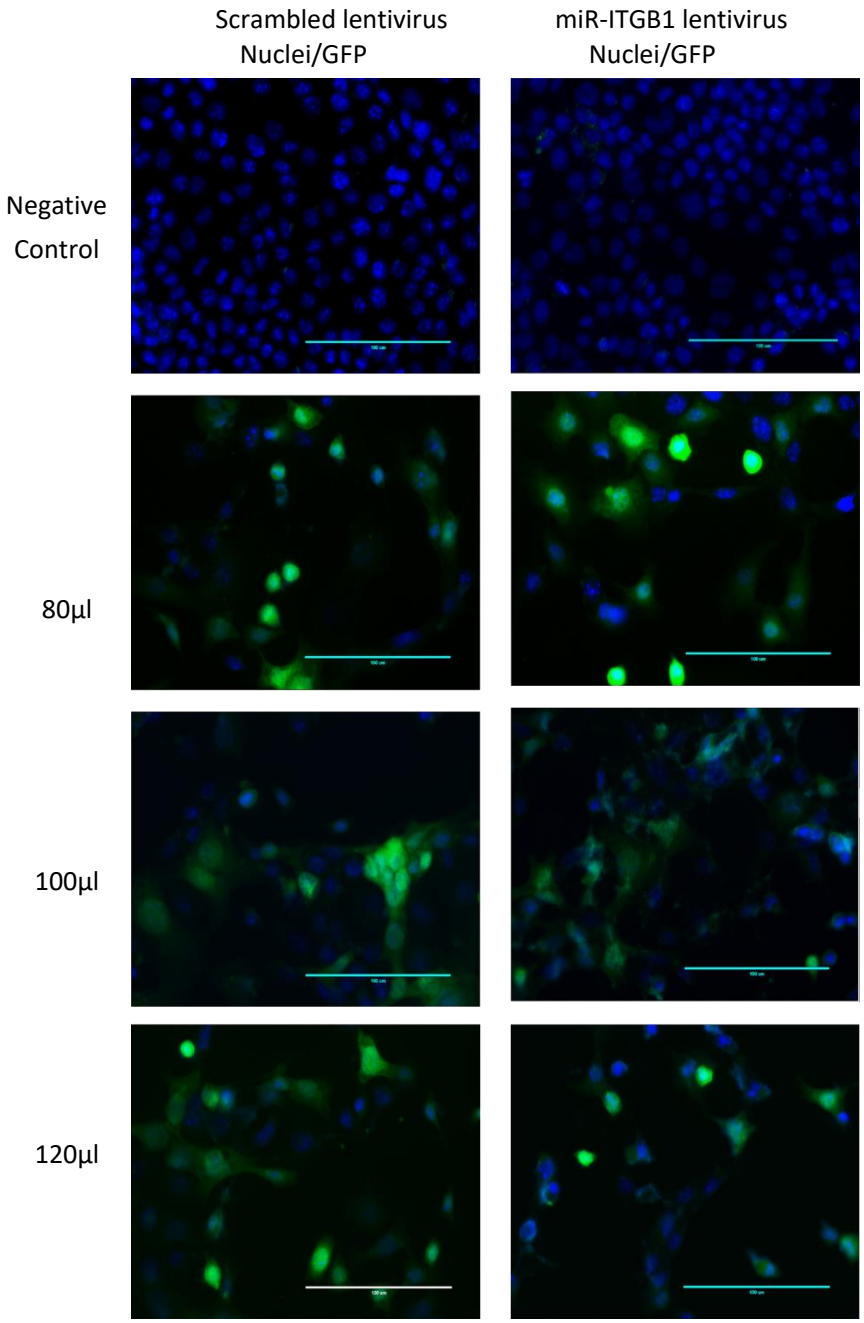

XII. 1 Representative images of higher concentrations (80, 100 and 120 µl) of virus titration in EpH4 cells. Cell density decreases in the coverslips with the highest volume of lentivirus. GFP (green) was expressed by the infected cells, and nuclei (blue) were stained with Hoechst 33258. Scale bar=100µm. Microscope magnification= 20X.

XIII. Example of MECs with and without ZO-1 expression.

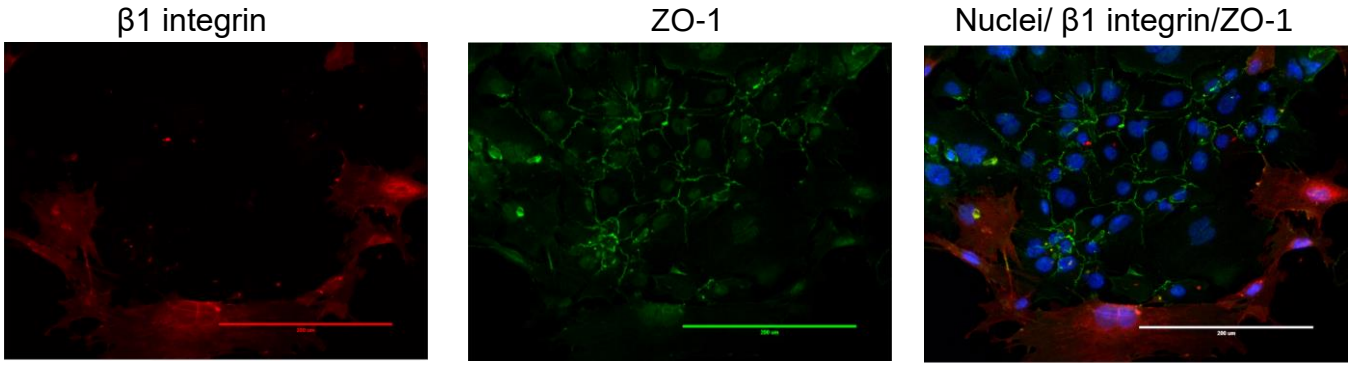

XIII. 1 Example of some primary MECs expressing or not ZO-1 (green). In red is the β1 integrin expression, and in blue the nuclei. Scale bar=200µm. Microscope magnification= 40X.

XIV. Lentivirus infection inferior to 80% in a sample group.

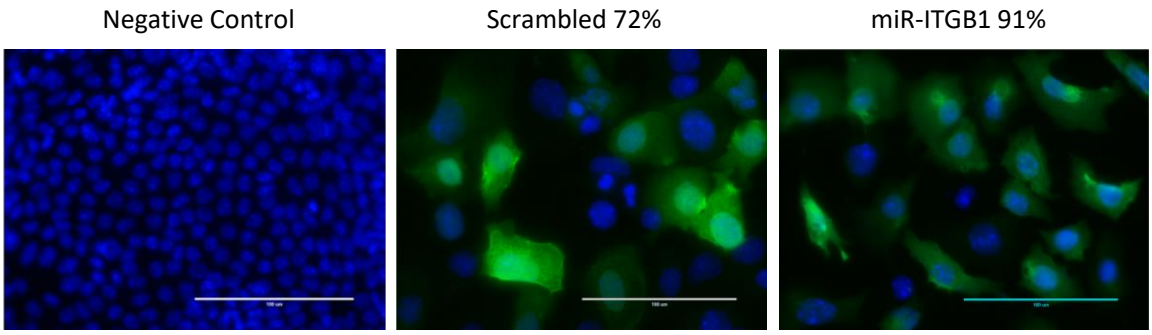

XIV.1 Example of the EpH4 cells infected expressing GFP. Although a previous virus titration was made to calculate the percentage of cells infected, the next experiment after that showed a different result. The group of scrambled lentivirus showed 72% infection and 91% the miR-ITGB1 lentivirus, although the lentivirus volume was previously calculated in the virus titration experiment. Scale bar= 100µm. Microscope magnification= 20X.

XV. License from Figure 1.4.

ELSEVIER LICENSE
TERMS AND CONDITIONS

Feb 20, 2024

This Agreement between University of Sheffield -- Aida Luna ("You") and Elsevier ("Elsevier") consists of your license details and the terms and conditions provided by Elsevier and Copyright Clearance Center.

License Number	5733130328344
License date	Feb 20, 2024
Licensed Content Publisher	Elsevier
Licensed Content Publication	Cell
Licensed Content Title	Integrins Bidirectional, Allosteric Signaling Machines
Licensed Content Author	Richard O. Hynes
Licensed Content Date	Sep 20, 2002

XVI. License from Figure 1.11. A

This is a License Agreement between Aida Luna ("User") and Copyright Clearance Center, Inc. ("CCC") on behalf of the Rightsholder identified in the order details below. The license consists of the order details, the Marketplace Permissions General Terms and Conditions below, and any Rightsholder Terms and Conditions which are included below.

All payments must be made in full to CCC in accordance with the Marketplace Permissions General Terms and Conditions below.

Order Date	19-Feb-2024	**Type of Use**	Republish in a thesis/dissertation
Order License ID	1451764-1	**Publisher**	COMPANY OF BIOLOGISTS,
ISSN	1477-9129	**Portion**	Image/photo/illustration

LICENSED CONTENT

Publication Title	Development	**Publication Type**	e-Journal
Article Title	Single continuous lumen formation in the zebrafish gut is mediated by smoothened-dependent tissue remodeling.	**Start Page**	1110
		End Page	1119
Author/Editor	Company of Biologists.	**Issue**	5
Date	01/01/1987	**Volume**	141
Language	English	**URL**	http://dev.biologists.org/
Country	United Kingdom of Great Britain and Northern Ireland		
Rightsholder	The Company of Biologists Ltd.		

XVII. License from Figure 1.11. B

SPRINGER NATURE LICENSE
TERMS AND CONDITIONS

Feb 19, 2024

This Agreement between University of Sheffield -- Aida Luna ("You") and Springer Nature ("Springer Nature") consists of your license details and the terms and conditions provided by Springer Nature and Copyright Clearance Center.

License Number	5732550899039
License date	Feb 19, 2024
Licensed Content Publisher	Springer Nature
Licensed Content Publication	Nature Cell Biology
Licensed Content Title	Genetic control of single lumen formation in the zebrafish gut
Licensed Content Author	Michel Bagnat et al
Licensed Content Date	Jul 15, 2007

XVIII. License from Figure 1.11. D

Order Date	19-Feb-2024	**Type of Use**	Republish in a thesis/dissertation
Order License ID	1451776-1	**Publisher**	COMPANY OF BIOLOGISTS,
ISSN	1477-9129	**Portion**	Image/photo/illustration

LICENSED CONTENT

Publication Title	Development	**Publication Type**	e-Journal
Article Title	Cftr controls lumen expansion and function of Kupffer's vesicle in zebrafish.	**Start Page**	1703
		End Page	1712
Author/Editor	Company of Biologists.	**Issue**	8
Date	01/01/1987	**Volume**	140
Language	English	**URL**	http://dev.biologists.org/
Country	United Kingdom of Great Britain and Northern Ireland		
Rightsholder	The Company of Biologists Ltd.		

XIX. License from Figure 1.12.

LICENSED CONTENT

Publication Title	Gene therapy	**Publication Type**	e-journal
Article Title	Splicing mutations in the CFTR gene as therapeutic targets	**Start Page**	399
		End Page	406
Date	01/01/1997	**Issue**	7-8
Language	English	**Volume**	29
Country	United Kingdom of Great Britain and Northern Ireland	**URL**	http://www.nature.com/gt/
Rightsholder	Springer Nature BV		

REQUEST DETAILS

Portion Type	Image/photo/illustration	**Distribution**	Worldwide
Number of Images / Photos / Illustrations	1	**Translation**	Original language of publication
Format (select all that apply)	Electronic	**Copies for the Disabled?**	No
		Minor Editing Privileges?	No
Who Will Republish the Content?	Academic institution	**Incidental Promotional Use?**	No
		Currency	GBP
Duration of Use	Life of current and all future editions		
Lifetime Unit Quantity	Up to 499		
Rights Requested	Main product		

NEW WORK DETAILS

marketplace.copyright.com/rs-ui-web/manage_account/orders/view-search/1500814

, 9:10 Manage Account

Title	THESIS	**Institution Name**	UNIVERSITY OF SHEFFIELD
Instructor Name	MARK FENWICK	**Expected Presentation Date**	2024-07-23

ADDITIONAL DETAILS

The Requesting Person / Organization to Appear on the License	AIDA AIDE LUNA PEREZ

REQUESTED CONTENT DETAILS

Title, Description or Numeric Reference of the Portion(s)	Figure 1 of the "Splicing mutations in the CFTR gene as therapeutic targets" paper	**Title of the Article / Chapter the Portion Is From**	Splicing mutations in the CFTR gene as therapeutic targets
Editor of Portion(s)	Deletang, Karine; Taulan-Cadars, Magali	**Author of Portion(s)**	Deletang, Karine; Taulan-Cadars, Magali
Volume / Edition	29	**Publication Date of Portion**	2022-08-01
Page or Page Range of Portion	399-406		

XX. License from Figure 1.13.

JOHN WILEY AND SONS LICENSE
TERMS AND CONDITIONS

Feb 19, 2024

This Agreement between University of Sheffield -- Aida Luna ("You") and John Wiley and Sons ("John Wiley and Sons") consists of your license details and the terms and conditions provided by John Wiley and Sons and Copyright Clearance Center.

License Number	5732531041265
License date	Feb 19, 2024
Licensed Content Publisher	John Wiley and Sons
Licensed Content Publication	Cell Biology International
Licensed Content Title	Promoter hypermethylation of the CFTR gene as a novel diagnostic and prognostic marker of breast cancer
Licensed Content Author	Chang Zou, Wenbin Zhou, Jianhong Wang, et al
Licensed Content Date	Dec 10, 2019

REFERENCES

Akhtar, N. and C. H. Streuli (2013). "An integrin-ILK-microtubule network orients cell polarity and lumen formation in glandular epithelium." Nat Cell Biol **15**(1): 17-27.

Alcorn, D., T. M. Adamson, T. F. Lambert, J. E. Maloney, B. C. Ritchie and P. M. Robinson (1977). "Morphological effects of chronic tracheal ligation and drainage in the fetal lamb lung." J Anat **123**(Pt 3): 649-660.

Almassy, J., E. Siguenza, M. Skaliczki, K. Matesz, J. Sneyd, D. I. Yule and P. P. Nanasi (2018). "New saliva secretion model based on the expression of Na(+)-K(+) pump and K(+) channels in the apical membrane of parotid acinar cells." Pflugers Arch **470**(4): 613-621.

Alvers, A. L., S. Ryan, P. J. Scherz, J. Huisken and M. Bagnat (2014). "Single continuous lumen formation in the zebrafish gut is mediated by smoothened-dependent tissue remodeling." Development **141**(5): 1110-1119.

Amaral, M. D., D. M. Hutt, V. Tomati, H. M. Botelho and N. Pedemonte (2020). "CFTR processing, trafficking and interactions." J Cyst Fibros **19 Suppl 1**: S33-S36.

Ameen, N., M. Silvis and N. A. Bradbury (2007). "Endocytic trafficking of CFTR in health and disease." J Cyst Fibros **6**(1): 1-14.

Anderson, J. M. and C. M. Van Itallie (2009). "Physiology and function of the tight junction." Cold Spring Harb Perspect Biol **1**(2): a002584.

Anderson, M. P., H. A. Berger, D. P. Rich, R. J. Gregory, A. E. Smith and M. J. Welsh (1991). "Nucleoside triphosphates are required to open the CFTR chloride channel." Cell **67**(4): 775-784.

Andrew, D. J. and A. J. Ewald (2010). "Morphogenesis of epithelial tubes: Insights into tube formation, elongation, and elaboration." Dev Biol **341**(1): 34-55.

Archangelidi, O., P. Cullinan, N. J. Simmonds, E. Mentzakis, D. Peckham, D. Bilton and S. B. Carr (2022). "Incidence and risk factors of cancer in individuals with cystic fibrosis in the UK; a case-control study." J Cyst Fibros **21**(2): 302-308.

Aszodi, A., E. B. Hunziker, C. Brakebusch and R. Fassler (2003). "Beta1 integrins regulate chondrocyte rotation, G1 progression, and cytokinesis." Genes Dev **17**(19): 2465-2479.

Atashgaran, V., J. Wrin, S. C. Barry, P. Dasari and W. V. Ingman (2016). "Dissecting the Biology of Menstrual Cycle-Associated Breast Cancer Risk." Front Oncol **6**: 267.

Baena-Lopez, L. A., A. Baonza and A. Garcia-Bellido (2005). "The orientation of cell divisions determines the shape of Drosophila organs." Curr Biol **15**(18): 1640-1644.

Bagnat, M., I. D. Cheung, K. E. Mostov and D. Y. Stainier (2007). "Genetic control of single lumen formation in the zebrafish gut." Nat Cell Biol **9**(8): 954-960.

Bagnat, M., A. Navis, S. Herbstreith, K. Brand-Arzamendi, S. Curado, S. Gabriel, K. Mostov, J. Huisken and D. Y. Stainier (2010). "Cse1l is a negative regulator of CFTR-dependent fluid secretion." Curr Biol **20**(20): 1840-1845.

Balda, M. S. and K. Matter (2000). "The tight junction protein ZO-1 and an interacting transcription factor regulate ErbB-2 expression." EMBO J **19**(9): 2024-2033.

Barwe, S. P., A. Skay, R. McSpadden, T. P. Huynh, S. A. Langhans, L. J. Inge and A. K. Rajasekaran (2012). "Na,K-ATPase beta-subunit cis homo-oligomerization is necessary for epithelial lumen formation in mammalian cells." J Cell Sci **125**(Pt 23): 5711-5720.

Belvindrah, R., D. Graus-Porta, S. Goebbels, K. A. Nave and U. Muller (2007). "Beta1 integrins in radial glia but not in migrating neurons are essential for the formation of cell layers in the cerebral cortex." J Neurosci **27**(50): 13854-13865.

Berger, H. A., S. M. Travis and M. J. Welsh (1993). "Regulation of the cystic fibrosis transmembrane conductance regulator Cl- channel by specific protein kinases and protein phosphatases." J Biol Chem **268**(3): 2037-2047.
Bergstralh, D. T., N. S. Dawney and D. St Johnston (2017). "Spindle orientation: a question of complex positioning." Development **144**(7): 1137-1145.
Bertrand, C. A. and R. A. Frizzell (2003). "The role of regulated CFTR trafficking in epithelial secretion." Am J Physiol Cell Physiol **285**(1): C1-18.
Bidaud-Meynard, A., F. Bossard, A. Schnur, R. Fukuda, G. Veit, H. Xu and G. L. Lukacs (2019). "Transcytosis maintains CFTR apical polarity in the face of constitutive and mutation-induced basolateral missorting." J Cell Sci **132**(10).
Biswas, S. K., S. Banerjee, G. W. Baker, C. Y. Kuo and I. Chowdhury (2022). "The Mammary Gland: Basic Structure and Molecular Signaling during Development." Int J Mol Sci **23**(7).
Blasky, A. J., A. Mangan and R. Prekeris (2015). "Polarized protein transport and lumen formation during epithelial tissue morphogenesis." Annu Rev Cell Dev Biol **31**: 575-591.
Blaug, S., K. Hybiske, J. Cohn, G. L. Firestone, T. E. Machen and S. S. Miller (2001). "ENaC- and CFTR-dependent ion and fluid transport in mammary epithelia." Am J Physiol Cell Physiol **281**(2): C633-648.
Bocchinfuso, W. P., J. K. Lindzey, S. C. Hewitt, J. A. Clark, P. H. Myers, R. Cooper and K. S. Korach (2000). "Induction of mammary gland development in estrogen receptor-alpha knockout mice." Endocrinology **141**(8): 2982-2994.
Bonvin, E., P. Le Rouzic, J. F. Bernaudin, C. H. Cottart, C. Vandebrouck, A. Crie, T. Leal, A. Clement and M. Bonora (2008). "Congenital tracheal malformation in cystic fibrosis transmembrane conductance regulator-deficient mice." J Physiol **586**(13): 3231-3243.
Borthwick, L. A., P. Botha, B. Verdon, M. J. Brodlie, A. Gardner, D. Bourn, G. E. Johnson, M. A. Gray and A. J. Fisher (2011). "Is CFTR-delF508 really absent from the apical membrane of the airway epithelium?" PLoS One **6**(8): e23226.
Bradbury, N. A., J. A. Clark, S. C. Watkins, C. C. Widnell, H. S. t. Smith and R. J. Bridges (1999). "Characterization of the internalization pathways for the cystic fibrosis transmembrane conductance regulator." Am J Physiol **276**(4): L659-668.
Bradbury, N. A., J. A. Cohn, C. J. Venglarik and R. J. Bridges (1994). "Biochemical and biophysical identification of cystic fibrosis transmembrane conductance regulator chloride channels as components of endocytic clathrin-coated vesicles." J Biol Chem **269**(11): 8296-8302.
Brakebusch, C., R. Grose, F. Quondamatteo, A. Ramirez, J. L. Jorcano, A. Pirro, M. Svensson, R. Herken, T. Sasaki, R. Timpl, S. Werner and R. Fassler (2000). "Skin and hair follicle integrity is crucially dependent on beta 1 integrin expression on keratinocytes." EMBO J **19**(15): 3990-4003.
Braten, O., I. Livneh, T. Ziv, A. Admon, I. Kehat, L. H. Caspi, H. Gonen, B. Bercovich, A. Godzik, S. Jahandideh, L. Jaroszewski, T. Sommer, Y. T. Kwon, M. Guharoy, P. Tompa and A. Ciechanover (2016). "Numerous proteins with unique characteristics are degraded by the 26S proteasome following monoubiquitination." Proc Natl Acad Sci U S A **113**(32): E4639-4647.
Brisken, C., S. Park, T. Vass, J. P. Lydon, B. W. O'Malley and R. A. Weinberg (1998). "A paracrine role for the epithelial progesterone receptor in mammary gland development." Proc Natl Acad Sci U S A **95**(9): 5076-5081.
Broackes-Carter, F. C., N. Mouchel, D. Gill, S. Hyde, J. Bassett and A. Harris (2002). "Temporal regulation of CFTR expression during ovine lung development: implications for CF gene therapy." Hum Mol Genet **11**(2): 125-131.

Bryant, D. M., A. Datta, A. E. Rodriguez-Fraticelli, J. Peranen, F. Martin-Belmonte and K. E. Mostov (2010). "A molecular network for de novo generation of the apical surface and lumen." Nat Cell Biol **12**(11): 1035-1045.
Bryant, D. M. and K. E. Mostov (2008). "From cells to organs: building polarized tissue." Nat Rev Mol Cell Biol **9**(11): 887-901.
Bryant, D. M., J. Roignot, A. Datta, A. W. Overeem, M. Kim, W. Yu, X. Peng, D. J. Eastburn, A. J. Ewald, Z. Werb and K. E. Mostov (2014). "A molecular switch for the orientation of epithelial cell polarization." Dev Cell **31**(2): 171-187.
Bui, T., J. Rennhack, S. Mok, C. Ling, M. Perez, J. Roccamo, E. R. Andrechek, C. Moraes and W. J. Muller (2019). "Functional Redundancy between beta1 and beta3 Integrin in Activating the IR/Akt/mTORC1 Signaling Axis to Promote ErbB2-Driven Breast Cancer." Cell Rep **29**(3): 589-602 e586.
Burstein, H. J., K. Polyak, J. S. Wong, S. C. Lester and C. M. Kaelin (2004). "Ductal carcinoma in situ of the breast." N Engl J Med **350**(14): 1430-1441.
Butt, M. H., M. Zaman, A. Ahmad, R. Khan, T. H. Mallhi, M. M. Hasan, Y. H. Khan, S. Hafeez, E. E. S. Massoud, M. H. Rahman and S. Cavalu (2022). "Appraisal for the Potential of Viral and Nonviral Vectors in Gene Therapy: A Review." Genes (Basel) **13**(8).
Byron, A., J. D. Humphries and M. J. Humphries (2013). "Defining the extracellular matrix using proteomics." Int J Exp Pathol **94**(2): 75-92.
Cabrita, I., A. Kraus, J. K. Scholz, K. Skoczynski, R. Schreiber, K. Kunzelmann and B. Buchholz (2020). "Cyst growth in ADPKD is prevented by pharmacological and genetic inhibition of TMEM16A in vivo." Nat Commun **11**(1): 4320.
Caci, E., A. Caputo, A. Hinzpeter, N. Arous, P. Fanen, N. Sonawane, A. S. Verkman, R. Ravazzolo, O. Zegarra-Moran and L. J. Galietta (2008). "Evidence for direct CFTR inhibition by CFTR(inh)-172 based on Arg347 mutagenesis." Biochem J **413**(1): 135-142.
Camerino, D. C., D. Tricarico and J. F. Desaphy (2007). "Ion channel pharmacology." Neurotherapeutics **4**(2): 184-198.
Campbell, J. J. and C. J. Watson (2009). "Three-dimensional culture models of mammary gland." Organogenesis **5**(2): 43-49.
Cao, F., X. Xie, T. Gollan, L. Zhao, K. Narsinh, R. J. Lee and J. C. Wu (2010). "Comparison of gene-transfer efficiency in human embryonic stem cells." Mol Imaging Biol **12**(1): 15-24.
Chatterjee, S. J. and L. McCaffrey (2014). "Emerging role of cell polarity proteins in breast cancer progression and metastasis." Breast Cancer (Dove Med Press) **6**: 15-27.
Chen, W., W. Wei, L. Yu, Z. Ye, F. Huang, L. Zhang, S. Hu and C. Cai (2021). "Mammary Development and Breast Cancer: a Notch Perspective." J Mammary Gland Biol Neoplasia **26**(3): 309-320.
Cheng, S. H., D. P. Rich, J. Marshall, R. J. Gregory, M. J. Welsh and A. E. Smith (1991). "Phosphorylation of the R domain by cAMP-dependent protein kinase regulates the CFTR chloride channel." Cell **66**(5): 1027-1036.
Clevers, H. (2016). "Modeling Development and Disease with Organoids." Cell **165**(7): 1586-1597.
Cohen, J. C. and J. E. Larson (2006). "Cystic fibrosis transmembrane conductance regulator (CFTR) dependent cytoskeletal tension during lung organogenesis." Dev Dyn **235**(10): 2736-2748.
Contreras, R. G., L. Shoshani, C. Flores-Maldonado, A. Lazaro and M. Cereijido (1999). "Relationship between Na(+),K(+)-ATPase and cell attachment." J Cell Sci **112 (Pt 23)**: 4223-4232.
Daly, J. W. (1984). "Forskolin, adenylate cyclase, and cell physiology: an overview." Adv Cyclic Nucleotide Protein Phosphorylation Res **17**: 81-89.

Datta, A., D. M. Bryant and K. E. Mostov (2011). "Molecular regulation of lumen morphogenesis." Curr Biol **21**(3): R126-136.
Debnath, J., K. R. Mills, N. L. Collins, M. J. Reginato, S. K. Muthuswamy and J. S. Brugge (2002). "The role of apoptosis in creating and maintaining luminal space within normal and oncogene-expressing mammary acini." Cell **111**(1): 29-40.
Debnath, J., S. K. Muthuswamy and J. S. Brugge (2003). "Morphogenesis and oncogenesis of MCF-10A mammary epithelial acini grown in three-dimensional basement membrane cultures." Methods **30**(3): 256-268.
Dekkers, J. F., C. L. Wiegerinck, H. R. de Jonge, I. Bronsveld, H. M. Janssens, K. M. de Winter-de Groot, A. M. Brandsma, N. W. de Jong, M. J. Bijvelds, B. J. Scholte, E. E. Nieuwenhuis, S. van den Brink, H. Clevers, C. K. van der Ent, S. Middendorp and J. M. Beekman (2013). "A functional CFTR assay using primary cystic fibrosis intestinal organoids." Nat Med **19**(7): 939-945.
Deletang, K. and M. Taulan-Cadars (2022). "Splicing mutations in the CFTR gene as therapeutic targets." Gene Ther **29**(7-8): 399-406.
Dimova, N. V., N. A. Hathaway, B. H. Lee, D. S. Kirkpatrick, M. L. Berkowitz, S. P. Gygi, D. Finley and R. W. King (2012). "APC/C-mediated multiple monoubiquitylation provides an alternative degradation signal for cyclin B1." Nat Cell Biol **14**(2): 168-176.
Du, K., M. Sharma and G. L. Lukacs (2005). "The DeltaF508 cystic fibrosis mutation impairs domain-domain interactions and arrests post-translational folding of CFTR." Nat Struct Mol Biol **12**(1): 17-25.
Durgan, J., N. Kaji, D. Jin and A. Hall (2011). "Par6B and atypical PKC regulate mitotic spindle orientation during epithelial morphogenesis." J Biol Chem **286**(14): 12461-12474.
Elias, B. C., S. Mathew, M. B. Srichai, R. Palamuttam, N. Bulus, G. Mernaugh, A. B. Singh, C. R. Sanders, R. C. Harris, A. Pozzi and R. Zent (2014). "The integrin beta1 subunit regulates paracellular permeability of kidney proximal tubule cells." J Biol Chem **289**(12): 8532-8544.
Evans, R. L., K. Park, R. J. Turner, G. E. Watson, H. V. Nguyen, M. R. Dennett, A. R. Hand, M. Flagella, G. E. Shull and J. E. Melvin (2000). "Severe impairment of salivation in Na+/K+/2Cl- cotransporter (NKCC1)-deficient mice." J Biol Chem **275**(35): 26720-26726.
Fanning, A. S., C. M. Van Itallie and J. M. Anderson (2012). "Zonula occludens-1 and -2 regulate apical cell structure and the zonula adherens cytoskeleton in polarized epithelia." Mol Biol Cell **23**(4): 577-590.
Farquhar, M. G. and G. E. Palade (1963). "Junctional complexes in various epithelia." J Cell Biol **17**(2): 375-412.
Farrell, P. M., B. J. Rosenstein, T. B. White, F. J. Accurso, C. Castellani, G. R. Cutting, P. R. Durie, V. A. Legrys, J. Massie, R. B. Parad, M. J. Rock, P. W. Campbell, 3rd and F. Cystic Fibrosis (2008). "Guidelines for diagnosis of cystic fibrosis in newborns through older adults: Cystic Fibrosis Foundation consensus report." J Pediatr **153**(2): S4-S14.
Fassler, R. and M. Meyer (1995). "Consequences of lack of beta 1 integrin gene expression in mice." Genes Dev **9**(15): 1896-1908.
Fernandez-Minan, A., M. D. Martin-Bermudo and A. Gonzalez-Reyes (2007). "Integrin signaling regulates spindle orientation in Drosophila to preserve the follicular-epithelium monolayer." Curr Biol **17**(8): 683-688.
Filipowicz, W., L. Jaskiewicz, F. A. Kolb and R. S. Pillai (2005). "Post-transcriptional gene silencing by siRNAs and miRNAs." Curr Opin Struct Biol **15**(3): 331-341.
Fire, A., S. Xu, M. K. Montgomery, S. A. Kostas, S. E. Driver and C. C. Mello (1998). "Potent and specific genetic interference by double-stranded RNA in Caenorhabditis elegans." Nature **391**(6669): 806-811.

Folkesson, H. G., M. A. Matthay, H. Hasegawa, F. Kheradmand and A. S. Verkman (1994). "Transcellular water transport in lung alveolar epithelium through mercury-sensitive water channels." Proc Natl Acad Sci U S A **91**(11): 4970-4974.
Foskett, J. K. (1990). "[Ca2+]i modulation of Cl- content controls cell volume in single salivary acinar cells during fluid secretion." Am J Physiol **259**(6 Pt 1): C998-1004.
Frizzell, R. A. and J. W. Hanrahan (2012). "Physiology of epithelial chloride and fluid secretion." Cold Spring Harb Perspect Med **2**(6): a009563.
Fus-Kujawa, A., P. Prus, K. Bajdak-Rusinek, P. Teper, K. Gawron, A. Kowalczuk and A. L. Sieron (2021). "An Overview of Methods and Tools for Transfection of Eukaryotic Cells in vitro." Front Bioeng Biotechnol **9**: 701031.
Gao, L., Z. Yang, C. Hiremath, S. E. Zimmerman, B. Long, P. R. Brakeman, K. E. Mostov, D. M. Bryant, K. Luby-Phelps and D. K. Marciano (2017). "Afadin orients cell division to position the tubule lumen in developing renal tubules." Development **144**(19): 3511-3520.
Garcia, F. U., L. M. Galindo and D. S. Holsclaw, Jr. (1998). "Breast abnormalities in patients with cystic fibrosis: previously unrecognized changes." Ann Diagn Pathol **2**(5): 281-285.
Grant, B. D. and J. G. Donaldson (2009). "Pathways and mechanisms of endocytic recycling." Nat Rev Mol Cell Biol **10**(9): 597-608.
Gregory, R. J., S. H. Cheng, D. P. Rich, J. Marshall, S. Paul, K. Hehir, L. Ostedgaard, K. W. Klinger, M. J. Welsh and A. E. Smith (1990). "Expression and characterization of the cystic fibrosis transmembrane conductance regulator." Nature **347**(6291): 382-386.
Gresch, O. and L. Altrogge (2012). "Transfection of difficult-to-transfect primary mammalian cells." Methods Mol Biol **801**: 65-74.
Grobstein, C. (1967). "Mechanisms of organogenetic tissue interaction." Natl Cancer Inst Monogr **26**: 279-299.
Gudjonsson, T., M. C. Adriance, M. D. Sternlicht, O. W. Petersen and M. J. Bissell (2005). "Myoepithelial cells: their origin and function in breast morphogenesis and neoplasia." J Mammary Gland Biol Neoplasia **10**(3): 261-272.
Gumbiner, B., B. Stevenson and A. Grimaldi (1988). "The role of the cell adhesion molecule uvomorulin in the formation and maintenance of the epithelial junctional complex." J Cell Biol **107**(4): 1575-1587.
Guo, J., A. Garratt and A. Hill (2022). "Worldwide rates of diagnosis and effective treatment for cystic fibrosis." J Cyst Fibros **21**(3): 456-462.
Halaoui, R. and L. McCaffrey (2015). "Rewiring cell polarity signaling in cancer." Oncogene **34**(8): 939-950.
Halaoui, R., C. Rejon, S. J. Chatterjee, J. Szymborski, S. Meterissian, W. J. Muller, A. Omeroglu and L. McCaffrey (2017). "Progressive polarity loss and luminal collapse disrupt tissue organization in carcinoma." Genes Dev **31**(15): 1573-1587.
Harris, A. and B. E. Argent (1993). "The cystic fibrosis gene and its product CFTR." Semin Cell Biol **4**(1): 37-44.
Hartsock, A. and W. J. Nelson (2008). "Adherens and tight junctions: structure, function and connections to the actin cytoskeleton." Biochim Biophys Acta **1778**(3): 660-669.
Hasler, U., X. Wang, G. Crambert, P. Beguin, F. Jaisser, J. D. Horisberger and K. Geering (1998). "Role of beta-subunit domains in the assembly, stable expression, intracellular routing, and functional properties of Na,K-ATPase." J Biol Chem **273**(46): 30826-30835.
Haws, C. M., I. B. Nepomuceno, M. E. Krouse, H. Wakelee, T. Law, Y. Xia, H. Nguyen and J. J. Wine (1996). "Delta F508-CFTR channels: kinetics, activation by forskolin, and potentiation by xanthines." Am J Physiol **270**(5 Pt 1): C1544-1555.
Hogan, B. L. and P. A. Kolodziej (2002). "Organogenesis: molecular mechanisms of tubulogenesis." Nat Rev Genet **3**(7): 513-523.

Hogg, N. A., C. J. Harrison and C. Tickle (1983). "Lumen formation in the developing mouse mammary gland." J Embryol Exp Morphol **73**: 39-57.
Hoover, K. B., S. Y. Liao and P. J. Bryant (1998). "Loss of the tight junction MAGUK ZO-1 in breast cancer: relationship to glandular differentiation and loss of heterozygosity." Am J Pathol **153**(6): 1767-1773.
Horikoshi, Y., A. Suzuki, T. Yamanaka, K. Sasaki, K. Mizuno, H. Sawada, S. Yonemura and S. Ohno (2009). "Interaction between PAR-3 and the aPKC-PAR-6 complex is indispensable for apical domain development of epithelial cells." J Cell Sci **122**(Pt 10): 1595-1606.
Horseman, N. D. (1999). "Prolactin and mammary gland development." J Mammary Gland Biol Neoplasia **4**(1): 79-88.
Hu, B., L. Zhong, Y. Weng, L. Peng, Y. Huang, Y. Zhao and X. J. Liang (2020). "Therapeutic siRNA: state of the art." Signal Transduct Target Ther **5**(1): 101.
Huang, E. N., H. Quach, J. A. Lee, J. Dierolf, T. J. Moraes and A. P. Wong (2021). "A Developmental Role of the Cystic Fibrosis Transmembrane Conductance Regulator in Cystic Fibrosis Lung Disease Pathogenesis." Front Cell Dev Biol **9**: 742891.
Hug, M. J., T. Tamada and R. J. Bridges (2003). "CFTR and bicarbonate secretion by [correction of to] epithelial cells." News Physiol Sci **18**: 38-42.
Hynes, R. O. (1999). "Cell adhesion: old and new questions." Trends Cell Biol **9**(12): M33-37.
Hynes, R. O. (2002). "Integrins: bidirectional, allosteric signaling machines." Cell **110**(6): 673-687.
Ingthorsson, S., E. Briem, J. T. Bergthorsson and T. Gudjonsson (2016). "Epithelial Plasticity During Human Breast Morphogenesis and Cancer Progression." J Mammary Gland Biol Neoplasia **21**(3-4): 139-148.
Iruela-Arispe, M. L. and G. J. Beitel (2013). "Tubulogenesis." Development **140**(14): 2851-2855.
Jacquot, J., E. Puchelle, J. Hinnrasky, C. Fuchey, C. Bettinger, C. Spilmont, N. Bonnet, A. Dieterle, D. Dreyer, A. Pavirani and et al. (1993). "Localization of the cystic fibrosis transmembrane conductance regulator in airway secretory glands." Eur Respir J **6**(2): 169-176.
Jaffe, A. B., N. Kaji, J. Durgan and A. Hall (2008). "Cdc42 controls spindle orientation to position the apical surface during epithelial morphogenesis." J Cell Biol **183**(4): 625-633.
Javed, A. and A. Lteif (2013). "Development of the human breast." Semin Plast Surg **27**(1): 5-12.
Jewett, C. E. and R. Prekeris (2018). "Insane in the apical membrane: Trafficking events mediating apicobasal epithelial polarity during tube morphogenesis." Traffic.
Jones, J. L., D. R. Critchley and R. A. Walker (1992). "Alteration of stromal protein and integrin expression in breast--a marker of premalignant change?" J Pathol **167**(4): 399-406.
Jorgensen, P. L. (1983). "Conformational changes in the alpha-subunit, and cation transport by Na+, K+-ATPase." Ciba Found Symp **95**: 253-272.
Katz, E. and C. H. Streuli (2007). "The extracellular matrix as an adhesion checkpoint for mammary epithelial function." Int J Biochem Cell Biol **39**(4): 715-726.
Kaushik, S., M. W. Pickup and V. M. Weaver (2016). "From transformation to metastasis: deconstructing the extracellular matrix in breast cancer." Cancer Metastasis Rev **35**(4): 655-667.
Kenny, P. A., G. Y. Lee, C. A. Myers, R. M. Neve, J. R. Semeiks, P. T. Spellman, K. Lorenz, E. H. Lee, M. H. Barcellos-Hoff, O. W. Petersen, J. W. Gray and M. J. Bissell (2007). "The morphologies of breast cancer cell lines in three-dimensional assays correlate with their profiles of gene expression." Mol Oncol **1**(1): 84-96.
Khajah, M. A., P. M. Mathew and Y. A. Luqmani (2018). "Na+/K+ ATPase activity promotes invasion of endocrine resistant breast cancer cells." PLoS One **13**(3): e0193779.

Khan, Y. S., A. O. Fakoya and H. Sajjad (2024). Anatomy, Thorax, Mammary Gland. StatPearls. Treasure Island (FL) ineligible companies. Disclosure: Adegbenro Fakoya declares no relevant financial relationships with ineligible companies. Disclosure: Hussain Sajjad declares no relevant financial relationships with ineligible companies.
Khundmiri, S. J., M. A. Metzler, M. Ameen, V. Amin, M. J. Rane and N. A. Delamere (2006). "Ouabain induces cell proliferation through calcium-dependent phosphorylation of Akt (protein kinase B) in opossum kidney proximal tubule cells." Am J Physiol Cell Physiol **291**(6): C1247-1257.
Kilanowska, A., A. Ziolkowska, P. Stasiak and M. Gibas-Dorna (2022). "cAMP-Dependent Signaling and Ovarian Cancer." Cells **11**(23).
Kim, E. J. Y., L. Sorokin and T. Hiiragi (2022). "ECM-integrin signalling instructs cellular position sensing to pattern the early mouse embryo." Development **149**(1).
Kim, H., M. Kim, S. K. Im and S. Fang (2018). "Mouse Cre-LoxP system: general principles to determine tissue-specific roles of target genes." Lab Anim Res **34**(4): 147-159.
Kim, T. K. and J. H. Eberwine (2010). "Mammalian cell transfection: the present and the future." Anal Bioanal Chem **397**(8): 3173-3178.
Kirshner, J., C. J. Chen, P. Liu, J. Huang and J. E. Shively (2003). "CEACAM1-4S, a cell-cell adhesion molecule, mediates apoptosis and reverts mammary carcinoma cells to a normal morphogenic phenotype in a 3D culture." Proc Natl Acad Sci U S A **100**(2): 521-526.
Klahan, S., W. C. Huang, C. M. Chang, H. S. Wong, C. C. Huang, M. S. Wu, Y. C. Lin, H. F. Lu, M. F. Hou and W. C. Chang (2016). "Gene expression profiling combined with functional analysis identify integrin beta1 (ITGB1) as a potential prognosis biomarker in triple negative breast cancer." Pharmacol Res **104**: 31-37.
Kopelman, H., M. Corey, K. Gaskin, P. Durie, Z. Weizman and G. Forstner (1988). "Impaired chloride secretion, as well as bicarbonate secretion, underlies the fluid secretory defect in the cystic fibrosis pancreas." Gastroenterology **95**(2): 349-355.
Kravtsov, D. V. and N. A. Ameen (2013). "Molecular motors and apical CFTR traffic in epithelia." Int J Mol Sci **14**(5): 9628-9642.
Kreda, S. M., C. W. Davis and M. C. Rose (2012). "CFTR, mucins, and mucus obstruction in cystic fibrosis." Cold Spring Harb Perspect Med **2**(9): a009589.
Kreda, S. M. and M. Gentzsch (2011). "Imaging CFTR protein localization in cultured cells and tissues." Methods Mol Biol **742**: 15-33.
Kreda, S. M., M. C. Gynn, D. A. Fenstermacher, R. C. Boucher and S. E. Gabriel (2001). "Expression and localization of epithelial aquaporins in the adult human lung." Am J Respir Cell Mol Biol **24**(3): 224-234.
Larre, I., A. Lazaro, R. G. Contreras, M. S. Balda, K. Matter, C. Flores-Maldonado, A. Ponce, D. Flores-Benitez, R. Rincon-Heredia, T. Padilla-Benavides, A. Castillo, L. Shoshani and M. Cereijido (2010). "Ouabain modulates epithelial cell tight junction." Proc Natl Acad Sci U S A **107**(25): 11387-11392.
Lee, B. H., I. Seijo-Barandiaran and A. Grapin-Botton (2022). "Epithelial morphogenesis in organoids." Curr Opin Genet Dev **72**: 30-37.
Lee, S. L., P. Y. Huang, P. Roller, E. G. Cho, D. Park and R. B. Dickson (2010). "Matriptase/epithin participates in mammary epithelial cell growth and morphogenesis through HGF activation." Mech Dev **127**(1-2): 82-95.
Li, H., I. A. Findlay and D. N. Sheppard (2004). "The relationship between cell proliferation, Cl- secretion, and renal cyst growth: a study using CFTR inhibitors." Kidney Int **66**(5): 1926-1938.

Li, H., W. Yang, F. Mendes, M. D. Amaral and D. N. Sheppard (2012). "Impact of the cystic fibrosis mutation F508del-CFTR on renal cyst formation and growth." Am J Physiol Renal Physiol **303**(8): F1176-1186.
Li, N., Y. Zhang, M. J. Naylor, F. Schatzmann, F. Maurer, T. Wintermantel, G. Schuetz, U. Mueller, C. H. Streuli and N. E. Hynes (2005). "Beta1 integrins regulate mammary gland proliferation and maintain the integrity of mammary alveoli." EMBO J **24**(11): 1942-1953.
Liu, K., F. Dong, H. Gao, Y. Guo, H. Li, F. Yang, P. Zhao, Y. Dai, J. Wang, W. Zhou and C. Zou (2020). "Promoter hypermethylation of the CFTR gene as a novel diagnostic and prognostic marker of breast cancer." Cell Biol Int **44**(2): 603-609.
Liu, Z., J. D. Anderson, L. Deng, S. Mackay, J. Bailey, L. Kersh, S. M. Rowe and J. S. Guimbellot (2020). "Human Nasal Epithelial Organoids for Therapeutic Development in Cystic Fibrosis." Genes (Basel) **11**(6).
Lobert, V. H., M. L. Skardal, L. Malerod, J. E. Simensen, H. A. Algra, A. N. Andersen, T. Fleischer, H. A. Enserink, K. Liestol, J. K. Heath, T. E. Rusten and H. A. Stenmark (2022). "PHLPP1 regulates CFTR activity and lumen expansion through AMPK." Development **149**(20).
Lu, Y., Z. Zhou, J. Tao, B. Dou, M. Gao and Y. Liu (2014). "Overexpression of stearoyl-CoA desaturase 1 in bone marrow mesenchymal stem cells enhance the expression of induced endothelial cells." Lipids Health Dis **13**: 53.
Lukacs, G. L., X. B. Chang, C. Bear, N. Kartner, A. Mohamed, J. R. Riordan and S. Grinstein (1993). "The delta F508 mutation decreases the stability of cystic fibrosis transmembrane conductance regulator in the plasma membrane. Determination of functional half-lives on transfected cells." J Biol Chem **268**(29): 21592-21598.
Lukasiewicz, S., M. Czeczelewski, A. Forma, J. Baj, R. Sitarz and A. Stanislawek (2021). "Breast Cancer-Epidemiology, Risk Factors, Classification, Prognostic Markers, and Current Treatment Strategies-An Updated Review." Cancers (Basel) **13**(17).
Luo, B. H., C. V. Carman and T. A. Springer (2007). "Structural basis of integrin regulation and signaling." Annu Rev Immunol **25**: 619-647.
Lyons, W. R. (1958). "Hormonal synergism in mammary growth." Proc R Soc Lond B Biol Sci **149**(936): 303-325.
Ma, T., Y. Song, A. Gillespie, E. J. Carlson, C. J. Epstein and A. S. Verkman (1999). "Defective secretion of saliva in transgenic mice lacking aquaporin-5 water channels." J Biol Chem **274**(29): 20071-20074.
Macias, H. and L. Hinck (2012). "Mammary gland development." Wiley Interdiscip Rev Dev Biol **1**(4): 533-557.
Mailleux, A. A., M. Overholtzer, T. Schmelzle, P. Bouillet, A. Strasser and J. S. Brugge (2007). "BIM regulates apoptosis during mammary ductal morphogenesis, and its absence reveals alternative cell death mechanisms." Dev Cell **12**(2): 221-234.
Maisonneuve, P., B. C. Marshall, E. A. Knapp and A. B. Lowenfels (2013). "Cancer risk in cystic fibrosis: a 20-year nationwide study from the United States." J Natl Cancer Inst **105**(2): 122-129.
Martin-Belmonte, F., A. Gassama, A. Datta, W. Yu, U. Rescher, V. Gerke and K. Mostov (2007). "PTEN-mediated apical segregation of phosphoinositides controls epithelial morphogenesis through Cdc42." Cell **128**(2): 383-397.
Martin-Belmonte, F., W. Yu, A. E. Rodriguez-Fraticelli, A. J. Ewald, Z. Werb, M. A. Alonso and K. Mostov (2008). "Cell-polarity dynamics controls the mechanism of lumen formation in epithelial morphogenesis." Curr Biol **18**(7): 507-513.

Maurisse, R., D. De Semir, H. Emamekhoo, B. Bedayat, A. Abdolmohammadi, H. Parsi and D. C. Gruenert (2010). "Comparative transfection of DNA into primary and transformed mammalian cells from different lineages." BMC Biotechnol **10**: 9.
McCaffrey, L. M. and I. G. Macara (2009). "The Par3/aPKC interaction is essential for end bud remodeling and progenitor differentiation during mammary gland morphogenesis." Genes Dev **23**(12): 1450-1460.
McClure, M. L., S. Barnes, J. L. Brodsky and E. J. Sorscher (2016). "Trafficking and function of the cystic fibrosis transmembrane conductance regulator: a complex network of posttranslational modifications." Am J Physiol Lung Cell Mol Physiol **311**(4): L719-L733.
McNeil, E., C. T. Capaldo and I. G. Macara (2006). "Zonula occludens-1 function in the assembly of tight junctions in Madin-Darby canine kidney epithelial cells." Mol Biol Cell **17**(4): 1922-1932.
Mehta, G., A. Y. Hsiao, M. Ingram, G. D. Luker and S. Takayama (2012). "Opportunities and challenges for use of tumor spheroids as models to test drug delivery and efficacy." J Control Release **164**(2): 192-204.
Melvin, J. E. (1999). "Chloride channels and salivary gland function." Crit Rev Oral Biol Med **10**(2): 199-209.
Meyerholz, D. K., D. A. Stoltz, N. D. Gansemer, S. E. Ernst, D. P. Cook, M. D. Strub, E. N. LeClair, C. K. Barker, R. J. Adam, M. R. Leidinger, K. N. Gibson-Corley, P. H. Karp, M. J. Welsh and P. B. McCray, Jr. (2018). "Lack of cystic fibrosis transmembrane conductance regulator disrupts fetal airway development in pigs." Lab Invest **98**(6): 825-838.
Meyerholz, D. K., D. A. Stoltz, E. Namati, S. Ramachandran, A. A. Pezzulo, A. R. Smith, M. V. Rector, M. J. Suter, S. Kao, G. McLennan, G. J. Tearney, J. Zabner, P. B. McCray, Jr. and M. J. Welsh (2010). "Loss of cystic fibrosis transmembrane conductance regulator function produces abnormalities in tracheal development in neonatal pigs and young children." Am J Respir Crit Care Med **182**(10): 1251-1261.
Monteleon, C. L., A. Sedgwick, A. Hartsell, M. Dai, C. Whittington, S. Voytik-Harbin and C. D'Souza-Schorey (2012). "Establishing epithelial glandular polarity: interlinked roles for ARF6, Rac1, and the matrix microenvironment." Mol Biol Cell **23**(23): 4495-4505.
Montesano, R., J. V. Soriano, I. Fialka and L. Orci (1998). "Isolation of EpH4 mammary epithelial cell subpopulations which differ in their morphogenetic properties." In Vitro Cell Dev Biol Anim **34**(6): 468-477.
Moran, O. (2017). "The gating of the CFTR channel." Cell Mol Life Sci **74**(1): 85-92.
Muthuswamy, S. K., D. Li, S. Lelievre, M. J. Bissell and J. S. Brugge (2001). "ErbB2, but not ErbB1, reinitiates proliferation and induces luminal repopulation in epithelial acini." Nat Cell Biol **3**(9): 785-792.
Narayanan, V., L. E. Schappell, C. R. Mayer, A. A. Duke, T. J. Armiger, P. T. Arsenovic, A. Mohan, K. N. Dahl, J. P. Gleghorn and D. E. Conway (2020). "Osmotic Gradients in Epithelial Acini Increase Mechanical Tension across E-cadherin, Drive Morphogenesis, and Maintain Homeostasis." Curr Biol **30**(4): 624-633 e624.
Nauntofte, B. and S. Dissing (1988). "K+ transport and membrane potentials in isolated rat parotid acini." Am J Physiol **255**(4 Pt 1): C508-518.
Navis, A. and M. Bagnat (2015). "Developing pressures: fluid forces driving morphogenesis." Curr Opin Genet Dev **32**: 24-30.
Navis, A., L. Marjoram and M. Bagnat (2013). "Cftr controls lumen expansion and function of Kupffer's vesicle in zebrafish." Development **140**(8): 1703-1712.
Naylor, M. J., N. Li, J. Cheung, E. T. Lowe, E. Lambert, R. Marlow, P. Wang, F. Schatzmann, T. Wintermantel, G. Schuetz, A. R. Clarke, U. Mueller, N. E. Hynes and C. H. Streuli (2005).

"Ablation of beta1 integrin in mammary epithelium reveals a key role for integrin in glandular morphogenesis and differentiation." J Cell Biol **171**(4): 717-728.
Neglia, J. P., S. C. FitzSimmons, P. Maisonneuve, M. H. Schoni, F. Schoni-Affolter, M. Corey and A. B. Lowenfels (1995). "The risk of cancer among patients with cystic fibrosis. Cystic Fibrosis and Cancer Study Group." N Engl J Med **332**(8): 494-499.
Nelson, C. M. and M. J. Bissell (2005). "Modeling dynamic reciprocity: engineering three-dimensional culture models of breast architecture, function, and neoplastic transformation." Semin Cancer Biol **15**(5): 342-352.
Nguyen, T. and J. E. Shively (2016). "Induction of Lumen Formation in a Three-dimensional Model of Mammary Morphogenesis by Transcriptional Regulator ID4: ROLE OF CaMK2D IN THE EPIGENETIC REGULATION OF ID4 GENE EXPRESSION." J Biol Chem **291**(32): 16766-16776.
Nir, I., D. Huttner and A. Meller (2015). "Direct Sensing and Discrimination among Ubiquitin and Ubiquitin Chains Using Solid-State Nanopores." Biophys J **108**(9): 2340-2349.
Nistico, P., F. Di Modugno, S. Spada and M. J. Bissell (2014). "beta1 and beta4 integrins: from breast development to clinical practice." Breast Cancer Res **16**(5): 459.
Noel, S., P. O. Strale, L. Dannhoffer, M. Wilke, H. DeJonge, C. Rogier, Y. Mettey and F. Becq (2008). "Stimulation of salivary secretion in vivo by CFTR potentiators in Cftr+/+ and Cftr-/- mice." J Cyst Fibros **7**(2): 128-133.
O'Riordan, C. R., A. L. Lachapelle, J. Marshall, E. A. Higgins and S. H. Cheng (2000). "Characterization of the oligosaccharide structures associated with the cystic fibrosis transmembrane conductance regulator." Glycobiology **10**(11): 1225-1233.
Oakes, S. R., H. N. Hilton and C. J. Ormandy (2006). "The alveolar switch: coordinating the proliferative cues and cell fate decisions that drive the formation of lobuloalveoli from ductal epithelium." Breast Cancer Res **8**(2): 207.
Okiyoneda, T., H. Barriere, M. Bagdany, W. M. Rabeh, K. Du, J. Hohfeld, J. C. Young and G. L. Lukacs (2010). "Peripheral protein quality control removes unfolded CFTR from the plasma membrane." Science **329**(5993): 805-810.
Ornoy, A., J. Arnon, D. Katznelson, M. Granat, B. Caspi and J. Chemke (1987). "Pathological confirmation of cystic fibrosis in the fetus following prenatal diagnosis." Am J Med Genet **28**(4): 935-947.
Ostedgaard, L. S., D. K. Meyerholz, J. H. Chen, A. A. Pezzulo, P. H. Karp, T. Rokhlina, S. E. Ernst, R. A. Hanfland, L. R. Reznikov, P. S. Ludwig, M. P. Rogan, G. J. Davis, C. L. Dohrn, C. Wohlford-Lenane, P. J. Taft, M. V. Rector, E. Hornick, B. S. Nassar, M. Samuel, Y. Zhang, S. S. Richter, A. Uc, J. Shilyansky, R. S. Prather, P. B. McCray, Jr., J. Zabner, M. J. Welsh and D. A. Stoltz (2011). "The DeltaF508 mutation causes CFTR misprocessing and cystic fibrosis-like disease in pigs." Sci Transl Med **3**(74): 74ra24.
Ou, Y., C. X. Pan, J. Zuo and F. A. van der Hoorn (2017). "Ouabain affects cell migration via Na,K-ATPase-p130cas and via nucleus-centrosome association." PLoS One **12**(8): e0183343.
Overeem, A. W., D. M. Bryant and I. S. C. van (2015). "Mechanisms of apical-basal axis orientation and epithelial lumen positioning." Trends Cell Biol **25**(8): 476-485.
Palk, L., J. Sneyd, T. J. Shuttleworth, D. I. Yule and E. J. Crampin (2010). "A dynamic model of saliva secretion." J Theor Biol **266**(4): 625-640.
Park, C. C., H. Zhang, M. Pallavicini, J. W. Gray, F. Baehner, C. J. Park and M. J. Bissell (2006). "Beta1 integrin inhibitory antibody induces apoptosis of breast cancer cells, inhibits growth, and distinguishes malignant from normal phenotype in three dimensional cultures and in vivo." Cancer Res **66**(3): 1526-1535.

Patil, P. U., J. D'Ambrosio, L. J. Inge, R. W. Mason and A. K. Rajasekaran (2015). "Carcinoma cells induce lumen filling and EMT in epithelial cells through soluble E-cadherin-mediated activation of EGFR." J Cell Sci **128**(23): 4366-4379.
Pearson, J. F., S. Hughes, K. Chambers and S. H. Lang (2009). "Polarized fluid movement and not cell death, creates luminal spaces in adult prostate epithelium." Cell Death Differ **16**(3): 475-482.
Pechoux, C., T. Gudjonsson, L. Ronnov-Jessen, M. J. Bissell and O. W. Petersen (1999). "Human mammary luminal epithelial cells contain progenitors to myoepithelial cells." Dev Biol **206**(1): 88-99.
Petersen, O. W., L. Ronnov-Jessen, A. R. Howlett and M. J. Bissell (1992). "Interaction with basement membrane serves to rapidly distinguish growth and differentiation pattern of normal and malignant human breast epithelial cells." Proc Natl Acad Sci U S A **89**(19): 9064-9068.
Picciotto, M. R., J. A. Cohn, G. Bertuzzi, P. Greengard and A. C. Nairn (1992). "Phosphorylation of the cystic fibrosis transmembrane conductance regulator." J Biol Chem **267**(18): 12742-12752.
Pignatelli, M., A. M. Hanby and G. W. Stamp (1991). "Low expression of beta 1, alpha 2 and alpha 3 subunits of VLA integrins in malignant mammary tumours." J Pathol **165**(1): 25-32.
Pitelka, D. R., S. T. Hamamoto, J. G. Duafala and M. K. Nemanic (1973). "Cell contacts in the mouse mammary gland. I. Normal gland in postnatal development and the secretory cycle." J Cell Biol **56**(3): 797-818.
Pivert, A., C. Lefeuvre, C. T. Tran, C. Baillou, D. Durantel, H. Le Guillou-Guillemette, F. M. Lemoine, F. Lunel-Fabiani and A. Ducancelle (2021). "Publisher Correction: A first experience of transduction for differentiated HepaRG cells using lentiviral technology." Sci Rep **11**(1): 18051.
Plachot, C., L. S. Chaboub, H. A. Adissu, L. Wang, A. Urazaev, J. Sturgis, E. K. Asem and S. A. Lelievre (2009). "Factors necessary to produce basoapical polarity in human glandular epithelium formed in conventional and high-throughput three-dimensional culture: example of the breast epithelium." BMC Biol **7**: 77.
Prince, L. S., A. Tousson and R. B. Marchase (1993). "Cell surface labeling of CFTR in T84 cells." Am J Physiol **264**(2 Pt 1): C491-498.
Prosser, S. L. and L. Pelletier (2017). "Mitotic spindle assembly in animal cells: a fine balancing act." Nat Rev Mol Cell Biol **18**(3): 187-201.
Ramsay, D. T., J. C. Kent, R. A. Hartmann and P. E. Hartmann (2005). "Anatomy of the lactating human breast redefined with ultrasound imaging." J Anat **206**(6): 525-534.
Rathbun, L. I., E. G. Colicino, J. Manikas, J. O'Connell, N. Krishnan, N. S. Reilly, S. Coyne, G. Erdemci-Tandogan, A. Garrastegui, J. Freshour, P. Santra, M. L. Manning, J. D. Amack and H. Hehnly (2020). "Cytokinetic bridge triggers de novo lumen formation in vivo." Nat Commun **11**(1): 1269.
Ratjen, F., S. C. Bell, S. M. Rowe, C. H. Goss, A. L. Quittner and A. Bush (2015). "Cystic fibrosis." Nat Rev Dis Primers **1**: 15010.
Recillas-Targa, F. (2006). "Multiple strategies for gene transfer, expression, knockdown, and chromatin influence in mammalian cell lines and transgenic animals." Mol Biotechnol **34**(3): 337-354.
Reddy, M. M., M. J. Light and P. M. Quinton (1999). "Activation of the epithelial Na+ channel (ENaC) requires CFTR Cl- channel function." Nature **402**(6759): 301-304.
Rejon, C., M. Al-Masri and L. McCaffrey (2016). "Cell Polarity Proteins in Breast Cancer Progression." J Cell Biochem **117**(10): 2215-2223.

Richter, M., O. Piwocka, M. Musielak, I. Piotrowski, W. M. Suchorska and T. Trzeciak (2021). "From Donor to the Lab: A Fascinating Journey of Primary Cell Lines." Front Cell Dev Biol **9**: 711381.
Riising, E. M., R. Boggio, S. Chiocca, K. Helin and D. Pasini (2008). "The polycomb repressive complex 2 is a potential target of SUMO modifications." PLoS One **3**(7): e2704.
Riordan, J. R. (2008). "CFTR function and prospects for therapy." Annu Rev Biochem **77**: 701-726.
Riordan, J. R., J. M. Rommens, B. Kerem, N. Alon, R. Rozmahel, Z. Grzelczak, J. Zielenski, S. Lok, N. Plavsic, J. L. Chou and et al. (1989). "Identification of the cystic fibrosis gene: cloning and characterization of complementary DNA." Science **245**(4922): 1066-1073.
Robinson, G. W., A. B. Karpf and K. Kratochwil (1999). "Regulation of mammary gland development by tissue interaction." J Mammary Gland Biol Neoplasia **4**(1): 9-19.
Rodgers, L. S., M. T. Beam, J. M. Anderson and A. S. Fanning (2013). "Epithelial barrier assembly requires coordinated activity of multiple domains of the tight junction protein ZO-1." J Cell Sci **126**(Pt 7): 1565-1575.
Rooney, N., P. Wang, K. Brennan, A. P. Gilmore and C. H. Streuli (2016). "The Integrin-Mediated ILK-Parvin-alphaPix Signaling Axis Controls Differentiation in Mammary Epithelial Cells." J Cell Physiol **231**(11): 2408-2417.
Rott, R., R. Szargel, J. Haskin, R. Bandopadhyay, A. J. Lees, V. Shani and S. Engelender (2011). "alpha-Synuclein fate is determined by USP9X-regulated monoubiquitination." Proc Natl Acad Sci U S A **108**(46): 18666-18671.
Ruan, W. and D. L. Kleinberg (1999). "Insulin-like growth factor I is essential for terminal end bud formation and ductal morphogenesis during mammary development." Endocrinology **140**(11): 5075-5081.
Ruan, Y. C., Y. Wang, N. Da Silva, B. Kim, R. Y. Diao, E. Hill, D. Brown, H. C. Chan and S. Breton (2014). "CFTR interacts with ZO-1 to regulate tight junction assembly and epithelial differentiation through the ZONAB pathway." J Cell Sci **127**(Pt 20): 4396-4408.
Rubin, J. L., L. O'Callaghan, C. Pelligra, M. W. Konstan, A. Ward, J. K. Ishak, C. Chandler and T. G. Liou (2019). "Modeling long-term health outcomes of patients with cystic fibrosis homozygous for F508del-CFTR treated with lumacaftor/ivacaftor." Ther Adv Respir Dis **13**: 1753466618820186.
Russ, A., J. M. Louderbough, D. Zarnescu and J. A. Schroeder (2012). "Hugl1 and Hugl2 in mammary epithelial cells: polarity, proliferation, and differentiation." PLoS One **7**(10): e47734.
Saint-Criq, V. and M. A. Gray (2017). "Role of CFTR in epithelial physiology." Cell Mol Life Sci **74**(1): 93-115.
Sassone-Corsi, P. (2012). "The cyclic AMP pathway." Cold Spring Harb Perspect Biol **4**(12).
Sato, K. and F. Sato (1984). "Defective beta adrenergic response of cystic fibrosis sweat glands in vivo and in vitro." J Clin Invest **73**(6): 1763-1771.
Sato, T., R. G. Vries, H. J. Snippert, M. van de Wetering, N. Barker, D. E. Stange, J. H. van Es, A. Abo, P. Kujala, P. J. Peters and H. Clevers (2009). "Single Lgr5 stem cells build crypt-villus structures in vitro without a mesenchymal niche." Nature **459**(7244): 262-265.
Schatzmann, H. J. (1953). "[Cardiac glycosides as inhibitors of active potassium and sodium transport by erythrocyte membrane]." Helv Physiol Pharmacol Acta **11**(4): 346-354.
Schedin, P., T. Mitrenga, S. McDaniel and M. Kaeck (2004). "Mammary ECM composition and function are altered by reproductive state." Mol Carcinog **41**(4): 207-220.
Schneider-Poetsch, T. and M. Yoshida (2018). "Along the Central Dogma-Controlling Gene Expression with Small Molecules." Annu Rev Biochem **87**: 391-420.

Schutgens, F., M. B. Rookmaaker, T. Margaritis, A. Rios, C. Ammerlaan, J. Jansen, L. Gijzen, M. Vormann, A. Vonk, M. Viveen, F. Y. Yengej, S. Derakhshan, K. M. de Winter-de Groot, B. Artegiani, R. van Boxtel, E. Cuppen, A. P. A. Hendrickx, M. M. van den Heuvel-Eibrink, E. Heitzer, H. Lanz, J. Beekman, J. L. Murk, R. Masereeuw, F. Holstege, J. Drost, M. C. Verhaar and H. Clevers (2019). "Tubuloids derived from human adult kidney and urine for personalized disease modeling." Nat Biotechnol **37**(3): 303-313.
Schwander, M., M. Leu, M. Stumm, O. M. Dorchies, U. T. Ruegg, J. Schittny and U. Muller (2003). "Beta1 integrins regulate myoblast fusion and sarcomere assembly." Dev Cell **4**(5): 673-685.
Schwank, G., B. K. Koo, V. Sasselli, J. F. Dekkers, I. Heo, T. Demircan, N. Sasaki, S. Boymans, E. Cuppen, C. K. van der Ent, E. E. Nieuwenhuis, J. M. Beekman and H. Clevers (2013). "Functional repair of CFTR by CRISPR/Cas9 in intestinal stem cell organoids of cystic fibrosis patients." Cell Stem Cell **13**(6): 653-658.
Seamon, K. B. and J. W. Daly (1981). "Forskolin: a unique diterpene activator of cyclic AMP-generating systems." J Cyclic Nucleotide Res **7**(4): 201-224.
Sigurbjornsdottir, S., R. Mathew and M. Leptin (2014). "Molecular mechanisms of de novo lumen formation." Nat Rev Mol Cell Biol **15**(10): 665-676.
Silberstein, G. B. (2001). "Tumour-stromal interactions. Role of the stroma in mammary development." Breast Cancer Res **3**(4): 218-223.
Stastna, N., K. Brat, L. Homola, A. Os and D. Brancikova (2023). "Increasing incidence rate of breast cancer in cystic fibrosis - relationship between pathogenesis, oncogenesis and prediction of the treatment effect in the context of worse clinical outcome and prognosis of cystic fibrosis due to estrogens." Orphanet J Rare Dis **18**(1): 62.
Stephens, L. E., A. E. Sutherland, I. V. Klimanskaya, A. Andrieux, J. Meneses, R. A. Pedersen and C. H. Damsky (1995). "Deletion of beta 1 integrins in mice results in inner cell mass failure and peri-implantation lethality." Genes Dev **9**(15): 1883-1895.
Sternlicht, M. D. (2006). "Key stages in mammary gland development: the cues that regulate ductal branching morphogenesis." Breast Cancer Res **8**(1): 201.
Sternlicht, M. D., H. Kouros-Mehr, P. Lu and Z. Werb (2006). "Hormonal and local control of mammary branching morphogenesis." Differentiation **74**(7): 365-381.
Streuli, C. H., N. Bailey and M. J. Bissell (1991). "Control of mammary epithelial differentiation: basement membrane induces tissue-specific gene expression in the absence of cell-cell interaction and morphological polarity." J Cell Biol **115**(5): 1383-1395.
Sun, Z., M. Costell and R. Fassler (2019). "Integrin activation by talin, kindlin and mechanical forces." Nat Cell Biol **21**(1): 25-31.
Taddei, I., M. M. Faraldo, J. Teuliere, M. A. Deugnier, J. P. Thiery and M. A. Glukhova (2003). "Integrins in mammary gland development and differentiation of mammary epithelium." J Mammary Gland Biol Neoplasia **8**(4): 383-394.
Tanimura, A. and Y. Tojyo (2006). "[Regulation of fluid and electrolyte secretion and exocytosis in salivary acinar cells]." Nihon Yakurigaku Zasshi **127**(4): 249-255.
Tizzano, E. F., D. Chitayat and M. Buchwald (1993). "Cell-specific localization of CFTR mRNA shows developmentally regulated expression in human fetal tissues." Hum Mol Genet **2**(3): 219-224.
Tizzano, E. F., H. O'Brodovich, D. Chitayat, J. C. Benichou and M. Buchwald (1994). "Regional expression of CFTR in developing human respiratory tissues." Am J Respir Cell Mol Biol **10**(4): 355-362.
Tsukita, S. and M. Furuse (2000). "The structure and function of claudins, cell adhesion molecules at tight junctions." Ann N Y Acad Sci **915**: 129-135.

Umeda, K., J. Ikenouchi, S. Katahira-Tayama, K. Furuse, H. Sasaki, M. Nakayama, T. Matsui, S. Tsukita, M. Furuse and S. Tsukita (2006). "ZO-1 and ZO-2 independently determine where claudins are polymerized in tight-junction strand formation." Cell **126**(4): 741-754.
Veit, G., R. G. Avramescu, A. N. Chiang, S. A. Houck, Z. Cai, K. W. Peters, J. S. Hong, H. B. Pollard, W. B. Guggino, W. E. Balch, W. R. Skach, G. R. Cutting, R. A. Frizzell, D. N. Sheppard, D. M. Cyr, E. J. Sorscher, J. L. Brodsky and G. L. Lukacs (2016). "From CFTR biology toward combinatorial pharmacotherapy: expanded classification of cystic fibrosis mutations." Mol Biol Cell **27**(3): 424-433.
Venglovecz, V., P. Pallagi, L. V. Kemeny, A. Balazs, Z. Balla, E. Becskehazi, E. Gal, E. Toth, A. Zvara, L. G. Puskas, K. Borka, M. Sendler, M. M. Lerch, J. Mayerle, J. P. Kuhn, Z. Rakonczay, Jr. and P. Hegyi (2018). "The Importance of Aquaporin 1 in Pancreatitis and Its Relation to the CFTR Cl(-) Channel." Front Physiol **9**: 854.
Vergani, P., A. C. Nairn and D. C. Gadsby (2003). "On the mechanism of MgATP-dependent gating of CFTR Cl- channels." J Gen Physiol **121**(1): 17-36.
Verkman, A. S., D. Synder, L. Tradtrantip, J. R. Thiagarajah and M. O. Anderson (2013). "CFTR inhibitors." Curr Pharm Des **19**(19): 3529-3541.
Vidi, P. A., M. J. Bissell and S. A. Lelievre (2013). "Three-dimensional culture of human breast epithelial cells: the how and the why." Methods Mol Biol **945**: 193-219.
Vijay-Kumar, S., C. E. Bugg and W. J. Cook (1987). "Structure of ubiquitin refined at 1.8 A resolution." J Mol Biol **194**(3): 531-544.
Vukicevic, S., H. K. Kleinman, F. P. Luyten, A. B. Roberts, N. S. Roche and A. H. Reddi (1992). "Identification of multiple active growth factors in basement membrane Matrigel suggests caution in interpretation of cellular activity related to extracellular matrix components." Exp Cell Res **202**(1): 1-8.
Walker, N. I., R. E. Bennett and J. F. Kerr (1989). "Cell death by apoptosis during involution of the lactating breast in mice and rats." Am J Anat **185**(1): 19-32.
Wang, F., V. M. Weaver, O. W. Petersen, C. A. Larabell, S. Dedhar, P. Briand, R. Lupu and M. J. Bissell (1998). "Reciprocal interactions between beta1-integrin and epidermal growth factor receptor in three-dimensional basement membrane breast cultures: a different perspective in epithelial biology." Proc Natl Acad Sci U S A **95**(25): 14821-14826.
Wang, P., X. Liu, C. Kong, X. Liu, Z. Teng, Y. Ma, L. Yong, C. Liang, G. He and S. Lu (2019). "Potential role of the IL17RC gene in the thoracic ossification of the posterior longitudinal ligament." Int J Mol Med **43**(5): 2005-2014.
Wang, Z., D. Wang, K. Jiang, Y. Guo, Z. Li, R. Jiang, R. Han, G. Li, Y. Tian, H. Li, X. Kang and X. Liu (2021). "A Comprehensive Proteome and Acetyl-Proteome Atlas Reveals Molecular Mechanisms Adapting to the Physiological Changes From Pre-laying to Peak-Laying Stage in Liver of Hens (Gallus gallus)." Front Vet Sci **8**: 700669.
Ward, C. L. and R. R. Kopito (1994). "Intracellular turnover of cystic fibrosis transmembrane conductance regulator. Inefficient processing and rapid degradation of wild-type and mutant proteins." J Biol Chem **269**(41): 25710-25718.
Watson, C. J. (2006). "Involution: apoptosis and tissue remodelling that convert the mammary gland from milk factory to a quiescent organ." Breast Cancer Res **8**(2): 203.
Weir, M. L., M. L. Oppizzi, M. D. Henry, A. Onishi, K. P. Campbell, M. J. Bissell and J. L. Muschler (2006). "Dystroglycan loss disrupts polarity and beta-casein induction in mammary epithelial cells by perturbing laminin anchoring." J Cell Sci **119**(Pt 19): 4047-4058.
Whiting, P., M. Al, L. Burgers, M. Westwood, S. Ryder, M. Hoogendoorn, N. Armstrong, A. Allen, H. Severens and J. Kleijnen (2014). "Ivacaftor for the treatment of patients with cystic fibrosis and the G551D mutation: a systematic review and cost-effectiveness analysis." Health Technol Assess **18**(18): 1-106.

WHO. (2020). "Breast cancer." Retrieved 01/06/2020, 2020, from http://www.who.int/cancer/prevention/diagnosis-screening/breast-cancer/en/.
Wicha, M. S., G. Lowrie, E. Kohn, P. Bagavandoss and T. Mahn (1982). "Extracellular matrix promotes mammary epithelial growth and differentiation in vitro." Proc Natl Acad Sci U S A **79**(10): 3213-3217.
Wilson, S. M., R. E. Olver and D. V. Walters (2007). "Developmental regulation of lumenal lung fluid and electrolyte transport." Respir Physiol Neurobiol **159**(3): 247-255.
Wrighton, K. H. (2013). "Cell adhesion: the 'ins' and 'outs' of integrin signalling." Nat Rev Mol Cell Biol **14**(12): 752.
Yang, J. M., P. Schiapparelli, H. N. Nguyen, A. Igarashi, Q. Zhang, S. Abbadi, L. M. Amzel, H. Sesaki, A. Quinones-Hinojosa and M. Iijima (2017). "Characterization of PTEN mutations in brain cancer reveals that pten mono-ubiquitination promotes protein stability and nuclear localization." Oncogene **36**(26): 3673-3685.
Yao, E. S., H. Zhang, Y. Y. Chen, B. Lee, K. Chew, D. Moore and C. Park (2007). "Increased beta1 integrin is associated with decreased survival in invasive breast cancer." Cancer Res **67**(2): 659-664.
Yates, L. L., C. Schnatwinkel, L. Hazelwood, L. Chessum, A. Paudyal, H. Hilton, M. R. Romero, J. Wilde, D. Bogani, J. Sanderson, C. Formstone, J. N. Murdoch, L. A. Niswander, A. Greenfield and C. H. Dean (2013). "Scribble is required for normal epithelial cell-cell contacts and lumen morphogenesis in the mammalian lung." Dev Biol **373**(2): 267-280.
Yokoyama, S., C. J. Chen, T. Nguyen and J. E. Shively (2007). "Role of CEACAM1 isoforms in an in vivo model of mammary morphogenesis: mutational analysis of the cytoplasmic domain of CEACAM1-4S reveals key residues involved in lumen formation." Oncogene **26**(55): 7637-7646.
Young, P. G., J. Levring, K. Fiedorczuk, S. C. Blanchard and J. Chen (2024). "Structural basis for CFTR inhibition by CFTR(inh)-172." Proc Natl Acad Sci U S A **121**(10): e2316675121.
Yu, E. and S. Sharma (2023). Cystic Fibrosis. StatPearls. Treasure Island (FL) ineligible companies. Disclosure: Sandeep Sharma declares no relevant financial relationships with ineligible companies.
Yu, W., X. Fang, A. Ewald, K. Wong, C. A. Hunt, Z. Werb, M. A. Matthay and K. Mostov (2007). "Formation of cysts by alveolar type II cells in three-dimensional culture reveals a novel mechanism for epithelial morphogenesis." Mol Biol Cell **18**(5): 1693-1700.
Zeng, D., A. Ferrari, J. Ulmer, A. Veligodskiy, P. Fischer, J. Spatz, Y. Ventikos, D. Poulikakos and R. Kroschewski (2006). "Three-dimensional modeling of mechanical forces in the extracellular matrix during epithelial lumen formation." Biophys J **90**(12): 4380-4391.
Zhang, J., Y. Wang, X. Jiang and H. C. Chan (2018). "Cystic fibrosis transmembrane conductance regulator-emerging regulator of cancer." Cell Mol Life Sci **75**(10): 1737-1756.
Zhang, J. T., X. H. Jiang, C. Xie, H. Cheng, J. Da Dong, Y. Wang, K. L. Fok, X. H. Zhang, T. T. Sun, L. L. Tsang, H. Chen, X. J. Sun, Y. W. Chung, Z. M. Cai, W. G. Jiang and H. C. Chan (2013). "Downregulation of CFTR promotes epithelial-to-mesenchymal transition and is associated with poor prognosis of breast cancer." Biochim Biophys Acta **1833**(12): 2961-2969.
Zhang, Z., F. Liu and J. Chen (2018). "Molecular structure of the ATP-bound, phosphorylated human CFTR." Proc Natl Acad Sci U S A **115**(50): 12757-12762.
Zhao, Z., X. Chen, A. M. Dowbaj, A. Sljukic, K. Bratlie, L. Lin, E. L. S. Fong, G. M. Balachander, Z. Chen, A. Soragni, M. Huch, Y. A. Zeng, Q. Wang and H. Yu (2022). "Organoids." Nat Rev Methods Primers **2**.
Zheng, B. and L. C. Cantley (2007). "Regulation of epithelial tight junction assembly and disassembly by AMP-activated protein kinase." Proc Natl Acad Sci U S A **104**(3): 819-822.

Zhu, J., W. Wen, Z. Zheng, Y. Shang, Z. Wei, Z. Xiao, Z. Pan, Q. Du, W. Wang and M. Zhang (2011). "LGN/mInsc and LGN/NuMA complex structures suggest distinct functions in asymmetric cell division for the Par3/mInsc/LGN and Galphai/LGN/NuMA pathways." Mol Cell **43**(3): 418-431.
Zovein, A. C., A. Luque, K. A. Turlo, J. J. Hofmann, K. M. Yee, M. S. Becker, R. Fassler, I. Mellman, T. F. Lane and M. L. Iruela-Arispe (2010). "Beta1 integrin establishes endothelial cell polarity and arteriolar lumen formation via a Par3-dependent mechanism." Dev Cell **18**(1): 39-51.
Zucca-Matthes, G., C. Urban and A. Vallejo (2016). "Anatomy of the nipple and breast ducts." Gland Surg **5**(1): 32-36.
Zutter, M. M., H. R. Krigman and S. A. Santoro (1993). "Altered integrin expression in adenocarcinoma of the breast. Analysis by in situ hybridization." Am J Pathol **142**(5): 1439-1448.
Zutter, M. M., G. Mazoujian and S. A. Santoro (1990). "Decreased expression of integrin adhesive protein receptors in adenocarcinoma of the breast." Am J Pathol **137**(4): 863-870.
Zutter, M. M., S. A. Santoro, W. D. Staatz and Y. L. Tsung (1995). "Re-expression of the alpha 2 beta 1 integrin abrogates the malignant phenotype of breast carcinoma cells." Proc Natl Acad Sci U S A **92**(16): 7411-7415.